EFFECT OF DIVALENT METAL CATIONS ON HYDROXYAPATITE DISSOLUTION KINETICS RELEVANT TO DENTAL CARIES AND EROSION

HANADI SAUD LINGAWI

BDS MSc Dent Rad MClin Dent Paeds

Thesis submitted in fulfilment of the requirements for the degree of Doctor of Philosophy in the Faculty of Medicine, University of London

May 2012

Centre for Oral Growth and Development
Institute of Dentistry
Queen Mary's School of Medicine and Dentistry
University of London

Barts and The London
School of Medicine and Dentistry

Declaration regarding plagiarism

I declare that the coursework material attached herewith is entirely my own work and that I have attributed any brief quotations both at the appropriate point in the text and in the bibliography at the end of this piece of work.

I also declare that I have not used extensive quotations or close paraphrasing and that I have neither copied from the work of another person, nor used the ideas of another person, without proper acknowledgement.

Name: Hanadi Saud Lingawi Course: PhD

Title of work submitted:
Effect of Divalent Metal Cations on Hydroxyapatite Dissolution Kinetics Relevant to Dental Caries and Erosion

Examination: A thesis submitted for the degree of Doctor of Philosophy, University of London

Signature: Date

Abstract

In recent years there has been an increasing awareness of the influence of various trace elements on reducing the progression of dental caries and of erosion. However, there are few clinical and even fewer *in-vitro* studies of the cariostatic effect of some trace elements on the progression of dental caries. Further, there is currently no consensus on the underlying physico-chemical mechanism on the influence of trace elements on these processes.

The aim of this study was to investigate the effect of three divalent cations; zinc (Zn^{2+}), strontium (Sr^{2+}) and copper (Cu^{2+}), on the physical-chemistry influencing hydroxyapatite (HAp) dissolution kinetics, using scanning microradiography (SMR), under simulated cariogenic and erosive conditions relevant to the oral environment.

Compressed and sintered porous HAp discs were used as model systems for dental enamel. These discs were exposed to demineralising solutions containing a range of concentrations of Zn^{2+}, Sr^{2+} and Cu^{2+}, and either 0.1% acetic acid at pH 4.0 resembling dental caries, or 0.3% citric acid at pH 2.8 resembling erosion conditions.

SMR is a development of the photographic microradiography technique of mineral quantification by means of X-ray absorption, but allows real-time quantification measurement of the rate of HAp mineral loss (RD_{HAp}). Sequential SMR experiments during which the HAp disc was exposed to demineralising solution, containing each cation in either increasing or decreasing concentration order (separated by 30 minutes of washing with de-ionised water) allowed evaluation of the persistence of the influence of the divalent cations being investigated.

The results showed that all three divalent cations decreased RD_{HAp} significantly under both investigated conditions but via two different mechanisms.

It was proposed that Zn^{2+} and Cu^{2+} decrease the RD_{HAp} through a surface controlled mechanism whereas Sr^{2+} decreases the RD_{HAp} through a solid phase change. This information will be useful as part of the development of therapeutic products which include these ions for the prevention of dental caries and erosion.

I dedicate this research work to the soul of my beloved mother

Hayat Bakhsh

(1941-2012)

May God rest her soul in Heaven

Acknowledgements

Here I would like to thank all those who were involved in and supported me in my PhD research.

I am thankful to my academic supervisor, Dr Paul Anderson, who stood by me through this entire PhD journey. Also I would like to thank my second supervisor, Dr Michele Barbour from the University of Bristol, for making me feel welcome, giving me access to her department facilities and giving me the chance to experience and enjoy the taste of collaborative work between different institutes.

I am also grateful to Dr Richard Lynch from GlaxoSmithKline (GSK) and Honorary Research Fellow at University of Liverpool, who was generous with his time and advice regarding our zinc experiments; Dr Rory Wilson for his help with XRD; Professor Robert Hill for his enriching discussions linking the academic research and industrial worlds; Dr Natalia Karpukhina for her valuable discussions about strontium; and Dr Siân Jones from the University of Bristol for her patient tutoring that made my trips to Bristol such a joy.

A special thanks to Dr Sharif Islam at QMUL who offered me the guidance during the statistical analysis of the data.

I cannot thank enough Professor Mark Hector, now the Dean of Dentistry at University of Dundee, who has been a great support and enormous help during the process of my GDC registration and during my work as an honorary clinical lecturer at the Paediatric Dentistry Department at QMUL.

I am deeply thankful to Dr Jacqueline Brown at King's College, University of London for being such an inspiration since I was her student at King's College during my MSc in Dental Radiology course.

I wish to thank the Dental Materials Science Laboratory at the School of Oral and Dental Sciences, University of Bristol for supplying this project with the HIMED hydroxyapatite discs.

My deep appreciation and gratitude go to the Saudi Ministry of Higher Education and the Saudi Cultural Bureau in UK for their financial grant and their continuous support throughout my course of studies.

My immense gratitude goes to my parents for their continued love and support, and to my sister Dr Arij, without whose encouragement I would have never reached this stage of my PhD.

Table of contents

PART III : DEVELOPMENT OF A PROTOCOL

List of figures

List of tables

List of abbreviations

a	Intercept
Al	Aluminium
°C	Degree celsius
Ca^{2+}	Calcium ion
CMR	Conventional contact microradiography
Cu^{2+}	Copper ion
DEJ	Dentine enamel junction
DMFT	Decayed, missing, filled permanent tooth
ESEM	Environmental scanning electron microscopy
h	Hour
H^{+}	Hydrogen ion
HAp	Hydroxyapatite
I	Transmitted X-rays intensity
I_o	Incident of X-rays intensity
LAC	Linear attenuation coefficient
m	Mass per unit area
MAC	Mass attenuation coefficient
MCA	Multiple channel analyser
min	Minute
RD_{HAp}	Hydroxyapatite demineralisation rate
s	Seconds
SD	Standard deviation
SE	Standard error
SEM	Scanning electron microscopy
SMR	Scanning microradiography
Sr^{2+}	Strontium ion
WHO	World Health Organisation
XRD	X-ray diffraction
XMT	X-ray microtomography
Zn^{2+}	Zinc ion
μ	LAC in cm^{-1}
μ_m	Mass attenuation coefficient

PART I: INTRODUCTION AND LITERATURE REVIEW

CHAPTER 1

Introduction

1.1 General introduction

Dental caries is a result of mineral dissolution of dental hard tissue, caused by the acid metabolic end products of oral bacteria that are capable of fermenting carbohydrates, particularly sugars. It is a multifactorial process and the presence of other factors, such as the host and enough time for the fermentation and acid production to take place, is required for caries to develop.

Dental caries is a worldwide health problem affecting both industrial and developing countries. According to Peterson (2003) approximately five billion people worldwide have experienced dental caries. It continues to be a major problem in dentistry and therefore should receive attention in everyday practice, not only considering treatment and restorative aspects but also preventive aspect.

Dental erosion is the loss of tooth hard tissue caused by acids without bacterial involvement. It is generally agreed that the reported prevalence of dental erosion is increasing. This may be due to greater awareness of the condition among dentists, and the increase in ageing populations worldwide, and the adult population retaining more natural teeth as they age due to developments in dentistry and dental care. In addition, younger individuals appear to exhibit increased dental erosion,

which may be due to more acidic diets and dietary eating disorders such as bulimia and anorexia.

Although dental erosion is increasingly recognised as an important aetiology in the loss of tooth structure, not only in adults but in adolescents and children as well, little is established concerning diagnostic criteria, treatment and preventive strategies. There is still a lot to be done in this field.

Mature dental enamel is acellular highly mineralised dental tissue that consists mostly of impure forms of hydroxyapatite (HAp). Carbonate, sodium and magnesium are the most abundant impurities; however a large number of impurities may exist. These may alter the physical and chemical properties of HAp and accordingly affect its demineralisation process. This thesis will address the effect of three divalent cations, zinc (Zn^{2+}), strontium (Sr^{2+}) and copper (Cu^{2+}), on the HAp demineralisation process under caries and erosion-like conditions in an attempt to understand their effect on the kinetics of HAp demineralisation process and their potential usefulness as a part of a preventive oral regimen against dental caries and erosion.

In this thesis the technique used for studying the effect of divalent cations on HAp demineralisation, is scanning microradiography (SMR). It is a method of mineral quantification by means of X-ray absorption in which the radiographic emulsion is replaced by a solid state detector. As part of the experimental work done for this thesis, the standard SMR technique has been modified to allow reliable quantitative data to be obtained over a short period of time (24 h or less), and the newly developed technique has been used in all the studies in this thesis.

1.2 General aim

The general aim of this study was to investigate the effect of the divalent cations zinc, strontium and copper on the physical chemistry influencing HAp dissolution kinetics, using scanning microradiography under simulated cariogenic and erosive conditions relevant to the oral environment.

1.3 Thesis layout

This thesis has been divided into four parts:

Part I, comprises the introduction to the thesis and the literature review. It is divided into nine chapters. The first three chapters deal with the literature review of dental enamel, dental caries and dental erosion with a brief overview of some of the available dissolution models for calcium phosphates. Chapters 5, 6 and 7 contain a detailed literature review of Zn^{2+}, Sr^{2+}, and Cu^{2+} respectively, as the divalent cations of interest in this thesis. Chapter 8 and Chapter 9 are concerned with the review of X-ray microradiography including X-ray generation, types of X-ray tubes, X-ray interactions with matter, X-ray attenuation and X-ray detection. Finally, the last chapter in Part I is a review of the literature on scanning microradiography as a technique of interest to this thesis.

Part II contains the methodology. It describes in detail the modifications made to the SMR technique, as part of the work in this thesis, so that it can be used to produce a reliable quantitative data over a short period of time (24 h or less).

Part III describes the protocol development. It consists of five chapters investigating the several changeable SMR parameters aimed at developing a protocol to be used for the rest of the experiments in this thesis.

Part IV consists of three chapters investigating the three divalent cations. Each chapter includes its own introduction, aims and objectives, materials and methods, results and discussion.

Finally, the work presented in this thesis is collectively summarised and addressed in Part V through an overall discussion, conclusions, discussion of the clinical implications and recommendations for future work.

CHAPTER 2

Human Dental Enamel

2.1 Dental enamel chemical composition

Dental enamel is a highly mineralised acellular dental tissue that is often referred to as an inorganic-organic two-phase system. It consists of ≈ 98 wt.% or 96 volume % calcium HAp, with multiple impurities, and ≈ 2 wt.% organic matrix and water (Elliott, 1994).

The organic matrix consists mainly of proteins. However, lipids, carbohydrates, and other organic molecules are also present (Wilson *et al.*, 1999). The protein concentration in dental enamel varies in a systematic manner. A high concentration of proteins has been reported to be located at the inner enamel of fissures and at the cervical margins (Robinson *et al.*, 1983).

The inorganic components are mainly in the form of impure HAp. Hydroxyapatite is a naturally occurring mineral with the chemical formula $Ca_5(PO_4)_3(OH)$, but now usually written as the stoichiometrically correct atomic composition containing 10 calcium atoms: $Ca_{10}(PO_4)_6(OH)_2$. Inclusion of carbonate, sodium, fluoride and other ions result in the impure form of the HAp that is present in human dental enamel (Elliott, 1997). In enamel crystal, phosphate ions can be replaced by carbonate ions, calcium ions can be replaced by sodium, and hydroxyl ions can be replaced by fluoride ions. Although there is no limit to the possible

extent of this substitution, 100% replacement is very rare. For example a 100% substitution of hydroxyl ions by fluoride ions lead to the formation of fluorapatite which is rarely found in biological tissue (except in shark enameloid) (Elliott, 1994). Substitution and distribution of some common impurities will be discussed in detail in Section 2.4.

2.2 Dental enamel structure

The basic structural units of human enamel are ≈5 μm wide enamel rods or sometimes referred to as enamel prisms (Boyde, 1997). Enamel rods extend from the enamel-dentine junction to the tooth surface and are separated by the interrod region. Each enamel rod is formed by tightly compacted highly organised enamel mineral crystals (crystallites). The mature enamel crystallites are narrow crystals with flattened hexagonal cross section (≈30 to 50 nm in width and elongated along the c-axis) (Boyde *et al.*, 1988). In cross section, the enamel rods may be compared to a keyhole with the top, or head, oriented toward the crown of the tooth and the tail, oriented toward the root of the tooth. The angle at which the rods approach the enamel surface varies from 90° in the cervical region to approximately 10° in the cuspal region. Many authors like Ripa *et al.* (1966), Whittaker (1982), Shellis (1984), Kodaka *et al.* (1989) and Kodaka *et al.* (1991) have reported that unlike the enamel bulk, surface enamel is prismless. The crystallites at the outer enamel are aligned parallel to each other and perpendicular to the enamel surface resulting in a more mineralised and densely packed layer with lack of inter-rod space.

2.3 Physical properties of dental enamel

Through crystallographic work Brudevold *et al.* (1960) concluded that the composition of enamel crystal is of pure HAp and therefore the mineral density of enamel would be equal to that of HAp (≈ 3.15 g/cm^3). However, later studies (Elliott, 1997) showed that enamel consists mainly of the impure form of HAp with multiple impurities, particularly carbonate ions that partially replace the phosphate ions. This significantly reduces enamel density (between 2.99 and 3.02 g/cm^3). Even though enamel density is less than was previously thought, still dental enamel is considered very dense and rigid material. The high rigidity and density makes it very brittle unless supported by the underlying dentine.

Another characteristic feature of enamel that affects its physical properties is enamel pores, which result from the imperfections in the packing of enamel crystallites. They are usually filled or partially filled with inter-prismatic substance. Authors have classified enamel pores into three main categories (Boyde and Oksche, 1989, Shellis and Dibdin, 2000). The first type is the small hexagonal tubule like pores (1-10 nm in diameter). They are located within the body of the enamel prism due to the random crystal orientation around the *c*-axis. They are the more abundant type of pores and count for 1-5 vol% of enamel. The second type is the prisms junctions pores. They are the largest in size but fewer in number and represent a minor fraction of the total enamel porosity. The third type is the intra-prismatic but their porosity is difficult to measure and little is known about them.

As a result of enamel structural architecture, particularly porosity, dental enamel is considered permeable to water, ions and small size organic molecules. The diffusion of water, ions and small organic molecules is controlled by many factors. Principally they are controlled by pore number, pore size and the inter-connectivity

between the pores. The partial acceptance or rejection of ion transport through the enamel pores depending on the charge of the diffusing ions is another controlling factor. To a lesser extent; the organic matrix also plays a role in affecting the permeability and transport process through enamel. For example, protein in the enamel matrix limits ionic diffusion. Also the mobility of water through enamel pores is significantly affected by the hydration of proteins (Shellis and Dibdin, 2000).

2.4 Trace elements in dental enamel

Dental enamel is composed mostly of biological apatites. They are impure form of HAp and differ from HAp in their composition, crystal size, morphology and stoichiometry. For example the Ca:P molar ratio in dental enamel is 1.62 - 1.64 while the Ca:P molar ratio in pure HAp is 1.67. This leads to the general idea that biological apatites are calcium deficient or non-stoichiometric. Pure HAp consists of calcium, phosphate and hydroxyl ions (Figure 2.1(a)) while biological apatites contain small amounts of various trace elements such as CO_3^{2-}, Mg^{2+}, Na^{+}, F^{-}, Zn^{2+}, Cu^{2+}, Sr^{2+} and others in addition to the main components, Ca^{2+}, PO_4^{3-}, and OH^{-} (Figure 2.1(b)).

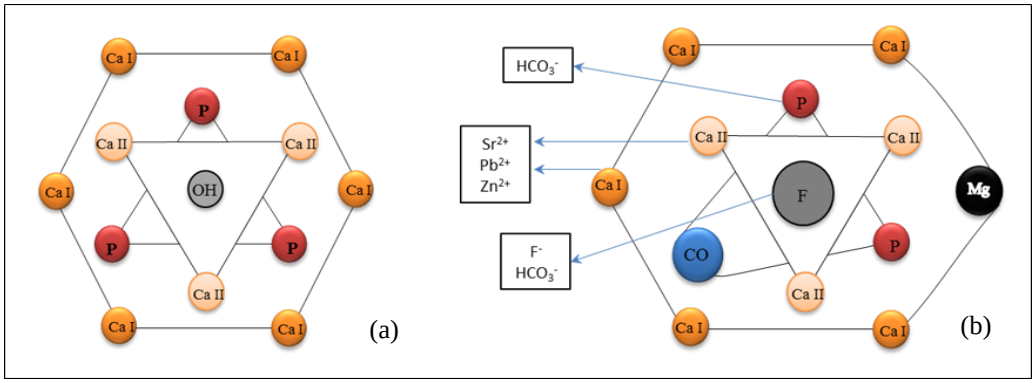

FIGURE 2.1 (a) Hexagonal unit structure of HAp with ions arranged around the central hydroxyl column (*c*-axis). (b) Examples of substitutes in biological apatite straining the lattice parameters and changing the crystal behaviour (schematic drawing idea after Robinson (2000))

Once the anions or cations become incorporated into the apatite structural lattice they alter the physico-chemical properties of the apatite. Such changes involve changes in crystal lattice parameters (reflecting the size and amount of substituents), change in crystallinity (crystal size and strain), change in crystal morphology and change in dissolution properties. The following section discusses some common substituents in dental enamel.

2.4.1 Carbonate

There has been controversy about the carbonate (CO_3^{2-}) substitution site in the apatite lattice. However, there is now general agreement that carbonates can either substitute for the phosphate ions which is called the B-type substitution (LeGeros and Tung, 1983) or substitute for the hydroxyl group which is called the A-type substitution (Elliott *et al.*, 1985). Carbonates poorly fit into the HAp lattice causing lattice strain and accordingly more soluble crystals. This is typically illustrated in the A-type substitution, when the hydroxyl group is substituted by less well-fitting carbonate which weakens the core of the crystal lattice along the *c*-axis.

The weak central core has been suggested to be responsible for the greater solubility of the crystals at the centre (Marshall and Lawless, 1981).

B-type substitution is usually associated with sodium ion replacement for calcium. Therefore, the sodium concentration of the lattice is considered an indirect indicator of carbonate concentration.

Like many other elements, carbonate distribution and concentration vary throughout enamel thickness, with increasing concentration from the surface (1 wt%) towards the inner enamel (4 wt%)(Robinson, 2000).

2.4.2 Fluoride

Fluoride can substitute in the apatite crystal either as F^- or $CO_3F_3^-$ by filling hydroxyl vacancies or by substituting the hydroxyl ion (Elliott, 1994). When fluoride ion (ionic radius ≈ 1.36Å) substitutes the hydroxyl ion (ionic radius, 1.40Å) on the *c*-axis it causes a reduction in the crystal volume and the lattice becomes more dense which reduces the crystal dissolution constant and enhances its chemical stability (Aoba, 1997). This substitution involves reduction at both the *a* and the *c*-axis (Kay et al., 1964) and reduces the lattice energy bringing more stability to the lattice (Robinson *et al.*, 1995b).

Unlike carbonate, fluoride shows a higher distribution concentration at the outer enamel surface than the inner enamel(Robinson, 2000).

2.4.3 Magnesium

Magnesium is considered a principal minor constituent of biological apatite. There is uncertainty about the incorporation of magnesium in the HAp lattice (Verbeeck, 1986). It has been reported that magnesium can substitute for calcium ions. However this is a very minimal substitution as only a small amount of

magnesium can be accommodated in the HAp crystal lattice (0.3 wt%) (Featherstone *et al.*, 1983b). Another possibility is that magnesium adheres to the crystal surface layer, either as an adsorbed element on the surface or attached loosely in the hydration layer, rather than being incorporated in the structure (Robinson, 2000). Like carbonates, magnesium shows higher concentrations in the inner enamel layer than in the outer surface (Robinson, 2000).

In conclusion, the topic of structure, chemistry and properties of enamel apatite has received a lot of attention from researchers and lots of fundamental work has been published in this area including published textbooks and review papers such as LeGeros (1991), Ten Cate and Featherstone (1991), Johnsson and Nancollas (1992), Elliott (1994), Shellis and Duckworth (1994) and Aoba (1997). It is particularly important to remember that dental enamel mineral contains not only HAp, but an apatite like structure with a wide variety of substitutes that might alter its physico-chemical properties. Zinc, strontium and copper as divalent metal cations are of special interest to this thesis. Their effect will be discussed in details in Chapter 5, 6 and 7 respectively.

2.5 Hydroxyapatite as a model system for dental enamel

Hydroxyapatite is commonly used as laboratory and, to a lesser extent, mathematical model for dental enamel mineral. However, there is still some controversy as to whether HAp can be used as a good representative of dental enamel mineral.

In this section a brief over view of the similarities and differences between HAp and dental enamel is discussed.

1. Crystal lattice parameter: the mineral of enamel has a different crystal lattice parameter (spacing) from HAp. According to crystallographic studies for HAp, a = 9.418 Å and c = 6.881 Å, while for dental enamel, a = 9.455 Å and c = 6.881 Å (Wilson *et al.*, 1999).
2. Chemical composition: HAp has a constant composition that can be summarised in the chemical formula $Ca_{10}(PO_4)_6(OH)_2$ while dental enamel has variable chemical composition with various impurities such as CO_3^{2-} 2 to 4 wt% replacing PO_4^{3-} and Na^+ 0.25 to 0.9 wt% (Section 2.3).
3. Density: due to the difference in chemical composition, enamel has a lower mineral density (2.99-3.02 g/cm^3) compared to the mineral density of HAp (3.15 g/cm^3).
4. Porosity: HAp typically has higher pores percentage, but pores are more evenly sized and distributed, while dental enamel has overall lower porosity. Pores size and distribution not only varies in dental enamel of different teeth, they even vary between different areas in the same tooth.

Even though HAp and dental enamel minerals differ in some aspects, HAp is still generally accepted as representative of dental enamel, and presents several significant advantages. From the practical point of view HAp is considered convenient to use as it is easier to obtain and requires no ethical approval. Further, HAp has a well-defined chemical composition and density when compared to enamel minerals. It also has the advantage of composition adaptability as it can be chemically adapted by the addition of impurities such as fluoride or sodium at precise levels of concentration, if needed, to mimic enamel minerals. Synthetic sintered HAp allows the use of larger size samples and gives reliable measurement repeatability due to its uniformity in chemical composition,

while for enamel minerals the repeatability of measurements is unreliable due to structural variations. So in conclusion, HAp aggregates are not expected to react identically to dental enamel as they are much more structurally and chemically homogeneous than enamel, but are believed to exhibit very similar dissolution kinetics and they can be used as a model for enamel in attempts to understand *in vivo* caries or erosion formation (Shellis *et al.*, 2010).

CHAPTER 3

Dental Enamel Caries and Erosion

3.1 Dental enamel caries

3.1.1 Introduction to dental enamel caries

Dental caries is the most common chronic disease affecting children (Filstrup *et al.*, 2003). It is five times more common than asthma (Donahue *et al.*, 2005). Its distribution varies between countries, regions within the same country as well as social class and ethnic groups (Petersen, 2005, Christensen *et al.*, 2010). According to the National Survey of Children's Health in the United Kingdom, almost 40% of the 5 years old children in England and Wales in 2003 had dental caries (Pitts *et al.*, 2007).

Although the prevalence and extent of dental caries have fallen greatly in the UK between the late 1970s and the current day, as well as in many other countries such as Nordic countries and Switzerland, yet this decline seems to have slowed down, and dental caries continues to be considered a significant problem.

According to the WHO 2003 report on oral health, caries remains a problem despite great improvements in the dental public health (Petersen and Yamamoto, 2005). The report showed that caries has declined in many developed countries from a decayed, missing and filled permanent teeth (DMFT) level of 4.5 to 2.5 for children aged 12 years between the years 1980 and 1998, however, over the same

period of time the DMFT of the same age group increased from 1.5 to 2.5 in developing countries. This is alarming considering that most of our world today is made up of developing countries (Sgan-Cohen and Mann, 2007).

Therefore, dental caries is still considered a problem worth manageing particularly through well-planned comprehensive dental health promotion and preventive strategies.

3.1.2 Aetiology of dental caries

For as long as the science of dentistry has existed, there have been theories about the causes of dental caries. However, today all experts in cariology generally agree that dental caries is a complicated multifactorial process that leads to destruction of dental hard tissue and that it is a localised destruction of dental hard tissue caused by acids produced by dental plaque bacteria (Fejerskov *et al.*, 2008). It can take place on any tooth surface in the oral cavity when dental plaque is left to accumulate for enough time to allow its bacteria to ferment the dietary carbohydrate (Kidd and Fejerskov, 2004). Bacterial carbohydrate fermentation results in acid production, such as, lactic acid, acetic acid, etc, which reduces the dental plaque pH below 5.0 within 1-3 minutes (Kidd, 2005). Exposure of tooth surface to repeated attacks of low pH may result in demineralisation. However, when the acid produced in dental plaque is neutralised by saliva, the pH increases again and minerals may be regained and remineralisation occur.

The cumulative result of the de- and remineralisation attacks determine whether the tooth will undergo demineralisation or remineralisation (Aoba, 2004). The process of demineralisation or remineralisation takes place frequently during the day leading to cavitation, repair or a maintenance state.

However dental caries is not only an infectious disease induced by diet. It is a complicated multifactorial process with multiple factors affecting the initiation and progression of the disease. There are factors that directly contribute to caries development. These include a host, dietary substrate, bacteria and sufficient time frame. Oral environmental factors include, saliva buffering capacity, salivary composition and flow rate, sugar consumption, frequency and sugar clearance rate. Also important are plaque pH, types of microbial species, and the use of fissure sealant, antimicrobial agents and fluoride. Finally, relevant personal factors include the level of education, behaviour and attitude towards oral care, sociodemographic status and many others (Harris *et al.*, 2004).

Dental caries is recognised as a preventable disease. Furthermore, it is known that cavitation is quite a late stage in the disease development and that before cavitation; the progress of the disease may be arrested or reversed if a favourable oral environment is achieved.

3.1.3 Histology and chemical changes in enamel caries

Silverstone (1981) has studied the histological changes of enamel in carious lesions and divided them into four zones, starting from the outer enamel surface layer to the enamel dentine junction (EDJ). These four zones are: surface, body of the lesion (25-50%), dark (5-10%) and translucent (Figure 3.1).

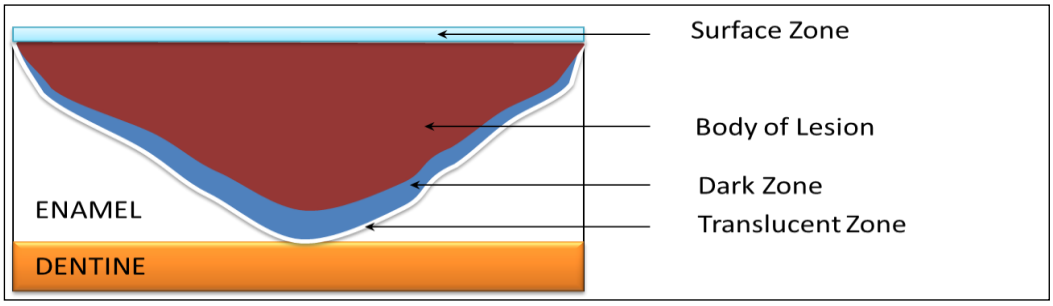

FIGURE 3.1 Schematic for enamel caries zones as classified by Silverstone (1981)

1. Surface Zone

The surface zone is the outermost zone, usually about 40 µm thick. During the process of dental caries, acids produced by bacteria diffuse into enamel and decrease its pH which starts the demineralisation process. As a result of the decrease in pH and the protonation of some phosphates (PO_4^{3-}) to hydrogen phosphates (HPO_4^{2-}), apatite crystals become unstable. This step is described as the formation of an active demineralisation site. As a result of the redistribution of charges and instability in the apatite crystal bonds, calcium is released. The release of calcium and protonation of phosphates, due to the drop in pH at the tooth outer surface, will form an undersaturated layer, a principal requirement for mineral dissolution.

As the demineralisation process continues, more acids will continue to diffuse inwards and more ions will be released and diffuse outwards. This outward and inward exchange is a key model in describing enamel caries-subsurface demineralisation. According to this theory, demineralisation starts at the subsurface layer while the outer surface layer remains intact (Silverstone, 1981).The subsurface demineralisation characteristic of dental enamel are cited in the literature to be due to irregularities in structure, the organic matrix in dental enamel, or the presence of a dental plaque layer (Isaac *et al.*, 1958, Zahradnik and Moreno, 1977). However, some *in vitro* studies on HAp aggregates have demonstrated subsurface demineralisation. This indicates that subsurface demineralisation is a characteristic of HAp rather than dental enamel (Mortimer and Tranter, 1971, Zahradnik *et al.*, 1976, Anderson and Elliott, 1985). Some models have been suggested in the literature to explain the mechanism that relates inward and outward flux of ions across the surface zone, such as the coupled diffusion model. The surface zone can

be considered as the relatively intact layer of enamel with mineral mass loss of less than 1%.

2. Translucent Zone

The enamel in this zone has more porosity and appears translucent when embedded with Canada balsam and looked at under a light microscope (Silverstone, 1981). This zone shows a 10-fold increase in pore volume when compared to intact enamel and accounts for approximately 1% of mineral loss, mostly mineral that is rich in carbonate and magnesium (Robinson, 2000).

3. Dark Zone

If a tooth section is put into quinoline and viewed with polarised light the body of the lesion will be outlined by a dark area (dark zone) (Kidd, 2005). The dark zone looks dark because quinoline, being a large molecule, cannot get into the little holes, which therefore remain filled with air giving a dark appearance while the body of lesion which looks dark in water now looks translucent with quinoline (Ten Cate, 1998).

The dark zone is similar to the translucent zone as they both show porosity and mineral loss, yet the dark zone shows mineral loss of about 5-10% and in addition to the large pores seen in the translucent zone small pores are seen in the dark zone (Robinson, 2000). The small pores in the dark zone show partial reversal of carious lesions when exposed to saliva or synthetic calcifying solution in experiments. Some studies (Crabb, 1966b, Crabb, 1966a, Silverstone, 1966, Clarkson *et al.*, 1984, Robinson *et al.*, 1990) have shown that when artificial caries-like lesions are exposed to saliva or synthetic calcifying solution, there is reduction in the pore volume throughout the whole lesion. This suggests that the dark zone represents a zone

where both demineralisation and remineralisation take place. This reflects the dynamic nature of the caries process which involves episodes of demineralisation and remineralisation simultaneously (Robinson, 2000).

Therefore, it has been suggested that the dark zone represent a dynamic stage between demineralisation and remineralisation according to the surrounding environment (Silverstone, 1981, Robinson *et al.*, 1990, Robinson, 2000).

4. Body of Lesion

The body of the lesion is the main part of the lesion and considered as the final stage of enamel demineralisation. The body of lesion is formed when the pore volume is so great that there is a catastrophic collapse of the enamel structure, followed by the collapse of the outer enamel surface layer (Robinson *et al.*, 1983, Shellis *et al.*, 1993).

3.1.4 Methods of dental caries detection

Dental caries diagnosis is mostly carried out using visual examination of the tooth surface with or without the use of a dental probe. This method of examination is well established, however studies have shown that almost half of occlusal carious lesions can be missed using this method of examination.

The use of the dental probe (explorer) in caries detection is controversial. In the USA it is considered that a sharp explorer tip should be used to detect any softness in the surface, while in Europe this practice is believed to add little benefit to caries detection. On the contrary, it might cause iatrogenic damage to the enamel surface and facilitate caries progression or initiation.

Proximal caries detection in posterior teeth can be challenging, especially in cases of heavy contact. The use of dental wedges, orthodontic separators or trans-

illumination might be of help. The use of dental radiographs is the method of choice by most dentists. However, radiographs are not helpful in detecting caries at early stages of development. In dental arches with crowding or rotated teeth the use of bite wings become of very little value, so accordingly the use of radiographs become more helpful in detecting advanced dentinal lesions.

Nowadays, a new caries detection and scoring system has been introduced, the International Caries Detection and Assessment System (ICDAS) (Ismail *et al.*, 2007). It is a clinical scoring system that can be used for dental education, clinical practice, research, and epidemiology (Pitts, 2004). It is designed to be based on a better quality of collective information to achieve appropriate diagnosis, prognosis, and clinical management at both the individual and public health levels. ICDAS has the advantage of enabling personalisation of caries management for each case independently, which helps in providing better and longer term results (Ismail *et al.*, 2008).

3.1.5 Prevalence of dental caries

In early 1900 the first statistics on dental decay were published (Yates, 1949, Marthaler, 2004). That was approximately the time when the first university dental faculties were training dental students. The number of these early statistics was very low and they are difficult to interpret. Around the 1950s, indices and methods of conducting surveys of dental diseases were developed, and in the 1960s many epidemiological studies started.

Until the 1960s the published surveys suggested that the prevalence of dental caries in children of Western European countries was high with an average of more

than 5 DMFT for 12 year old children and 10 DMFT for 15 year old children (Marthaler, 2004).

Between the 1970s and the 1980s there was a remarkable decline in the prevalence of dental decay in children in many industrialised countries. This reduction is mainly due to the development and the wide spread of use of fluoridated tooth pastes (Downer *et al.*, 1985, Downer, 1993).

During the decades since then, consensus from around the world shows that dental caries has declined significantly. In 1985, FDI data demonstrated caries declined particularly in nine countries: Denmark, Finland, Norway, Sweden, Australia, the Netherlands, New Zealand, the United Kingdom and the USA (Marthaler, 2004). In 12 year old children in the Netherlands the decrease in dental caries showed the average DMFT decreased steadily from eight in 1965 to one in 1993. Similarly, most of the European data showed that caries prevalence in children continued to decline until the 1990s (Downer *et al.*, 1985). Although the last National Children's Dental Health Survey in the UK in 2003 showed that overall dental caries in children continued to decline over the last decade yet there was an observation of an increase in caries prevalence among particular groups such as the lower social classes and migrants (Harker and Morris, 2005). This is shown in a Swedish study, with Turkish immigrant children having more caries than Swedish children both in the primary and permanent teeth (Mejàre and Mjönes, 1989). However, children born in Turkey had more caries in the primary dentition than those born in Sweden. Turkish immigrant children therefore constitute a high risk group for caries and need supervision early after immigration. Also, increasing immigration has been identified as a new factor, leading to increases in the overall

dental caries prevalence rate in Switzerland, given that migrants form 20% of Swiss residents.

Most recent studies have reported that dental caries is increasing particularly in developing countries. This is alarming given that most of today's world population is made of developing countries.

The National Oral Health Survey in the Philippines reported an alarming 97.1% of 6 year old with dental caries and 84.7% with symptoms of dental infection. The overall prevalence of dental caries among 6-12 year old school children was 92.3% (Carino *et al.,* 2003). In Mexico, the prevalence of dental caries increased by more than 20% among children in just over one year from 14.2% to 34.7% in fewer than 18 months. An epidemiological survey in Sao Paulo, Brazil showed that the prevalence of dental caries in permanent teeth among 12 year old children was 53.6% (Gomes *et al.*, 2004). In Palestine, the DMFT score was 6.5 in an oral health survey (Bagramian *et al.,* 2009). In Saudi Arabia there is lack of national oral health survey. However local and regional surveys reported a high DMFT score in 12 years old children. In Riyadh area for example the mean DMFT was 5.06 (AlDosari *et al.*, 2004). Another study conducted in the western region (Jeddah) reported a mean DMFT of 5.71(Alamoudi *et al.*, 1996).

In summary dental caries remains a major health concern worldwide and an action is needed to control the spread of this problem.

3.2 Dental erosion

3.2.1 Introduction to dental erosion

Dentists have been aware of the phenomenon of dental hard tissue loss that is not attributed to dental caries but for years only little has been done about it. Recently, such dental hard tissue loss has been increasingly seen in the younger population (Welbury *et al.*, 2005). The phenomenon of tooth wear can be classified as attrition, abrasion or erosion. Attrition is loss of the tooth hard surface due to tooth to tooth contact (bruxism). Abrasion is physical wear due to tooth surface contact against hard surfaces such as a faulty brushing technique with a hard toothbrush or the habit of nail biting or biting against a pen or pencil while thinking. Erosion can be defined as the loss of dental hard tissue due to acids without the involvement of bacteria (Figure 3.2).

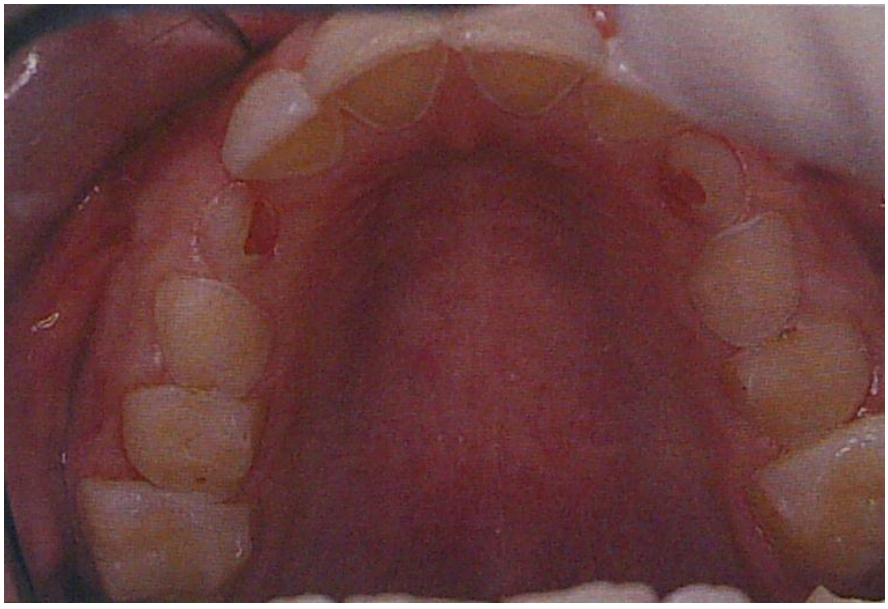

FIGURE 3.2 Upper arch of child with gastro-oesophageal reflux showing generalised erosion affecting maxillary teeth particularly on the palatal surface (Welbury *et al.*, 2005)

3.2.2 Aetiology of dental erosion

Erosion can be due to intrinsic factors or extrinsic factors. For example the pH of stomach acid can reach below 1.0 and therefore any regurgitation or vomiting is harmful to the teeth and causes more severe destruction than that caused by other dietary acids (Bartlett and Coward, 2001). Gastro-intestinal tract disorders or eating disorders (e.g. bulimia and anorexia nervosa) are the most common causes of dental erosion by gastric acid (Meurman *et al.*, 1994, Schroeder *et al.*, 1995). However, extrinsic factors are considered the most common cause of dental erosion. Extrinsic factors are most commonly in the form of acidic foods or drinks such as fruit, fruit juices, carbonated drinks, and sports drinks. Many of these acids are usually unnoticed by their consumers and their effect is underestimated (Gandara and Truelove, 1999). Pure baby fruit juices, for example, have been shown to have a pH value below 5.5. Many of these drinks are given to infants in a feeding bottle and the combination of the prolonged exposure of the tooth to the juice and its highly acidic nature may result in excessive tooth surface loss (Zerob, 2004). Soft drinks represent a major factor of dental erosion through their ability to cause enamel and dentin dissolution, and they are in particular available to all age groups (Nyvad, 1999). In 1995, one study showed that 56-85% of USA school children consumed at least one soft drink per day, from this group 20% consumed four or more servings daily (Grenby, 1996). Although the nature of the acidic food or drink has a strong effect on the degree of dental erosion, it is not the only controlling factor (Amaechi and Higham, 2005).

It was found that the volume, frequency and time of consumption affect the degree of dental erosion as erosive tooth surface loss tends to be higher in cases of high volume of consumption and when the intake is at bed time (Moazzez *et al.*,

2000). Behavioural factors can influence the impact of these dietary acids on the dentition. For example, excessive consumption of acidic food or beverages, or unusual eating and drinking habits such as sipping an acidic drink over a long period of time, will increase the acid challenge to the teeth (Johansson *et al.*, 2004). Other acidic foods and drinks such as wine, and vinegar are potentially erosive (Chaudhry *et al.*, 1997, Piekarz *et al.*, 2008). The most commonly found acids in soft drinks are; citric, phosphoric, malic and tartaric acids (Grenby, 1996). A study of sour sweets, which are popular among children came to an important conclusion: that all the sour sweets tested were found to be erosive, and some of them were even more erosive than orange juice (Chu *et al.*, 2010). This is important to know, especially for paediatricians and paediatric dentists who are concerned about children's dietary habits and diet analysis (Chadwick, 2008, Brand *et al.*, 2009, Wagoner *et al.*, 2009). Oral hygiene products such as toothpastes, and some low pH medications, like vitamin C tablets, have been reported to show erosive potential (Lussi, 2006). Environmental acids are also potential risk factors. Acidic fumes such as sulfuric and hydrochloric acid fumes in some working places have been reported to show erosive potential (Petersen and Gormsen, 1991).

Dental erosion can be clinically observed at early stages of development as a loss of surface contour with a shiny, glass like appearance (Asher and Read, 1987). In the past it was thought that erosion involved the total loss and destruction of the whole enamel thickness while some studies have demonstrated signs of subsurface demineralisation (Meurman and Gate, 1996). Therefore the chemical processes of dental enamel erosion and dental enamel caries are quite similar, apart from the source of acids and the lack of dark zone. The absence of dark zone might be due to the very low pH in the case of erosion. Lussi and Featherstone have studied the

chemistry of dental erosion (Lussi, 2006). A key factor in dental erosion is that it takes place in a highly acidic environment and the mineral loss can be a result of simple interaction with hydrogen ions such as in the case of acetic acid.

$$CH_3COOH \leftrightarrow CH_3COO^- + H^+ \quad (3.1)$$

However, it is more likely that erosion is a complex interaction involving the effect of the hydrogen ions as well as the effect of the chelating agent. A typical example of this complex interaction is citric acid. As citric acid dissolves in water, it dissociates into a mixture of hydrogen ions, acid anion (citrate) and non-dissociated acid. Citric acid has the capability of producing three hydrogen ions from each molecule:

$$HOOCCH_2COH(COOH)CH_2COOH \leftrightarrow HOOCCH_2COH(COOH)CH_2COO^- + H^+ \quad (3.2)$$

$$HOOCCH_2COH(COOH)CH_2COO^- \leftrightarrow {}^-OOCCH_2COH(COOH)CH_2COO^- + H^+ \quad (3.3)$$

$${}^-OOCCH_2COH(COOH)CH_2COO^- \leftrightarrow {}^-OOCCH_2COH(COO^-)CH_2COO^- + H^+ \quad (3.4)$$

Citric acid has three pK_a values (pK_{a1}= 3.13, pK_{a2} = 4.76 and pK_{a3}= 6.40). Therefore citric acid can be found in solution in any of the forms showed in the equations above depending on the solution pH (Lussi, 2006).

On one side the hydrogen ion can interact with the enamel surface crystals and combine with phosphate and/or carbonate ions, while on the other hand the chelating agent (citrate) has high affinity to attract calcium ions as illustrated in Figure 3.3.

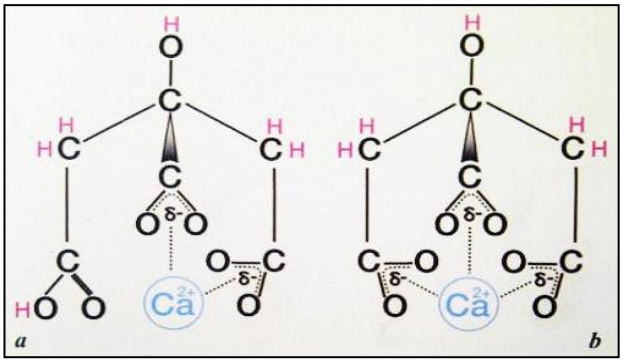

FIGURE 3.3 Schematics of citrate ion where two and three of the hydrogen ions have been lost (*a* and *b* respectively) and calcium ion is attracted (Lussi, 2006)

3.2.3 Prevalence of dental erosion

The prevalence of dental erosion is not well documented since national dental surveys are not commonly conducted worldwide and rarely include measures of erosive tooth wear. In addition, it is often difficult to compare the outcomes of different epidemiological studies on dental erosion due to the use of different examination standards, including scoring systems, samples and groups examined (Lussi, 2006). There is however some evidence that the prevalence of erosion is increasing (Linnett and Seow, 2001, Nunn *et al.*, 2003).

In 1993 the UK National Child Dental Health Survey (Nunn *et al.*, 2003) included an assessment of the prevalence of erosion of both primary and permanent incisor teeth. The survey reported that 52% of 5 year old children had erosion on the palatal surface of their primary incisors with 24% advanced approaching the pulp. On the other hand the prevalence of erosion on the palatal surface of permanent incisor was 27% of 15 years old children with 2% showed progression into the pulp (Lussi, 2006). Studies have shown that socio-economic status may also play a role in the prevalence of erosion, which could be due to different eating, drinking and possibly oral hygiene habits. Some studies reported more erosion in higher socio-economic classes other studies have reported different results, so the issue is still controversial (Millward *et al.*, 1994, Al-Dlaigan *et al.*, 2001).

At the present time it is clear that dental erosion is an important condition affecting the dental hard tissues. But there is no clear answer to whether this problem is actually increasing or whether it has remained constant with figures reflecting only an increased awareness of the condition.

3.2.4 Methods of dental erosion detection and assessments

Enamel erosion at its early stages is detected as loss of surface contour with a shiny, glass like appearance which can easily go unnoticed by the patient and/or the dentist. This is followed by a stage of tooth sensitivity and fracture of thinned enamel, particularly thinned incisal edges. As erosion progresses more of the yellowish dentin layer becomes exposed (Figure 3.4).

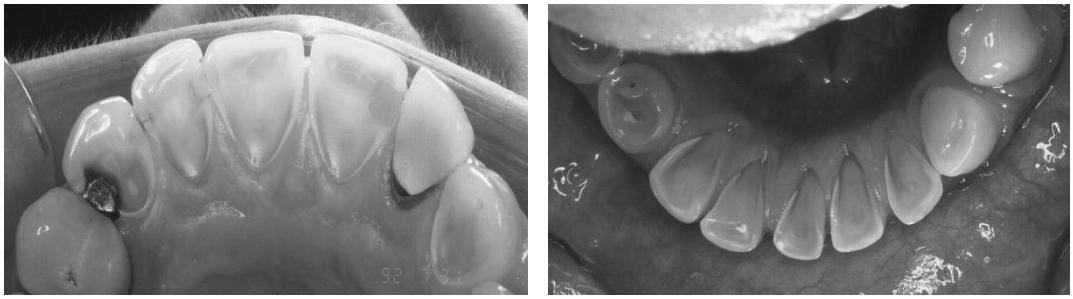

FIGURE 3.4 Dental erosion affecting both maxillary and mandibular teeth particularly palatal and lingual surfaces (Lazarchik and Filler, 1997)

Eroded lesions classically look dished out, hard and smooth (Lazarchik and Filler, 1997). Eccles and Jenkins proposed a set of diagnostic criteria to classify erosion based on its clinical appearance (Table 3.1).

TABLE 3.1 Eccles and Jenkins erosion grading scale (Lazarchik and Filler, 1997)

Rating	Erosion Severity
Grade 0	No involvement of surface
Grade 1	Loss of enamel surface features; no dentin involvement
Grade 2	Exposure of dentin on less than 1/3 of surface
Grade 3	Exposure of dentin on more than 1/3 of surface

There are several other classifications used in the literature. Some are only applicable for adults and not children, such as the Smith and Knight Tooth Wear Index (Smith and Knight, 1984). A modified version of the Smith and Knight Tooth Wear Index that can be used for children was developed by O'Sullivan *et al.* (1998). It is a more detailed index that takes into consideration the site, severity and area affected. A third index, considered more simple and practical was proposed by Aine *et al.* (1993). This index is mainly used for children with gastro-oesophageal reflux but is suitable for adults and children, primary, mixed and permanent dentition. The number of different indices for dental erosion indicates that there is no single index fulfilling all the relevant required criteria. This complicates comparisons between data obtained from different studies.

3.3 Laboratory techniques for assessment of dental hard tissue loss

There are many techniques to assess the loss of dental hard tissue and the softness of the enamel surface. With all the available literature it is now clear that the complex mechanism of dental enamel mineral dissolution might not be fully understood and evaluated by a single technique, but instead would require many techniques with different approaches for full understanding. This section will briefly mention some of the commonly used techniques.

3.3.1 Scanning electron microscopy

Scanning electron microscopy (SEM) is a qualitative measure. It can be used to image the surface changes after erosive attacks. It can be used on both polished and unpolished surfaces after gold sputtering. In enamel, acid attacks due to

immersion of specimens in erosive solutions lead to a surface etching and exposure of enamel prisms to various extents. For SEM, sample preparation would involve drying of the specimen which may cause additional alteration to the eroded surface. Precipitates formed by dissolved enamel minerals may block some enamel surface and SEM might not detect the blocked enamel prisms in such cases.

3.3.2 Environmental scanning electron microscopy (ESEM)

The ESEM has an advantage over the SEM in that it does not require sample preparation, and sample examination can be performed without metal or carbon coating, which reduces the artefacts. Both SEM and ESEM are suitable for use with native surfaces yet both methods provide qualitative assessment and do not provide detailed quantitative information about the eroded surface.

3.3.3 Atomic force microscopy (AFM)

Atomic force microscopy (AFM) also provides qualitative measures. The main application of the AFM is high resolution imaging of different materials. AFM enables imaging of surface topography as well as differences in elasticity. AFM was used in many studies for qualitative evaluation of eroded surfaces. It can also be used to quantitatively measure hardness changes.

3.3.4 Surface profilometry

Surface profilometry involves scanning specimens with a light beam or a contact stylus with diameter of about 2-20 µm. The contact stylus is loaded with a force of a few milliNewtons. With surface profilometry complete surface mapping can be achieved. In cases involving thin and weak enamel surfaces, profilometry might be affected by the tendency of the contact stylus to penetrate this fragile layer.

The laser or white light beam stylus has the advantage of having a higher resolution over the contact stylus and of course beams will not penetrate a fragile surface. Yet it has the disadvantage of producing over shots at sharp edges such as at the bottom of a groove and these will result in artefacts.

3.3.5 Nanoindentation and microindentation

The nanoindentation technique is used to investigate enamel dissolution by measuring the hardness of the enamel surface. It is known that enamel dissolution involves softening of the enamel surface; therefore the surface hardness measurement would represent an indirect method in measuring the degree of erosion or dissolution. Mostly the indenter is a diamond tip which is pressed onto a surface with a given load and duration, resulting in three sided pyramidal indentation. Microindentations in sound enamel have typical indentation depths of micrometers or tens of micrometers, while on the other hand, nanoindentations in sound enamel have sub-micrometer indentation depths, typically hundreds of nanometres. We should not forget the fact that the hardness of the surface measured is affected by many factors like the immediate surrounding material, and material as far away as ten times the diameter of the indentation itself.

3.3.6 Chemical analysis

Chemical analysis methods are based on the principle that dental enamel consists of 34%-39% calcium (dry weight) and 16%-18% phosphorus (Lussi, 2006). Measuring the amount of calcium and/or phosphate dissolved in any solution in which a dental structure has been placed for some time, gives an indirect estimate of the amount of demineralisation that has occurred. A calcium sensitive electrode and

a specific pH for the surrounding environment are required for this technique to work precisely.

Chemical analysis is considered the main competing technique for measuring mineral loss. It has the advantages of being much cheaper than X-ray based techniques and its small size makes it easy to carry out in any laboratory. The chemical method also has the advantage of being able to detect very small mineral loss using unpolished uncoated native tooth samples, yet these methods are applied *in vitro* only (Barbour, 2002).

However it is important to remember that dental enamel dissolution involves the formation of other phases of calcium phosphate complexes and does not simply dissolve to its basic constituents of calcium and phosphate. Therefor the measurement of calcium and/or phosphate in the demineralisation solution may not be an accurate representative of the amount of demineralisation that took place in the dental hard structure. Also an intensive solution preparation is required to allow the measurement of calcium and phosphate with a minimal amount of solution no less than 100µl.

3.3.7 Microradiography

Microradiography is a method of special interest to this thesis as it is the technique to be used in all the experiments in this thesis. Therefore, it is discussed in details in Chapter 9.

The selection of SMR as the technique of choice for the experimental work in this thesis was based on that SMR was initially developed by Jim Elliott in QMUL around 1980 and modified by JIM Elliott and Paul Anderson around 1985 giving the Dental Physical Science Department at QMUL a worldwide reputation in SMR technology with pioneers working in this field.

CHAPTER 4

Calcium Apatites Dissolution Models

4.1 Introduction

There have been many proposed dissolution models for HAp dissolution (Dorozhkin, 2002). Each of these models has its own strengths, weaknesses and limitations. These models provide important information with regards to factors affecting HAp dissolution. These factors can be classified into:

I: Factors associated with solutions such as pH, composition, saturation, and hydrodynamics

II: Factors associated with bulk solid such as chemical composition, solubility and particle size

III: Factors associated with the surface such as defects, absorbed ions, and phase transformation

In this chapter some of the previously published models for calcium apatite dissolution models will be discussed in an attempt to highlight the part of the dissolution mechanism that each model focuses on.

4.1.1 Diffusion controlled and surface controlled models

These types of models are concerned with the study of the dissolution reaction controlling step, and the transport rates of chemical reagents (H^+ and anions of acids) from solution to the HAp crystal surface and the transport of the

dissolution products away from the HAp crystal surface to the bulk solution ($Ca^{2+}$and PO_4^{3-}). Both mechanisms are concerned with the rate controlling mechanism (driving force), which is the concentration gradient with in the Nernst diffusion layer in the case of the diffusion model or the gradient of the ionic chemical potential at the apatite-solution interface in the case of the surface controlled model (Margolis, 1992).

The question of whether enamel dissolution is a surface or diffusion controlled or a combination of both is a question that still has no single defined answer. Some early studies such as those by White and Nancollas (1977) and Higuchi *et al.* (1965) described the dissolution of HAp as a diffusion controlled. Other more recent studies suggest that the dissolution of HAp is not limited purely by diffusion and that surface processes play an important role in controlling the overall kinetics depending on the surrounding conditions (Budz and Nancollas, 1988, Anderson *et al.*, 2004).

4.1.2 Self-inhibition (calcium rich layer formation) model

This model was created following studies of the dissolution kinetics of apatite powders in acidic buffer with solution pH between 3.7 and 6.9, under constant composition (Dorozhkin, 2002, Tang *et al.*, 2003). It was noticed that during the initial period of dissolution (first 2-5 min) the amount of Ca^{2+} released into the bulk of solution was less than the uptake of H^+. This was explained as follows: as the first amount of Ca^{2+} is released into the solution some Ca^{2+} ions probably through coupled diffusion are returned from the solution back to the apatite and adsorb to its surface. This Ca^{2+} rich surface layer acts as a semipermeable ionic membrane (Dorozhkin, 1997b).

As the dissolution process continues, more Ca^{2+} released into the solution increases, and therefore H^+ uptake decreases until electric neutrality is achieved. Therefore, the overall apatite dissolution process decreases with time (Thomann *et al.*, 1990, Mafe *et al.*, 1992).

4.1.3 Stoichiometric/Non-stoichiometric dissolution models

Stoichiometric dissolution is also called congruent dissolution; it is the type of dissolution that occurs when the ions present in the solid dissolve simultaneously with dissolution rates proportional to their molar concentrations in the solid (Dorozhkin, 2002). Non stoichiometric dissolution (incongruent dissolution) occurs when the ions present in the solid dissolve with different dissolution rates from their molar concentrations (Dorozhkin, 2002), resulting in a situation where a surface layer is formed with a chemical composition different from that of the bulk of the solid. It has been reported that in calcium phosphate apatite with a calcium to phosphate ratio between 1.67 to 2, the calcium ions are the first to dissolve while when the calcium to phosphate ratio is less than 1.67, the phosphate ions tend to be the first ions to dissolve. Studies have shown that stoichiometric and non-stoichiometric dissolution of apatite can occur at the same apatite crystal at different stages of dissolution, and that whether the apatite will dissolve stoichiometrically or non-stoichiometrically depends on its chemical composition (Margolis, 1992, Pearce *et al.*, 1995).

4.1.4 Chemical model

The chemical dissolution model for dissolution of HAp was introduced with the concept that HAp unit cell ($Ca_{10}(PO_4)_6(OH)_2$) is unlikely to dissolve by detachment of a single molecule at a time, breaking down to its 18 ionic components.

Instead, it is expected that HAp would dissolve via a series of chemical reactions (Dorozhkin, 1997b, Dorozhkin, 1997a)

Previously, the chemical equation for HAp dissolution was thought to be:

$$Ca_{10}(PO_4)_6(F,OH)_2 + 14H^+ \longrightarrow 10Ca^{2+} + 6H_2PO_4^- + 2HF\ ,\ 2H_2O \quad (4.1)$$

or

$$Ca_{10}(PO_4)_6(F,OH)_2 \longrightarrow 10Ca^{2+} + 6PO_4^{3-} + 2F^-\ ,\ 2OH^- \quad (4.2)$$

The new concept of HAp dissolution is that apatite would pass through four stages of chemical reactions to dissolve (Dorozhkin, 2002).

$$Ca_5(PO_4)_3(F,OH) + H_2O + H^+ \longrightarrow Ca_5(PO_4)_3(H_2O)^+ + HF\ ,\ H_2O \quad (4.3)$$

$$2Ca_5(PO_4)_3(H_2O)^+ \longrightarrow 3Ca_3(PO_4)_2 + Ca^{2+} + 2H_2O \quad (4.4)$$

$$Ca_3(PO_4)_2 + 2\,H^+ \longrightarrow Ca^{2+} + 2CaHPO_4 \quad (4.5)$$

$$CaHPO_4 + H^+ \longrightarrow Ca^{+2} + H_2PO_4 \quad (4.6)$$

During the stages of the dissolution process, different calcium phosphates and biological apatites can be formed with various stoichiometries which control the dissolution process by either facilitating or inhibiting it according to the type of compound being formed.

4.1.5 Nanoscale enamel dissolution model

Traditional understanding of the dissolution process assumes that the dissolution of minerals is spontaneous and continuous and that all the solid phase can be dissolved in under saturated solutions until equilibrium is reached. Wang has lately introduced another vision for the dissolution process (Wang *et al.*, 2005, Wang *et al.*, 2006) in which the reaction is accompanied by the formation of dissolution pits and subsequent displacement of pit steps. Pit formation increases surface

roughness. This roughness leads to an increase in the crystal/solution interfacial area. Subsequent dissolution proceeds through the growth of these pits. However, it has been found that demineralisation reactions actually involve particle size dependent critical conditions of energetic control at the molecular level. Only when the pits are larger than a critical size do they contribute to the reaction, this critical value is of a nanoscale level. This model of dissolution establishes a clear link between the microscopic physics of step dynamics and the bulk behaviour of the crystals during dissolution. It also emphasises the importance of surface energy during dissolution.

4.2 Summary

This brief discussion of the different available models for the study of apatite dissolution, shows that a complete understanding of HAp demineralisation cannot be achieved using a single model and whether the model is concerned with the dissolution process at the solid solution interface, at the solid itself or at the bulk solution external to the dissolving solid. They all explain HAp demineralisation at different sites of the HAp that might be taking place simultaneously and are complementary to each other.

CHAPTER 5

Zinc

5.1 Introduction

Zinc (Zn^{2+}) is a metallic chemical element with an atomic number 30. It has atomic weight 65.39. Its pure metal has a hexagonal close-packed crystal structure. Its melting point is 420ºC and boiling point 907ºC. Its only common oxidation state is 2^{+}.

Zinc is found abundantly in tissues throughout the body. Approximately 60% of total zinc pool is found in muscle tissues, ≈ 30% in bone, ≈ 5% in skin and as a trace element in teeth (section 2.4) (Christianson, 1991, Hambidge, 2000). It is involved in many body functions; it is necessary for normal collagen synthesis, mineralisation of bone, immune system function and proper healing (Thomas and Bishop, 2007) Therefore, it is considered a dietary essential trace element. It can be naturally present in some food such as oysters, lobster, most sea food, red meat, beans and nuts. It is also added to other foods such as cereals and is available as a dietary supplement (Lawler and Klevay, 1984, Hambidge, 2000, Brooks *et al.*, 2005). In addition to standard tablets and capsules, some zinc is added to lozenges and nasal sprays for treatment of the common cold (Weismann *et al.*, 1990, McElroy and Miller, 2002).

The current Recommended Dietary Allowances (RDAs) for zinc are 8 mg/day for a female adult and 11 mg/day for a male adult. For pregnant and lactating women, the RDAs increase up to 12-14 mg/day. The upper margin for the daily intake of zinc should not exceed 40 mg/day (Maret and Sandstead, 2006). Iron supplements might interfere with zinc absorption, therefore taking iron supplements between meals helps reducing their effect on zinc absorption. On the other hand high zinc intake can inhibit copper absorption sometimes causing copper deficiency and associated anaemia (Lawler and Klevay, 1984, Milne *et al.*, 1984). For this reason dietary supplements containing high level of zinc sometimes contain copper as well.

Zinc deficiency is characterised by growth retardation and reduced bone density as zinc stimulates both bone growth and mineralisation as well as regulating osteoclast activities (Yamaguchi *et al.*, 1987, Kishi and Yamaguchi, 1994, Yamaguchi, 1998). Other symptoms include loss of appetite and impaired immune defense. In more severe cases, zinc deficiency, can cause weight loss, taste abnormalities, mental lethargy and delayed wound healing. Hair loss, diarrhoea, delayed sexual maturation, impotence, hypogonadism in males, eye and skin lesions are also not uncommon (Maret and Sandstead, 2006) in severely zinc-deficient patients.

The difficulty of diagnosing zinc deficiency lies in that none of these symptoms is specific and they are often associated with other health conditions. Therefore, a medical examination is necessary to diagnose zinc deficiency (Golden, 1989). Zinc ion levels in the body are difficult to measure using laboratory tests, because of their distribution throughout the body as a component of many proteins and nucleic acids. Plasma and serum zinc level are the most commonly used for testing zinc deficiency. People with gastrointestinal diseases such as Crohn’s disease

and ulcerative colitis are more susceptible to zinc deficiency as gastrointestinal diseases may increase the loss of zinc from the gastrointestinal tract and lower zinc absorption or uptake (Wapnir, 2000).

Zinc toxicity can occur in both acute and chronic forms. Acute adverse effects of high zinc intake include nausea, vomiting, loss of appetite, abdominal cramps, diarrhoea, and headache. Approximately 500 mg zinc can cause acute toxicity while the intake of 150-450 mg zinc per day is enough to cause chronic toxicity (Fosmire, 1990).

5.2 Zinc in the oral cavity

Zinc is naturally present in the oral cavity, in the teeth, saliva and dental plaque. It is one of the trace elements present in teeth and shows a distribution pattern similar to that of fluoride and lead (Robinson *et al.*, 1995a) with higher concentration at the surface structure of dental enamel and lower concentrations at the subsurface. Concentrations of zinc in the subsurface enamel of teeth range from 430 to 2100 parts per million (ppm), with most zinc deposition taking place before tooth eruption (Brudevold *et al.*, 1963, Brudevold *et al.*, 1975). After eruption, zinc concentration at the enamel surface increases further, suggesting incorporation occurring during post eruption exposure to oral fluids. With ageing excessive zinc content is lost over the years in a similar fashion to fluoride (Weatherell *et al.*, 1972, Weatherell *et al.*, 1973).

Zinc concentration analysis through cross sections of the tooth crown show highest zinc concentration in the enamel surface layer and decrease in concentrations towards the dentino-enamel junction. In dentine there is also a gradient in zinc level

with the greatest concentration occurring adjacent to the pulp. The level of zinc in the bulk of the coronal dentine is approximately the same as that in junctional enamel. Near the pulp zinc concentrations increase sharply and approach those of external enamel (Brudevold *et al.*, 1963).

Much research has been conducted to investigate zinc concentrations in saliva. A range of values between 0.01 to 0.2 ppm have been reported (Bales *et al.*, 1990, Oezdemir *et al.*, 1998, Watanabe *et al.*, 2005, Burguera-Pascu *et al.*, 2007). Zinc is also naturally present in dental plaque and researchers have studied zinc concentrations in both dry as well as wet dental plaque. It was found that zinc concentrations in dry plaque ranged between 6 ppm and 31 ppm, which is estimated to be around seven folds more than the reported zinc concentration in wet plaque. The difference in concentrations between the dry and wet plaque is justifiable assuming that drying increases the apparent concentration (Tatevossian, 1978, Agus *et al.*, 1980, Duckworth *et al.*, 1987).

5.3 Effect of zinc on calculus formation

5.3.1 Zinc containing mouthwashes

Mouthwashes containing zinc salts were first reported to reduce dental plaque growth in the early 1970s (Picozzi *et al.*, 1972, Fischman *et al.*, 1973), followed by other studies investigating the effect of zinc containing mouthwashes on dental plaque growth, and calculus formation (Schmid *et al.*, 1974, Compton and Beagrie, 1975, Skjörland *et al.*, 1978),

The role of zinc in calculus formation was confirmed in later work (Harrap *et al.*, 1983) which stressed the importance of the use of high concentrations of zinc

and sufficient frequency of application to suppress calculus formation (Harrap *et al.*, 1984). Prolonged retention of zinc in the mouth is thought to be important for its activity (Bonesvoll and Gjermo, 1978, Afseth *et al.*, 1983a)

After using mouthwashes containing zinc salts, approximately 40% of the amount of the applied zinc is retained in the oral cavity. Its concentration rapidly decreases to a low concentration yet significantly above the zinc baseline in 30 to 60 min. This rapid clearance phase is followed by a slow clearance phase that extends for many hours. The elevated zinc concentration persists in dental plaque for up to 13 hours (h) after application. The incorporation of zinc citrate to mouthwashes was reported to successfully reduce plaque by approximately 8% (Addy *et al.*, 1980), but the clinical significance is unknown.

5.3.2 Zinc containing toothpastes

Toothpastes are more widely used than mouthwashes. Therefore they are considered a more desirable method for delivering an antiplaque agent. Yet the incorporation of antiplaque ingredients into toothpastes presents several difficulties. Toothpastes formulations are quite complex and some of the ingredients may affect activity of the therapeutic agent. For example the availability of chlorhexidine is reported to be affected by anionic detergents usually present in toothpastes (Addy *et al.*, 1992). Also the concentrations of the antiplaque ingredients should be higher than in mouthwashes as the dose of dentifrice used in the mouth is only about 0.1 to 0.2 of that used in the mouthwashes.

Zinc was introduced into toothpastes in the form of zinc citrate. Literature review shows much research done on this. Studies have managed to clearly show that zinc containing toothpastes show the same antiplaque activity as that reported

for zinc in mouthwashes (Fischman *et al.*, 1973, Schmid *et al.*, 1974, Skjörland *et al.*, 1978, Harrap *et al.*, 1983, Harrap *et al.*, 1984).

The mechanism by which zinc affects plaque growth is not clearly established. Zinc might bind to the oral bacterial surface altering its surface potential (Ollsenn and Glantz, 1977) and accordingly might affect bacterial adhesion to teeth (Skjörland *et al.*, 1978). Or, it might be zinc's capability to inhibit acid production by bacteria in plaque (Oppermann and Rölla, 1980, Oppermann *et al.*, 1980, Harrap *et al.*, 1983) by altering the metabolic activity of the oral bacteria hence reducing bacterial growth (Afseth, 1983, Afseth *et al.*, 1983c, Saxton *et al.*, 1986, Hall *et al.*, 2003).

Zinc has been used for a long time for its antiplaque activity as well as to reduce oral malodor. Oral malodor (halitosis) is a condition that originates from bacterial metabolism of proteins from saliva, sloughed oral tissue and food debris leading to the formation of amines, alcohol and particularly volatile sulphur compounds such as hydrogen sulfide (H_2S) (Young *et al.*, 2001, Young *et al.*, 2003). Zinc salts are found to be highly effective in reducing H_2S since they are chemically able to neutralise H_2S as well as acting as antimicrobial agents (Bradshaw *et al.*, 1993).

Oral availability in adequate quantities is a necessary prerequisite of any agent for antiplaque activity *in vivo.* Data demonstrates that approximately 30% of zinc citrate is retained in the oral cavity after brushing (Cummins, 1991). Gilbert and Ingramm (1988) had demonstrated that after brushing with 1gm toothpaste containing zinc, 25 to 38% of the zinc was retained in the oral tissues. Zinc levels in saliva remained significantly above baseline level for at least 2 h after application.

Another study determined a significant increase in salivary zinc levels, highest 5 minutes after brushing with toothpaste containing 0.75% zinc citrate. This was followed up by gradual reduction in zinc concentration, approximately reaching the base line levels after 7 h (Oezdemir *et al.*, 1998).

5.4 Effect of zinc on dental caries

Due to the success of incorporating zinc in toothpastes and mouthwashes and the demonstration of their ability to reduce plaque and calculus, zinc containing toothpastes and mouthwashes have been used in treating and preventing periodontal diseases (Mellberg and Chomicki, 1983).

Since zinc incorporation in toothpastes has extended to involve its incorporation in some fluoridated toothpastes, more research work was needed to determine if zinc might affect fluoride deposition in dental enamel and whether its incorporation in fluoridated toothpastes showed a synergistic/ antagonist or no effect.

Mellberg and Chomicki (1983) suggested that zinc citrate inhibits fluoride uptake by artificial enamel caries and gave two explanations: either the inhibition is due to zinc reaction with monofluorophosphate (MFP) ions in the solution inhibiting its reaction with enamel, or most likely there is reaction of zinc with the phosphate ions in the enamel lesion (caries) which leads to the formation of insoluble zinc phosphate complex. Zinc phosphate complex coats the HAp surface, precipitates and blocks the diffusion of fluoride into the carious sites.

On the other hand more recent *in vivo* studies have demonstrated a reduction in enamel demineralisation with the use of zinc containing fluoride toothpastes (Lynch, 2011). However the demineralisation reduction could not be entirely due to the interaction of zinc with HAp as it may, to a degree, be the result of the

antimicrobial effect of zinc (Ten Cate, 1993, Churchley *et al.*, 2011). Further research is recommended to study the direct and individual effect of Zn^{2+} on enamel demineralisation.

5.5 Effect of zinc on dental erosion

As mentioned before, most of the research done on zinc has concentrated on zinc effects on dental plaque and calculus formation which is indirectly linked to, management of oral malodor, and to a lesser extent on zinc anti-caries effects.

A review of the literature on the effect of zinc on dental erosion did not reveal any work done on the use of zinc as a preventive aspect or in cases of dental erosion. In fact many publications have studied the erosive potential of zinc fumes (zinc oxide, zinc chloride) specially on industrial workers (Remun *et al.*, 1982).

Zinc's ability to inhibit apatite dissolution under acidic erosive like conditions and the potential usefulness of zinc as an ingredient in toothpastes for erosion prevention purposes is a subject that has been overlooked and requires further research.

5.6 Effect of zinc on hydroxyapatite dissolution

The exact mechanism by which the divalent cations reduced enamel dissolution has been an issue of controversy as ion uptake by HAp from solution can occur via two methods.

Method 1: As HAp dissolves in the acidic environment, phosphates are released. Phosphates can react with metal cations in the solution to form new low soluble

divalent metal (Me) phosphate crystals with an apatitic structure that precipitates according to the Equation 5.1 and 5.2:

$$Ca_{10}(PO_4)_6(OH)_2 + 14H^+ \longrightarrow 10Ca_2^+ + 6H_2PO_4^- + 2H_2O \quad (5.1)$$

$$10Me_2^+ + 6H_2PO_4^- + 2H_2O \longrightarrow Me_{10}(PO_4)_6(OH)_2 + 14H^+ \quad (5.2)$$

Method 2: This involves some Ca^{2+} being substituted with the divalent metal cation by a diffusion process and adsorbed onto the surface (Equation 5.3)

$$Ca_{10}(PO_4)_6(OH)_2 + xMe^{2+} \longrightarrow (Ca_{10-x})Me_x(PO_4)_6(OH)_2 + xCa^{2+} \quad (5.3)$$

Therefore, we can say that zinc might adsorb on to the HAp surface and block high energy "kink" sites on the outer surface. According to Xu *et al.* the adsorption method occurs at pre equilibrated HAp. Otherwise zinc might be incorporated in the HAp lattice forming new zinc phosphate crystals that precipitate (Xu *et al.*, 1994). At zinc concentrations of ≥1ppm, hopeite ($Zn_3(PO_4)_2.4H_2O$) is formed. Zinc is incorporated into the HAp lattice forming a hopeite layer at the surface (Xu *et al.*, 1994). Hopeite is usually formed at low pH. As the pH increases, other forms of apatitic structures such as scholzite ($CaZn_2(PO_4)_2.2H_2O$) and zincite (ZnO) are formed.

The incorporation of zinc as a divalent metal cation in HAp and in particular its binding site is still not clearly understood. One reason for this uncertainty is the presence of two structurally distinct cation sites Ca1 and Ca2, in the HAp lattice which appear to be suitable for zinc substitution (Figure 5.1). A considerable amount of research has been done on metal ion preference in the HAp structure (Mayer *et al.*, 1994, Terra *et al.*, 2002, Tamm and Peld, 2006, Matsunaga, 2008, Tang *et al.*, 2009, Matsunaga *et al.*, 2010) and still the debate continues regarding the selection criteria influencing how metal ions choose between Ca1 and Ca2 sites.

When Zn^{2+} occupies the Ca2 site, the result is an overall shrinkage and more stability in the crystal. The local HAp lattice shrinkage brings the ZnO_4 tetrahedron and the channel OH^- groups in the HAp lattice closer, minimising the effect on the adjacent Ca1 sites and avoiding any disruption of the framework (Elliott, 1994).

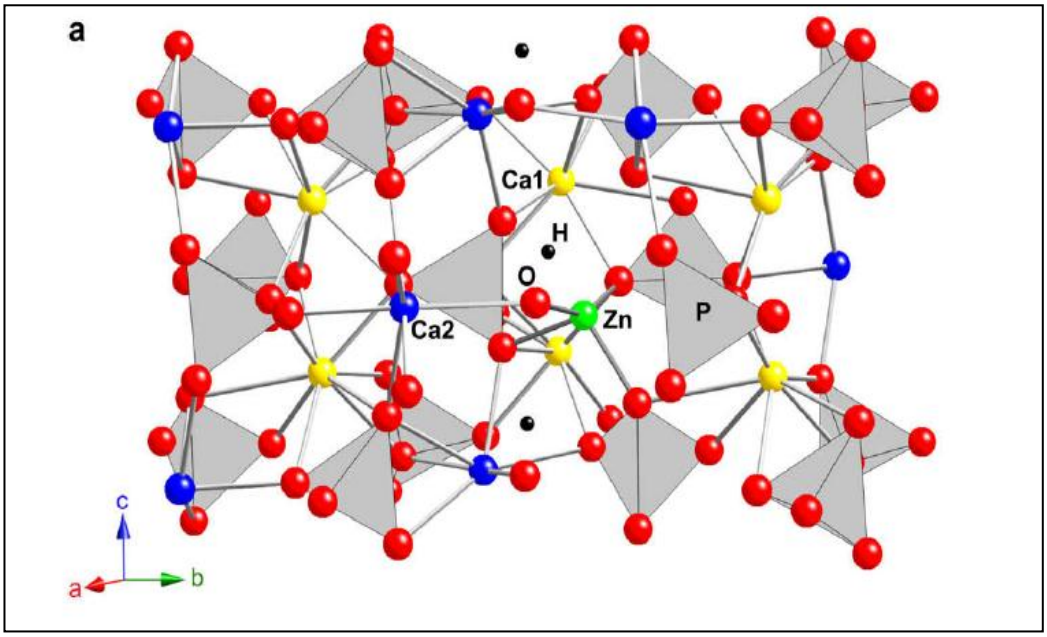

FIGURE 5.1 Schematic figure for the structure of Zn-doped HAp, where yellow, blue, red, black, green and gray refer to calcium1 site,calcium2 site,oxygen, hydrogen, zinc and phosphate groups respectively (Tang *et al.*, 2009)

Ca2 site preference is in case of pure HAp, but in biological apatite when there is an especially high concentration of carbonate (CO_3^{2-}) and which also may be Ca^{2+} deficient which is the case in teeth, this might influence the uptake of Zn^{2+} and its site binding. From reviewing the literature and the mechanism through which Zn^{2+} affects the hydroxyapatite demineralisation rate (RD_{HAp}) it seems that both, adsorption and incorporation are not mutually exclusive, and it is likely that both mechanisms are implicated in reducing HAp solubility in the presence of Zn^{2+}, to a greater or lesser extent.

CHAPTER 6

Strontium

6.1 Introduction:

Strontium (Sr) is one of the most abundant elements on earth, forming about 0.04% of the earth's crust. It is element number 38 of the periodic table of elements, and was first discovered in 1808 near a village in Scotland called Strontian, after which the metal was named (Murray, 1993). It has mass number 87.62, a melting point of 777°C and a boiling point of 1384°C. Strontium can exist in two oxidation states: Sr^{+} and Sr^{2+}. Under normal environmental conditions, only the Sr^{2+}oxidation state is stable enough to be important. Strontium is reactive with water to produce strontium hydroxide and hydrogen gas. Natural strontium is not radioactive and exists in four stable types (or isotopes), each of which can be written as ^{84}Sr, ^{86}Sr, ^{87}Sr, and ^{88}Sr. Rocks, soil, dust, coal, oil, surface and underground water, air, plants, and animals all contain varying amounts of strontium. Strontium concentrations in most materials are a few ppm, yet strontium is considered abundant trace element in seawater, at an average concentration of 8.1 ppm (Angino *et al.*, 1966). The human body contains an average of 320 mg of strontium, almost all of it is in bone, teeth and connective tissue (Schweissing and Grupe, 2003).

Strontium compounds, such as strontium carbonate, are used in making ceramics and glass products, paint, fluorescent lights, medicines, and other products.

Strontium can also exist as radioactive isotopes. ^{90}Sr, or strontium ninety, is the most hazardous of the radioactive isotopes of the chemical element strontium. ^{90}Sr is formed in nuclear reactors or during the explosion of nuclear weapons. The radioactive half-life is the time that it takes for half of a radioactive strontium isotope to give off its radiation and change into a different element. ^{90}Sr has a half-life of 29 years.

Strontium is not an essential trace element, and therefore, there is no established recommended daily intake, no defined level of deficiency and no identified symptoms of strontium toxicity or strontium overdose. It is usually abundant in milk, dairy products, vegetables (such as spinach, lettuce, and carrots), red meat as well as seafood. Therefore the body usually gets the little strontium it needs through diet. However, therapeutic doses of strontium supplements range from 10 mg to 1000 mg and more daily. Such a high dose is usually prescribed for the treatment of osteoporosis, as strontium plays a role in promoting osteoblastic, and inhibiting osteoclastic, activity (Meunier *et al.*, 2004).

Once strontium enters the bloodstream, it is distributed throughout the body, where it can enter and leave the cells quite easily. In the body, strontium behaves very much like calcium. Most of the strontium will accumulate mainly in bone (in adults, strontium mostly attaches to the surfaces of bones). Strontium is eliminated from the body through urine, faeces, and sweat.

6.2 Strontium in bone

Strontium has close chemical similarity to calcium; therefore it behaves in a similar manner to calcium and is involved in the development of tooth and bone at times when calcification is taking place. Strontium can replace calcium to some extent in various situations in the body, such as replacing a proportion of calcium in the hydroxyapatite lattice in bone and teeth.

The human placenta plays a selective role against strontium transfer from maternal blood to the foetus during early pregnancy; this selective permeability becomes free passage towards the end of pregnancy. The strontium concentration of the foetus is determined entirely by the strontium level in the mother's blood (ingested by the mother during pregnancy).

According to very early studies, strontium deposition in bone can take place through two methods (Likins *et al.*, MacDonald *et al.*, 1951, Glas and Lagergren, 1961).

Method one: involves rapid incorporation of strontium. It refers to the blood strontium deposited by ionic exchange, surface adsorption, and preosseous protein binding.

Method two: involves slow incorporation of strontium into the lattice structure of the bone crystals during their formation.

Method one and method two are both considered valid and we cannot be certain about which of the two strontium deposition processes contributes to the initially formed bone and tooth tissues.

Most recent studies have shown that postnatal and through life, strontium accumulates in bone, in particular where active remodeling is taking place as it stimulates the cell replication of osteoblasts which ultimately increase the rate of

new bone formation and decrease bone resorption by inhibiting osteoclast differentiation and activity (Canalis *et al.*, 1996, Marie *et al.*, 2001, Baron and Tsouderos, 2002). Accordingly strontium has been used in medications for the treatment and prevention of osteoporosis (Bonnelye *et al.*, 2008).

6.3 Strontium in the oral cavity

Strontium in the oral cavity is present in teeth, dental plaque as well as in saliva. There has been considerable research on the role and distribution of trace elements in dental enamel, and these have succeeded in demonstrating the concentration distribution pattern through the dental enamel thickness. While most of the trace elements studied (eg. Zn^{2+}, Cu^{2+}, F^{-}, Fe^{2+}, Mn^{2+}) showed a higher concentration at the outer enamel layer, Sr^{2+} and Mg^{2+} showed a different distribution pattern. Their concentration gradually increased with age and more towards the dentino-enamel junction (Frank *et al.*, 1989, Reitznerová *et al.*, 2000). Human enamel was reported to have mean values between 70 and 286 µg/g of strontium, with a median value of 115 µg/g (Curzon and Cutress, 1983). Less strontium is found in dentine than in enamel (Frostell *et al.*, 1977, Frank *et al.*, 1989). Strontium concentrations on tooth surfaces can be affected by the amount of strontium in the drinking water. The issue of the relationship between Sr^{2+} concentration in water and in the enamel surface and its relation to caries resistance has been a topic of interest since the 1950s (Steadman *et al.*, 1958, Barmes, 1969).

Although Sr^{2+} is not considered one of the elements with significant quantities in dental plaque, it has been detected in plaque fluid from subjects who lived in an area where the strontium level in drinking water ranged between 0.4 and 17.9 mmol/l (Margolis, 1994).

Curzon studied the whole resting saliva for 14 year old school children in different areas with different strontium levels in drinking water in Wisconsin (U.S.A.) and found that strontium concentrations in saliva were weakly related to its concentrations in drinking water. He also reported a negative relationship between strontium concentrations in saliva and caries prevalence (Curzon, 1984).

6.4 Effect of strontium on hydroxyapatite dissolution

The mechanism of Sr^{2+} behaviour in HAp is controversial. Grynpas (1993) thought that the incorporation of Sr^{2+} in the HAp lattice weakened the lattice structure and increased its solubility. Le Geros (1991) also found that the substitution of some Ca^{2+} in calcium apatite by Sr^{2+} causes the crystal lattice to expand and the solubility to increase. This is due to the larger ionic radius of Sr^{2+} (≈1.12Å) than the ionic radius of Ca^{2+} (≈0.99Å) (Kikuchi *et al.*, 1994). On the other hand Christoffersen *et al.* (1997) and Dedhiya *et al.* (1973) found that Sr^{2+} strongly inhibited HAp dissolution due to the formation of a $Ca_3Sr_2(PO_4)_3OH$ surface complex, with up to 40% strontium substitution (Heslop *et al.*, 2003). It was also indicated by Christoffersen *et al.* (1997) that the solubility of strontium-substituted apatite increases with the increase in strontium content. In comparison with results obtained from Verbeeck *et al.* (1981), up to 10% Strontium substituted apatite give a reduction in HAp dissolution (Li *et al.*, 2007).

6.5 Effect of strontium on dental caries

Research work on the effect of strontium on dental caries goes back to as the mid-1960s, when Losee and Adkins showed that post eruption exposure to high

strontium doses had an anti-carious effect. Gedalia and Curzon also studied the effect of prenatal, pre-eruptive and postnatal administered strontium on rat teeth and found that strontium showed an anti-carious effect (Gedalia *et al.*, 1975, Joseph *et al.*, 1977, Ashrafi *et al.*, 1980, Curzon *et al.*, 1982). The pre-and post-eruptive effects of low doses of strontium on dental caries in rats were reported to be associated with the lowest caries level. It was also reported that the uptake of strontium by enamel was significantly correlated with its concentration in diet (Ashrafi *et al.*, 1980).

In 1969 Losee and Adkins (1969) published a 10 year study carried out by the United States Naval Dental Service which involved dental examination of approximately 270,000 naval recruits, and showed only 360 completely caries-free individuals. Out of the 360 caries-free individuals, 36 individuals belonged to one small area near Rossburg, Ohio, where the water had a higher strontium concentration. Likewise, Curzon (1985) conducted studies on 80 young boys from five different communities in Ohio and his results indicated an inverse relationship between caries prevalence and strontium level in drinking water. Curzon *et al.* (1978) also carried out a study on 1313 children aged 12 to 14 years and suggested that strontium in drinking water supplies may be associated with an inhibition of dental caries, particularly during the tooth development period, presumably through incorporation in the apatite crystal. Similar results were obtained from Athanassouli *et al*. (1983) who investigated the possible cariostatic effect of high strontium levels in drinking water and concluded that a low DMFT index was associated with high strontium concentration in drinking water.

Studies on the effects of strontium and fluoride applied together showed that the combination appeared to be more effective in controlling dental caries than

fluoride alone (Featherstone *et al.*, 1983a, Curzon, 1985, Curzon, 1988, Thuy *et al.*, 2008).

6.6 Effect of strontium on dentine hypersensitivity

Strontium containing toothpastes for the treatment of tooth hypersensitivity were introduced to the market around five decades ago. Strontium chloride was introduced commercially as the first tubule occluding agent in the original Sensodyne™ toothpaste (Dowell and Addy, 1983). Due to the reaction that occurs between strontium chloride and fluoride, an insoluble strontium fluoride is formed and that is the rational for calling the original Sensodyne™ product a fluoride free toothpaste. In the 1970s however, strontium chloride was mostly replaced by potassium nitrate. Strontium containing toothpastes were later modified by the incorporation of strontium acetate in place of strontium chloride. Strontium acetate is compatible with fluoride and does not form insoluble precipitates (Cummins, 2010). Eight percent strontium acetate showed rapid and lasting relief of hypersensitivity (Layer and Hughes, 2010). Together 8% strontium acetate with 1040 ppm fluoride are considered the optimal combination available currently on the market for the treatment of tooth hypersensitivity (Hughes *et al.*, 2010, Mason *et al.*, 2010). Three potential mechanisms of action for strontium salts, in terms of treatment for dentine hypersensitivity have been proposed in the literature. First, it is believed that strontium causes some degree of nerve depolarisation. Second, strontium shows chemical similarities to calcium and is capable of replacing lost calcium in the HAp lattice. Third, a layer of fine particles may be deposited by the strontium salts leading to the occlusion of the dentinal tubules.

In conclusion, strontium has proved its effectiveness in the management of tooth hypersensitivity. However, its anti-carious effect is still an area of controversy and more research is needed.

CHAPTER 7

Copper

7.1 Introduction:

Copper (Cu^{2+}) is a highly conductive metal (thermally and electrically). It has atomic number 29 and mass 63.546. Its melting point is 1084.62ºC and its boiling point is 2562ºC. Copper is a transition metal with different oxidation states: Cu^{1+} (cuprous), Cu^{2+} (cupric), Cu^{3+} and Cu^{4+}. The cupric state is found most often in biological systems. The name copper originates from the word Cyprium (means metal of Cyprus) which was later on shortened to Cuprum and this goes back to the Roman Empire when copper was discovered in Cyprus (Dhavalikar, 1997).

Copper is an essential trace element for human metabolism. It is needed for many body functions such as red blood cell synthesis, synthesis of particular enzymes responsible for body metabolism and, energy production, and it also assists in iron absorption (Danks, 1988). Copper also forms part of the enzyme imine oxidase which is involved in collagen crosslinking (Knott and Bailey, 1998).

Copper is abundant in regular diets. The RDA of 2 mg is usually obtained easily from a balanced diet. It is rare to be truly deficient in copper (Klevay, 1998). Copper is found in seafood, organ meat (such as liver, kidney and heart), nuts (such as cashew and almond), soybeans, lentils as well as dried fruits (Klevay, 1998). Humans may also obtain copper inadvertently using copper cookware. When food is

prepared and left to set for an extended period of time in copper cookware, this may allow copper transfer from the cookware surface. One may also get copper unnoticeably from water coming through copper pipes. In many regions of the world, drinking water supplies are constructed from copper tubing. Copper plumbing leaches a small amount of copper into drinking tap water supplies. The WHO has published a document in 2004 about copper in drinking water (WHO, 2004).

Copper deficiency can occur in early life due to insufficient copper in infants exclusively fed a cow's milk diet, because of the low copper content of cow's milk, and its limited absorption into cow's milk (Dorner *et al.*, 1989). In adult life, copper deficiency can arise after burns, chronic diarrhoea, intestinal diseases and pancreatic diseases.

Acute copper toxicity is very rare and mainly restricted to the accidental drinking of solutions of copper nitrate or copper sulphate. However, these solutions and other organic copper salts have a powerful emetics effect and in large doses they are normally rejected by the body by vomiting. Chronic copper poisoning is also very rare in healthy humans as healthy human livers are capable of excreting considerable amount of copper (Turnlund *et al.*, 1990, Turnlund *et al.*, 1998).

7.2 Effect of copper on dental plaque

In 1940, Hanke reported the effect of copper on dental plaque and referred to this as the "destruction of plaque" (Hanke, 1940). Since then, the antimicrobial effect of copper ions on oral bacteria has been a subject of interest for researchers, but the antibacterial effect of ions other than copper, particularly zinc or silver on biofilm formation, appears to have received much more attention.

In vitro studies have reported the antibacterial effect of copper ions against oral bacteria. Due to the variety of oral microorganisms and the variety of tests, the extent of the effect of copper ions has been different across the various studies, and therefore difficult to compare. For example, Maltz and Emilson (1982) studied the effects of various fluoride salts on oral bacteria. They and others reported bactericidal effects of copper fluoride on several species of oral bacteria, and concluded that metal salts of fluoride (SnF_2 and CuF_2) showed a stronger antibacterial effect than non-metal fluoride compounds, which is in accordance with other studies (Andres *et al.*, 1974, Yoon and Berry, 1979, Mayhew and Brown, 1981).

In vivo studies have also shown that copper ions have antibacterial activity. There is a controversy about whether chlorhexidine is more of an efficient antibacterial agent than copper. Waerhaug *et al.* (1984) reported that the antibacterial effect of copper ions was not as noticeable as that of chlorhexidine, which has been reported to be the most effective antibacterial agent for the reduction of plaque and gingivitis (Waerhaug *et al.*, 1984, Ciancio, 1992). However, Waler and Rolla (1982) have studied and compared the effect of chlorhexidine, copper, and silver containing solutions, and found that although chlorhexidine showed the best results it was not significantly different from the effects of copper ions, whereas the efficacy of silver was the least statistically significant. Whether the antimicrobial effect of chlorhexidine is significantly better than that of copper or not, copper has the advantage of causing less staining than chlorhexidine which causes darker and more difficult stains to remove (Mandel, 1988). Also, the taste of both copper and chlorhexidine mouthwashes is a problem, but copper containing mouthwash is considered to be more acceptable than chlorhexidine mouthwashes (Waerhaug *et al.*,

1984). Thus, copper containing products show promise for future use in the treatment of oral infections and deserve further study (Mandel, 1988).

7.3 Effect of copper on dental caries

As discussed in Section 7.2, studies have shown that copper salts exhibit an inhibitory effect on bacterial dental plaque. Studies on the ability of copper to inhibit dental caries initiation and progression go back as far as the 1950s when it was reported that copper has an inhibitory effect on dental caries in hamsters (Hein, 1953). Later Afseth *et al.* studies investigated the cariostatic effect of copper on rats and on human dental enamel (Afseth *et al.*, 1980, Afseth *et al.*, 1983b, Afseth *et al.*, 1984a, Afseth *et al.*, 1984b).

Both *in vivo* and *in vitro* studies, showed copper as a potent cariostatic agent. Its cariostatic property is demonstrated through its ability to reduce the number of bacteria in dental plaque as well as decrease smooth surface dental caries scores (Oppermann and Johansen, 1980, Afseth *et al.*, 1983b, Mandel, 1988, Davey and Embery, 1992).

Afseth *et al.* studied the effects of copper sulphate (in the form of a mouthwash), fluoride (in the form of fluoridated water), and the combination of both, on dental caries in rats. They noticed that the group receiving topical Cu^{2+} treatment together with fluoride in the drinking water gave the lowest smooth surface caries score and the lowest number of bacteria in dental plaque. These results were comparable to results found in previous studies (Larson and Amsbaugh, 1975, Afseth *et al.*, 1984a).

According to the literature, copper exerts its cariostatic function through two mechanisms. First, is the antibacterial action of copper on dental plaque bacteria (bactericidal/bacteriostatic effect). Copper has the ability to a) limit bacterial growth, by inhibiting glycolysis through oxidation of thiol groups in the enzymes involved in the glycolysis process, leading to decreased acid production by bacteria, and b) stopping important metabolic reactions in plaque bacteria such as the bacterial ability to convert urea to ammonia (Maltz and Emilson, 1982, Afseth *et al.*, 1984b, Rosalen *et al.*, 1996a, Rosalen *et al.*, 1996b). Second is the ability of copper to form copper phosphate crystals on the tooth surface that protect the enamel and increase its resistance to acidic mediated dissolution. However, very few studies have been carried out to verify this second mechanism (Koulourides *et al.*, 1968, Rosalen *et al.*, 1996a, Brookes *et al.*, 2003, Abdullah *et al.*, 2006) and this is one of the aims of this thesis.

7.4 Effect of copper on enamel demineralisation

A literature review of the effects of copper on dental enamel demineralisation shows that most research has been done to explore its cariostatic effects due to its bactericidal properties. Only a few studies have been carried out to examine the direct effect of Cu^{2+} on the acid mediated dissolution mechanism of dental enamel.

Afseth *et al.* studied the effect of copper applied topically or in drinking water on the caries experience in rats. They reported that 1.0 mmol/l Cu^{2+} in drinking water and 5.0 mmol/l Cu^{2+}, topically applied, inhibited caries formation in a rat model. They also reported that although the *Streptococcus mutans* count was lowered when copper was delivered topically or in drinking water, the *Streptococcus*

mutans count was only statistically significantly reduced when copper was delivered in drinking water. This shows that copper may have a direct effect on enamel demineralisation, which Afseth *et al.* explained with reference to the ability of Cu^{2+} to electrostatically bind to various acid groups in dental plaque and stay retained in dental plaque for a long duration (Afseth *et al.*, 1984a, Afseth *et al.*, 1984b).

Brookes *et al*. (2003) studied the inhibitory effect of copper in the form of copper sulphate under erosion-like conditions using acetic acid pH 3.2. They found that copper decreased enamel dissolution, and by studying a range of copper concentrations, they found that the peak of the reduction in enamel dissolution was achieved by 90 ppm Cu^{2+}, whereas higher copper concentrations did not show a statistically significant reduction in enamel dissolution rate.

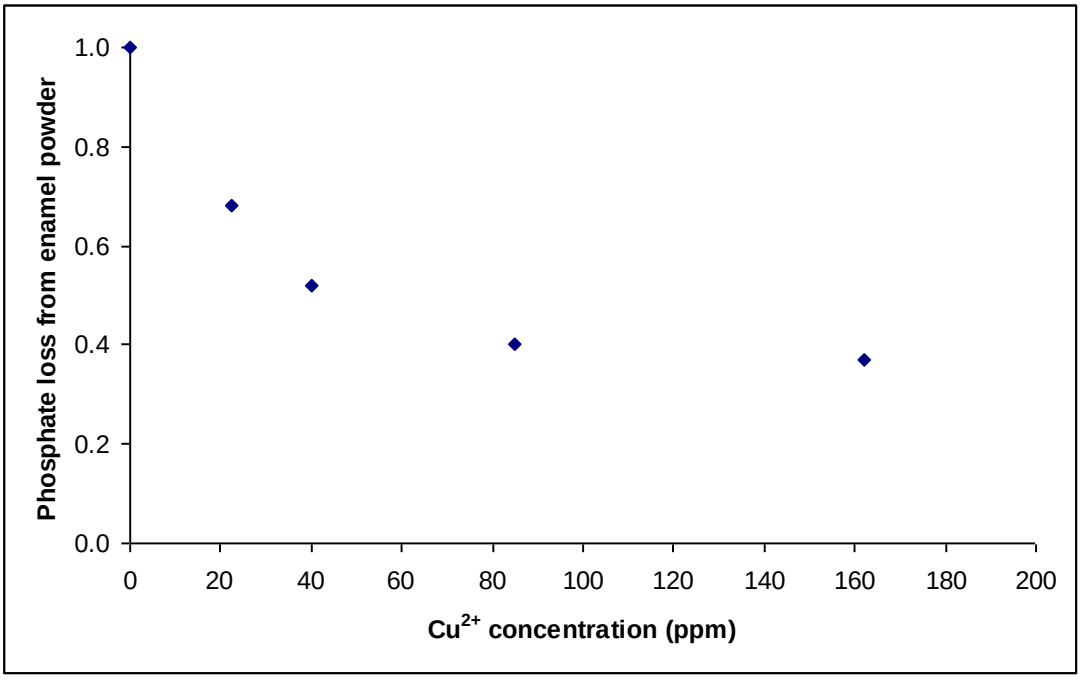

FIGURE 7.1 The effect of Cu^{2+} concentration on the phosphate released form powdered human enamel (Brookes *et al.*, 2003) after the conversion of Cu^{2+} concentrations from mmol/L to ppm

The same group measured the molar calcium to phosphate ratio in the demineralisation solution in the presence of Cu^{2+}, it was found that there is a higher calcium to phosphate ratio in the demineralisation solution compared to the calcium

to phosphate ratio in enamel (≈1.88 compared and ≈1.55, respectively) suggesting that copper ions replace calcium ions, forming copper phosphate crystals on the enamel surface. This has a more stable structure which has a lower dissolution rate when exposed to an acidic attack (Abdullah *et al.*, 2006). They concluded that the Cu^{2+} inhibition effect of enamel demineralisation may be a surface controlled mechanism rather than a change in structural phase (Brookes *et al.*, 2003) and might even occur at the level of the Stern layer as discussed by Mafe *et al.* (1992).

In conclusion, this literature review shows that Cu^{2+} has potential usefulness as a cariostatic agent both as an antimicrobial agent against dental plaque bacteria causing caries and periodontal disease, and as a mineral mass loss protective agent, against caries and erosion. More research is needed to explore the mechanisms by which Cu^{2+} alters HAp dissolution kinetics.

CHAPTER 8

X-ray microscopy

8.1 Nature of electromagnetic radiation

Radiation can be defined as the transmission of energy through space and matter (White and Pharoah, 2008). This transmission can take place in two forms; particulate and electromagnetic. Particulate radiation consists of atomic nuclei or subatomic particles moving in a high velocity such as α-rays and β-rays, while electromagnetic radiation is the movement of energy through space as a combination of electric and magnetic fields (White and Pharoah, 2008).

Electromagnetic radiation is a wave in space or through matter with the electric and magnetic field components perpendicular to each other and perpendicular to the direction of energy propagation as demonstrated in Figure 8.1 (Seibert, 2004) .

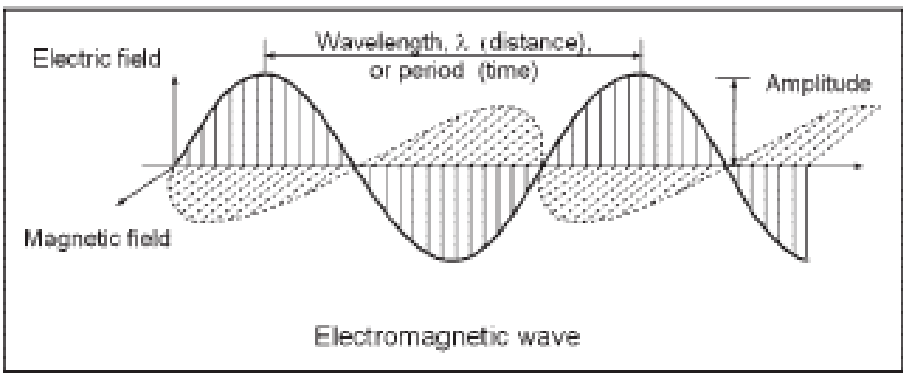

FIGURE 8.1 X-ray is an electromagnetic wave, where the electric and magnetic fields are perpendicular to each other and to the direction of propagation (Seibert, 2004)

Electromagnetic radiation is classified into several types according to their wave frequency. Radio waves, microwaves, infrared radiation, visible light, ultraviolet radiation, X-ray and gamma rays are all examples of electromagnetic waves. Of these, radio waves have the longest wave length and gamma rays have the shortest (Figure 8.2).

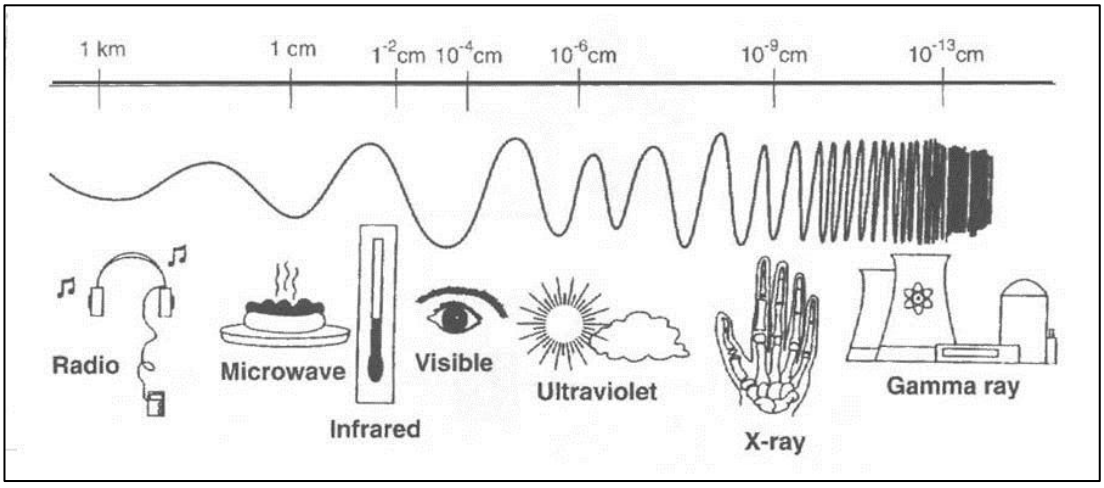

FIGURE 8.2 The electromagnetic spectrum in terms of wave length (http://www.centennialofflight.gov/essay/Dictionary/ELECTROSPECTRUM/DI159.htm)

8.2 X-ray generation

8.2.1 Introduction

More than one hundred years ago, in 1895, Wilhelm Conrad Roentgen discovered X-ray generation. He was the first to call them X-rays. One of the first X-ray photographs taken was the hand of Roentgen's wife taken three days before Christmas on 22 December 1895 (Figure 8.3). The image displayed both her wedding ring and bones (Assmus, 1995).

FIGURE 8.3 First X-ray photograph taken by Roentgen showing his wife's fingers (Assmus, 1995)

To generate X-rays Roentgen used a large induction coil connected to vacuumed glass tube. His detection system comprised of a paper screen covered with crystals of barium platinocyanide, set up in a dark room. On 28 December 1895 he announced his discovery and gave an accurate description of many of the basic properties of the rays (Assmus, 1995).

8.2.2 Modern X-ray tube

Roentgen's idea of X-ray generation was to introduce a high voltage to a residual gas at 10^{-3} mmHg pressure, leading to the formation of electrons and positively charged ions. The positive ions bombard a curved cathode releasing electrons which are accelerated towards the anode under high voltage producing X-ray. In roentgen X-ray generation, it was essential to maintain the gas pressure constant because changes in the pressure resulted in change in voltage between the anode and cathode of the tube.

In 1913 William Coolidge introduced a new source of electrons in the form of a hot tungsten spiral filament in a vacuumed glass. The filament is heated by a current provided by a battery and accordingly the electron current could be controlled independently of the applied voltage (Assmus, 1995).

The basic operating equipment for generating X-rays is the X-ray tube, and is composed of cathode and anode. The cathode acts as a source of the electrons to be directed at the anode. Both anode and cathode are enclosed in an evacuated glass tube. Electrons from the cathode are generated and when they strike the target in the anode they produce X-rays.

In order for an X-ray tube to generate X-rays it is fundamental that it should have a power supply that is capable of establishing a high voltage potential between the anode and the cathode which is required to accelerate the electrons (Figure 8.4).

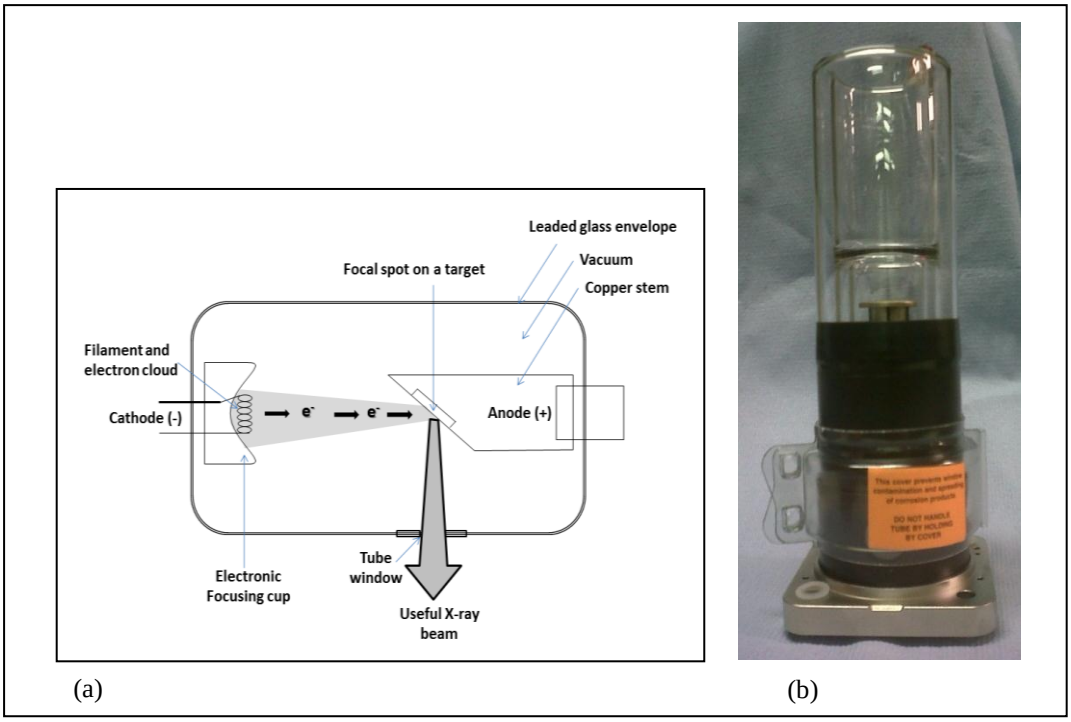

FIGURE 8.4 Schematic diagram showing basic components of an X-ray tube (a) and X-ray tube used in SMR machine (PANalytical®) with silver (Ag) target (b)

I. Cathode

The cathode consists of a filament and a focusing cup (Figure 8.4(a)). The filament is the source of electrons. It is a coil of tungsten wire about 2 mm in diameter and 1 cm in length, mounted on two stiff wires that act as holder and at the same time supply the filament with electrical current. To achieve a small focal spot the electrons are focused by a small metal focusing cup maintained at the same high voltage as the filament.

II. Anode

The anode is a target embedded in a copper block that is usually cooled. The target material is made up of an element that has a high atomic number, high melting point and a low vapour pressure at the X-ray operating temperature. In an X-ray tube the anode is kept at a high positive potential in comparison to the filament. When the filament is heated electrons are generated. These electrons accelerate through the potential difference between the anode and the cathode. They hit the target and transfer their kinetic energy to X-ray photons. Only a small amount of the electrons' kinetic energy produces X-ray photons, while about 99% is converted to heat. This explains the need for a target material with high melting point. X-ray tube anodes can be the fixed (stationary) type or the rotating anode type. In this study a fixed anode X-ray set was used (Figure 8.4 (b)).

III. X-ray tube envelope

The X-ray tube components are engulfed by a tightly air evacuated glass envelope. When the accelerated electrons generated by the cathode hit the target at the anode, they transfer their kinetic energy into heat and X-ray photons and the X-rays leave the X-ray tube case through two or more windows, usually made from

beryllium as they need to be vacuum tight but highly transparent to X-rays (Figure 8.4).

8.2.3 Microfocus tubes

Microfocus X-ray tubes are used in situations when a fine X-ray beam size is critical. With a microfocus tube, a high resolution and high magnification is achievable (Figure 8.4(b)). They are usually demountable X-ray tubes with a very small focal spot. The focal spot size determines the size of the actual X-ray source.

8.2.4 Electron impact X-ray source

When the accelerated electrons hit the target on the anode they are capable of producing two different types of radiation; continuous spectrum radiation and characteristic radiation (Figure 8.5).

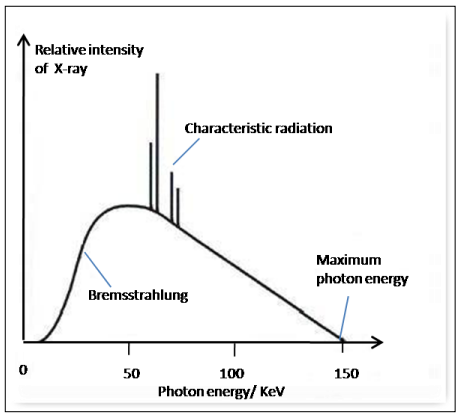

FIGURE 8.5 A typical X-ray spectrum produced by a tube with tungsten target showing continuous and characteristic radiation

I. Continuous radiation

There is a small probability that some electrons from the filament may penetrate the electron cloud and pass close to or interact with the nucleus or nuclear field of the target atoms. This interaction involves the deflection of the electron by

the nucleus accompanied by large energy loss by the electron. This energy is emitted as high energy electromagnetic X-radiation that is usually referred to as continuous or Brehmsstrahlung or braking radiation. Continuous radiation contains many energy levels. When the tube voltage is increased, the intensity of all wavelengths in the continuous spectrum increases as well as the maximum energy position.

II. Characteristic radiation

This type of radiation occurs simultaneously with Brehmsstrahlung production. This process involves the interaction of an electron from the filament with individual orbital electrons in the atoms of the target material. If it has enough energy, a filament electron may eject an orbital electron from an inner shell (K, L or M) of the target atom. This is followed by an outer-shell electrons dropping into inner shells to fill the vacancy, and the difference in energy is emitted in the form of characteristic radiation. This is called characteristic radiation because it is "characteristic" for the element and named according to the shell which captured the electron. For example, characteristic radiation resulting from an outer shell electron filling a vacant site in the K shell is named K-characteristic radiation.

8.2.5 Factors affecting X-ray beam quantity and quality

X-ray beam quantity usually refers to a measure of the amount or number of photons in the beam. The words quantity, exposure and intensity are interchangeable as the higher the quantity or amount of radiation the greater the exposure. On the other hand, quality of X-ray beam refers to the measurements of its penetrating power *ie.* its average photon energy.

There are many factors affecting the quantity and quality of the final X-ray beam. These include: tube voltage, tube current, distance from target, target material and position across the beam and filtration (Figure 8.6).

I. Tube voltage (V)

Increasing the voltage (V) accelerates the electrons emitted from the heated filament, and the total intensity (I) is proportional to V^2:

$$I \alpha V^2 \tag{8.1}$$

Also the higher the tube voltage, the higher the maximum photon energy will be, and hence the more penetrative the beam:

$$E_{max} \alpha V^2 \tag{8.2}$$

II. Tube current (A)

The total intensity increases on increasing the filament current since this result in an increase in the tube current which increases the number of electrons hitting the target:

$$I \propto A \tag{8.3}$$

III. Distance from target

There is an inverse square relation between the X-ray intensity (I) and the distance (d) from the target:

$$I \propto \frac{1}{d^2} \tag{8.4}$$

IV. Target material

Target materials with high atomic number (Z) and high density are more efficient in X-ray production:

$$I \propto Z \tag{8.5}$$

V. Filtration

The purpose of using of filters is to modify the beam spectrum by differential attenuation of different photon energies. For example in diagnostic radiology the filters are designed to remove the unwanted low energy photons which will be otherwise absorbed by the body tissue without contribution to the final radiographic image.

VI. Summary

Summarising the effect of the above factors on the X-ray spectrum is illustrated in Figure 8.6, and the X-ray intensity equation can be written as:

$$I \propto \frac{V^2 . A . Z}{d^2} \qquad (8.6)$$

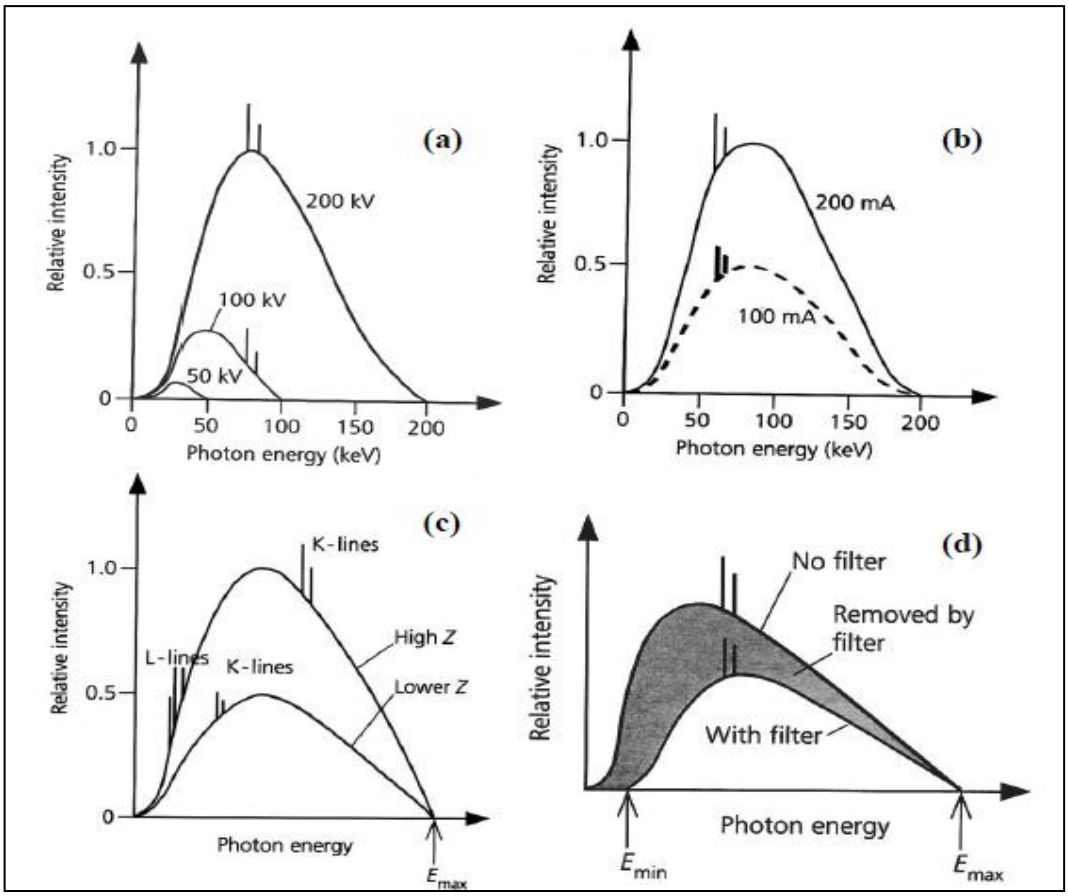

FIGURE 8.6 Factors affecting the X-ray spectrum. (a) changing the tube voltage changes the X-ray spectrum; (b) effect of tube current on the X-ray spectrum; (c) effect of target material on the spectrum; (d) adding a filter changes the shape of the X-ray spectrum (Pobe, 1998)

8.3 X-ray interaction with matter

As an X-ray beam passes through an object, there are three possible ways in which the photons will react:

I. Penetrate the section of matter without interacting.

II. Interact with the matter and be completely absorbed by depositing their energy.

III. Interact and be scattered or deflected from their original direction and deposit part of their energy.

X-rays attenuation depends on the X-rays energy level, density, and atomic number of the material.

8.3.1 Attenuation mechanisms

The attenuation mechanisms in general of any object are summarised in (Figure 8.7) and described as follows:

I. Photoelectric absorption

The photoelectric interaction involves an interaction between a photon and an electron from an inner orbital shell at the matter. Usually inner shells electrons bind firmly to the atom and when their binding energy is only slightly less than the energy of the photon, they get ejected from the atom and move a relatively short distance from their original location. The energy transfer is a two-step process; the first step involves the photoelectric interaction in which the photon transfers its energy to the electron, the second step involves the electron depositing its energy in the surrounding matter. The photon's energy is divided into two parts by the interaction. A portion of the energy is used to overcome the electron's binding energy and to

remove it from the atom. The remaining energy is transferred to the electron as kinetic energy and is deposited near the interaction site. When the electron is ejected out of the shell a vacancy is created, usually in shell K or L. This vacancy is then filled by an electron moving from an outer shell. The difference in energy between the two shells produces a characteristic X-ray photon (Aichinher *et al.*, 2004, White and Pharoah, 2004).

II. Compton scattering

Compton scatter occurs when incoming photon has greater energy than the binding energy of the electron in the atom. As a result only part of the photon energy is used to eject the electron from its shell (usually outer shell electron). The photon leaves the site of the interaction in a different direction with reduced energy and the electron (called recoil electron) distributes its energy via ionisation.

III. Pair production

Pair production is a photon-matter interaction. It takes place when the incident X-ray has energy greater than 1.02 MeV. The interaction of the incident photon with the electric field of the nucleus produces an electron-positron pair. This is not a very common type of interaction and not relevant to this study.

IV. Coherent scattering

In coherent scattering, an incident photon interacts with matter and excites an atom, causing it to vibrate. The vibration causes the photon to scatter. The coherent scattering can be also referred to as Thompton scattering.

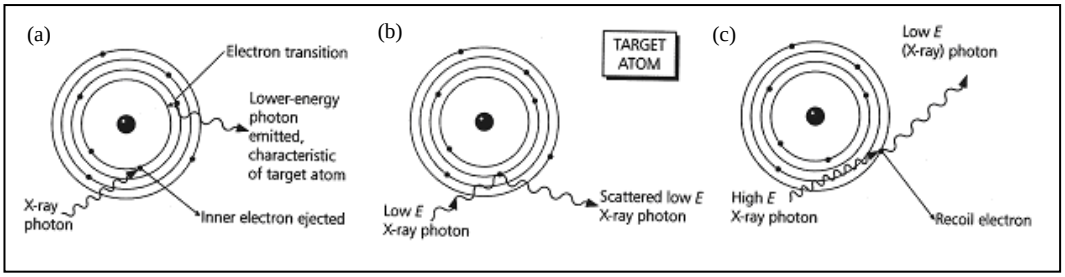

FIGURE 8.7 X-ray attenuation mechanism: (a) Photoelectric effect; (b) Simple scatter; (c) Compton scatter

8.3.2 X-ray attenuation: Beer's law

Beer's law, also known as Beer–Lambert law or the Lambert–Beer law relates the absorption of electromagnetic radiation to the properties of the attenuating material. A monochromatic X-ray beam is attenuated exponentially as it passes through a medium (Figure 8.8). This relationship is expressed by Beer's law as:

$$I = I_o \, e^{-\mu x} \qquad (8.7)$$

where

I is the intensity of the attenuated beam

I_o is the initial intensity of the beam

x is the thickness of the medium

μ is the linear attenuation coefficient (LAC)

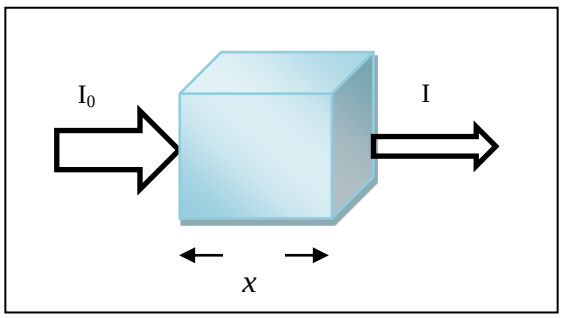

FIGURE 8.8 Attenuation of a monochromatic X-ray beam of intensity I_0 by a homogenous material thickness x

8.3.3 Types of attenuation coefficient (LAC)

I. Linear attenuation coefficient (LAC)

The linear attenuation coefficient (μ) of an element or material refers to the fraction of the beam of X-rays that is absorbed or scattered per unit thickness of the material. It has units of cm^{-1}.

II. Mass attenuation coefficient (MAC)

The mass attenuation coefficient describes the attenuation per unit area density of material, and has units of m^2kg^{-1} but is normally expressed as cm^2g^{-1}. This is because at a given photon energy, the linear attenuation coefficient can vary significantly for the same material if it exhibits differences in physical density.

$$\mu_m = \frac{\mu}{\rho} \tag{8.8}$$

where

μ is the linear attenuation coefficient

p is the density

8.4 X-ray detection

8.4.1 Introduction to semiconductors

There are different types of X-ray detection system, these include: solid state semiconductor detectors, X-ray films, gas detectors and scintillation detectors. In this section only the semiconductor detectors are going to be discussed in details, as this is the type of detector used in this study.

In semiconductors and insulators the electrons are confined to different bands of energy and are forbidden from other regions. The band gap represents the energy difference between the valence band and the conduction band. For semiconductors the band gap energy is small but not zero with an upper limit of ≈ 4eV, while for insulators the band gap is large. The main example of these solid state semiconductor detectors are high purity germanium detectors (HPGe) and lithium drifted silicon detectors (Si(Li)). A high purity germanium detector is used in this study.

The basic principle behind the operation of semiconductor detectors is that as the photon passes through the detector, an electron–hole pair is created. These electron-hole pairs are produced when an electron acquires enough energy to overcome the band gap and jump from the valence band to the conduction band in the detector material. Electron–hole pairs are considered the basic information carriers in solid state detectors (Singh, 2000, Seibert and Boone, 2005).

8.4.2 Multichannel analysers (MCA)

The role of the MCA is to convert the voltage pulses from the detector preamplifier into digital pulses. These digital pulses are organised in electric "bins" which correspond to different ranges of voltage pulse. Important characteristics of an MCA are linearity and stability with respect to temperature changes, and analogue to digital conversion time. In this study a DSPEC Plus (EG & G ORTEC, TN, USA) is used as both amplifier and MCA. This MCA system uses a zero dead-time correction technique developed by ORTEC to correct the actual number of counts by determining the number of events that must be added to account for pulse pile-up.

CHAPTER 9

Scanning Microradiography (SMR) Theory and Methodology

9.1 Introduction

Scanning microradiography is an X-ray attenuation technique which was initially developed by Elliott *et al*. (1981). It was later modified by Anderson and Elliott (1985) to observe real-time physical and chemical changes in specimens. The aim behind the concept of developing the SMR was to overcome the difficulties associated with the conventional contact microradiography (CMR) such as inhomogeneity of the film emulsion due to manufacture variation, saturation of the photographic emulsion as well as nonlinear response and noise at low X-ray exposures (Anderson, 1988, Anderson, 1993).

SMR is a point by point X-ray absorption technique which enables measurement of the intensity of approximately 15 μm transmitted X-ray beams as they are attenuated by passing through a specimen mounted on the SMR moving specimen holder stage. The stage has an accuracy of movement of approximately 0.1 μm. It travels a distance of 600 mm horizontally in the X-axis direction and 200 mm vertically in the Y-axis direction, driven by a stepper motor and controlled by a computer (Anderson, 1993). The transmitted photons are detected and counted via a high purity Germanium detector which eliminates the need for close contact between

specimen and detector. This allows for the creation of separate environmental chambers enclosing each specimen, which can be altered by, for example, changing the degree of saturation, chemical composition, pH and the circulating rate of the solution, all independently of other chambers. SMR allows the study of more than one specimen simultaneously during an experiment on a single stage. Computer control of the stage enables the order of scanning of the specimens as well as parameters of the scanning to be controlled independently. SMR can be considered the technique of choice for precise measurement of changes in mineral mass as the experiment conditions can be modified and the effect of the modifications on the experimented sample can be observed, measured and monitored in real time over a selected period of time that can be up to 1000 h. The disadvantages of SMR include that it is much more complex than CMR, it needs a very stable X-ray source and has a lower spatial resolution, and areas need more time for measurements (Anderson, 1993).

Scanning can be achieved in either a “parallel” or a “perpendicular” direction depending on the direction of the acid attack in relation to the X-ray beam. When the acid attack is perpendicular to the central X-ray beam it is called “perpendicular mode” (Anderson *et al.*, 1998). When the acid attack is parallel to the central beam, it is called “parallel mode” (Anderson *et al.*, 1998). In this study the “parallel mode” was used.

9.2 SMR system apparatus

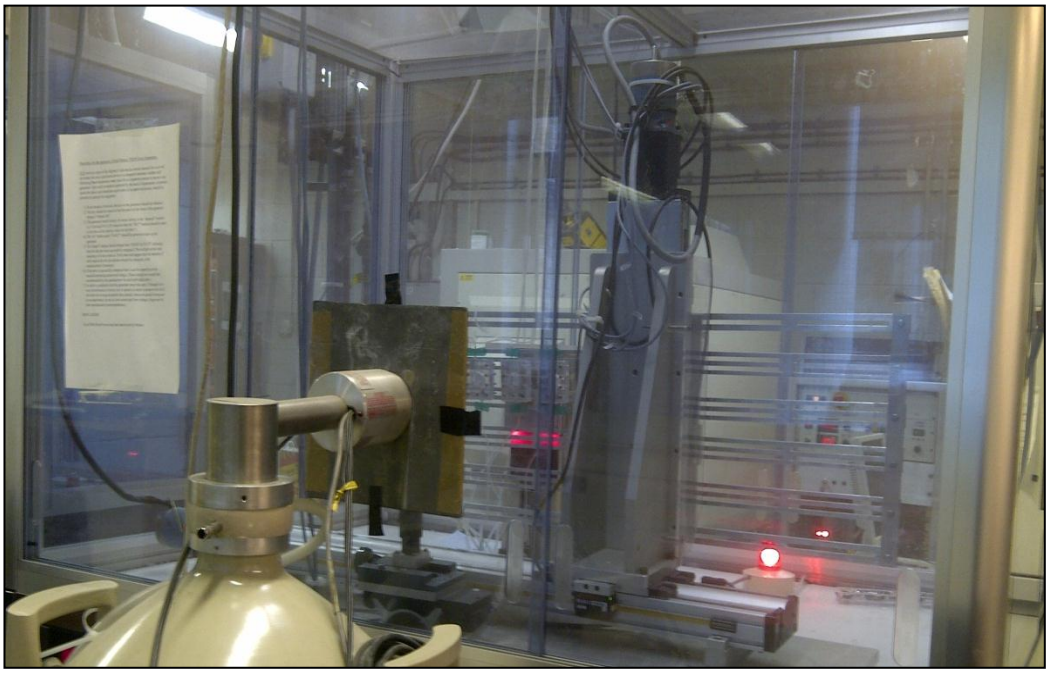

FIGURE 9.1 SMR machine with its main components X-ray source, X-Y stage, and detector

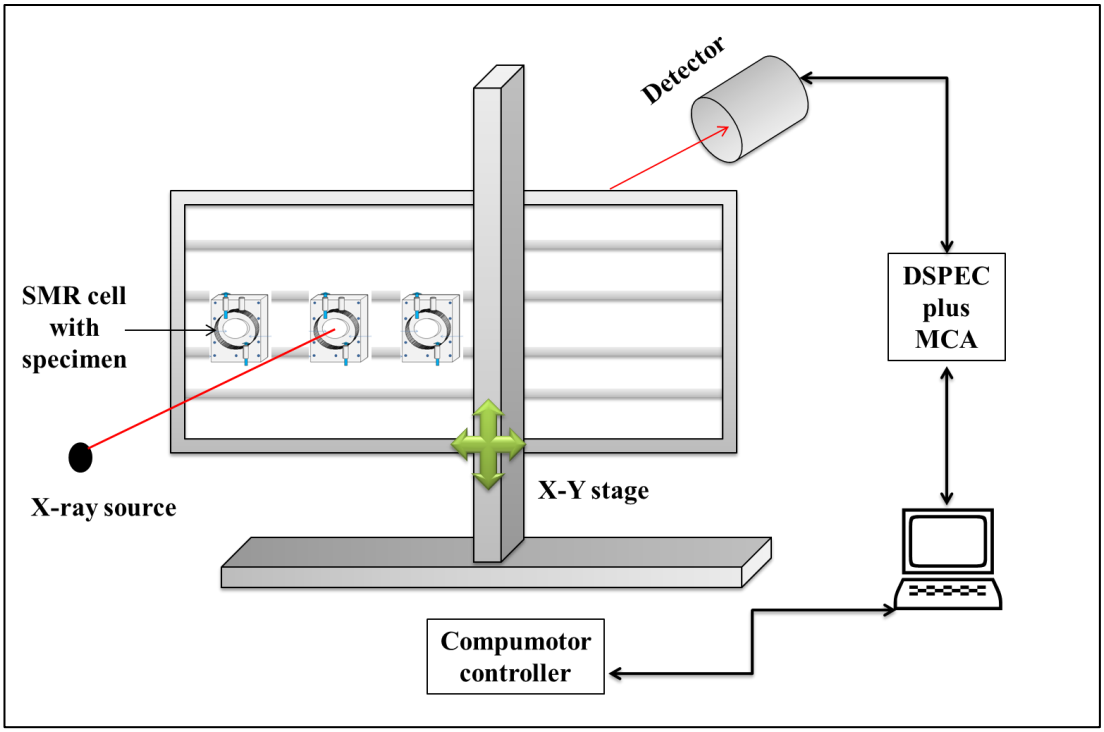

FIGURE 9.2 Schematic representation of the SMR system main components and their connections

The SMR system apparatus consists of three main components; X-ray generator, SMR stage with SMR cell's mounting frame, and X-ray detector (Figure 9.1 and Figure 9.2).

9.2.1 X-ray generator

SMR requires a very stable X-ray source that demands a high voltage high stability power supply. An Enraf-Nonious® FR590 X-ray microfocus generator was used with a PANalytical ® X-ray tube with a silver (Ag) target that gives a characteristic Kα peak at 22.1 keV (Figure 8.4). An approximately 15 μm aperture made up from 90% gold and 10% platinum is used to produce an X-ray beam of approximately 15 μm diameter (Siscoglou, 2008).

9.2.2 X-ray detector

The X-ray detector used is a high purity germanium detector (Ametek, PA, USA). The detector was coupled to digital spectrometer and multichannel analyser DSPEC PLUS™ (Digital Gamma-Ray Spectrometer, ORTEC®, Ametec, PA, USA), which allows spectrum capture (for details of the multichannel analyser refer to Section 8.4.2). The information in a single voltage (analogue) pulse from a detector and amplifier is then sent to a digital converter where it is converted into a sequence of digital values. Counting can be narrowed to only those energy values that fall within a certain range of energy and therefore monochromatisation of the X-ray beam can be achieved (Kosoric, 2006).

9.2.3 SMR stage

The SMR apparatus has two stages that move in X and Y directions (Micromech, UK). The horizontal stage moves in the X-axis direction for a distance

of 600 mm while the vertical stage moves in the Y-axis direction for a distance of 200 mm. Each stage is controlled by a stepper of 0.1 μm resolution linear encoder and moved by stepper motors controlled by software (written by Dr P. Anderson, Queen Mary University of London) and connected to a computer terminal. The software was designed to enable the stage to perform up to 30 experiments simultaneously with 30 different parameters (time, number of steps, step size, standards, etc.).

9.2.4 SMR cells

The SMR cells are made up of polymethyl methacrylate-PMMA. The dimensions of the cells are 4.0 cm x 5.0 cm. Each cell has a centrally located chamber of 2.5 cm in diameter and 4.0 mm depth. Each cell has a cover made up of the same material and dimensions as the cell itself but with 1.0 mm thickness (refer to Section 10.3 for SMR cell details). Once the SMR cells are ready with the specimen disc securely positioned in the centre of the chamber, and the covers securely sealed with silicon and screws, the SMR cells can then be mounted on to the SMR stage.

9.2.5 Area scanning

Before the main experiment begins, an area scanning of each specimen should be performed. The area scan gives an indication of the status of the specimen and its exact location coordinates on the SMR scanning stage (Figure 9.3).

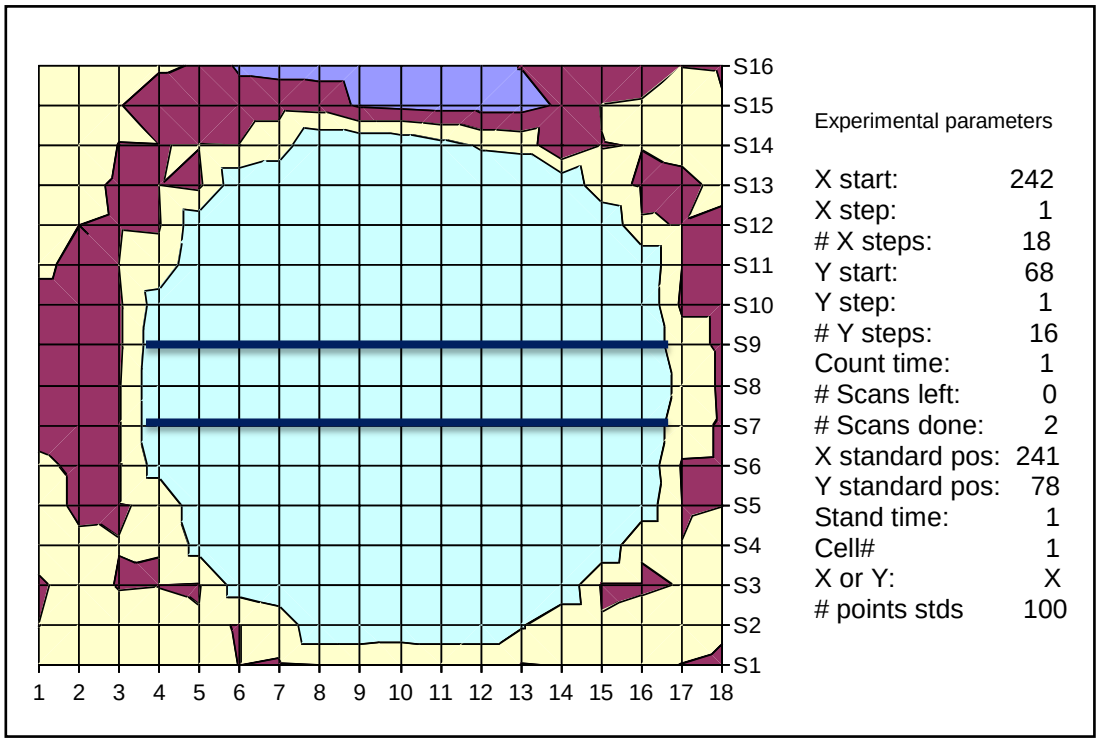

FIGURE 9.3 Area scan of an SMR cell with the specimen centrally located where X and Y axis represents specimen position coordinates on the SMR stage. Two line scans drawn across the specimen (▬) and scanning parameters are shown on the side

From the specimen area scan, two horizontal lines are chosen at approximately 2 mm apart. These lines are called line scans. On each line scan 13 points are chosen. The points are called scanning positions and refer to the points on the specimen that are going to be scanned throughout the experiment to determine any change in their mineral content. The 1st and the last scanning positions are located outside the specimen and are used as a reference (I_o) value.

9.2.6 Data analysis

For the duration of the experiment the 13 scanning positions on each line scan are continuously scanned and real time counts are detected by the detector. Data analysis begins by standardising the counts at the chosen point against a standard measurement which is a point outside the specimen, to correct for variations in X-ray

generator and X-ray counting chain characteristics. According to Beer's law (Section 8.3.2), for monochromatic radiation the intensity of transmitted beam through a sample is:

$$I = I_o \ e^{-\mu x} \qquad (9.1)$$

where I is the transmitted X-ray intensity, I_o is the incident X-ray intensity, and x is the sample thickness and μ is the linear attenuation coefficient.

Knowing the density of the material, ρ, the linear attenuation coefficient is divided by the density of the material (μ/ρ) and the equation can be written as:

$$I = I_o \ e^{-\mu m M} \qquad (9.2)$$

where μ_m is the mass absorption coefficient and M is the mass per unit area of the specimen (g/cm^2).

Equation 9.2 can be also written as

$$m = \frac{1}{\mu_m}\left[ln\frac{1}{N} - ln\frac{1}{N_\circ}\right] \qquad (9.3)$$

where N is the number of transmitted photons and N_o is the number of incident photon, taken outside of the specimen.

Differentiating this gives the error of the m as:

$$\delta m = \frac{1}{\mu_m}\left[\frac{1}{\sqrt{N}} + \frac{1}{\sqrt{N_\circ}}\right] \qquad (9.5)$$

$\frac{1}{\sqrt{N_\circ}}$ can be neglected as the number of incident X-ray photons, N_o, is very high (≈500,000). N, the number of transmitted X-ray photons, is typically about 50,000 which give a fractional error in m of ≈ 0.5 % (Figure 9.4).

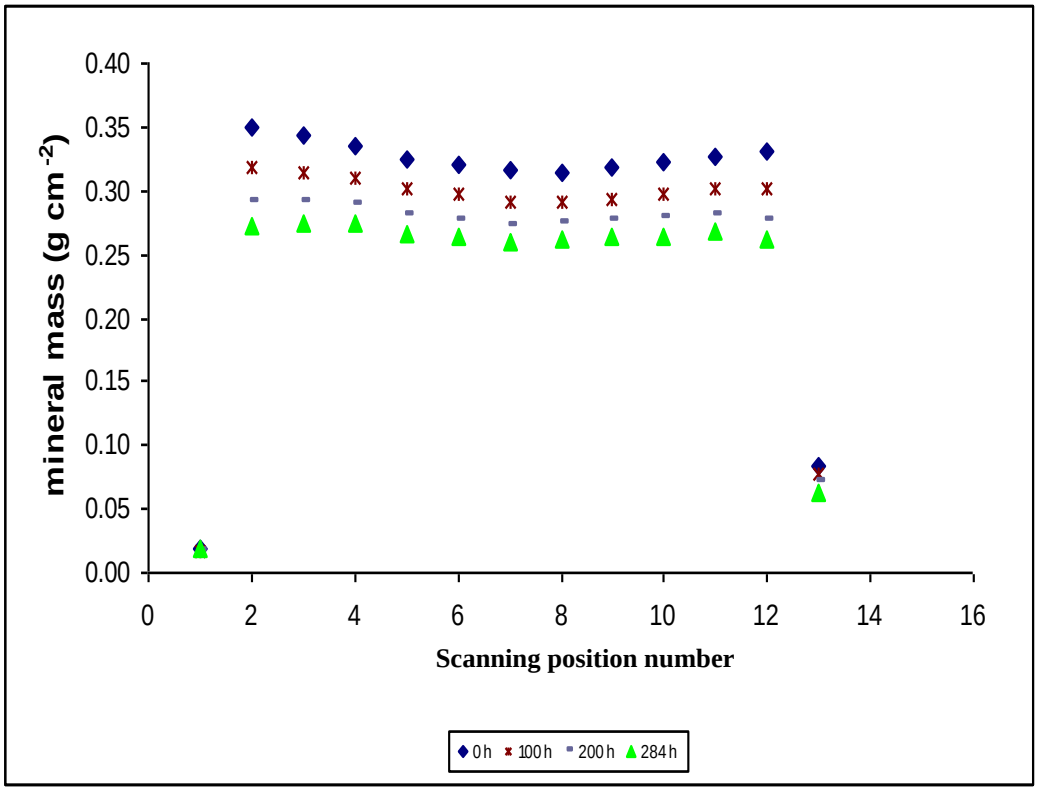

FIGURE 9.4 Example of data analysis and construction of time profile of HAp mineral mass loss at the scanning positions during the demineralisation process. The error in each point is of the order of 0.002 g/cm^2

Using Equation 9.3, the mass of HAp per unit area (g /cm^2) can be calculated by using the mass attenuation coefficient of HAp (4.69 cm^2/g) calculated for AgKα radiation. At the selected point the X-ray attenuation value can be then converted to a value for mass of HAp per unit area (g/cm^2). Based on the assumption that the mineral loss in HAp is linear with time, the demineralisation rate can then be calculated as:

$$m = at + b \qquad (9.4)$$

where m is the projected mass of HAp per unit area, t is the time, a is the rate of demineralisation, and b is the intercept on the y axis.

PART II: METHODOLOGY

CHAPTER 10

Modification of Real-time Scanning Microradiography for the Quantitative Measurements of Dissolution Kinetics of Compressed Hydroxyapatite Discs over Short Period of Time

10.1 Introduction

The development of the SMR technique has been on-going for over 20 years, with several generations. Early versions of SMR had significant drawbacks particularly associated with the SMR stage. The first drawback was the lengthy repeat time between measurements of the same point due to the slow movement of the stage. The second drawback was the low accuracy in stage positioning (5 μm accuracy).

Later versions of SMR were developed to overcome the problems associated with the stage by using a commercial X-Y stage. This provided much higher positioning accuracy, and a faster travel through the X and Y axes, which allowed a significant increase in sample positioning speed and reduced the length of the repeat time between successive measurements of the same point. Another improvement in the later version of SMR was the use of the same computer to control both stage motion, and detector photon counting system. The later versions were used to study mineral content changes in specimens over long periods of time and studying

multiple scanning positions. The experimental periods of time might extend for several weeks in order to allow accurate measurements of changes in specimens mineral mass content.

For the work described in this thesis, modifications to the operation technique were developed in order to allow the use of SMR for the detection of RD_{HAp} over short time periods of 24 h or less. In this Chapter, the SMR technique modification and the development of a new SMR protocol (short scanning protocol) will be discussed. This short scanning protocol was used in all the experiments described in this thesis.

10.2 SMR system apparatus used in this study

10.2.1 X-ray generation

An Enraf-Nonius® (now Bruker) FR590 X-ray microfocus generator was used with a silver (Ag) target PANalytical ® X-ray tube (Figure 8.4), and was run at 8 mA and 40 kV. The Ag target gives a characteristic Kα peak at 22.1 keV.

A 10 μm aperture (Imaging Equipment, UK) was used with this generator. The aperture has a cross section of 10 μm ± 0.5 μm, length of 20 μm ± 1 μm and is constructed from 90% gold and 10% platinum (Figure 10.1). The percentage of X-rays transmitted decreases the further the distance from the centre of the aperture and increases with higher energy levels, with 20% transmission at 47 keV, but almost 0% transmission at 20 keV. The number of SMR measurements is approximately 1800 in 24 h. Therefore a standardisation method was used to correct for variations in the X-ray generator throughout, and X-ray counting chain characteristics, by scanning a standard point usually located in the pure polymethyl methacrylate (PMMA) which

is unaffected by the experimental setup, by recording data for approximately 30 seconds repeatedly every 10 scan measurements.

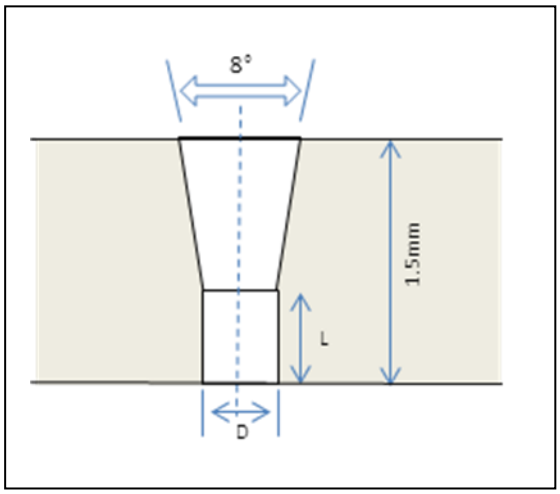

FIGURE 10.1 Schematic diagram of the cross section of the aperture assembly D= 10 µm ± 0.5, L= 20 µm ±1.0

10.2.2 X-ray detector

A solid state high purity germanium (HPGe) planar photon detector system (*ORTEC*® Ametek, PA, USA) was used for all studies reported in this thesis. This was an *ORTEC*® HPGe detector (GLP planar P-type detector) with 0.3 µm ion implanted window thickness, 0.127 mm beryllium absorbing layers and useful energy range 3 kV to 300 kV. It was connected to a DSPEC PLUS™ (Digital Gamma-Ray Spectrometer, ORTEC®, Ametec, PA, USA) which acts as both digital amplifier and a multi-channel analyser.

The information in a single voltage (analogue) pulse from the detector is amplified and then sent to an analogue-digital converter where the signal is converted into a sequence of digital values. Electronic monochromatisation of the beam was achieved by only counting pulses that fell within a particular energy range.

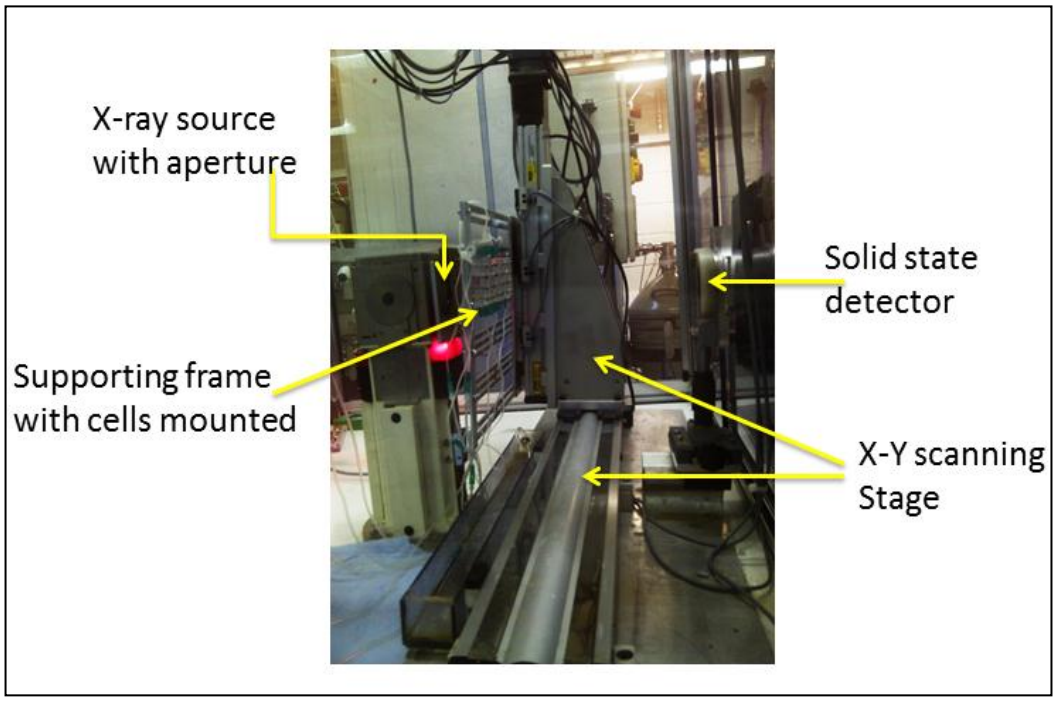

FIGURE 10.2 The main components of the SMR machine including the X-ray source, X-ray detector, X-Y scanning stage, and the mounting frame with SMR cells

10.2.3 SMR stage

As discussed in Section 9.2.3, the SMR apparatus consists of two orthogonally mounted stages (Parker Automation, UK) fitted with optical encoders (Renishaw). The horizontal stage moves in the X-axis direction for a distance of 600 mm, and the vertical stage moves in the Y-axis direction for a distance of 200 mm (Figure 10.2). The stages are fitted with end of travel and home sensors. They are controlled and moved by stepper motors with 0.1 μm accuracy linear encoders under computer control. The computer software was designed to enable the stage to perform up to 30 experiments simultaneously with 30 different parameters (time, number of steps, step size, standards, etc.) (Figure 10.2).

10.3 Area scanning

The area scanning technique followed in this study is the same as the standard area scanning technique discussed in Section 9.2.5 and gives the exact location of the HAp disc coordinates on the SMR scanning stage. However, in this study, one centrally located point at the centre of the HAp disc was chosen using the area scanning analysis and used as the scanning position. A second point, the standard point, was located in the SMR cell wall (PMMA) *ie*. not in the sample and therefore unaffected by changes in the experimental setup. The counting time for the centrally located scanning position was 30 seconds with a standard reading taken after every 10 measurements. The scanning time for the standard was 30 seconds. This modification resulted in a much shorter experiment time, as the considerable movement time between different scanning positions was not required. A large number of data points (≈ 1800) were obtained resulting in good statistical accuracy over the 24 h experimental duration.

10.4 Data analysis at a point

Data analysis begins by standardising the count data at the chosen point against the standard measurement to correct for any variations in the long term X-ray generation and X-ray counting chain characteristics. According to (Equation 9.2) and (Equation 9.3) the transmitted photon counts can be converted to mineral mass content per unit area and accordingly the projected mineral mass content of HAp per unit area (g/cm^2) can be calculated. This is followed by plotting the projected mineral content as a function of time (Figure 10.3).

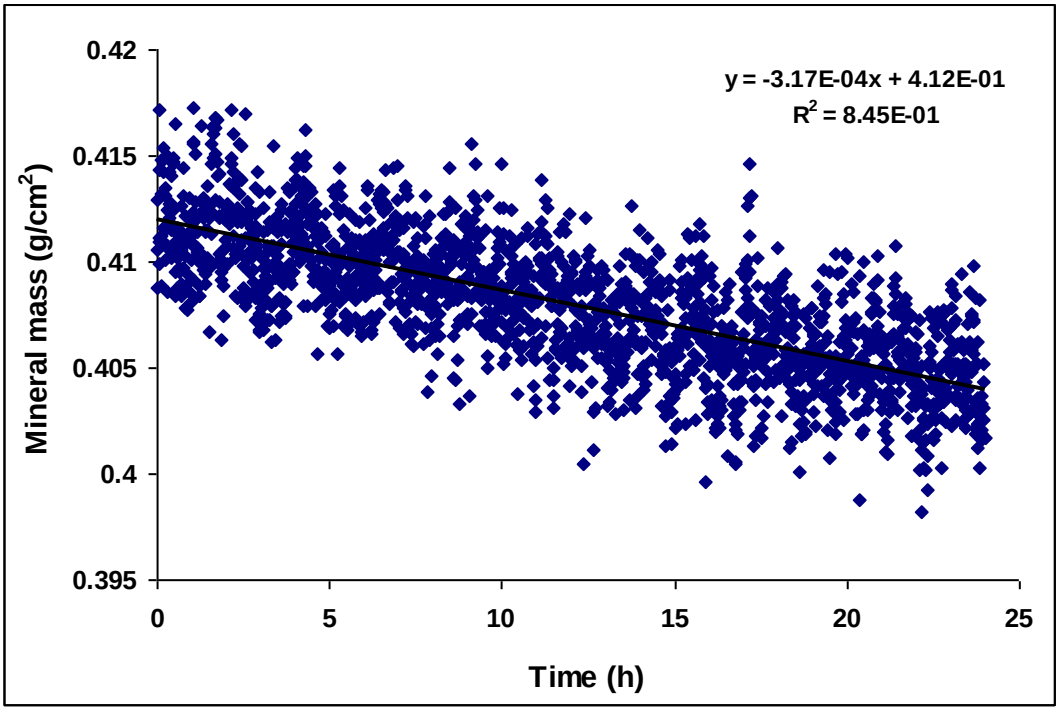

FIGURE 10.3 Typical example of linear change in projected mineral mass content over the experimental duration and the calculation of the RD_{HAp}

Based on the assumption that the change in the projected mineral mass content is linear with time, the demineralisation rate can then be calculated as:

$$y = a + bx \qquad (10.1)$$

where y is the projected mass of HAp per unit area, x is the time, b is the rate of demineralisation, and a is the intercept with the Y-axis.

Accordingly, Figure 10.3 shows that the change in the projected HAp mineral mass content over 24 h is ≈2% and the RD_{HAp} is 3.17×10^{-4} g/cm^2/h.

10.5 The effect of SMR data sampling frequency on the statistics of mineral mass loss calculation

One of the main advantages of the SMR technique is that it is designed to enable the scanning of up to 30 different SMR cells with 30 different scanning

parameters simultaneously. The SMR experiments are usually run for several weeks. This involves a large amount of the data collected over the experimental duration which allows the scanning of multiple SMR cells simultaneously.

However, in this thesis, a modified SMR technique was developed aiming at shorter experimental durations (24 h or less), involving a reduction in the number of data collected to ≈1800 data counts in 24 h.

10.5.1 Effect of even sampling frequency

Figures 10.4, 10.5, 10.6 and 10.7 show the changes in the projected HAp mineral mass content over 24h at 100%, 50%, 25% and 10% sampling frequencies respectively.

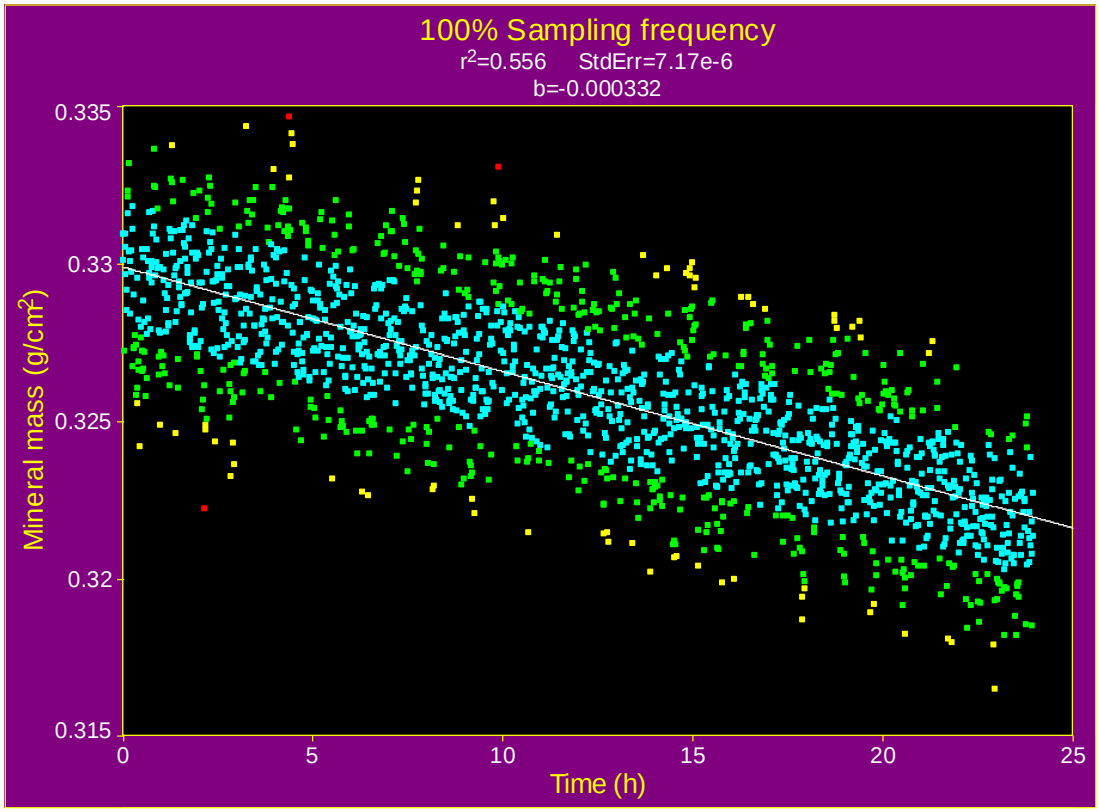

FIGURE 10.4 Change in the projected HAp mineral mass content over 24 h at 100% sampling frequency

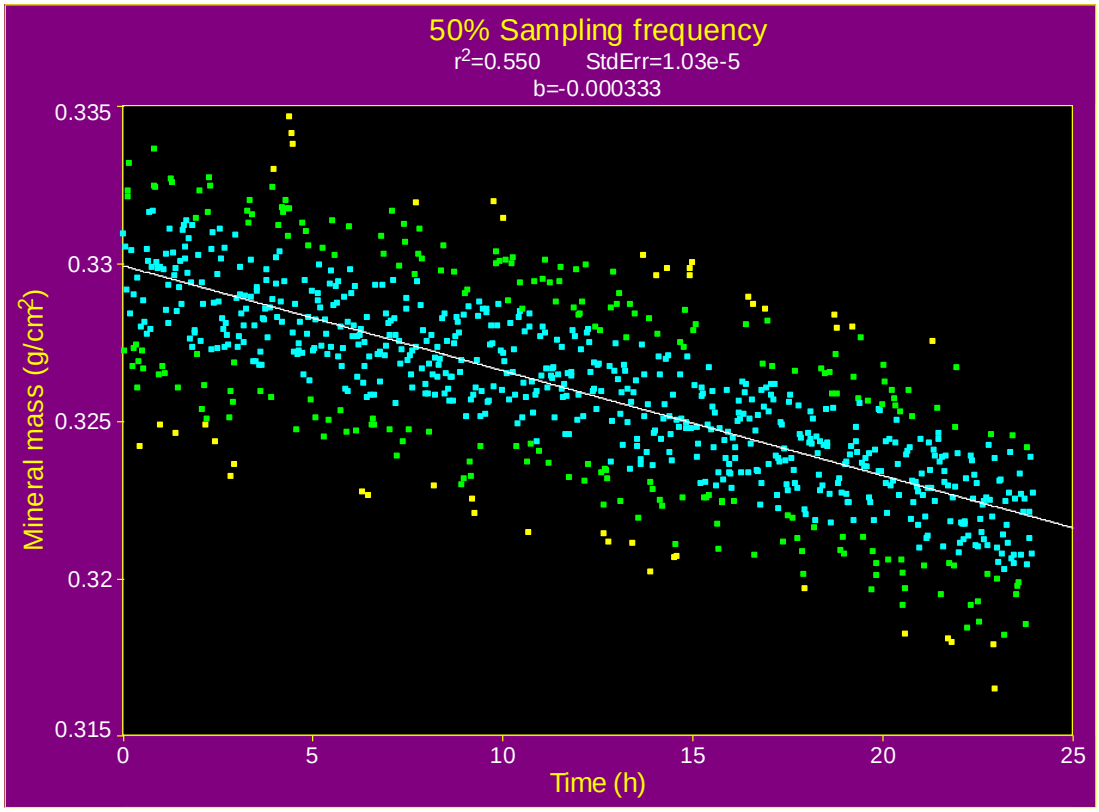

FIGURE 10.5 Change in the projected HAp mineral mass content over 24 h at 50% sampling frequency

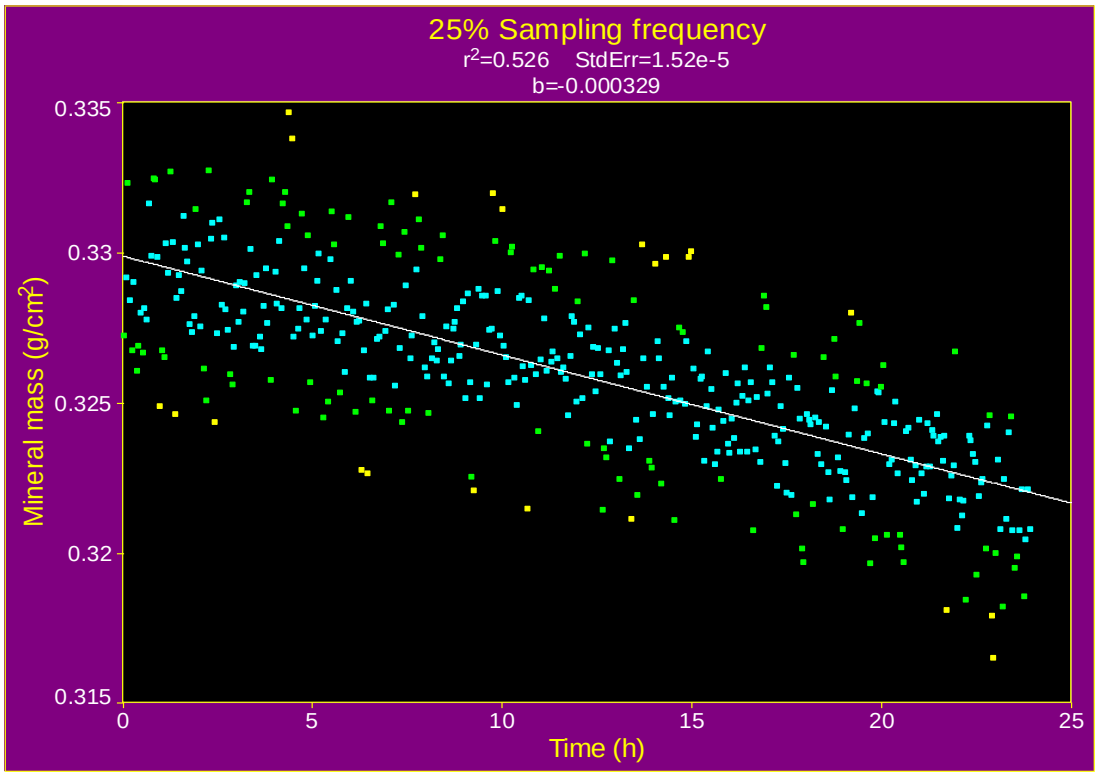

FIGURE 10.6 Change in the projected HAp mineral mass content over 24 h at 25% sampling frequency

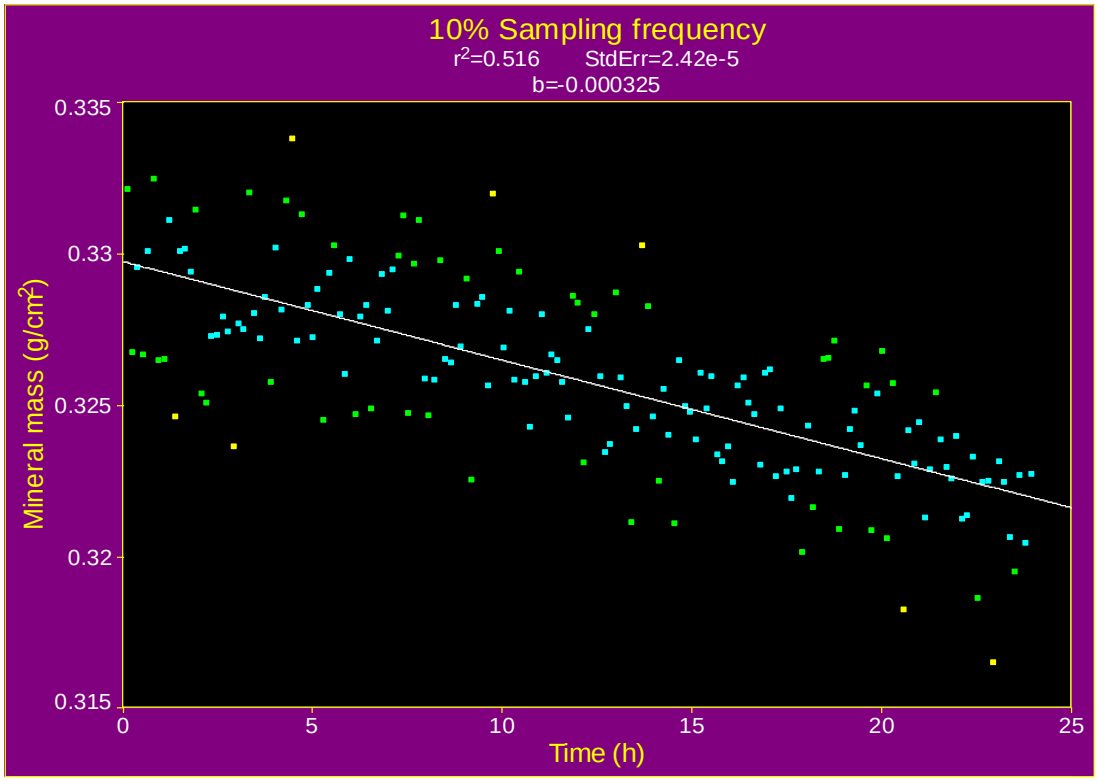

FIGURE 10.7 Change in the projected HAp mineral mass content over 24 h at 10% sampling frequency

Table 10.1 summarises the calculated changes in RD_{HAp}, R^2 and standard error (SE), using Microsoft Office Excel 2003® and TableCurve 2D® programs, at different sampling frequencies when a HAp disc was exposed to 0.1% acetic acid pH 4.0 demineralisation solution for 24 h.

TABLE 10.1 The RD_{HAp}, R^2 and SE calculated at different sampling frequencies using Microsoft Office Excel 2003® and TableCurve 2D® programs

Sampling frequency	RD_{HAp} ($g/cm^2/h$)		R^2		Standard error	Standard error in RD_{HAp} (%)
	calculated by Microsoft Office Excel	calculated by TableCurve 2D	calculated by Microsoft Office Excel	calculated by TableCurve 2D	data analysis using TableCurve 2D	
100%	$3.32x10^{-4}$	$3.32x10^{-4}$	$5.56\ x10^{-1}$	$5.56\ x10^{-1}$	$7.17x10^{-6}$	2
50%	$3.33x10^{-4}$	$3.33x10^{-4}$	$5.49\ x10^{-1}$	$5.50\ x10^{-1}$	$1.03\ x10^{-5}$	3
33.3%	$3.31x10^{-4}$	$3.31x10^{-4}$	$5.75\ x10^{-1}$	$5.75\ x10^{-1}$	$1.95\ x10^{-5}$	6
25%	$3.29x10^{-4}$	$3.29x10^{-4}$	$5.26\ x10^{-1}$	$5.26\ x10^{-1}$	$1.52\ x10^{-5}$	5
20%	$3.26x10^{-4}$	$3.26x10^{-4}$	$5.21\ x10^{-1}$	$5.21\ x10^{-1}$	$1.70\ x10^{-5}$	5
16.6%	$3.31x10^{-4}$	$3.31x10^{-4}$	$5.72\ x10^{-1}$	$5.72\ x10^{-1}$	$1.73\ x10^{-5}$	5
14.3%	$3.30x10^{-4}$	$3.30x10^{-4}$	$5.48\ x10^{-1}$	$5.50\ x10^{-1}$	$1.93\ x10^{-5}$	6
12.5%	$3.30x10^{-4}$	$3.30x10^{-4}$	$5.20\ x10^{-1}$	$5.20\ x10^{-1}$	$2.18\ x10^{-5}$	7
11.1%	$3.25x10^{-4}$	$3.25x10^{-4}$	$5.72\ x10^{-1}$	$5.72\ x10^{-1}$	$2.05\ x10^{-5}$	6
10%	$3.25x10^{-4}$	$3.25x10^{-4}$	$5.16\ x10^{-1}$	$5.16\ x10^{-1}$	$2.42\ x10^{-5}$	7

As observed from Table 10.1 the difference in the calculated RD_{HAp}, over different sampling frequencies ranged between 100% (1800 data counts) and 10% (180 data counts) using both Microsoft Office Excel 2003® and TableCurve 2D®, was $0.07x10^{-4}$ $g/cm^2/h$ which represents a maximum difference of 2%. Figures 10.4-10.7 are examples of different sampling frequencies, 100%, 50%, 25% and 10% respectively. This emphasises the advantage of using the standard error (SE) in statistical evaluation on the use of R^2, since the SE takes in account the sample size while R^2 represent the accuracy of fit.

10.5.2 Effect of multiple SMR cells simultaneous scanning

Some of the experiments in this thesis involved the scanning of two or three SMR cells simultaneously which led to a reduction in the observed data by 50% or 33% respectively. Figures 10.8-10.11 show real-data from simultaneous scanning of one to four SMR cells respectively. The reduction in the observed data counts was reflected in a systematic repetitive interrupted pattern (gaps) in the data points.

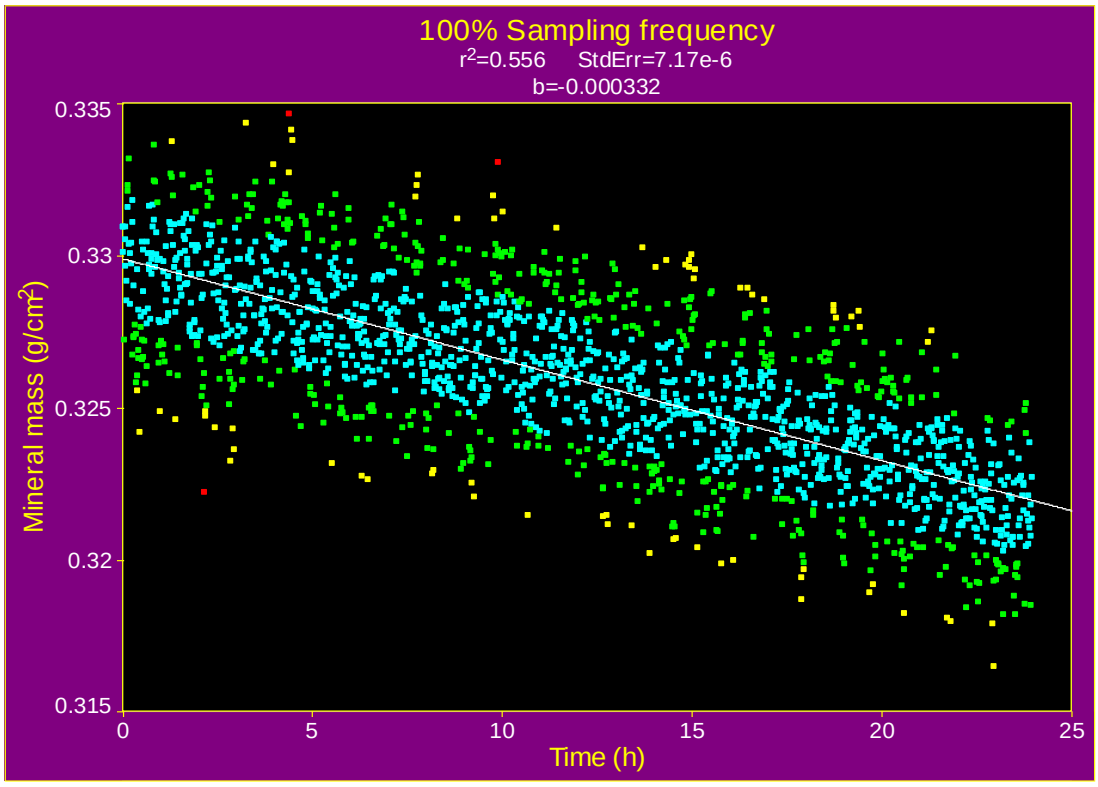

FIGURE 10.8 Change in the projected HAp mineral mass content over 24 h at 100% sampling frequency

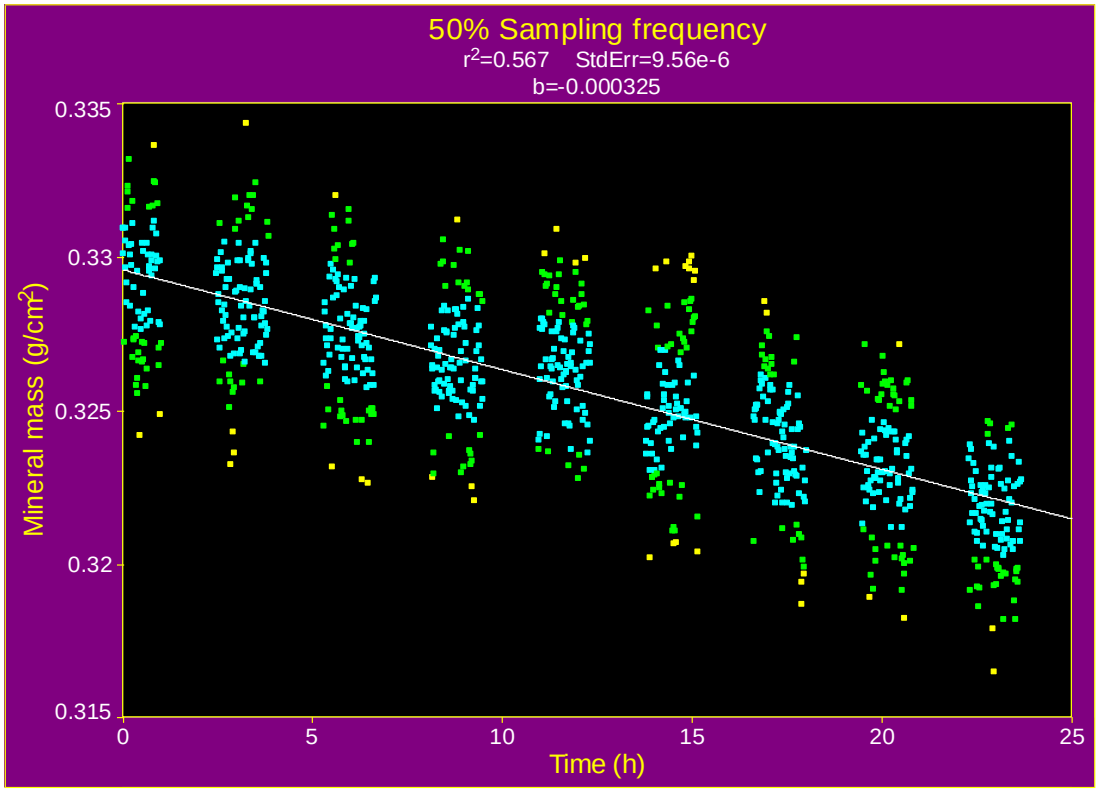

FIGURE 10.9 Change in the projected HAp mineral mass content over 24 h at 50% sampling frequency

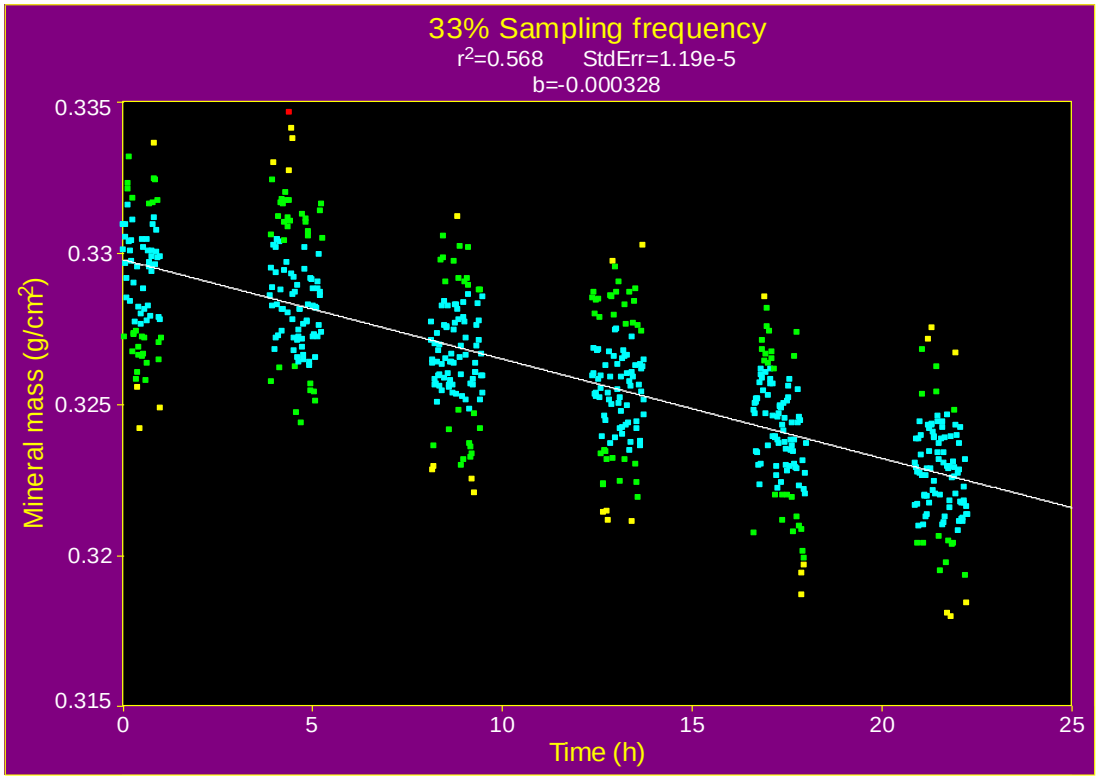

FIGURE 10.10 Change in the projected HAp mineral mass content over 24 h at 33% sampling frequency

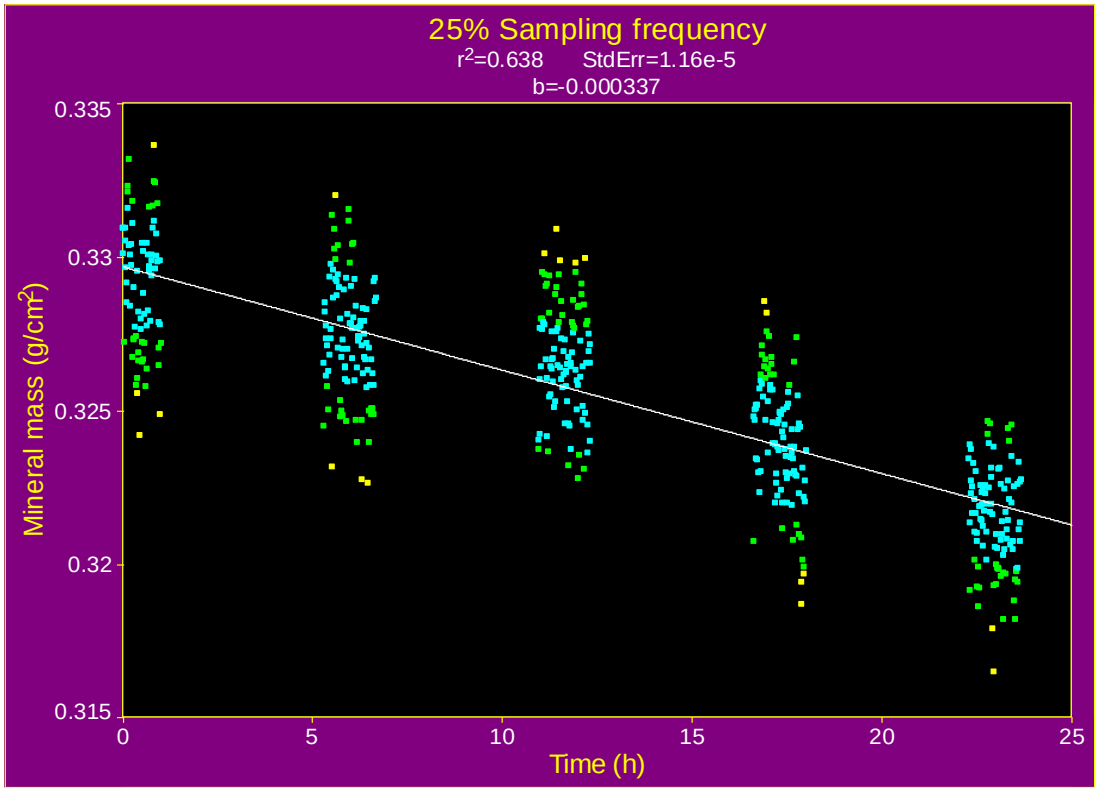

FIGURE 10.11 Change in the projected HAp mineral mass content over 24 h at 25% sampling frequency

As observed in Table 10.2, the difference in the calculated RD_{HAp} over different sampling frequencies ranged between $3.32x10^{-4}$ g/cm^2/h when one SMR cell was scanned at a time and $3.28x10^{-4}$ g/cm^2/h when three SMR cells were scanned simultaneously. However, the calculated standard of error shows that 33% reduction in data counts, scanning three SMR cells simultaneously, lead to approximately $0.04x10^{-4}$ change in SE which supports the reliability of scanning two or three SMR cells simultaneously.

In this thesis scanning of simultaneous scanning of up to three SMR cells was used in some of the experiments. TableCurve 2D® was used to demonstrate the results as it gives a higher level of statistical analysis by calculating the SE for both *a* and *b* (Section 9.2.6) which is more statistically important than R^2.

TABLE 10.2 The RD_{HAp}, R^2 and SE calculated at different sampling frequencies representing multiple SMR cells scanned simultaneously, using Microsoft Office Excel 2003® and TableCurve 2D® programs

Sampling frequency	# of SMR cells	RD_{HAp} ($g/cm^2/h$)		R^2		Standard error	Standard error in RD_{HAp} (%)
		calculated using Microsoft Office Excel	calculated using TableCurve 2D	calculated using Microsoft Office Excel	calculated using TableCurve 2D	calculated using TableCurve 2D	
100%	1	$3.32x10^{-4}$	$3.32x10^{-4}$	$5.56\ x10^{-1}$	$5.56\ x10^{-1}$	$7.17x10^{-6}$	2
50%	2	$3.25x10^{-4}$	$3.25x10^{-4}$	$5.67\ x10^{-1}$	$5.67\ x10^{-1}$	$9.56\ x10^{-6}$	3
33.3%	3	$3.28x10^{-4}$	$3.28x10^{-4}$	$5.68\ x10^{-1}$	$5.68\ x10^{-1}$	$1.19\ x10^{-5}$	4
25%	4	$3.37x10^{-4}$	$3.37x10^{-4}$	$6.38\ x10^{-1}$	$6.38\ x10^{-1}$	$1.16\ x10^{-5}$	3
20%	5	$3.19x10^{-4}$	$3.19x10^{-4}$	$5.62\ x10^{-1}$	$5.62\ x10^{-1}$	$1.45\ x10^{-5}$	4
16.6%	6	$3.00x10^{-4}$	$3.00x10^{-4}$	$5.08\ x10^{-1}$	$5.08\ x10^{-1}$	$1.77\ x10^{-5}$	6
14.3%	7	$3.10x10^{-4}$	$3.10x10^{-4}$	$5.48\ x10^{-1}$	$4.71\ x10^{-1}$	$1.71\ x10^{-5}$	6
12.5%	8	$3.50x10^{-4}$	$3.50x10^{-4}$	$7.17\ x10^{-1}$	$7.17\ x10^{-1}$	$1.33x10^{-5}$	4
11.1%	9	$3.00x10^{-4}$	$3.00x10^{-4}$	$5.53\ x10^{-1}$	$5.53\ x10^{-1}$	$1.90\ x10^{-5}$	6
10%	10	$3.72x10^{-4}$	$3.72x10^{-4}$	$4.02\ x10^{-1}$	$4.02\ x10^{-1}$	$2.51\ x10^{-5}$	7

10.6 SMR cell design and specimen preparation

10.6.1 SMR cells

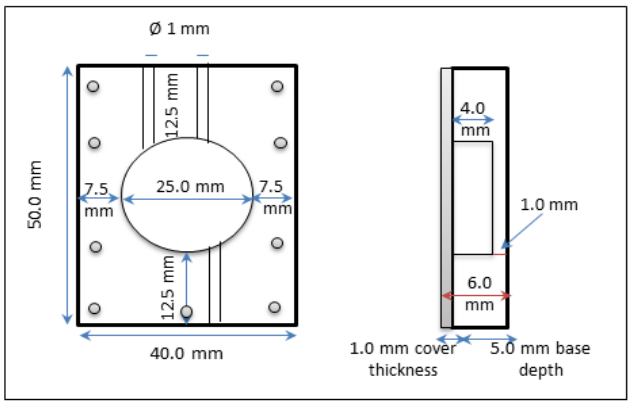

FIGURE 10.12 Schematic diagram showing top and side views of the new design for SMR cells with dimensions

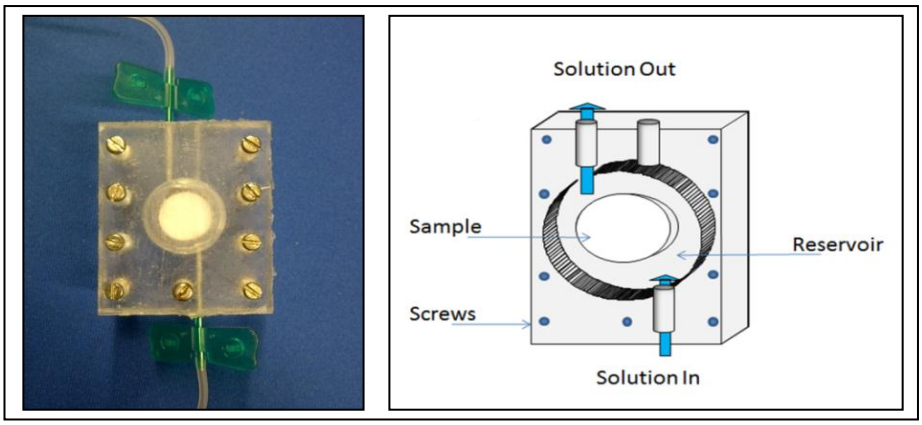

FIGURE 10.13 New SMR cell design developed to accommodate fitting of the complete HAp disc required in this thesis

Modifications of the previous SMR cells designs (either two wells design to allow experiments using powder or one small chamber design to test sections or small specimens) was required to enable fitting of the entire HAp disc (Figure 10.12). An SMR cell with one large (25.0 mm) central chamber was required for this study. Four SMR cells were prepared from polymethyl methacrylate (PMMA), with dimensions of 40.0 mm x 50.0 mm. Each cell has a centrally located chamber of 25.0 mm diameter and 4.0 mm depth and a cover made up of the same material as the cell itself, with the same dimensions but with 1.0 mm thickness (Figure 10.13). Each SMR cell has two holes on the top and one hole on the bottom. One butterfly needle is connected to the top hole and one to the hole at the bottom of the SMR cell, to allow solution to be pumped in and out, maintaining its circulation throughout the experiment. The butterfly needles are Hospira Venisystems Butterfly® (product # P293A05, needle length 20.0 mm, needle diameter 0.8 mm). The second top hole allows the escape of air and prevents building up of internal pressure within the cell and leakage within the cell in case of pump failure. A single permeable compressed HAp disc is securely placed in the centre of the SMR cell chamber and the cover is securely sealed with silicon and screws.

10.6.2 Specimen preparation

In this study permeable compressed sintered HAp discs were used as a representative of dental enamel. The HAp discs were all products of Plasma-Biotal Ltd, UK, with dimensions of 13.0 mm in diameter x 2.0 mm thickness and 20 wt % porous (HAp discs type selection will be discussed later in Chapter 11 and Chapter 12). All the compressed HAp discs were preconditioned by the preconditioning technique followed at the Oral Surface Science Department, School of Oral & Dental Sciences, University of Bristol, Bristol, UK. The idea behind preconditioning the HAp discs was to remove any loose particles or more soluble materials on the surface of the disc. The HAp discs were preconditioned by being submerged in a beaker containing a stirred solution of citric acid (0.3% normal pH) and turned over after 15 minutes. The discs were then washed by deionised water and left on filter paper for few hours to dry. The discs were then coated with acid resistant nail varnish on all surfaces leaving only one surface exposed so that the acid could diffuse through into the solid disc. Finally the discs were sterilised by autoclaving under usual conditions of 121°C (given by 15 p.s.i. pressure from 100% steam) for 30 min sterilisation time.

In this study a single HAp disc was placed in each SMR cell. The HAp disc was placed in the centre of the SMR cell chamber, covered by the SMR cell cover which was sealed with silicone rubber compound (RS Components Ltd, Corby, Northants, UK, product # 692-542) to prevent leakage and tightened up with nine screws (Figure 10.4). SMR cells were then mounted on the SMR cells mounting frame on the SMR X-Y stage. The cells were securely mounted on the SMR X-Y stage by screws, filled and circulated with de-ionised water to keep the specimen

hydrated. By this stage, the SMR cells with the HAp discs specimens were ready for area scanning.

10.7 Demineralisation solutions

10.7.1 0.1% acetic acid pH 4.0

In this study 0.1% acetic acid pH 4.0 was used as representative of caries-like conditions. In clinical situations dental caries develop in response to organic acids particularly lactic acid produced by plaque bacteria through fermentation of dietary carbohydrates. Therefore, in ideal situation lactic acid should have been used to resemble caries like condition but since lactic acid is quite expensive to obtain and difficult to find in pure form therefore acetic acid was chosen. Acetic acid has been used in many studies in this lab and other research centres and it has been shown that the role of acetic acid in demineralisation is similar to that of lactic acid (Margolis, 1992, Gao *et al.*, 1993, Anderson *et al.*, 2004, Elliott *et al.*, 2005). Acetic acid pH 4.0 was particularly selected because previous SMR studies using acetic acid pH 4.5 required a longer experimental duration to obtain a reliable data as the first 24h data were noisy.

One litre of 0.1% acetic acid pH 4.0 was prepared from acetic acid 100% (AnalaR NORMAPUR, VWR International Ltd. England, product # 20104.334, batch # 08G310506) and de-ionised water (Milipore, Direct-Q5; France). No additional calcium or phosphate was added and the solution was buffered with 1 Molar HCl or KOH solutions as necessary to reach the targeted pH level. The pH adjustment was done using Orion-pH/ISE meter Model 710.

10.7.2 0.3% citric acid pH 2.8

0.3% citric acid pH 2.8 was used as representative of erosion-like conditions. This is following protocol used by the Dental Materials Science Laboratory at the School of Oral and Dental Sciences, University of Bristol in studying dental erosion in vitro. One litre of 0.3% citric acid pH 2.8 was prepared from citric acid (AnalaR NORMAPUR, VWR International Ltd. England, product # 100813M, batch # K91366639 730) and de-ionised water (Milipore, Direct-Q5; France). No additional calcium or phosphate was added and the solution was buffered with 1 Molar HCl or KOH solutions as necessary to reach the targeted pH level. The pH adjustment was done using Orion-pH / ISE meter Model 710.

Each solution was stored separately in one litre bottle, sterilised by autoclaving at 121°C achieved with 15 psi pressure, 100% steam) and 30 minutes sterilisation time.

Demineralisation solutions were prepared fresh on the experiment day. When the same solution was used in a series of experiments on successive days or at different pH values, the demineralisation solution was made as a bulk solution and divided into multiple one litre bottles. Each solution was stored separately in one litre bottle, sterilised by autoclaving at 121°C achieved with 15 psi pressure, 100% steam) and 30 minutes sterilisation time. The pH was then adjusted on the day of the experiment. Solutions were circulated at 24 RPM (0.80 ml/min) using Watson Marlow Pump 205U, UK (Section 14.3). All experiments were carried out at room temperature, in a thermostatically controlled laboratory (at 22 ± 1°C).

Details of the specific solution used in the experiments are given in the materials and methods section of each experiment.

PART III: DEVELOPMENT OF A PROTOCOL

Introduction to Development of a Protocol

The scanning microradiography technique has been previously used to study the kinetics of enamel and HAp dissolution under erosive and caries simulating conditions, over a long period of time extending up to 1000 h. However, studying the kinetics of HAp dissolution over a short period of time (24 h or less) has not been studied previously using the SMR technique in this laboratory. Therefore, a development of a protocol was required.

The development of a protocol involved investigating several changeable parameters regarding the SMR technique, type of HAp discs to be used, demineralisation solution circulation rate and the concentration of divalent cations.

With regards to the SMR technique, it was modified and tested for its ability and reliability in detecting RD_{HAp} over a period of 24 h or less (Chapter 13).

In this thesis HAp was used as an analogue for dental enamel (Section 2.5). Similar studies in this laboratory have mostly used one of two types of HAp discs, either Plasma-Biotal HAp discs or Hitemco Medical Applications (HIMED) HAp discs. In order to choose between these two types of discs, they were investigated by X-ray microtomography (XMT), X-ray diffraction (XRD) and SMR to help in selecting the most suitable type for this thesis (Chapter 11 and Chapter 12).

The circulation rate of demineralising solution adjacent to a dissolving surface is an important parameter in SMR experiments since it has a considerable

influence on the rate of dissolution of solids. Therefore different demineralisation solution circulation speeds were investigated (Chapter 14).

Finally the effect of Sr^{2+} in high concentrations was investigated (Chapter 15). Summary of the experiments done to finalise the protocol is given in Table III.A.

TABLE III.A Experiments performed for developing the thesis protocol

Protocol component	Experiment
SMR technique and duration	▪ Modification of SMR technique to reliably detect RD_{HAp} over a short period of time ▪ Investigate the demineralisation of compressed HAp discs with altering acidic buffer with de-ionised water over short period of time
Selection of HAp discs	▪ Characterisation of HIMED and Plasma-Biotal compressed HAp discs using X-ray diffraction and X-ray microtomography ▪ Comparison between HIMED and Plasma-Biotal compressed HAp discs response (RD_{HAp}) to exposure to demineralisation solutions using SMR
Demineralisation solution circulation speed	▪ Study the effect of demineralisation solution circulation speed on compressed HAp discs dissolution kinetics using SMR
Sr^{2+} concentrations	▪ Study the effect of high concentration (desensitising toothpaste concentration) of Sr^{2+} on HAp dissolution kinetics studied using SMR

CHAPTER 11

Characterisation of HIMED and Plasma-Biotal Compressed Hydroxyapatite Discs

11.1 Introduction

In this thesis permeable HAp discs were used as an analogue for dental enamel. Similar studies in this laboratory have used one of two types of HAp discs. The first type was Plasma-Biotal Ltd, UK, permeable, compressed and sintered HAp discs with dimensions of 13.0 mm in diameter x 2.0 mm thickness and 20 wt% nominal porosity. The second type of HAp disc was the product of Hitemco Medical Applications, (HIMED), USA, permeable, compressed and sintered HAp discs with dimensions of 12.05 mm in diameter x 1.25 mm in thickness and 20 wt% nominal porosity.

11.2 Aims and objectives

The aim of this study was to compare the dissolution behaviour of the Plasma-Biotal and HIMED permeable compressed HAp discs and select the type of HAp discs to be used in this thesis.

The objectives were to investigate the HAp discs purity, uniformity and porosity using X-ray diffraction (XRD) and X-ray microtomography (XMT) techniques.

11.3 Materials and methods

11.3.1 X-ray microtomography

Three permeable compressed HAp discs of each type were randomly selected and scanned using the fourth generation in-house developed XMT system with a laboratory X-ray generator (Ultrafocus HMX 160, X-Tek system Ltd, 5µm source, tungsten target, 160 kV) operated at 90 kV and 200µA (Davis and Elliott, 1997).

Two permeable compressed HAp discs were placed flat and fixed by sticky wax to a Perspex stand that was mounted on the XMT rotation stage and oriented so that the XMT axis of rotation was as perpendicular as possible to the HAP disc surface (Figure 11.1)

FIGURE 11.1 HIMED and Plasma-Biotal HAp discs placed flat and fixed on a Perspex stand with aluminum wire to be mounted on the XMT rotation stage

11.3.2 X-ray diffraction

Three randomly selected compressed HAp discs of each type were tested for their mineral content and purity by X-ray diffraction. X-ray diffraction was carried out using an XPERT-PRO diffractometer system, 1500 W sealed tube with a copper (Cu) target ran at 40 mA tube current and 45 kV generator voltage to provide CuKα radiation. The diffraction patterns were then collected from continuous scans ranging from 5 to 120 2-theta angle.

11.4 Results

11.4.1 XMT

For the XMT, data analysis and visual display of the XMT data set was done using the Amira™ software package (TGS Template Graphics Software Inc., USA). The Amira™ program allows visualisation of single slices as well as surface and volume rendered images enabling viewing of a sample from any angle.

A comparison of the reconstructed images from both types of HAp discs reveals that they were of evenly uniformity in porosity, whereas HIMED compressed discs showed greater distribution and larger variety in pores sizes (Figure 11.2 and Figure 11.3).

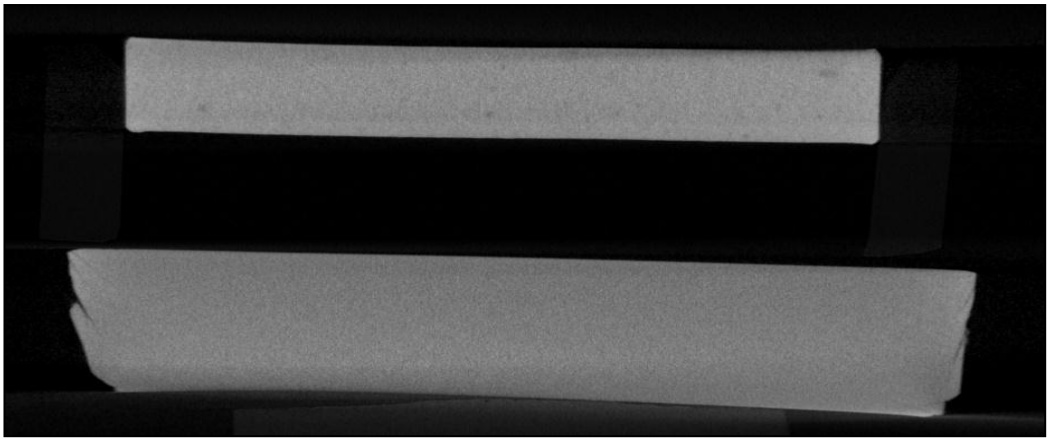

FIGURE 11.2 Reconstructed images of coronal sections through two compressed HAp discs showing larger pores in upper HAp disc (HIMED (a)) and evenly distributed and sized pores in lower HAp disc (Plasma- Biotal (b))

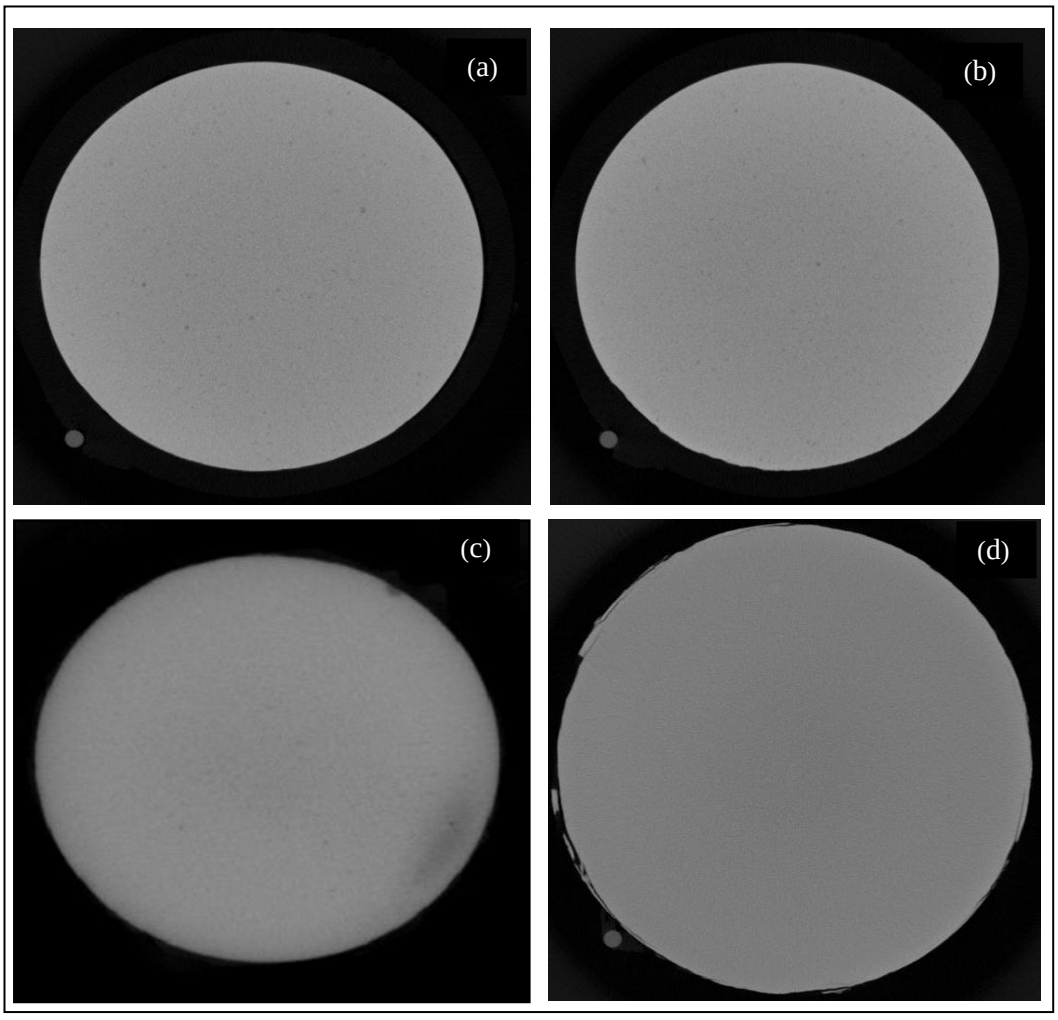

FIGURE 11.3 Reconstructed images of axial sections through HIMED HAp discs (a,b,and c) showing uneven distribution of larger sized pores while Plasma-Biotal HAp disc (d) shows even distribution of equally sized pores

11.4.2 XRD

Typical examples of the obtained XRD pattern for the HIMED compressed HAp discs and the Plasma-Biotal compressed HAp discs are shown in Figure 11.4 and Figure 11.5.

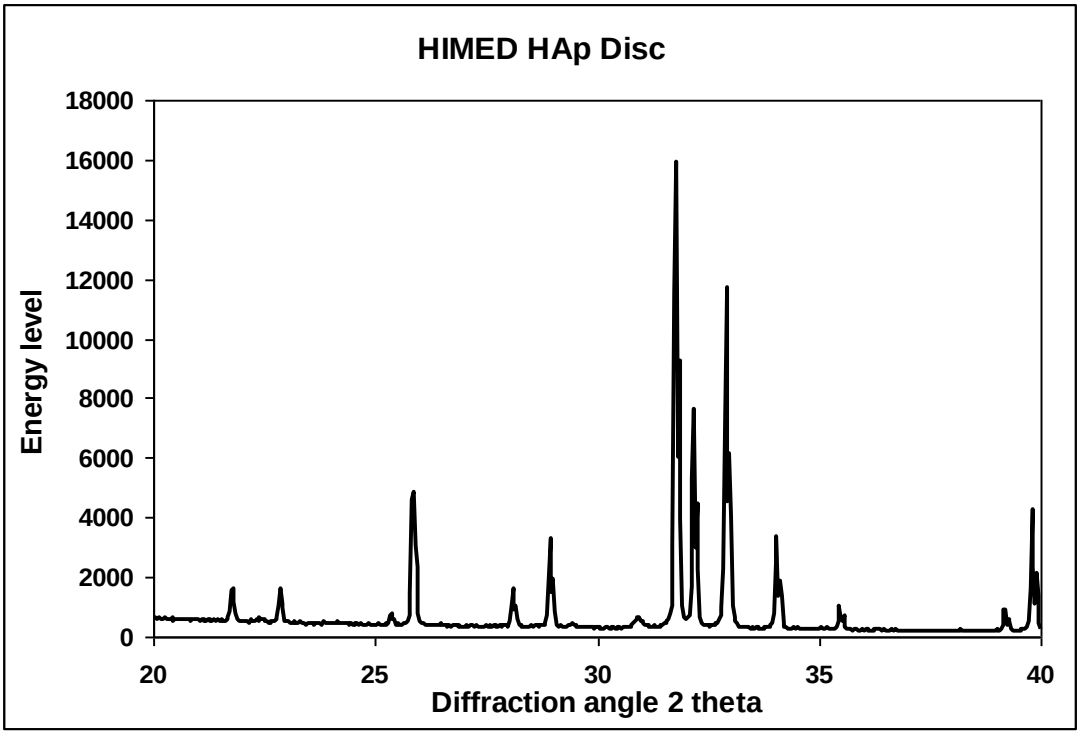

FIGURE 11.4 XRD pattern for HIMED HAp disc from 20-40 (2θ)

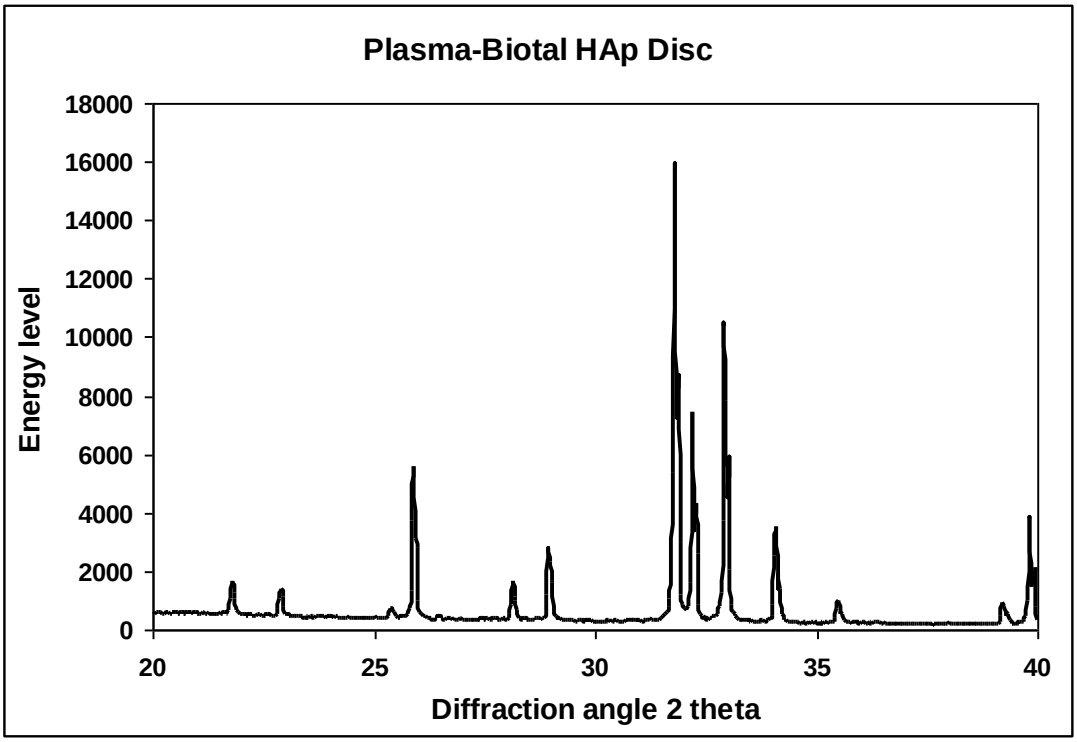

FIGURE 11.5 XRD pattern for Plasma-Biotal HAp disc from 20-40 (2θ)

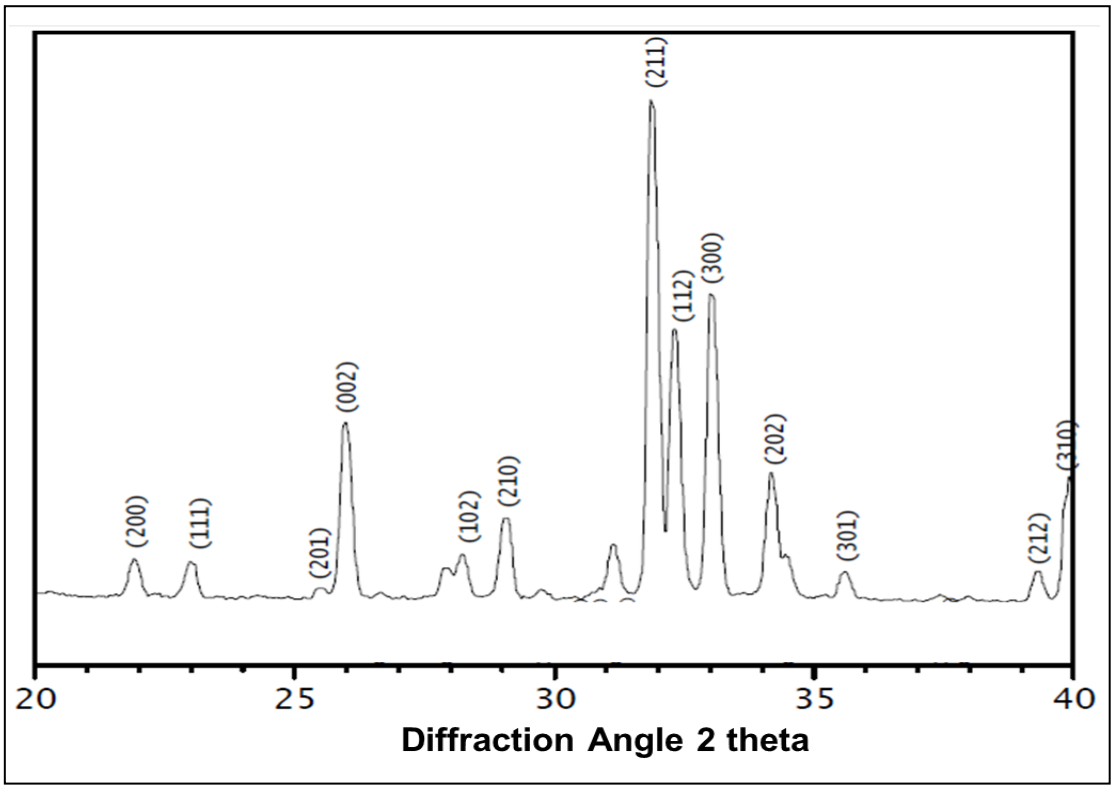

FIGURE 11.6 Typical XRD pattern of fully crystalline HAp with principal diffraction peaks (Prevéy, 2000)

11.5 Discussion

It was visually apparent from the XMT reconstructed images that the Plasma-Biotal HAp discs had better uniformity with regard to pore size and distribution, compared to HIMED HAp discs.

The results shown from the XRD confirmed that both types of HAp discs contain only hexagonal HAp. When compared to a classical HAp XRD pattern (Figure 11.6), both HIMED and Plasma-Biotal compressed HAp discs showed a classical HAp XRD pattern with no additional peaks. However, there is a peak missing in the Plasma-Biotal XRD results at about 31 degrees 2theta diffraction angle. There is no explanation to this finding and further research is needed in this area.

11.6 Conclusion

The narrow and sharp principal diffraction peaks indicate fully crystalline HAp with no difference in purity and crystal structure between the two types of discs.

CHAPTER 12

Comparison of Demineralisation Results of HIMED and Plasma-Biotal Hydroxyapatite Discs

12.1 Aims and objectives

The aim was to compare the demineralisation rate of HIMED and Plasma-Biotal HAp discs.

The objective was to measure RD_{HAp} of the two types of HAp discs in response to exposure to different demineralisation solutions of various pH values using the SMR technique.

12.2 Materials and methods

12.2.1 SMR

For details of the SMR technique refer to Chapter 10

12.2.2 HAp discs

Two randomly selected HAp discs from each type (HIMED and Plasma-Biotal) were preconditioned, sterilised and coated with acid resistant nail varnish on all surfaces except one and positioned in the centre of the SMR cells (for sample preparation details refer to Section 10.6.2).

12.2.3 Demineralisation solution

In this study, 4 litres of 0.1% acetic acid solution pH 2.8, 3.2, 3.6 and 4.0 were prepared. Similarly 0.3% citric acid solution was prepared (for demineralisation solution preparation details refer to Section 10.7). One HAp disc from each type of discs was exposed to the full series of 0.1% acetic acid demineralisation solutions (pH 2.8, followed by 3.2, 3.6 and 4.0) for 24 h for each pH value. The HAp disc was washed with de-ionised water (without pH adjustment) for 30 min between solutions with different pH values. The same applied to 0.3% citric acid. Each experiment was duplicated.

12.3 Results

The mineral mass content of each HAp disc was continuously measured though out the experiment duration. RD_{HAp} was calculated and the results are summarised in Table 12.1 and Figures 12.1 and 12.2.

TABLE 12.1 RD_{HAp} for both types of HAp discs in response to a change in demineralisation solution type and pH values

	0.1% acetic acid		0.3% citric acid	
pH	Plasma-Biotal disc RD_{HAp} ($g/cm^2/h$)	HIMED disc RD_{HAp} ($g/cm^2/h$)	Plasma-Biotal disc RD_{HAp}($g/cm^2/h$)	HIMED disc RD_{HAp} ($g/cm^2/h$)
2.8	4.44×10^{-4}	4.16×10^{-4}	1.22×10^{-3}	8.58×10^{-4}
3.2	4.32×10^{-4}	3.67×10^{-4}	7.65×10^{-4}	4.98×10^{-4}
3.6	3.79×10^{-4}	3.30×10^{-4}	4.72×10^{-4}	3.44×10^{-4}
4.0	3.69×10^{-4}	3.10×10^{-4}	4.02×10^{-4}	3.39×10^{-4}

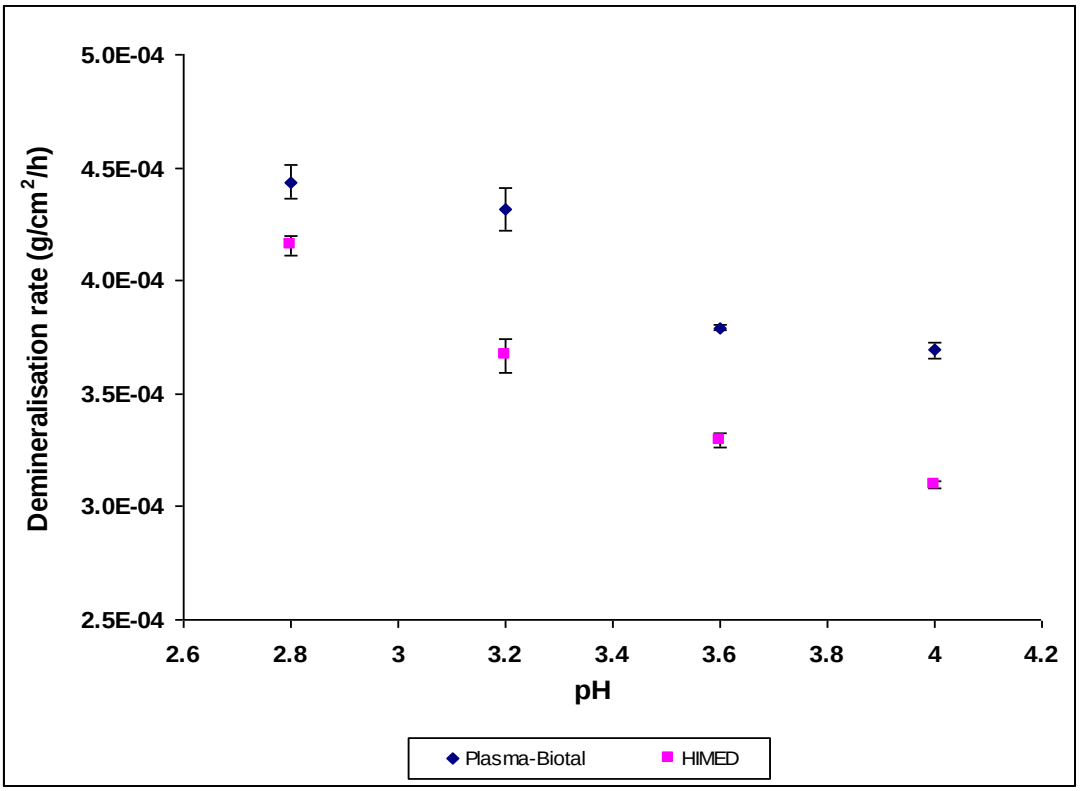

FIGURE 12.1 The change in RD_{HAp} for Plasma-Biotal and HIMED HAp discs as a function of 0.1% acetic acid at a range of pH values

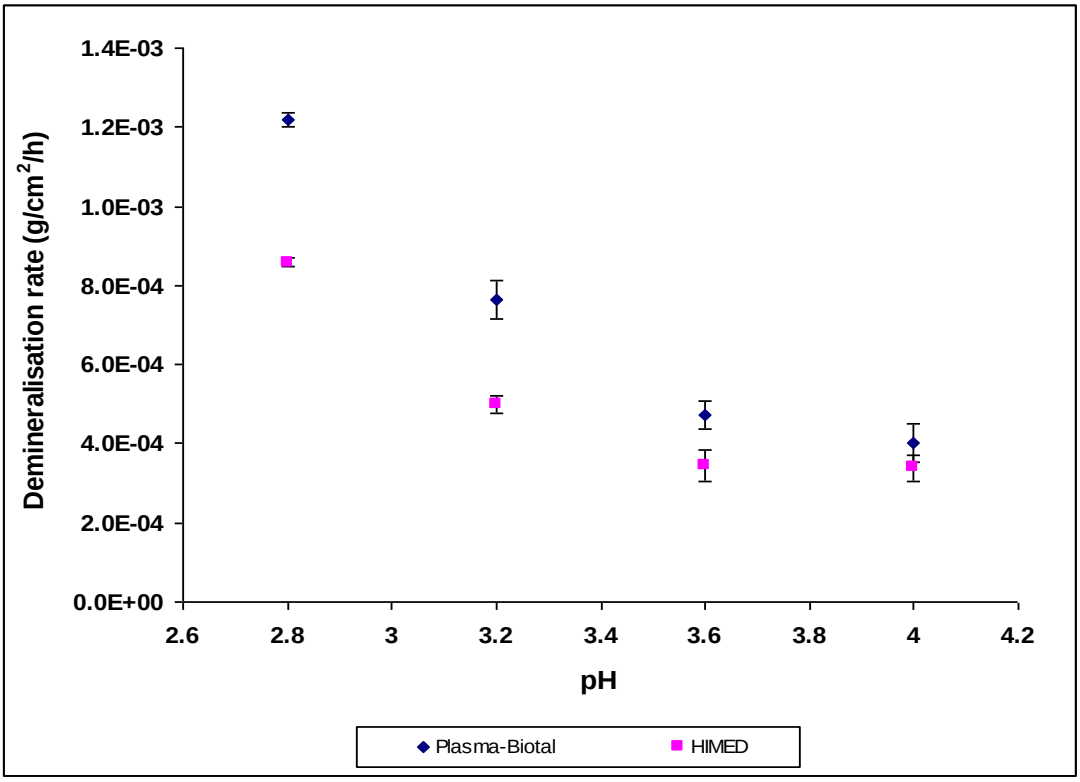

FIGURE 12.2 The change in RD_{HAp} for Plasma-Biotal and HIMED HAp discs as a function of 0.3% citric acid at a range of pH values

12.4 Discussion

The rate of hydroxyapatite dissolution can be affected by multiple factors (Section 4.1) among them; the chemical composition of the bulk solid, the pore size and distribution of the bulk solid, and the pH value of the demineralisation solution.

The use of XMT, XRD and the SMR in the experiments in Chapter 11 and Chapter 12 was to find the best HAp amongst the two available types to be used in this thesis.

Based on the results of the XMT study (Chapter 11), the Plasma-Biotal HAp discs showed better uniformity with regards to pore size and distribution compared to the HIMED HAp discs. Since larger pores are known to facilitate diffusive transport of ions, it was expected that the HIMED HAp discs will show faster demineralisation rates. The results shown in Table 12.1 demonstrate that RD_{HAp} for the Plasma-Biotal HAp discs was faster than that for the HIMED HAp discs though they both showed the same pattern in response to change in the pH value of the demineralisation solution. There is no clear explanation for this observation and further investigation is required.

12.5 Conclusions

SMR results showed that HIMED HAp discs were less soluble than Plasma-Biotal HAp discs when exposed to the demineralisation solutions particularly citric acid. However both discs followed a similar trend in change in RD_{HAp} when subjected to different demineralisation solutions with different pH values.

Based on the results obtained for the experiments described in Chapter 11 and Chapter 12 it was concluded that both types of discs are made up from fully

crystalline HAp with no difference in purity or crystal structure and showed a similar trend in change in RD_{HAp} when subjected demineralisation solutions, however according the XMT results Plasma-Biotal HAp discs had better uniformity and porosity than HIMED HAp discs. Therefore it was decided to use Plasma-Biotal HAp discs in all the experiments in this thesis.

CHAPTER 13

Demineralisation of Compressed Hydroxyapatite Discs with Acidic Buffers at a Range of pH Values over Short Period of Time

13.1 Introduction

In many *in vitro* studies of model systems for dental caries and erosion, the solid is usually exposed to demineralising or remineralising solution, but altering solution conditions involves interrupting the experiment. A major advantage of the SMR is that the experimental conditions can be altered without interrupting the experiment. Using the SMR technique in conjunction with pH cycling systems allows mimicking of pH conditions in the oral cavity (White, 1995, Harless and Wefel, 2003, Thaveesangpanich *et al.*, 2005).

13.2 Aims and objectives

The main aim of this experiment was to test the ability of the SMR technique to detect changes in HAp mineral mass content in response to exposure to acidic buffers at a range of pH values over a short period of time (24 h or less). A further aim was to investigate whether information could be obtained about the transient stage between exposure to acid buffer and the de-ionised water.

The objectives were to obtain reliable quantitative measures of the demineralisation rate of compressed HAp discs in acidic buffer followed by de-ionised water using SMR, over periods of 24 h or less.

13.3 Materials and methods

13.3.1 SMR

For details of the SMR technique refer to Chapter 10.

13.3.2 HAp discs

Four HAp compressed discs (Plasma-Biotal, UK) were used in this study. All discs were preconditioned, sterilised, and painted with acid resistant nail varnish on all surfaces but one, leaving this surface exposed to the demineralising solution. Each disc was placed in a separate SMR and mounted in the centre of the SMR cell chamber. For details of specimen preparation refer to Section 10.6.2.

13.3.3 Demineralisation solutions

In this study 0.1% acetic acid and 0.3% citric acid solutions of pH 2.8, 3.2, 3.6 and 4.0 were buffered with 1M KOH, with no addition of calcium or phosphate. Each demineralisation solution was stored separately in a 1 litre bottle (for details of solution preparation refer to Section 10.7). Demineralisation solutions were circulated through the SMR cell at a slow rate of 0.19cm^3/min. The circulation rate was set at a slow rate to avoid, as much as possible, any mechanical erosion that might arise from a fast circulation of acidic solutions. The same HAp disc was exposed to 0.1% acetic acid at pH 2.8 for 20 h followed by 4 h of de-ionised water,

then 0.1% acetic acid at pH 3.2 for 20 h, followed by 4 h of de-ionised water and similarly at pH 3.6 and 4.0. The HAp mineral mass content was measured continuously over the 24 h experiment time. The experiment was repeated with 0.3% citric acid solution. All experiments were performed in a thermostatically controlled laboratory at a temperature of 22°C ± 1°C and were duplicated.

13.4 Results

To assess the effect of the acidic buffers at a range of pH values, over a short periods of time, on RD_{HAp}, the mineral mass content of each HAp disc was continuously measured over the duration of the experiment of 24 h. Typical examples of the results obtained are illustrated in Figures 13.1 to 13.8.

13.4.1 0.3% citric acid demineralisation solution

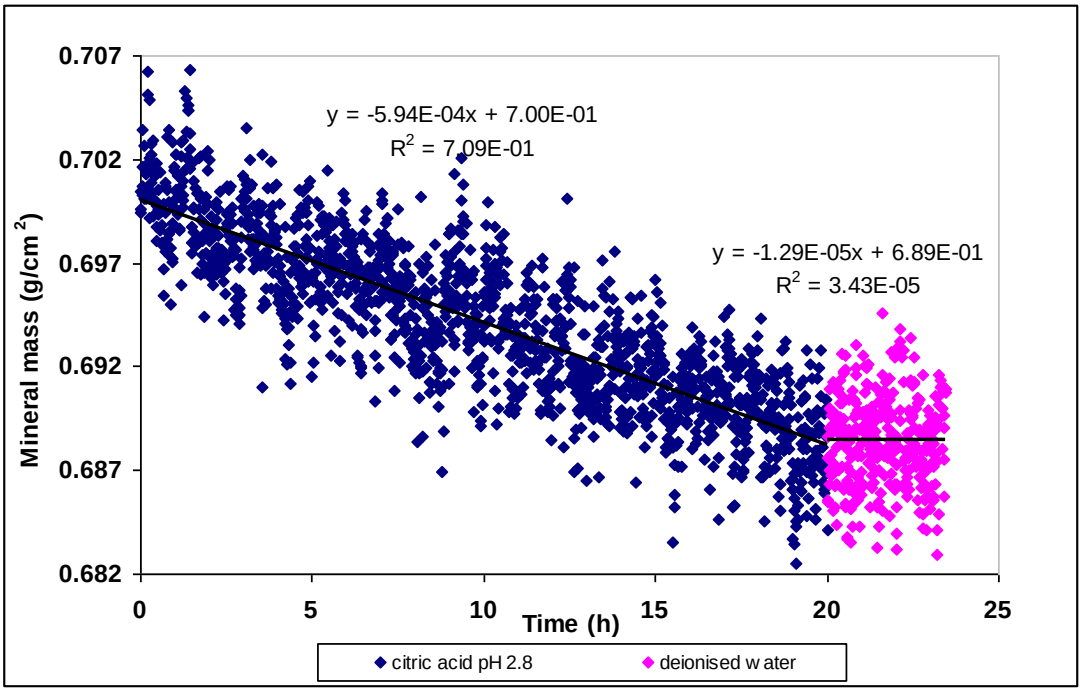

FIGURE 13.1 The change in projected HAp mineral mass content in response to 20 h of demineralisation by 0.3% citric acid pH 2.8 followed by 4 h of de-ionised water

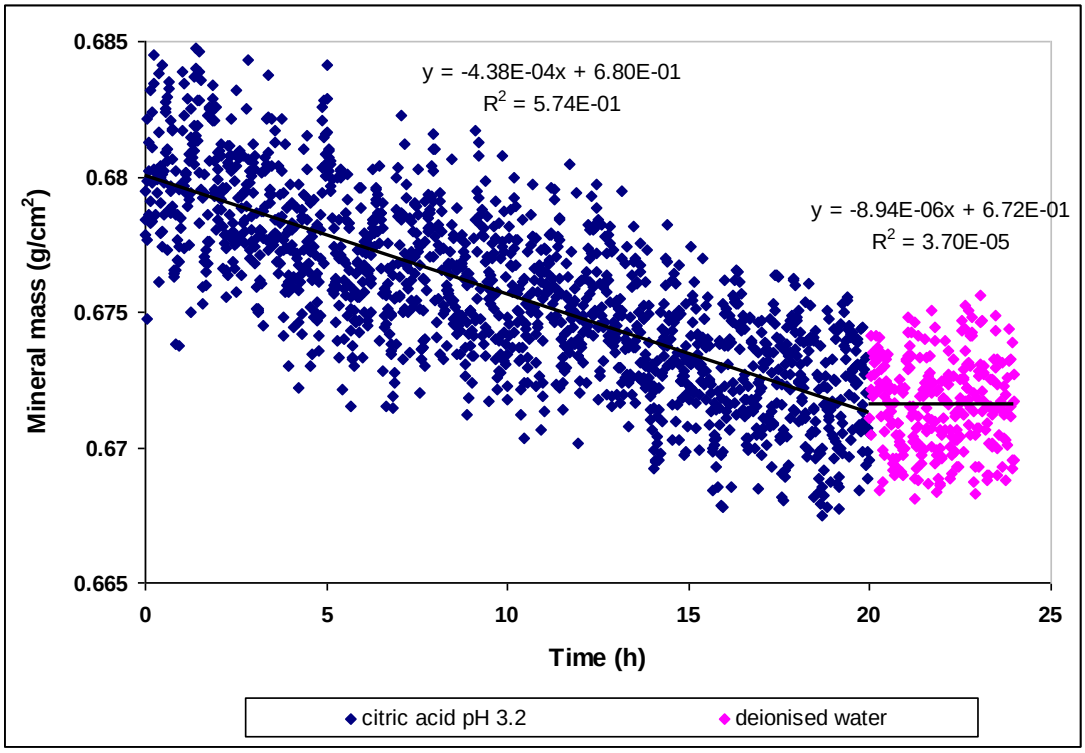

FIGURE 13.2 The change in projected HAp mineral mass content in response to 20 h of demineralisation by 0.3% citric acid pH 3.2 followed by 4 h of de-ionised water

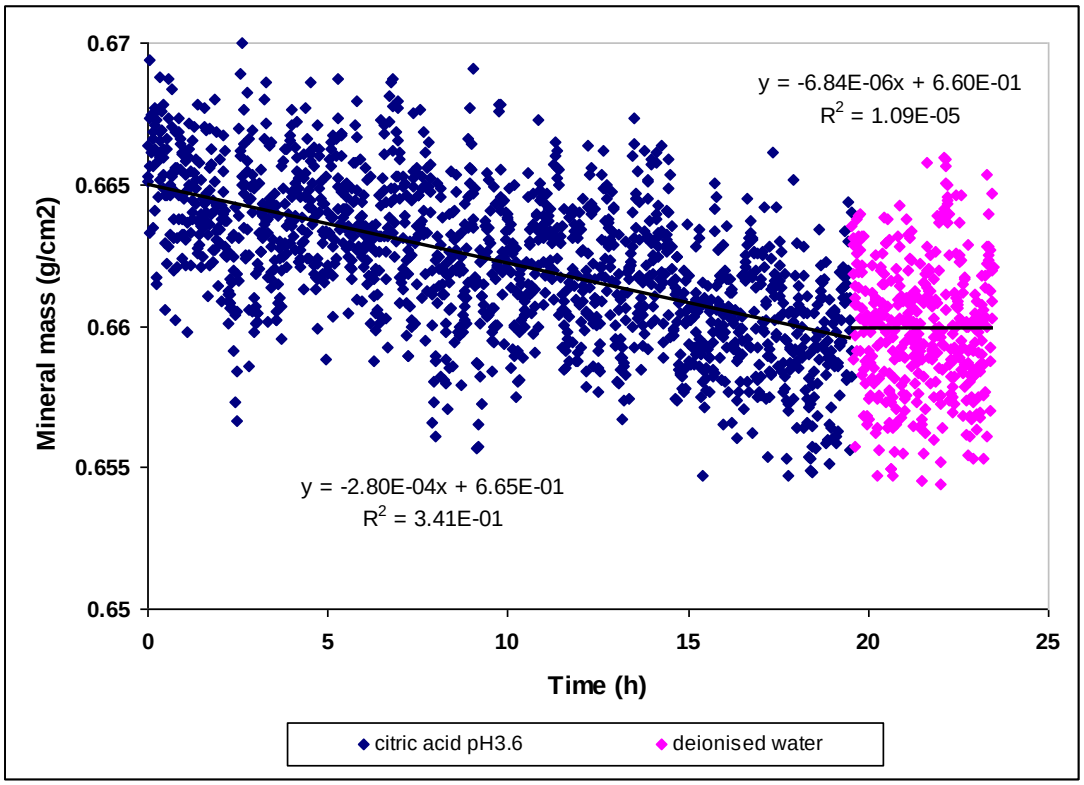

FIGURE 13.3 The change in projected HAp mineral mass content in response to 20 h of demineralisation by 0.3% citric acid pH 3.6 followed by 4 h of de-ionised water

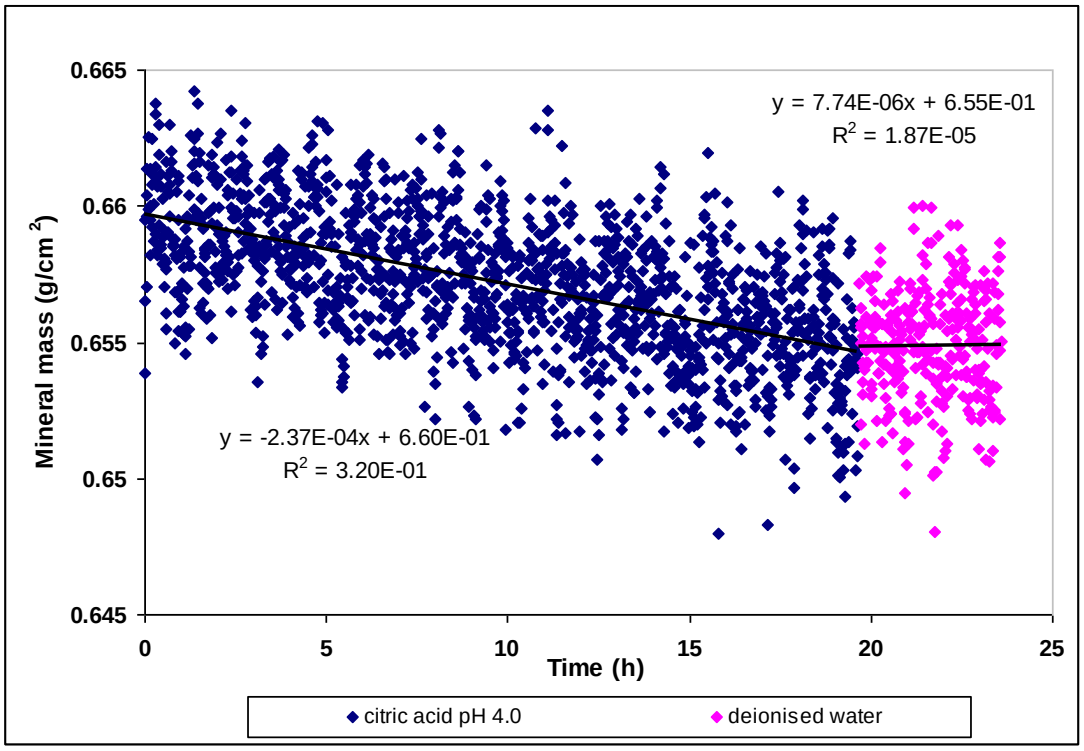

FIGURE 13.4 The change in projected HAp mineral mass content in response to 20 h of demineralisation by 0.3% citric acid pH 4.0 followed by 4 h of de-ionised water

13.4.2 0.1% acetic acid demineralisation solution

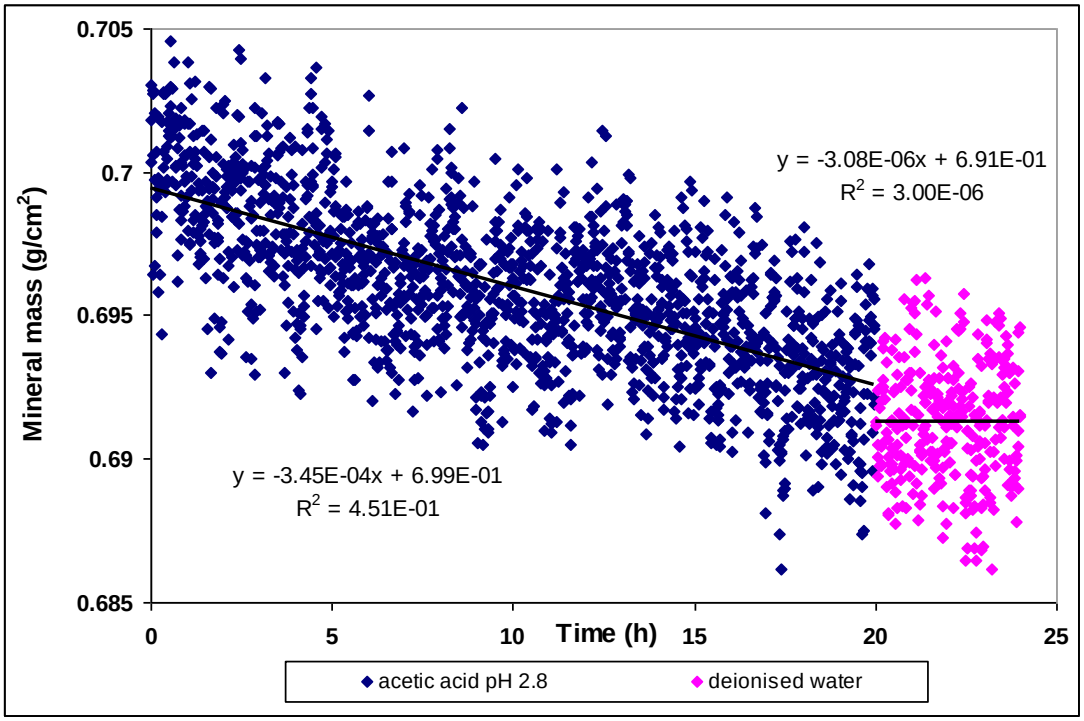

FIGURE 13.5 The change in projected HAp mineral mass content in response to 20 h of demineralisation by 0.1% acetic acid pH 2.8 followed by 4 h of de-ionised water

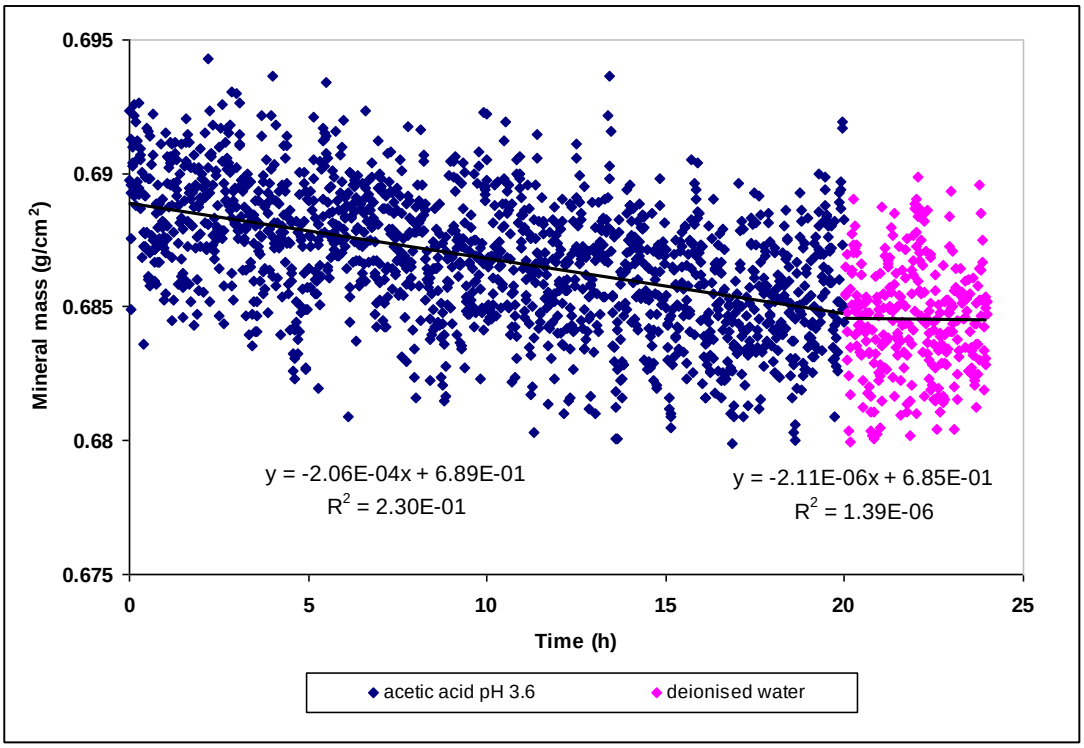

FIGURE 13.6 The change in projected HAp mineral mass content in response to 20 h of demineralisation by 0.1% acetic acid pH 3.2 followed by 4 h of de-ionised water

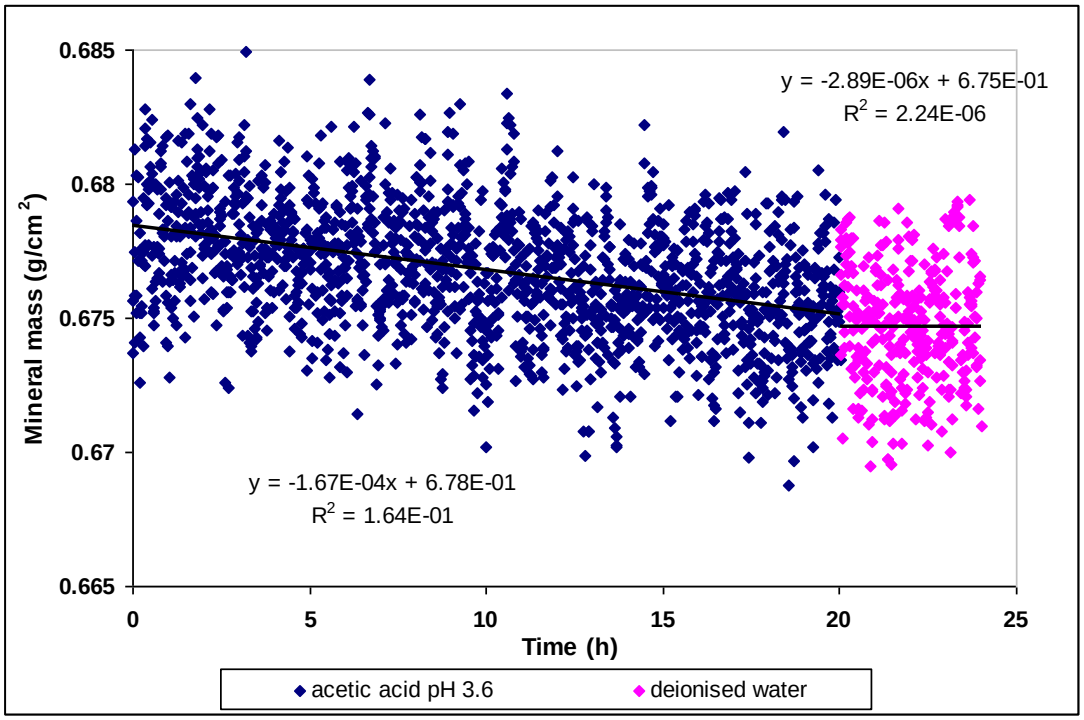

FIGURE 13.7 The change in projected HAp mineral mass content in response to 20 h of demineralisation by 0.1% acetic acid pH 3.6 followed by 4 h of de-ionised water

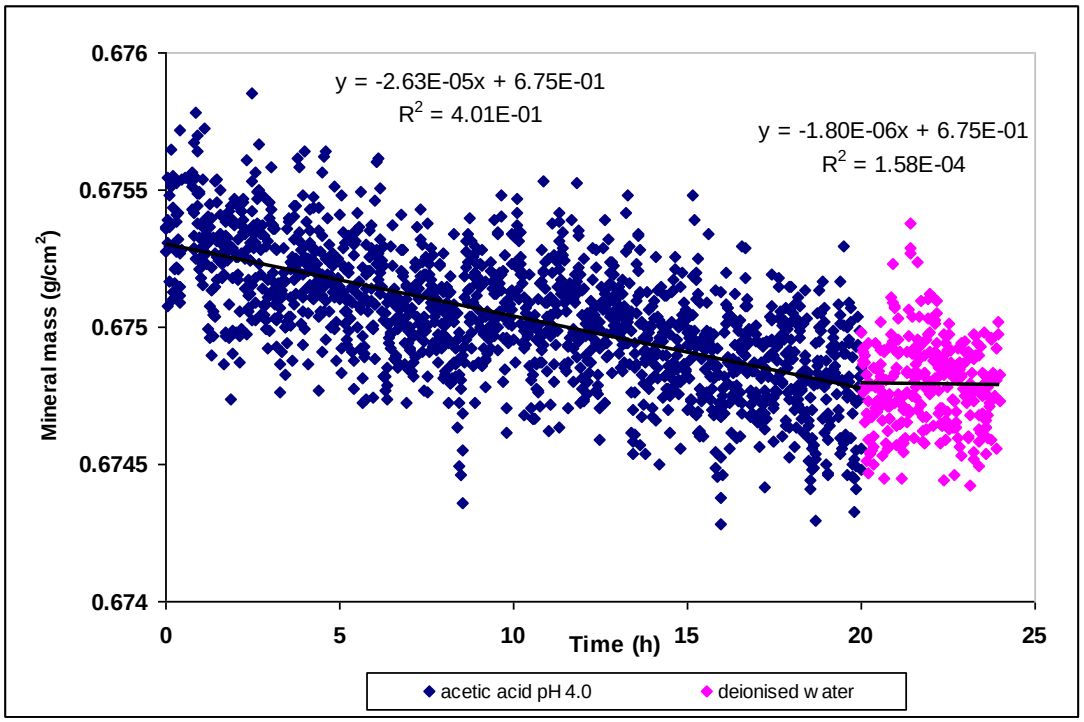

FIGURE 13.8 The change in projected HAp mineral mass content in response to 20 h of demineralisation by 0.1% acetic acid pH 4.0 followed by 4 h of de-ionised water

Figure 13.9 summarises the RD_{HAp} for all demineralisation solutions at the investigated pH range.

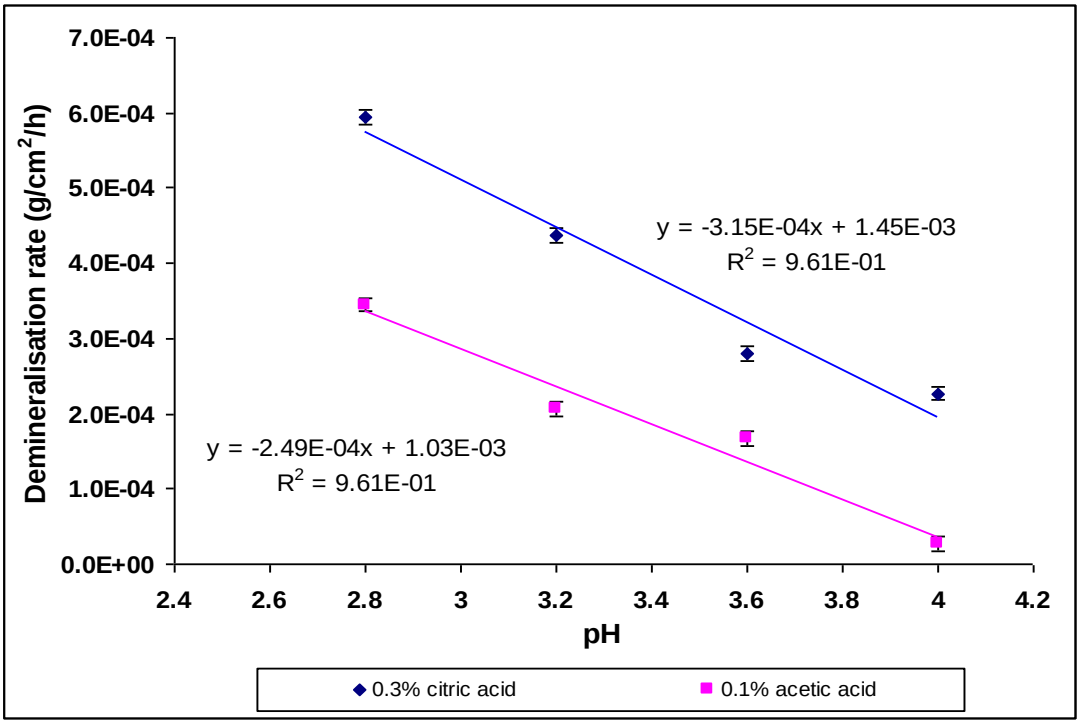

FIGURE 13.9 The change in RD_{HAp} in response to changing the demineralisation solution at a range of pH values

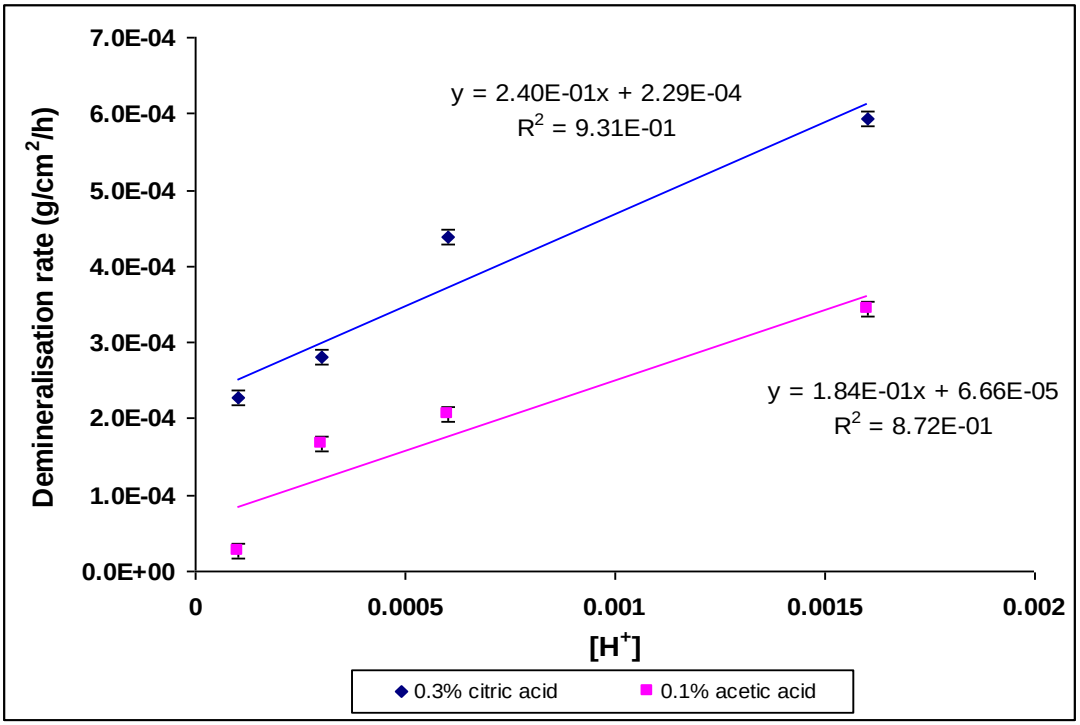

FIGURE 13.10 The change in RD_{HAp} in response to changing the demineralisation solution at a range of $[H^+]$

13.5 Discussion

Previously, SMR has been used to provide precise quantitative measurements of mineral mass changes in real-time in studies measuring the kinetics of demineralisation and remineralisation of enamel and HAp, particularly over long periods of time (up to 1000 h). These long periods of experiments (1 week or more) were required to obtain reliable quantitative kinetic dissolution data. This study has demonstrated that experimental time can be reduced to 20 h while still obtaining enough photon counts to obtain reliable data. This was achieved through optimising the X-ray generator and detection system parameters. In previous experiments, the generator was usually run at lower tube currents and voltages such as 6 mA and 36 kV or 1.5 mA and 45 kV which according to Equation 8.6 give a relative value of X-ray intensity *(I)* of 7776 and 3037 respectively. Increasing the photon energy means increasing the penetration power of the photons and accordingly increasing the photons counts. Therefore, in this study, the current and voltage were increased to 8 mA and 39 kV increased the spectrum intensity to 12108 which represent almost doubling the photon counts (for calculation details refer to Section 8.2.5). By doubling the photon counts, detection of more data over a shorter period of time was achievable and accordingly it became possible to obtain more accurate data during the first 24 h of HAp demineralisation. The results (Figure 13.9) demonstrated that the linear relationship between the loss of mineral mass content and time (previously found with longer SMR studies), is also observed by SMR over the shorter duration used in this study. The essentially linear loss of mineral with time has been attributed to a surface controlled process of dissolution of the mineral at the advancing front of the HAp disc.

A further finding was the instantaneous reduction in the demineralisation rate of the compressed HAp discs following the change to de-ionised water. This suggests that the demineralisation process is a surface controlled process rather than diffusion controlled. If switching from demineralisation solution to de-ionised water resulted in gradual decrease in RD_{HAp}, and hence a curve seen, this would have suggested that a diffusion controlled process in which the diffusion of the dissolution products out the acids and into the compressed HAp disc had an influence on RD_{HAp}. However, taking in consideration the small size and the porosity of the discs, the change in the circulating solution will not take more than few minutes to affect the diffusion whether at the HAp surface or within the pores. Therefore, studying the transient stage should include a close look at the data of the first few minutes of change in solutions. This is not possible with the current technique and experiment methodology. With the amount of data obtained within 1 h or less would be too noisy and inconclusive. Testing the transient stage is beyond the scope of this experiment (Bollet-Quivogne *et al.*, 2005, Bollet-Quivogne *et al.*, 2007).

13.6 Conclusions

In conclusion, the study in this chapter has demonstrated that SMR can be used to quantitatively measure the dissolution of permeable compressed HAp discs under artificial caries and erosion-like conditions for periods of 24 h or less. This technique can be used to measure the efficacy of various therapies to reduce the impact of dental caries and erosion.

CHAPTER 14

Effect of Circulation Speed of Demineralisation Solutions on Compressed Hydroxyapatite Discs Dissolution Rate Studied Using Scanning Microradiography*

14.1 Introduction

The circulation speed of demineralising solution adjacent to a dissolving surface has a considerable influence on the rate of dissolution of solids. This is particularly pertinent to dissolution studies of enamel and similar studies of model systems for dental caries using compressed hydroxyapatite discs as the substrate.

This chapter summarises the experimental study on the effect of the circulation speed of demineralisation solution on permeable compressed HAp disc dissolution kinetics.

14.2 Aims and objectives

The aim of this study was to compare the RD_{HAp} as a function of the demineralisation solution circulation speed.

* The work described in this chapter was presented at the European Organisation for Caries Research Conference (ORCA), Montpellier, France (September, 2010).

The objective of this study was to investigate the effect of pumping speed (solution circulating speed) on compressed HAp discs dissolution rates over a period of 24 h, using SMR.

14.3 Materials and methods

14.3.1 SMR

For details of the SMR technique refer to Chapter 10.

14.3.2 HAp discs

Three randomly selected compressed HAp discs (Plasma-Biotal, UK) were used in this study. All discs were preconditioned, sterilised, and painted with acid resistant nail varnish on all surfaces leaving one surface exposed to the demineralising solution. Each disc was placed in a separate SMR cell and mounted in the centre of the SMR cell chamber (Section 10.6.2).

14.3.3 Demineralisation solutions

0.1% acetic acid solution pH 4.0 was used in this study as representative of dental caries-like conditions. For solution details refer to Section 10.7. The HAp disc exposed surface was subjected to the demineralising solution for duration of 24 h followed by 30 min of de-ionised water. The circulation speed was then changed to the next investigated speed.

14.3.4 Circulating pump

An automatic/manual control multi-channel cassette pump (Watson-Marlow Bredel pumps, Cornwall UK, model 205U), Figure 14.1 and Figure 14.2, was used

with orange colour coded tubes (Altec™, Altec Products Limited, Cornwall, UK, product number116-0532-08, bore size = 0.89 mm) used for pumping solution into the cell, and blue colour coded tubes (product of Altec™, product number 116-0532-08, bore size = 1.65 mm) to pump the solution out of the cell. The pump tubes were then connected to 2.0 m long transmission tube of 1.5 mm diameter, and were securely connected (via Altec™ barbed straight tubing adapter, product number 05-44-5513), to butterfly needles (Hospira Venisystems Butterfly®, product number P293A05, needle length 20.0 mm, needle diameter 0.8 mm), which were inserted into the cells as shown in Figure 14.1 and 14.2.

FIGURE14.1 Watson Marlow 205U electric pump with circulating solution

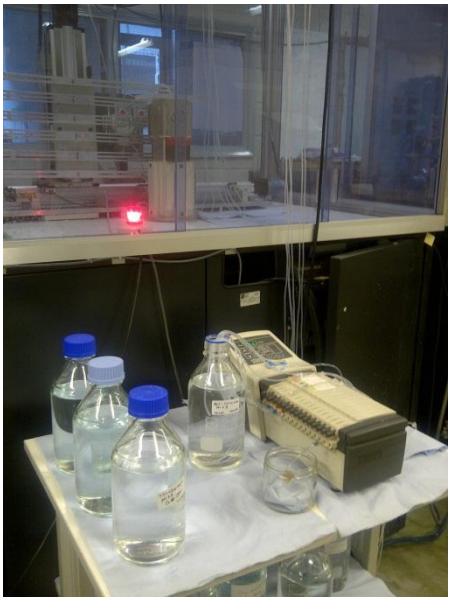

FIGURE 14.2 The electric pump connected to the SMR cells via tubing while the demineralisation solution circulates into and out of the SMR cells

TABLE 14.1 Manufacturer tubes specifications and flow rate as factor of change in pumping speed

Tube code	Orange / Orange	Blue / Blue
Pore size	0.89 mm	1.65 mm
Flow rate at 0.5 RPM	0.016 ml/min	0.043 ml/min
Flow rate at 90 RPM	2.92 ml/min	7.69 ml/min

The flow rate at each of the circulating speeds to be used in this experiment (0, 6, 12, 18, 24, 30, 36 RPM) was measured, using orange-orange tubes, and calculated in ml/min (Table 14.2).

TABLE 14.2 The measured flow rate in ml/min corresponding to each circulating speed in RPM.

Parestaltic pump speed (RPM)	**0**	**6**	**12**	**18**	**24**	**30**	**36**
Measured flow rate (ml/min)	0	0.19	0.39	0.58	0.80	0.97	1.17

The demineralising solutions were circulated around the compressed HAp disc at various circulating speeds of 0, 6, 12, 18, 24, 30, 36 RPM (0, 0.19, 0.39, 0.58, 0.80, 0.97, and 1.17 ml/min respectively). The investigated solution circulation speeds were chosen in the range of slow speeds in order to keep mechanical erosion of the surfaces to a minimum and avoid the possibility of cell tube/cell leakage while maintaining a continuous circulation. Each measurement was repeated in triplicate. All experiments were run in a thermostatically controlled laboratory at a temperature of 22°C ± 1°C.

14.4 Results

For each of the 21 experiments, the relative mass per unit area of the compressed HAp disc was measured over the 24 h demineralisation cycle and the RD_{HAp} was calculated (Table 14.3).

TABLE 14.3 The calculated RD_{HAP} during the exposure to 0.1% acetic acid pH 4.0 at various circulation speeds (in triplicate)

Peristaltic pump speed (RPM)	Peristaltic pump speed (ml/min)	RD_{HAp} (1) $g/cm^2/h$	RD_{HAp} (2) $g/cm^2/h$	RD_{HAp} (3) $g/cm^2/h$	Mean RD_{HAp} $g/cm^2/h$
0	0	$6.13x10^{-6}$	$6.85x10^{-6}$	$6.76x10^{-6}$	$6.58x10^{-6}$
6	0.19	$1.20x10^{-4}$	$1.13x10^{-4}$	$1.22x10^{-4}$	$1.18x10^{-4}$
12	0.39	$1.48x10^{-4}$	$1.62\ x10^{-4}$	$2.14x10^{-4}$	$1.70x10^{-4}$
18	0.58	$2.44x10^{-4}$	$2.56x10^{-4}$	$2.42x10^{-4}$	$2.40x10^{-4}$
24	0.80	$2.68x10^{-4}$	$2.92x10^{-4}$	$2.92x10^{-4}$	$2.72x10^{-4}$
30	0.97	$3.07x10^{-4}$	$3.03x10^{-4}$	$2.97x10^{-4}$	$3.13x10^{-4}$
36	1.17	$3.12x10^{-4}$	$3.17x10^{-4}$	$3.19x10^{-4}$	$3.16x10^{-4}$

Typical examples of the real-time change in HAp projected mineral mass following the exposure to 0.1% acetic acid pH 4.0 with demineralisation solution circulation speeds between 0.00 and 0.97 ml/min are demonstrated in Figure 14.4 and Figure 14.5 respectively.

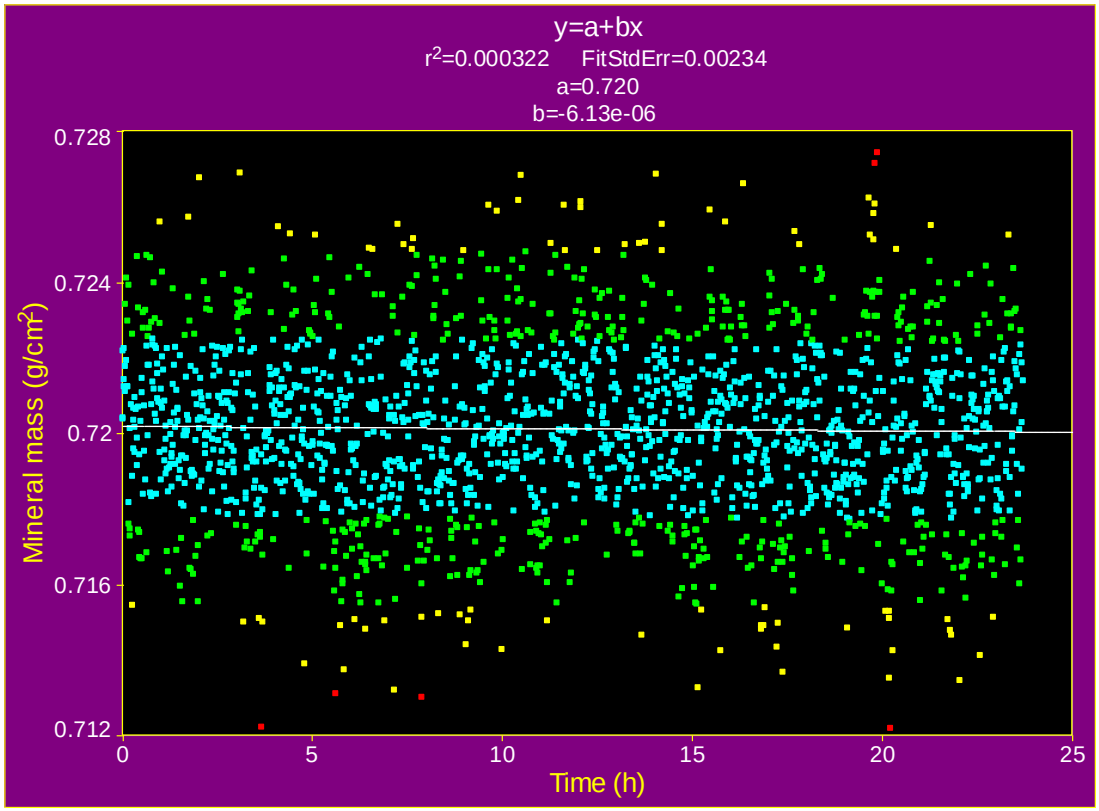

FIGURE 14.3 Typical example of the change in projected HAp mineral mass content over a period of 24 h in response to 0.1% acetic acid pH 4.0 demineralisation solution at 0 ml/min circulation speed

(■ Within 1 SD, 1 SD< ■ < 2 SD, 2 SD< ■ < 3 SD, 3 SD< ■ < 4 SD)

TABLE 14.4 Statistical analysis, for the data in Figure 14.3, using TableCurve 2D®

	Value	SE	t-value	95% Confidence Limits	
a (g/cm^2)	0.720	1.067e-04	6748.5202	0.7199	0.7204
b (g/cm^2/h)	-6.13e-6	7.791e-06	-0.786	-2.141e-5	9.154e-6

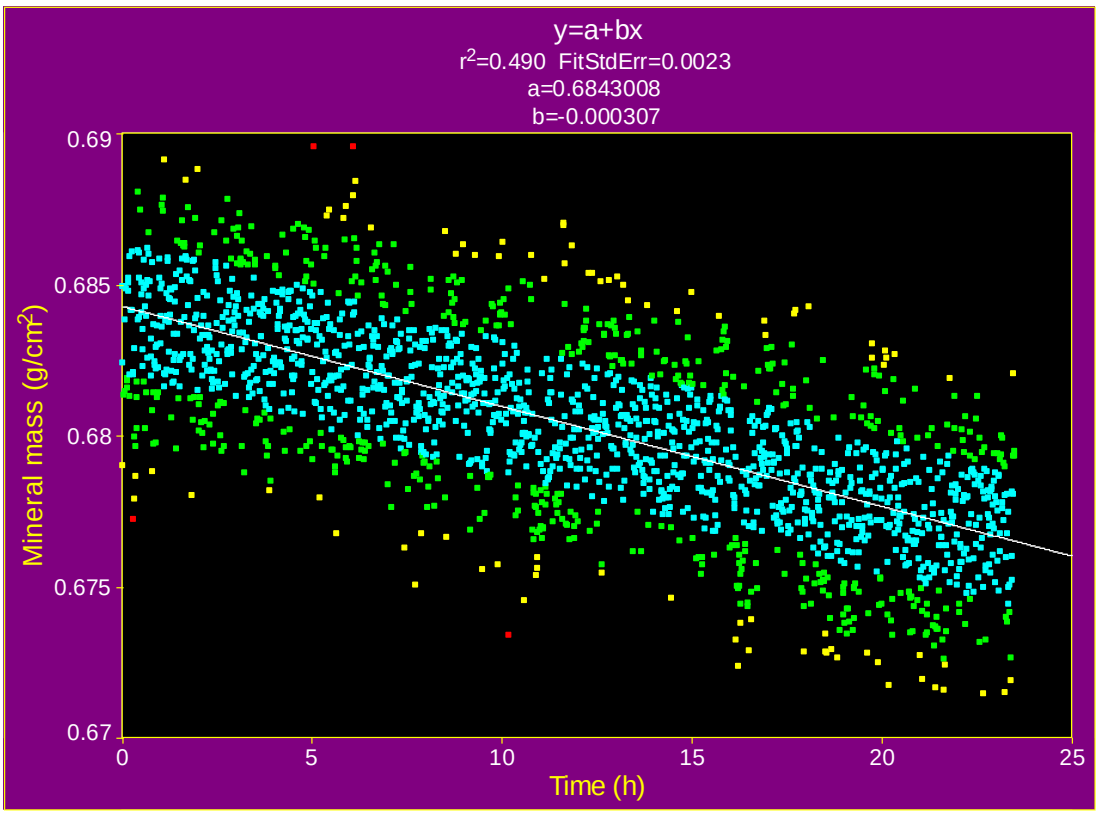

FIGURE 14.4 Typical example of the change in projected HAp mineral mass content over a period of 24 h in response to 0.1% acetic acid pH 4.0 demineralisation solution at 0.97 ml/min circulation speed

(■ Within 1 SD, 1 SD< ■ < 2 SD, 2 SD< ■ < 3 SD, 3 SD< ■ < 4 SD)

TABLE 14.5 Statistical analysis, for the data in Figure 14.4, using TableCurve 2D®

	Value	SE	t-value	95% Confidence Limits	
a (g/cm^2)	0.684	1.047e-04	6533	0.6840	0.6845
b($g/cm^2/h$)	-3.07e-4	7.71e-06	-42.86	-3.22e-4	- 2.92e-4

The mean RD_{HAp} ($g/cm^2/h$) for the triplicate experiments at each circulation speed was calculated and plotted against demineralisation solution circulation speed (ml/min) as demonstrated in Figure 14.5.

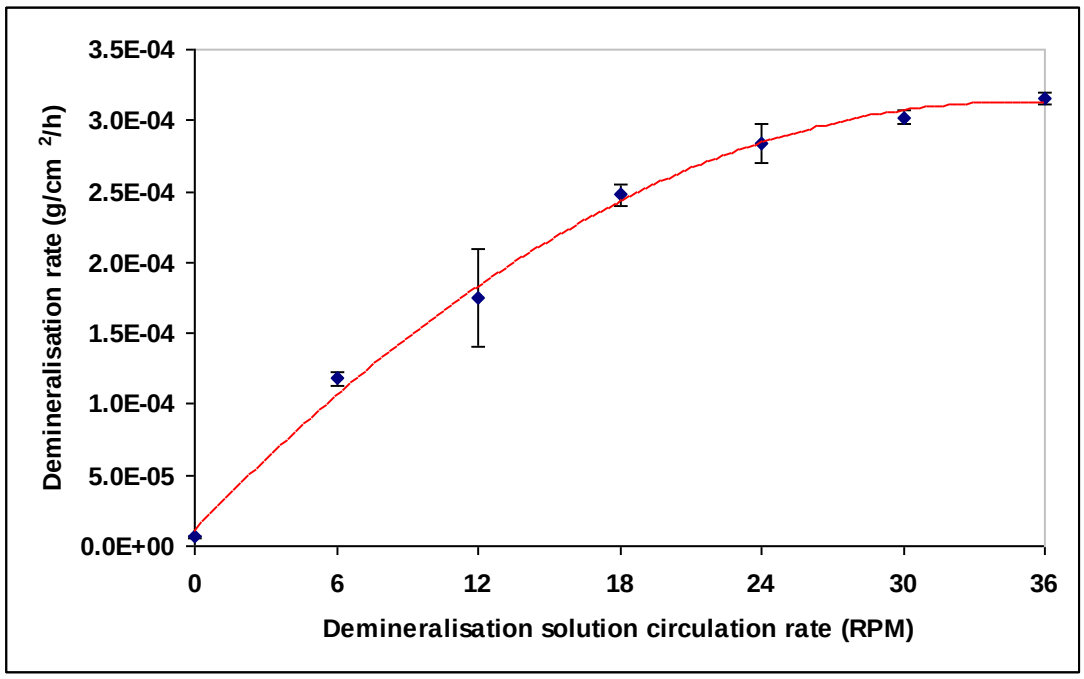

FIGURE 14.5 The mean rate of demineralisation ($g/cm^2/h$) plotted against the change in demineralisation solution circulation speed (RPM). A curve has been fitted for viewing purposes only

14.5 Discussion

In this study the demineralising solution circulation speed was altered with all other factors maintained constant in an attempt to study the effect of circulation speed on the RD_{HAp}. The selection criteria for the choice of the tested circulation speed involved; Firstly, the circulation rate should be fast enough to keep the solution in the SMR cell in state of pseudo constant composition without subjecting the fine SMR tubes to the danger of leakage/rupture. Secondly, to have a solution circulation rate that provides minimal possible physical erosion to the HAp disc. Therefore it was decided to test 0, 6, 12, 18, 24, 30, 36 RPM circulation rates. The calculated RD_{HAp} of the triplicate experiments at each circulation speed were similar

in value with a small standard deviation (Table 14.3). This represents the precision, repeatability and accuracy of the results.

Figure 14.3 represents a typical example of the effect of 0.1% acetic acid pH 4.0 on the RD_{HAp} when circulated at 0.00 ml/min. When the mineral mass content of the projected HAp was plotted against time for the 24 h scanning duration, 1800 scanning measurements were recorded. 1708 measurements were within 2 SE showing a good fit of the data. The data showed a hardly recognisable deceleration trend in the RD_{HAp} $6.13x10^{-6}$ $g/cm^2/h$ indicating that when the flow rate was zero, the compressed HAp discs dissolution rate was minimal. As the compressed HAp disc dissolves, its dissolution products of calcium, phosphate and hydroxyl ions neutralise the acidity of the acetic acid and quickly the acid loses its acidic strength.

When the circulation rate was increased to 0.97 ml/min the RD_{HAp} mineral mass content was measured by 1800 scanning measurements over 24 h. 1718 points from the obtained data fell within the range of 2 SE.

The mean of the triplicate experiment was $3.13x10^{-4}$ $g/cm^2/h$ with SE of $5.05x\ 10^{-6}$. The overall trend showed a linear and consistent regression in HAp mineral content over 24 h.

Figure 14.5 shows an exponential relationship between the mean RD_{HAp} in response to changes in the demineralisation solution circulation rate. Comparing the mean RD_{Hap} for each two successive circulation rates reveals that the change in RD_{HAp} was statistically significant as the demineralisation solution circulation rate increased from 0 RPM to 6 RPM, from 6 RPM to 12 RPM and from 12 RPM to 18 RPM. The calculated P value for each two successive circulation rates was 0.01, 0.05, and 0.01 respectively. However, as the demineralisation solution circulation

increased above 18 RPM the change in RD_{HAp} became statistically insignificant with P values of 1.78, 1.22 and 0.75 for demineralisation solution circulation rate changing from 18 RPM to 24 RPM, from 24 RPM to 30 RPM and from 30 RPM to 36 RPM respectively.

14.6 Conclusions

This study demonstrates that the solution composition in contact with a demineralising HAp surface achieved by sufficient circulation speed, or stirring, is an important parameter in HAp dissolution studies. Diffusive transport of dissolved substrate away from the dissolving HAp surface will influence the kinetics of the process.

This study helped in developing the research protocol to be used in the rest of the experiments in this thesis with regard to selecting the demineralisation solution circulation speed. It was decided to select 24 RPM (0.80 ml/min) as it was the highest circulating speed that showed a significant increase in RD_{HAp}.

CHAPTER 15

Effect of High Concentration of Strontium Ions (Sr^{2+}) on Hydroxyapatite Dissolution Kinetics Studied Using Scanning Microradiography

15.1 Introduction

Toothpastes containing Sr^{2+} were introduced to the market around five decades ago for the treatment of tooth hypersensitivity. Strontium chloride and strontium acetate were the most commonly used strontium compounds (Hughes *et al.*, 2010, Mason *et al.*, 2010). Strontium acetate has the advantage of being compatible with fluoride (Cummins, 2010). Toothpastes containing 6% and 8% strontium acetate showed rapid and lasting relief of hypersensitivity (Layer and Hughes, 2010). The chemical similarity between Sr^{2+} and Ca^{2+} made it possible for Sr^{2+} to replace Ca^{2+}, in various structures in the body, including HAp . The effect of Sr^{2+} on RD_{HAp} remains an area of controversy (Kikuchi *et al.*, 1994, Bigi *et al.*, 2007). For further details on Sr^{2+} background refer to Chapter 6.

15.2 Aims and objectives

The aim of this pilot study was to study the effect of Sr^{2+}, at concentrations comparable to those found in desensitising toothpastes, on the dissolution kinetics of porous HAp discs.

The objective was to measure the rate of HAp dissolution in permeable HAp discs using SMR under strictly controlled thermodynamic conditions at Sr^{2+} concentrations relevant to desensitising toothpastes.

15.3 Materials and methods

15.3.1 HAp discs

Two HAp discs were used in this study. The details of the HAp disc preparation are described in Section 10.6.2.

15.3.2 Demineralisation solutions

Four solutions were prepared at strontium concentrations reported in desensitizing toothpastes containing 6% and 8% strontium acetate (Layer and Hughes, 2010);

1) 1 litre of 0.1% acetic acid pH 4.0 with 6% strontium acetate *(SIGMA-ALDRICH*™ product # 388548-500G and batch # 01715JJ).

2) 1 litre of 0.1% acetic acid pH 4.0 with 8% strontium acetate.

3) 1 litre of de-ionised water pH 7.0 with 6% strontium acetate (60,000 ppm)

4) 1 litre of de-ionised water pH 7.0 with 8% strontium acetate (80,000 ppm).

The pH of each solution was adjusted following addition of strontium acetate by addition of HCl or KOH 1 Molar solutions as necessary. The solutions were circulated at 0.80 ml/min (Table 14.2).

15.3.3 SMR

SMR Cell 1 contained 1 HAp disc that was exposed to 0.1% acetic acid pH 4.0 with 6% (60,000 ppm) strontium acetate then 0.1% acetic acid pH 4.0 with 8%

(80,000 ppm) strontium acetate for 40 h each. The two demineralising solution cycles were separated by 24 hours of de-ionised water.

SMR Cell 2 contained 1 HAp disc exposed to 6% (60,000 ppm) strontium acetate in de-ionised water followed by 8% (80,000 ppm) strontium acetate for 40 h each, separated by 24 h of de-ionised water.

15.4 Results

15.4.1 0.1% acetic acid pH 4.0 with 6% strontium acetate

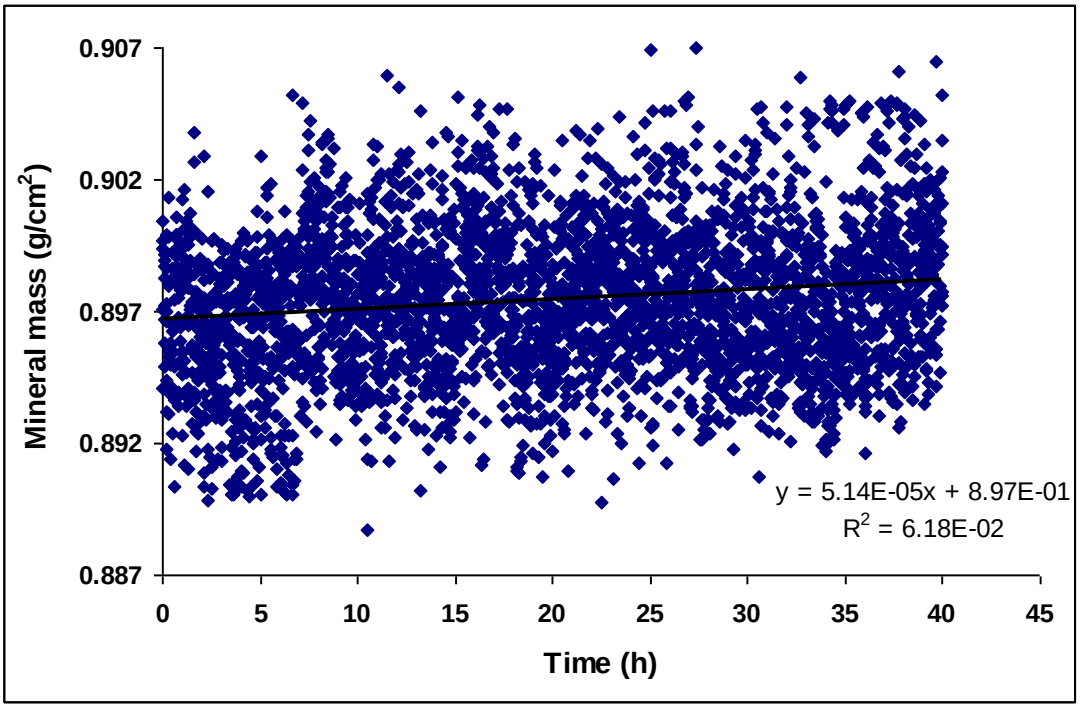

FIGURE 15.1 Increased projected HAp mineral mass content over a period of 40 h in response to exposure to 0.1% acetic acid pH 4.0 demineralisation solution containing 6% strontium acetate

The results of the effect of 0.1% acetic acid pH 4.0 with 6% strontium acetate on RD_{HAp} are shown in Figure 15.1. The RD_{HAp} was stopped and the projected HAp mineral mass content increased at a rate of 5.14×10^{-5} g/cm^2/h.

15.4.2 0.1% acetic acid pH 4.0 with 8% strontium acetate

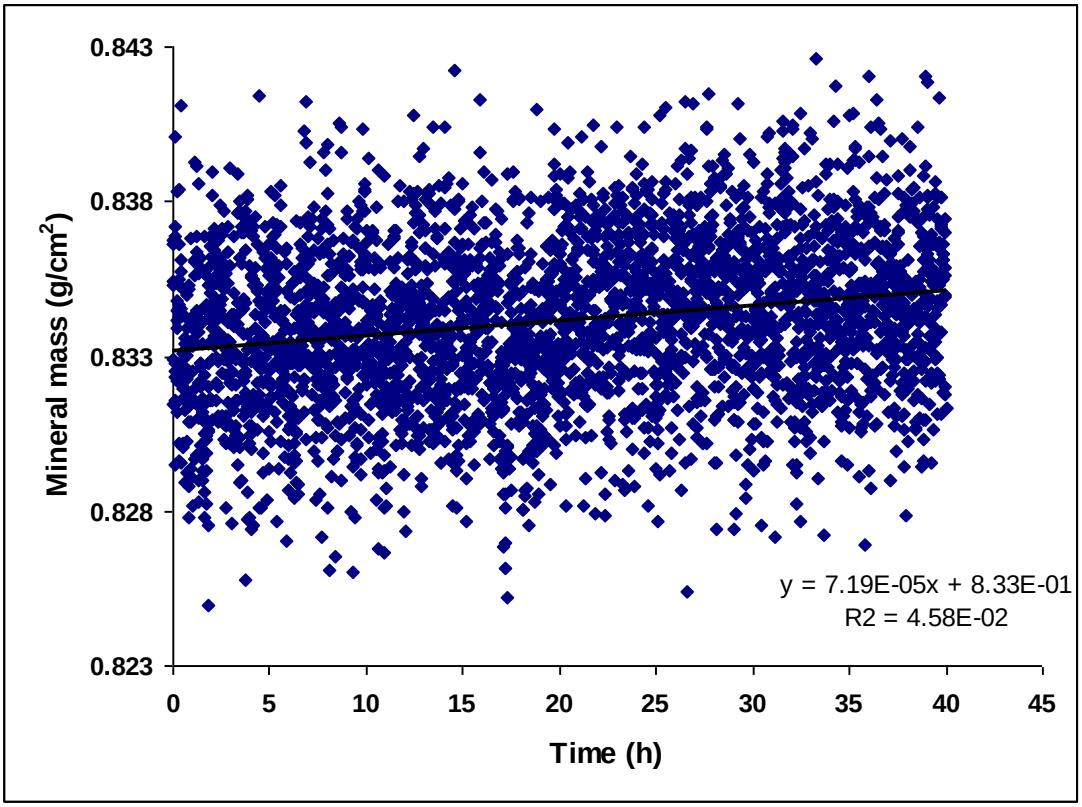

FIGURE 15.2 Increased projected HAp mineral mass content over a period of 40 h in response to exposure to 0.1% acetic acid pH 4.0 demineralisation solution containing 8% strontium acetate

The results of the effect of 0.1% acetic acid pH 4.0 with 8% strontium acetate on RD_{HAp} are shown in Figure 15.2. The RD_{HAp} was stopped and the projected HAp mineral mass content increased at a rate of 7.19×10^{-5} g/cm^2/h.

15.4.3 De-ionised water pH 7.0 with 6% strontium acetate

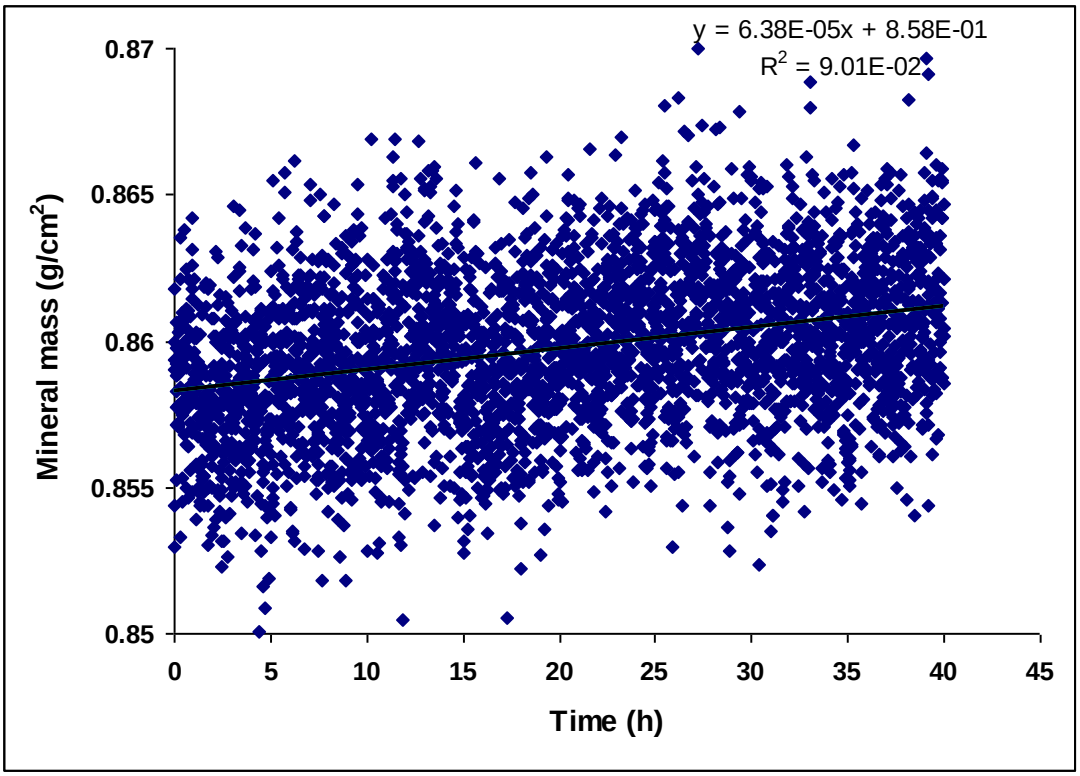

FIGURE 15.3 Increased projected HAp mineral mass content over a period of 40 h in response to exposure to de-ionised water pH7 containing 6% strontium acetate

The results of the effect of de-ionised water pH 7.0 with 6% strontium acetate on RD_{HAp} are shown in Figure 15.3. The RD_{HAp} was stopped and the projected HAp mineral mass content increased at a rate of 6.38×10^{-5} g/cm^2/h.

15.4.4 De-ionised water pH 7.0 with 8% strontium acetate

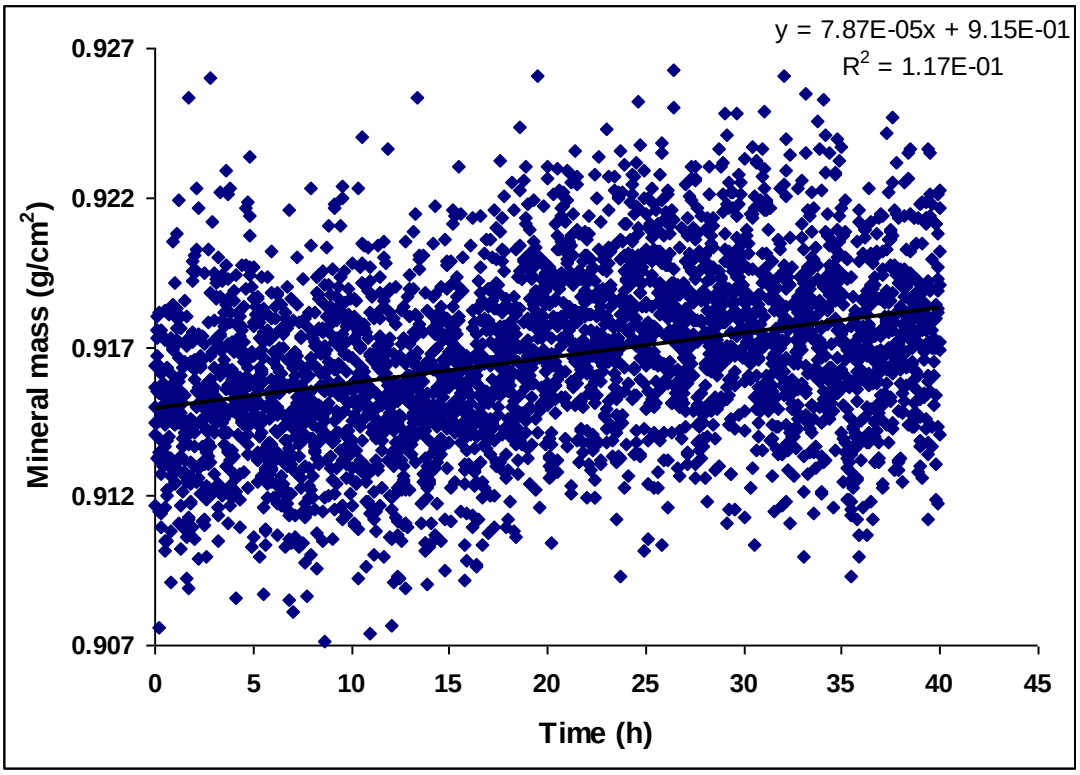

FIGURE 15.4 Increased projected HAp mineral mass content over a period of 40 h in response to exposure to de-ionised water pH7 containing 8% strontium acetate

The results of the effect of de-ionised water pH 7.0 with 8% strontium acetate on RD_{HAp} are shown in Figure 15.4. The RD_{HAp} was stopped and the projected HAp mineral mass content increased at a rate of 7.87×10^{-5} g/cm^2/h.

15.5 Discussion

Demineralisation halted when the porous HAp disc was exposed to 0.1% acetic acid solution pH 4.0 containing either 6% or 8% strontium acetate. Over a period of 40 hours the mineral mass content of the HAp disc exposed to the demineralisation solutions actually *increased*. Similar results were obtained when the

HAp disc was exposed to solutions containing 6% and 8% strontium acetate at pH 7.0.

The literature did not reveal any previous demineralisation experiments with solutions containing high strontium concentrations with which to compare the results. A possible explanation for the halt in RD_{HAp} and increase in the mineral mass content suggests that Sr^{2+} was precipitated on the HAp surface. Another possibility is that the high Sr^{2+} concentration in the solution might have affected the X-ray detection by the detector causing fewer photon counts, reflected as increased mineral mass content at the HAp disc.

Therefore in order to have good understanding of the effect of Sr^{2+} on RD_{HAp} it was decided to test the effect of strontium at low concentrations such as Sr^{2+} concentrations in water on the HAp dissolution kinetics.

15.6 Protocol summary

Based on the results obtained from Chapters 11-15, a final protocol for the experiments in this thesis has been developed.

Plasma-Biotal compressed permeable HAp discs will be used as a model for dental enamel (Chapter 11 and Chapter 12). The HAp discs should be preconditioned and sterilised (Section 10.6.2) prior to placement at the centre of the SMR cell. The HAp discs will be scanned using the modified SMR technique for measuring the RD_{HAp} over a period of 20 h to resemble the oral condition as much as possible while insuring obtaining enough photon counts for a reliable data. A statistician was consulted in regards to the sample size. Ideally the larger the sample size the more statistically sound and reliable the results are, but due to the nature of the SMR

experiments (length of the experiments and the large number of counts obtained over 20 h) it was justifiable to duplicate the experiments.

Based on the sampling time discussed in Section 10.5, scanning more than one SMR cell simultaneously would not affect the calculated RD_{HAp}, therefore the duplicate experiments will be run at the same time by scanning 2 SMR cells simultaneously. 0.1% acetic acid pH 4.0 demineralisation solution will be used a representative of caries-like condition and 0.3% citric acid pH 2.8 will be used for erosion-like conditions. These concentrations have been previously used in published work by the Dental Physical Sciences Laboratory at Queen Mary, University of London as well as by the Dental Materials Science Laboratory at the School of Oral and Dental Sciences, University of Bristol. The demineralisation solutions will be circulated at 24 RPM (0.80 ml/min) circulation speed (Section 14.6). The three divalent metal cations to be investigated are Zn^{2+}, Sr^{2+} and Cu^{2+}.

Zinc will be investigated at a range of concentrations relevant to Zn^{2+} concentrations in dental plaque (0, 5, 10, 15, and 20 ppm) (Section 16.2). Sr^{2+} will be investigated at a range of concentrations relevant to Sr^{2+} concentration in drinking water (0, 5, 10, 20, and 30 ppm) (Section 17.2) and Cu^{2+} will be investigated at a range of concentrations (0, 11.25, 22.50, 45, 90, 150 and 180 ppm) relevant to Cu^{2+} concentrations that have been investigated in other studies (Section 18.5).

Each cation will be investigated in a series of experiments in an increasing concentration sequence (e.g. 0, 5, 10, 15, and 20 ppm) or a series of experiments in a decreasing concentration sequence (e.g. 20, 15, 10, 5, and 0 ppm). All concentrations in one sequence, increasing or decreasing, should be done on the same HAp disc. For each cation concentration, the RD_{HAp} will be measured over a period of 20 h followed by 30 min of washing the HAp disc by de-ionised water at 90 RPM to

remove any loosely attached substances, followed by the next concentration for another 20 h and so on, through the whole series of increasing or decreasing concentration sequence. The idea behind investigating all different concentrations on a single HAp disc in a sequence of increasing or decreasing concentration sequence is an attempt to explore whether the investigated cation exhibits a long lasting effect. In that case the effect of the different concentrations, represented by RD_{HAp}, in an increasing concentration sequence will show a different trend (pattern) than the trend shown by the same concentrations when investigated in a decreasing concentration sequence. In reverse, if both sequences of cation increasing and decreasing concentrations showed the same trend of effect on RD_{HAp} regardless of the type of sequence, this would be an indication that the cation showed a surface effect.

A summary of the final developed protocol for the experiments in this thesis is shown in Table 15.1.

TABLE 15.1 A summary of the protocol to be used in the SMR studies in this thesis

Protocol component	Conclusion
SMR technique and scanning duration	▪ The modified SMR technique for measuring RD_{HAp} over 24 h or less, to be used in this thesis ▪ Twenty hours of demineralisation is sufficient to be used as scanning duration and HAp discs to be washed with de-ionised water at 90 RPM for 30 min between different experimental conditions to remove any loosely bound substances on the surface
Selection of HAp discs	▪ Permeable compressed sintered Plasma-Biotal HAp discs will be used in this thesis as

	representative of dental enamel
Types of demineralisation solutions	▪ 0.1% acetic acid pH 4.0 simulating caries-like conditions ▪ 0.3% citric acid pH 2.8 simulating erosion-like conditions
Demineralisation solution circulation rate	▪ 24 RPM (0.80 ml/min) demineralisation solution circulation speed
Zn^{2+} concentration	▪ Zn^{2+} will be investigated at concentrations relevant to Zn^{2+} concentration in dental plaque (e.g. 0, 5, 10, 15, and 20 ppm)
Sr^{2+} concentration	▪ High Sr^{2+} concentrations such as in desensitising toothpastes are not suitable for use in studying RD_{HAp} using the SMR technique, instead low Sr^{2+} concentrations such as Sr^{2+} concentrations in water (0, 5, 10, 20, and 30 ppm) will be used
Cu^{2+} concentration	▪ Cu^{2+} will be investigated at a range of concentrations (0, 11.25, 22.50, 45, 90, 150 and 180 ppm) relevant to Cu^{2+} concentrations that have been investigated in other studies

PART IV: EXPERIMENTAL WORK

CHAPTER 16

Effect of Zinc Ions (Zn^{2+}) on Hydroxyapatite Dissolution Kinetics Studied Using Scanning Microradiography *

16.1 Introduction

Zinc is a dietary essential trace element that was long ago incorporated in toothpastes because of its antiplaque activity and ability to reduce calculus formation as well as oral malodor (background information about Zn^{2+} was discussed in Chapter 5). Few studies have been conducted on the direct effects of Zn^{2+} on HAp dissolution under either erosion or caries-like conditions. The exact mechanism by which the Zn^{2+} divalent metal cation alters HAp dissolution kinetics has been an issue of controversy (Section 5.6).

16.2 Aims and objectives

The aim of this study was to study the effect of Zn^{2+} on the dissolution kinetics of permeable HAp discs, at a range of concentrations relevant to Zn^{2+} concentrations in plaque.

* The work described in this Chapter was presented at the 2nd Zinc-UK meeting, London, UK (October 2010) and at the European Organisation for Caries research Conference, Kaunas, Lithuania, (July, 2011)

The objectives were to measure the RD_{HAp} under strictly controlled thermodynamic conditions at a range of 0, 5, 10, 15 and 20 ppm Zn^{2+} over a period of 20 h using SMR.

16.3 Materials and methods

The general protocol of the experiment is illustrated in Figure 16.1.

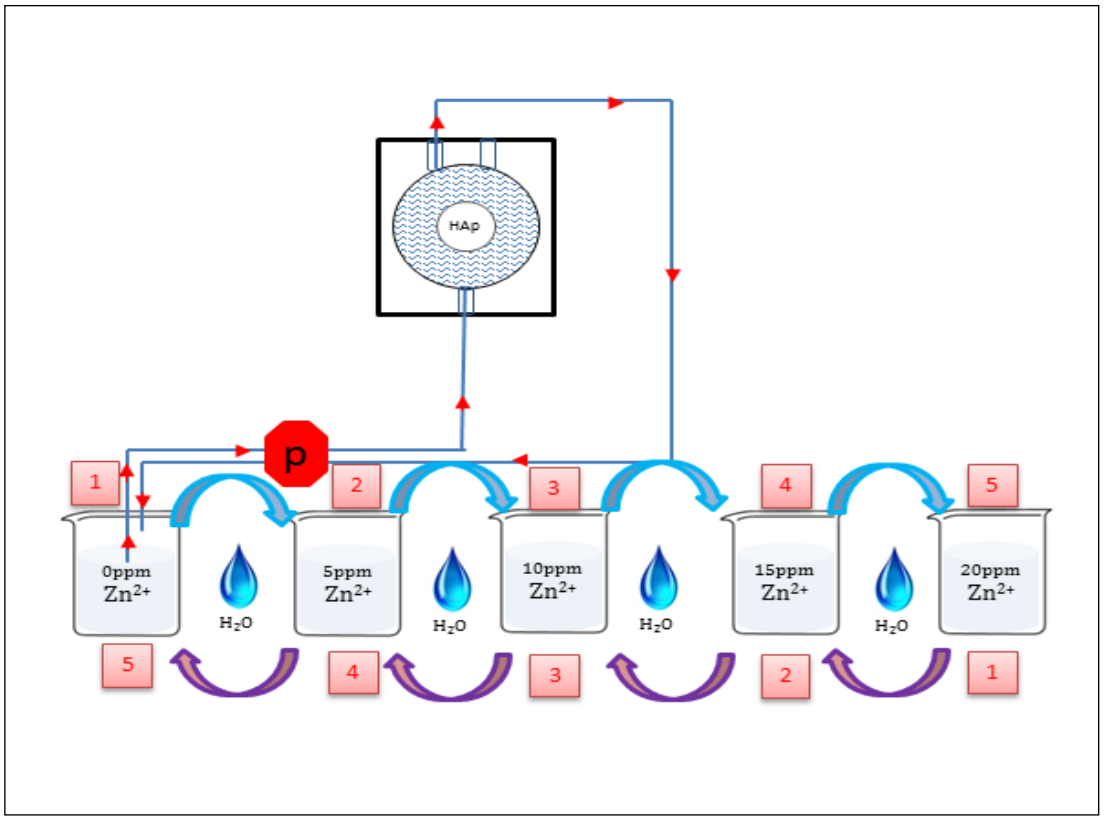

FIGURE 16.1 Schematic diagram of a SMR cell with HAp disc in place connected to the peristaltic pump (p) for circulating the demineralisation solution over a period of 20 h followed by 30 minutes of de-ionised water at both increasing ∩, and decreasing ∪ Zn^{2+} concentration sequence

16.3.1 HAP discs

Eight HAp discs were used in this study. The details of the HAp disc preparation were described in Section 10.6.2.

16.3.2 Demineralisation solutions

A 5 litre batch solution of 0.1% acetic acid pH 4.0 was divided into five x 1 litre bottles. Into each, zinc acetate (Fisher Scientific UK Limited, Leicesester, UK, code # Z/0700/50 and batch # 0951237) was added, so that the final Zn^{2+} concentration was 0, 5, 10, 15 or 20 ppm. The solution pH was adjusted following addition of zinc acetate by using 1 Molar HCl or KOH solutions as necessary.

Similarly, a 5 litre batch solution of 0.3% citric acid pH 2.8 was divided into five 1 litre bottles. Into each, zinc acetate (product of Fisher Scientific UK Limited, Leicesester, UK, code # Z/0700/50 and batch # 0951237) was added, so that the final concentration Zn^{2+} was 0, 5, 10, 15 and 20 ppm. The solution pH was adjusted following addition of zinc acetate by using 1 Molar HCl or KOH solutions as necessary (Section 10.7). The demineralisation solutions were circulated at 0.80 ml/min.

16.3.3 SMR

Four HAp discs were fixed centrally in four SMR cells and demineralising solutions were circulated at 0.80 ml/min. The RD_{HAp} was measured at a single centrally located point on each disc for approximately 20 h at 22 ± 1°C. Each experiment was repeated twice for both experiments with increasing, and decreasing Zn^{2+} concentration steps. The same HAp disc was used for the entire series of different Zn^{2+} concentrations, whether at increasing or decreasing Zn^{2+} concentration sequences, with the disc being washed with de-ionised water for 30 min between each Zn^{2+} concentrations sequences.

For the increasing Zn^{2+} concentration sequence 20 h experiments; the HAp disc was exposed to demineralising solution, with no Zn^{2+} added; followed by 30 min of washing by de-ionised water, followed by 20 h of exposure to demineralising

solution with 5 ppm Zn^{2+}, followed by 30 min of washing by de-ionised water and so on through all the Zn^{2+} different concentrations. All steps were performed using the same HAp disc. In reverse, the decreasing sequence Zn^{2+} concentration experiments, the same HAp disc was exposed for 20 h to demineralising solution with, 20 ppm Zn^{2+}, followed by 30 min of washing by de-ionised water, followed by 20 h of exposure to demineralising solution with 15 ppm Zn^{2+}, followed by 30 min of washing by de-ionised water and so on through the decreasing Zn^{2+} concentrations. Each experiment was duplicated.

16.4 Results

16.4.1 0.1% acetic acid pH 4.0

For each one of the 20 acetic acid pH 4.0 demineralisation solutions experiments (containing five different Zn^{2+} concentrations), the mineral mass loss of each HAp disc was continuously measured throughout the experimental duration. Figure 16.2 and Figure 16.3 are typical examples of the real-time change in the projected HAp mineral mass content in response to exposure to 0.1% acetic acid solution pH 4.0 with 5 ppm Zn^{2+} for both increasing and decreasing Zn^{2+} concentration sequences respectively.

Figure 16.2 shows that the HAp projected mineral mass content decreased from 0.722 g/cm^2 to 0.715 g/cm^2 in 20 h. This reduction represents only a 0.9% loss of the projected HAp mineral mass over 20 h. While for Figure 16.3 the HAp projected mineral mass content decreased from 0.691 g/cm^2 to 0.684 g/cm^2 in 20 h which represents only a 1% loss in the HAp projected mineral content over 20 h.

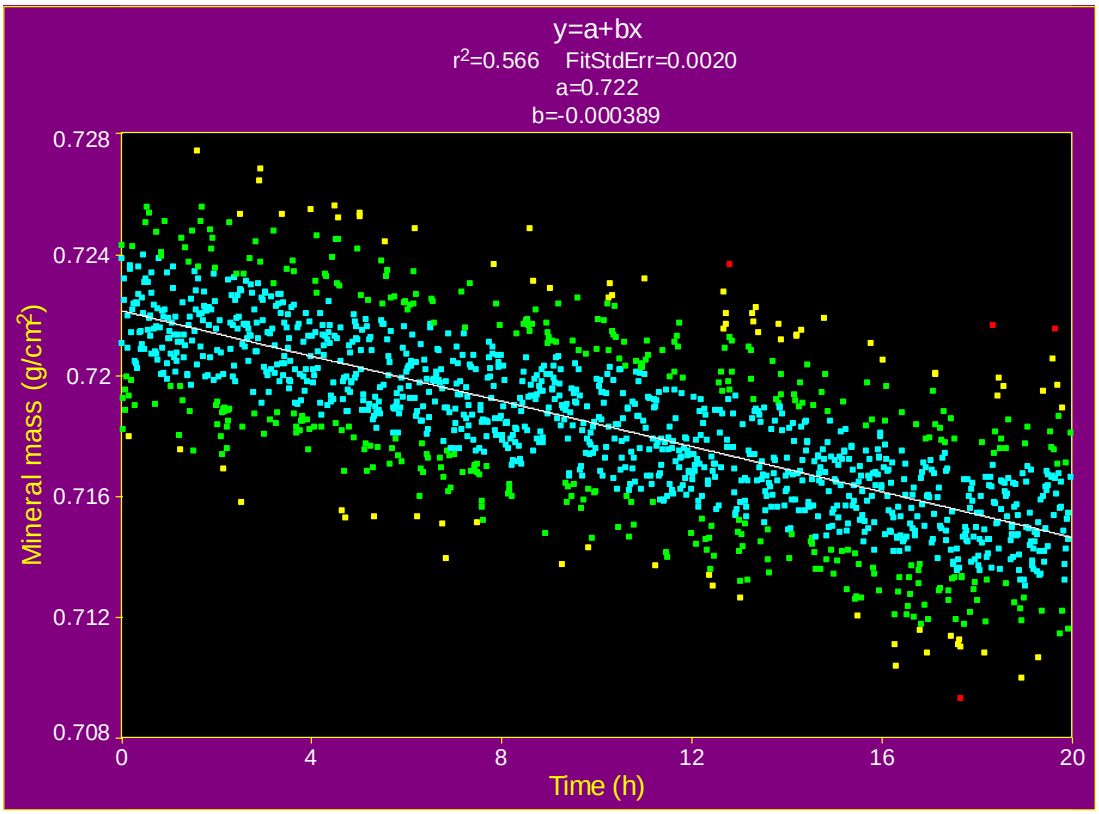

FIGURE 16.2 Typical example of the change in projected HAp mineral mass content over a period of 20 h in response to 0.1% acetic acid pH 4.0 with 5 ppm Zn^{2+} demineralisation solution at increasing Zn^{2+} concentration sequence

(■ Within 1 SD, 1 SD< ■ < 2 SD, 2 SD< ■ < 3 SD, 3 SD< ■ < 4 SD)

TABLE 16.1 Statistical analysis, for the data in Figure 16.2, using TableCurve 2D®

	Value	SE	t-value	95% Confidence Limits	
a (g/cm^2)	0.722	1.071e-04	6740.54	0.722	0.722
b ($g/cm^2/h$)	-3.89e-4	9.277e-06	-40.34	-3.982e-4	- 3.760e-4

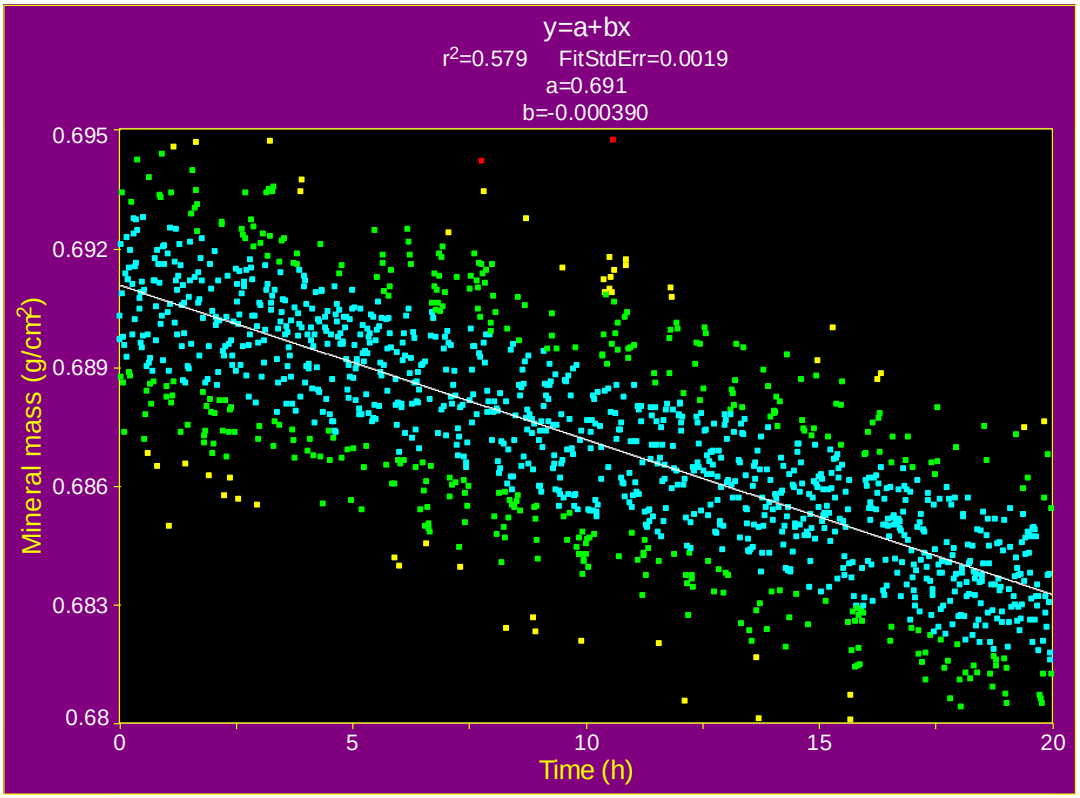

FIGURE 16.3 Typical example of the change in projected HAp mineral mass content over a period of 20 h in response to 0.1% acetic acid pH 4.0 with 5 ppm Zn^{2+} demineralisation solution at decreasing Zn^{2+} concentration sequence

(■ Within 1 SD, 1 SD< ■ < 2 SD, 2 SD< ■ < 3 SD, 3 SD< ■ < 4 SD)

TABLE 16.2 Statistical analysis, for the data in Figure 16.3, using TableCurve 2D®

	Value	SE	t-value	95% Confidence Limits	
a (g/cm^2)	0.691	1.039e-04	6651.835	0.6908	0.6913
b ($g/cm^2/h$)	-3.90e-4	9.001e-06	-43.387	-4.082e-4	- 3.729e-4

TableCurve 2D®, automated curve fitting and equation discovery program, version 5.1 for Windows (SYSTAT® Software Inc, Richmond CA), was used to calculate the standard error (SE) for each experiment.The RD_{HAp} was calculated and the resulting associated errors are summarised in Table 16.3.

TABLE 16.3 RD_{HAp} and calculated SE for each demineralising solution

0.1% acetic acid pH 4.0									
		RD_{HAp} (g/cm^2/h) for increasing Zn^{2+} concentration sequence				RD_{HAp} (g/cm^2/h) for decreasing Zn^{2+} concentration sequence			
Zn^{2+} concentration (ppm)		**HAp disc1**	**SE**	**HAp disc2**	**SE**	**HAp disc1**	**SE**	**HAp disc2**	**SE**
	20	2.97×10^{-4}	9.30×10^{-6}	2.44×10^{-4}	8.72×10^{-6}	2.65×10^{-4}	9.21×10^{-6}	2.50×10^{-4}	9.21×10^{-6}
	15	3.14×10^{-4}	9.11×10^{-6}	2.90×10^{-4}	8.90×10^{-6}	2.86×10^{-4}	8.78×10^{-6}	2.95×10^{-4}	8.78×10^{-6}
	10	3.22×10^{-4}	8.81×10^{-6}	3.15×10^{-4}	8.69×10^{-6}	3.09×10^{-4}	9.56×10^{-6}	3.19×10^{-4}	9.54×10^{-6}
	5	3.73×10^{-4}	9.25×10^{-6}	3.89×10^{-4}	9.00×10^{-6}	3.90×10^{-4}	9.27×10^{-6}	3.70×10^{-4}	9.30×10^{-6}
	0	4.27×10^{-4}	8.97×10^{-6}	4.48×10^{-4}	8.97×10^{-6}	4.48×10^{-4}	9.17×10^{-6}	4.30×10^{-4}	9.17×10^{-6}

16.4.2 0.3% citric acid pH 2.8

Figure 16.4 and Figure 16.5 demonstrate the real-time change of HAp projected mineral mass following exposure to 0.3% citric acid pH 2.8 solution at a range of Zn^{2+} concentrations, for both increasing and decreasing Zn^{2+} concentration respectively.

Figure 16.4 shows that the HAp projected mineral mass content decreased from 0.589 g/cm^2 to 0.535 g/cm^2 in 20 h. This reduction represents a 9% loss in projected HAp mineral mass over 20 h. While for Figure 16.5 the HAp projected mineral mass content decreased from 0.505 g/cm^2 to 0.449 g/cm^2 in 20 h which represents a 10% loss in the projected mineral content over 20 h.

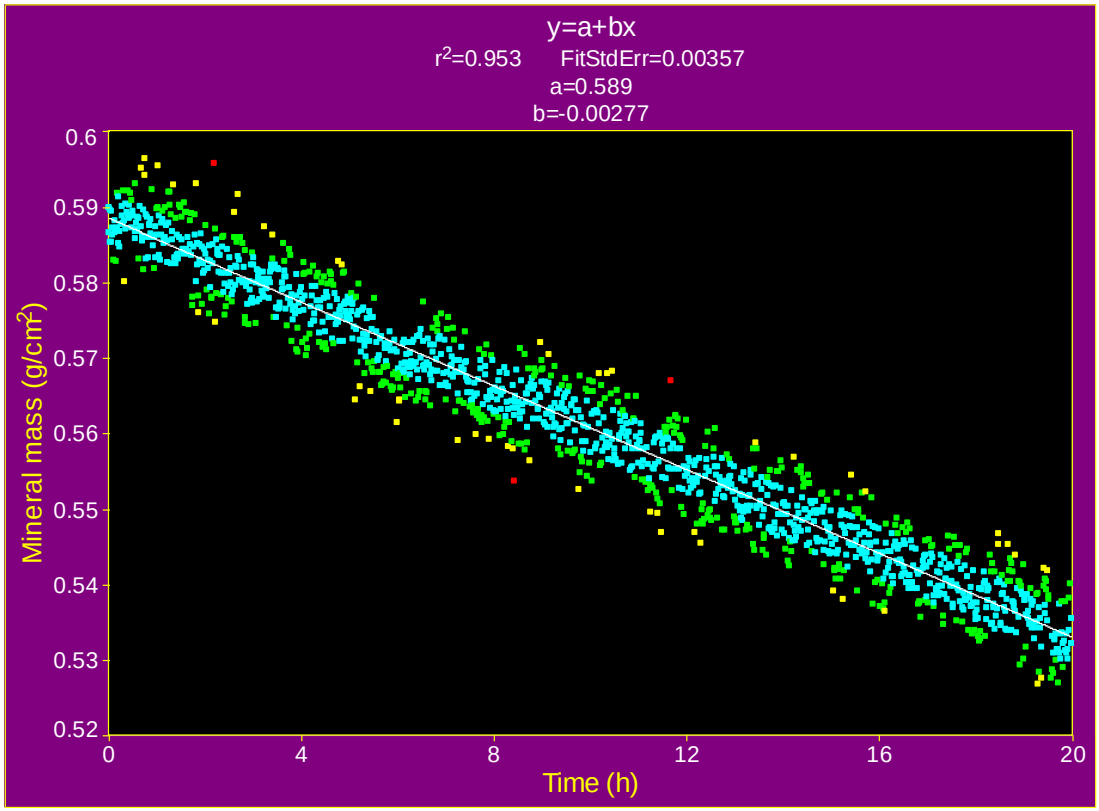

FIGURE 16.4 Typical example of the change in projected HAp mineral mass content over a period of 20 h in response to 0.3% citric acid pH 2.8 with 5 ppm Zn^{2+} demineralisation solution at increasing Zn^{2+} concentration sequence
(■ Within 1 SD, 1 SD< ■ < 2 SD, 2 SD< ■ < 3 SD, 3 SD< ■ < 4 SD)

TABLE 16.4 Statistical analysis, for the data in Figure 16.4, using TableCurve 2D®

	Value	SE	t-value	95% Confidence Limits	
a (g/cm^2)	0.589	1.87e-04	3143.845	0.5882	0.5889
b ($g/cm^2/h$)	-2.77e-3	1.62e-05	-170.807	-2.80e-3	- 2.74e-3

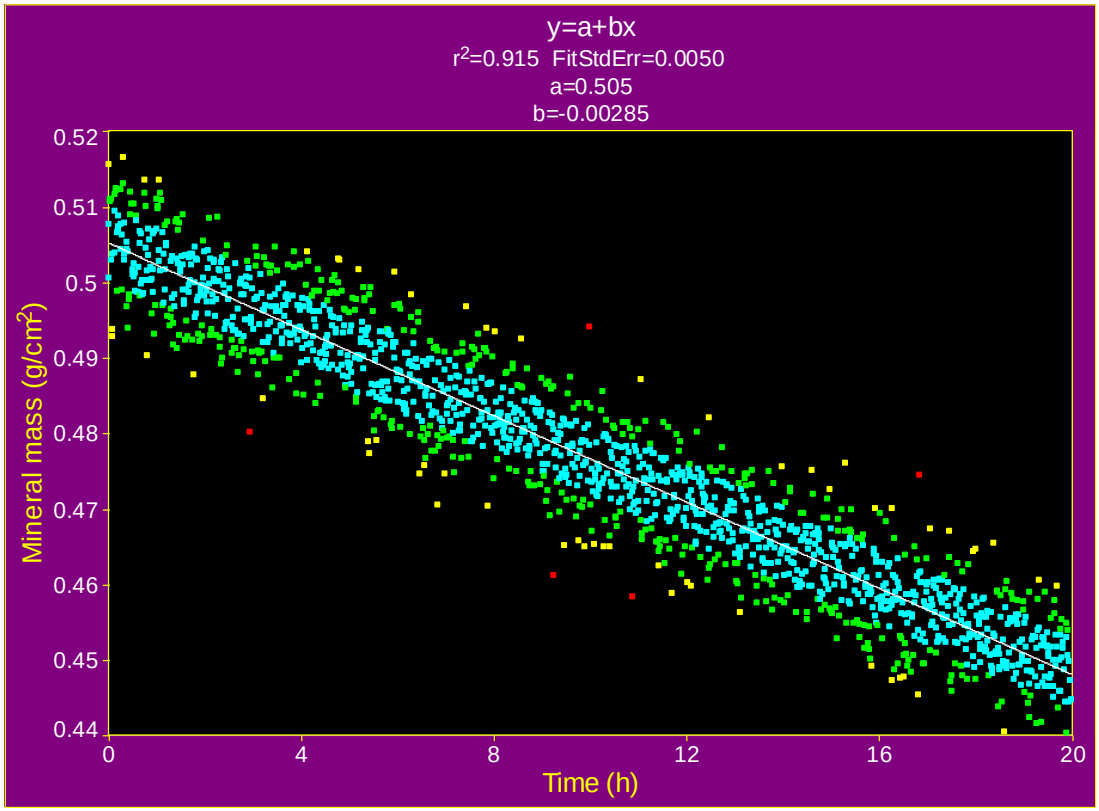

FIGURE 16.5 Typical example of the change in projected HAp mineral mass content over a period of 20 h in response to 0.3% citric acid pH 2.8 with 5 ppm Zn^{2+} demineralisation solution at decreasing Zn^{2+} concentration sequence

(■ Within 1 SD, 1 SD< ■ < 2 SD, 2 SD< ■ < 3 SD, 3 SD< ■ < 4 SD)

TABLE 16.5 Statistical analysis, for the data in Figure 16.5, using TableCurve 2D®

	Value	SE	t-value	95% Confidence Limits	
a (g/cm^2)	0.505	2.53e-04	1994.060	0.5048	0.5057
b ($g/cm^2/h$)	-2.85e-3	2.20e-05	-129.974	-2.90e-3	- 2.81e-3

The change in RD_{HAp} after the sequential exposure to 0.3% citric acid pH 2.8 with various Zn^{2+} concentrations was calculated and the results obtained are summarised in Table 16.6.

TABLE 16.6 RD_{HAp} and calculated SE for each demineralising solution

0.3% citric acid pH 2.8									
		RD_{HAp} ($g/cm^2/h$) for increasing Zn^{2+} concentration sequence				**RD_{HAp} ($g/cm^2/h$) for decreasing Zn^{2+} concentration sequence**			
Zn^{2+} concentration (ppm)		**HAp disc1**	**SE**	**HAp disc2**	**SE**	**HAp disc1**	**SE**	**HAp disc2**	**SE**
	20	$1.70x10^{-3}$	$1.65x10^{-5}$	$1.96x10^{-3}$	$1.48x10^{-5}$	$1.59x10^{-3}$	$1.46x10^{-5}$	$1.74x10^{-3}$	$1.40 x10^{-5}$
	15	$2.51x10^{-3}$	$1.87x10^{-5}$	$2.38x10^{-3}$	$1.54x10^{-5}$	$2.45x10^{-3}$	$1.76x10^{-5}$	$2.42x10^{-3}$	$1.73 x10^{-5}$
	10	$2.84x10^{-3}$	$2.19x10^{-5}$	$2.62x10^{-3}$	$1.60x10^{-5}$	$2.60x10^{-3}$	$1.58x10^{-5}$	$2.68x10^{-3}$	$1.74 x10^{-5}$
	5	$2.89x10^{-3}$	$2.36x10^{-5}$	$2.77x10^{-3}$	$1.62x10^{-5}$	$2.85x10^{-3}$	$2.20x10^{-5}$	$2.88x10^{-3}$	$2.25 x10^{-5}$
	0	$3.18x10^{-3}$	$2.15x10^{-5}$	$3.06x10^{-3}$	$1.73x10^{-5}$	$2.90x10^{-3}$	$2.26x10^{-5}$	$2.95x10^{-3}$	$2.18 x10^{-5}$

16.5 Discussion

Previous studies on the effect of Zn^{2+} on de/remineralisation of enamel concluded that Zn^{2+} interacts with the HAp either through adsorbing onto the surface of the crystals or through incorporation into the crystal lattice replacing Ca^{2+} and forming zinc calcium phosphates (Xu *et al.*, 1994, Stötzel *et al.*, 2009)

In this study, for caries-like conditions, Figure 16.2 and Figure 16.3 represent typical examples of the change in projected HAp mineral mass content, over a period of ≈20 h when exposed to 0.1% acetic acid pH 4.0 with 5 ppm Zn^{2+} demineralisation solution with increasing and decreasing concentration sequences respectively. In Figure 16.2 the change in mineral mass content (g/cm^2) was plotted as a function of time (h). The data showed a linear regression trend for the projected HAp mineral mass content over time. One thousand and five hundred data counts were measured at a centrally located point on the permeable HAp disc over 20 h, of which only 76 data counts were outside 2 SD (5%).

Figure 16.3 shows demineralisation in caries-like conditions similar to those in Figure 16.2 but in the sequence when the Zn^{2+} concentration experiments had been reversed. It shows a similar linear regression trend in projected HAp mineral mass content over the experimental duration. One thousand five hundred data counts were collected at a centrally located point on the permeable HAp disc over 20 h out of which 50 data counts were outside 2 SD (3.3%).

Table 16.3 shows the calculated demineralisation rates and the SE for each of the 20 experiments with various Zn^{2+} concentrations. Calculations of SE gives a better insight into the accuracy of the data than R^2, particularly when dealing with large data sets as it takes into consideration the sample size while R^2 only represents

a measure of goodness of fit. The calculated SE for the fitted parameters were low, as demonstrated in Table 16.3.

Figure 16.6 shows that as Zn^{2+} concentration increased at an increasing concentration sequence (0-20 ppm), the RD_{HAp} decreased. This reduction in RD_{HAp} was statistically significant ($P \leq 0.05$) for all Zn^{2+} concentrations investigated when compared to the control group (0 ppm). However, when the sequence of Zn^{2+} concentrations was reversed (20-0 ppm), the RD_{HAp} increased (Figure 16.7).

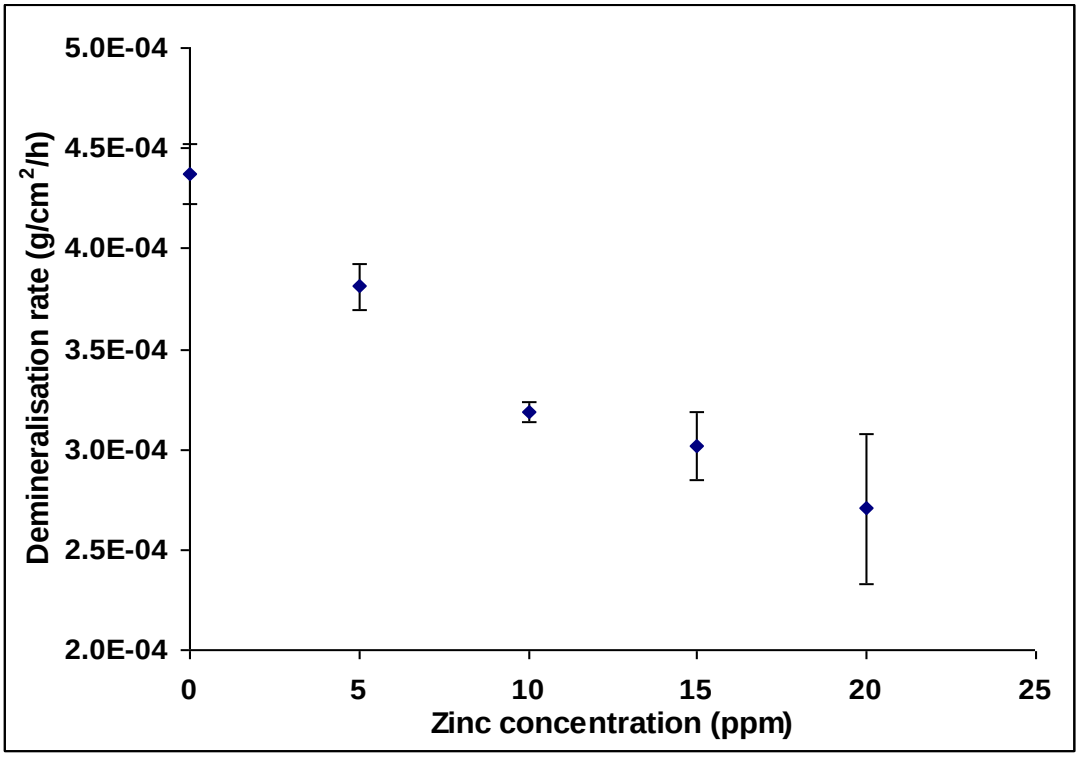

FIGURE 16.6 The effect of Zn^{2+} at a range of 0 – 20 ppm on mean RD_{HAp} at increasing Zn^{2+} concentration sequence under caries-like conditions

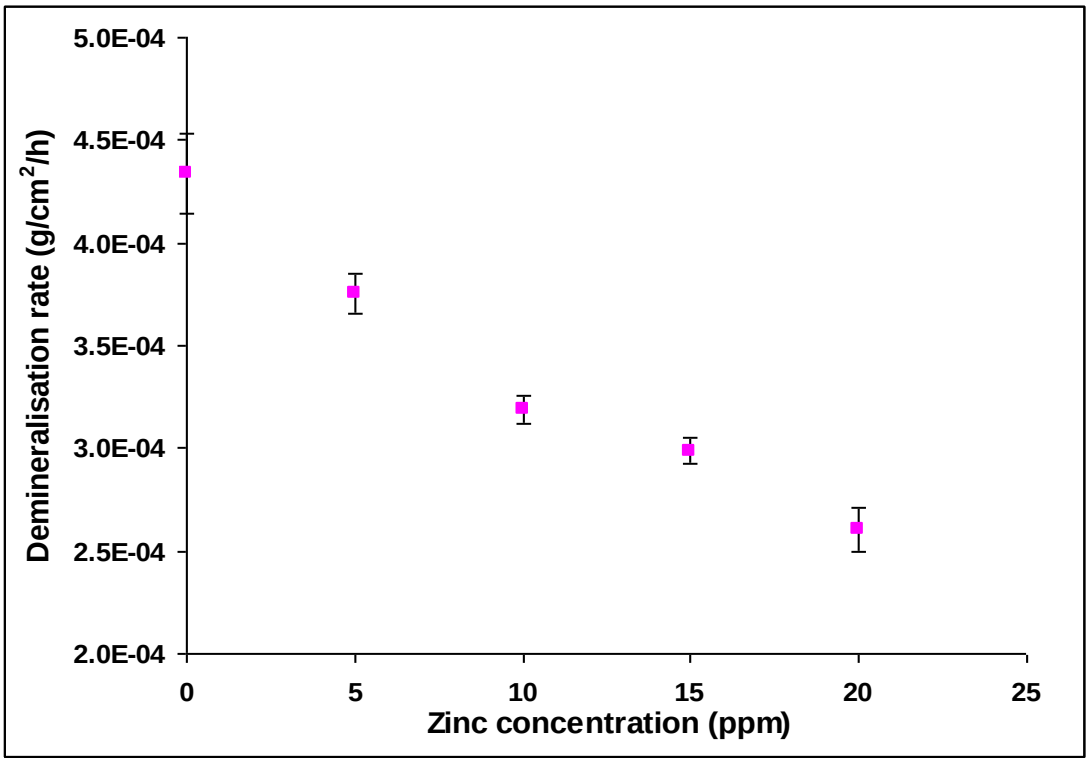

FIGURE 16.7 The effect of Zn^{2+} at a range of 20 - 0 ppm on mean RD_{HAp} at decreasing Zn^{2+} concentration sequence under caries-like conditions

The average of each duplicate experiment, at each Zn^{2+} concentration, in both increasing and decreasing Zn^{2+} concentration sequence was calculated and illustrated in Figure 16.8.

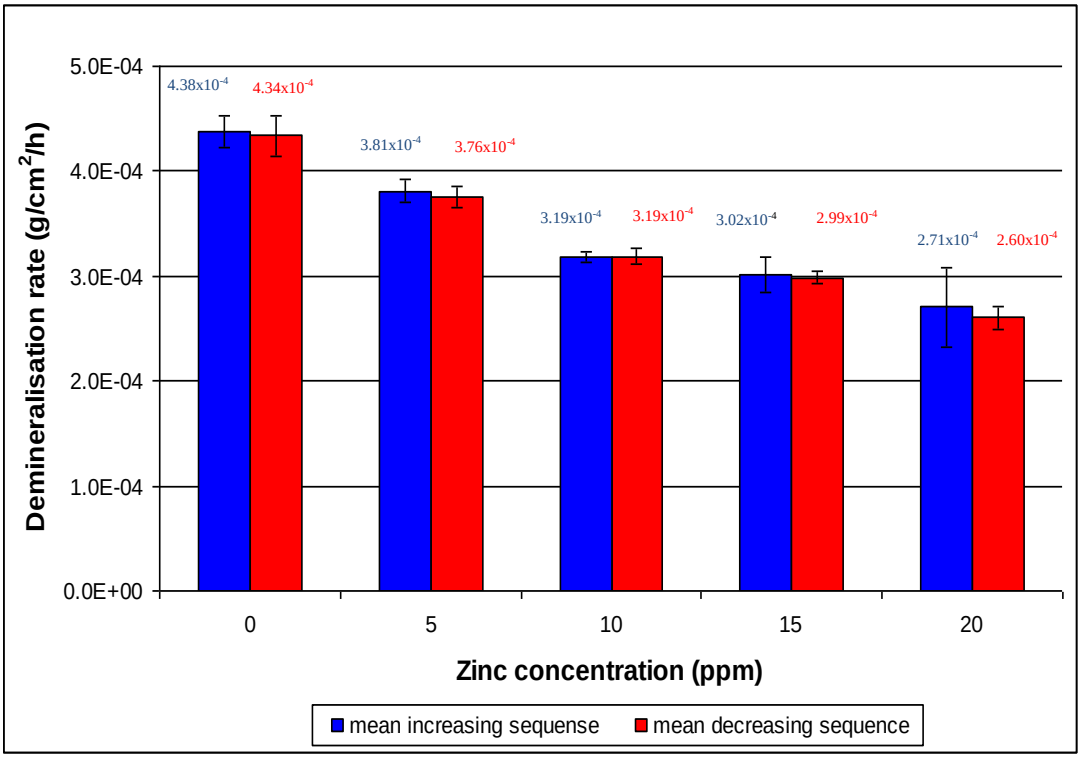

FIGURE 16.8 The effect of 0.1% acetic acid pH 4.0 with different Zn^{2+} concentrations (ppm) on RD_{HAp} ($g/cm^2/h$) at both increasing and decreasing concentration sequences

Figure 16.8 shows that the relation between Zn^{2+} concentration and RD_{HAp} is the same for both, increasing and decreasing concentration sequences. An important outcome of this study is that the direction of the sequence of Zn^{2+} concentration has no effect on its capability to reduce RD_{HAp}. This is as if Zn^{2+} was completely washed away when the HAp disc was rinsed by the de-ionised water between the different concentrations in each sequence. This supports the hypothesis that Zn^{2+} is not permanently incorporated into the HAp structure; but instead adheres to the HAp surface blocking dissolution nuclei and slowing the demineralisation rate.

For erosion-like conditions, Figure 16.4 and Figure 16.5 are typical examples of the change in projected HAp mineral mass content over a period of 20 h during exposure to 0.3% citric acid pH 2.8 with 5 ppm Zn^{2+} demineralisation solution during an increasing and a decreasing concentration sequences respectively.

Figure 16.4 shows a regression trend for the projected HAp mineral mass content over time. One thousand five hundred data counts were measured at a centrally located point on the permeable HAp disc over 20 h, of which only 55 data counts were outside 2 SD (3.6%).

Figure 16.5 shows demineralisation in erosion-like conditions similar to those for Figure 16.4 but with the sequence of the Zn^{2+} concentration experiments reversed. It shows a similar regression trend in projected HAp mineral mass content over the experimental duration. One thousand five hundred data counts were collected at a centrally located point on the permeable HAp disc over 20 h, out of which only 62 data counts were outside 2 SD (4.1%).

Table 16.4 shows the calculated demineralisation rates and the SE for each of the 20 experiments in which various Zn^{2+} concentrations were used.

Figure 16.9 shows the effect of Zn^{2+} on RD_{HAp} at an increasing concentration sequence (0-20 ppm), that RD_{HAp} decreased. This reduction in RD_{HAp} was statistically significant ($P \leq 0.05$) for all Zn^{2+} concentrations investigated when compared to the control group (0 ppm). However, when the sequence of Zn^{2+} concentrations was reversed, as Zn^{2+} concentrations decreased (20-0 ppm), the RD_{HAp} increased (Figure 16.10).

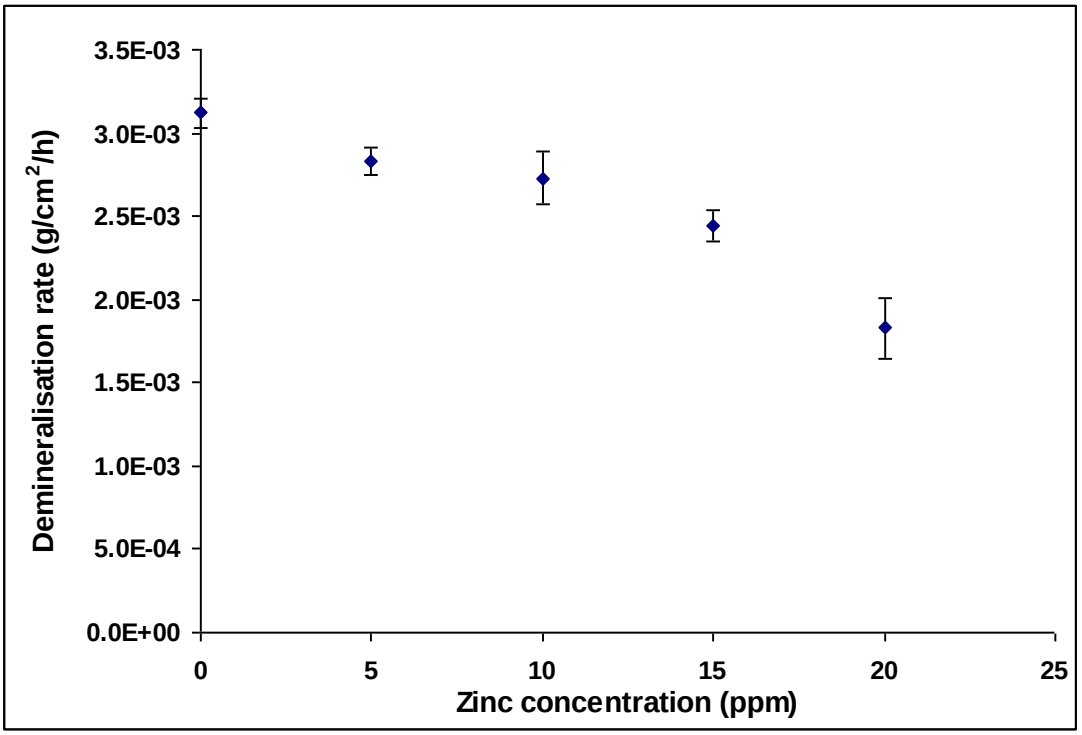

FIGURE 16.9 The effect of Zn^{2+} at a range of 0 – 20 ppm on mean RD_{HAp} at increasing Zn^{2+} concentration sequence under erosion-like conditions

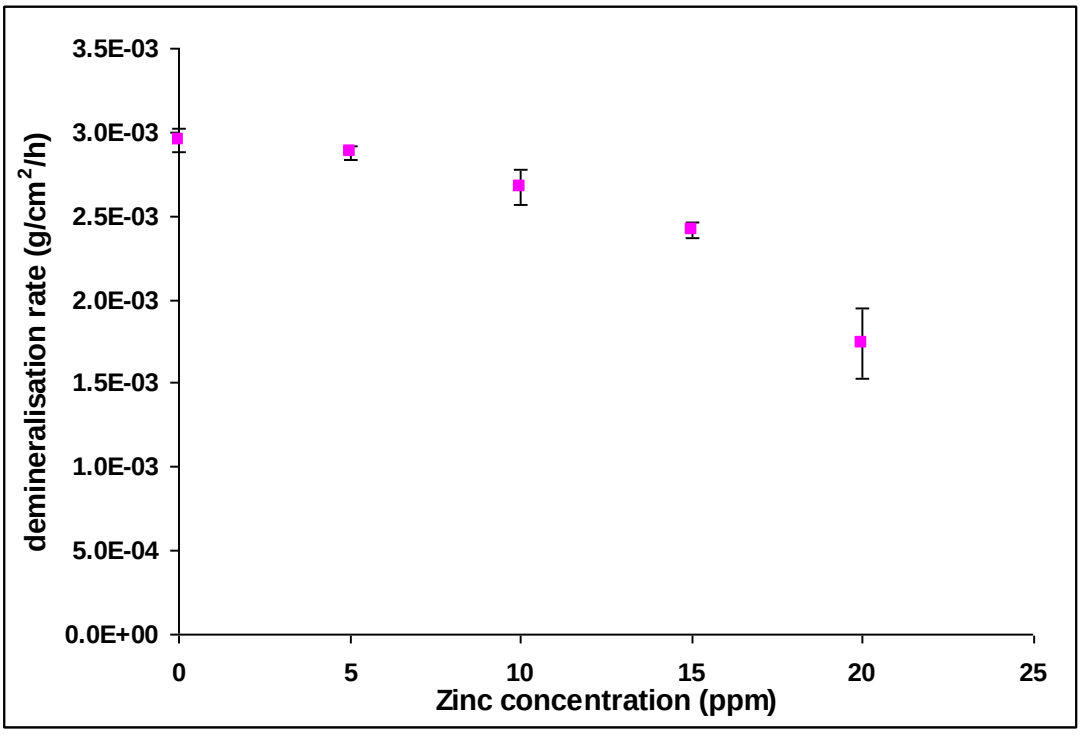

FIGURE 16.10 The effect of Zn^{2+} at a range of 20 – 0 ppm on mean RD_{HAp} at decreasing Zn^{2+} concentration sequence under erosion-like conditions

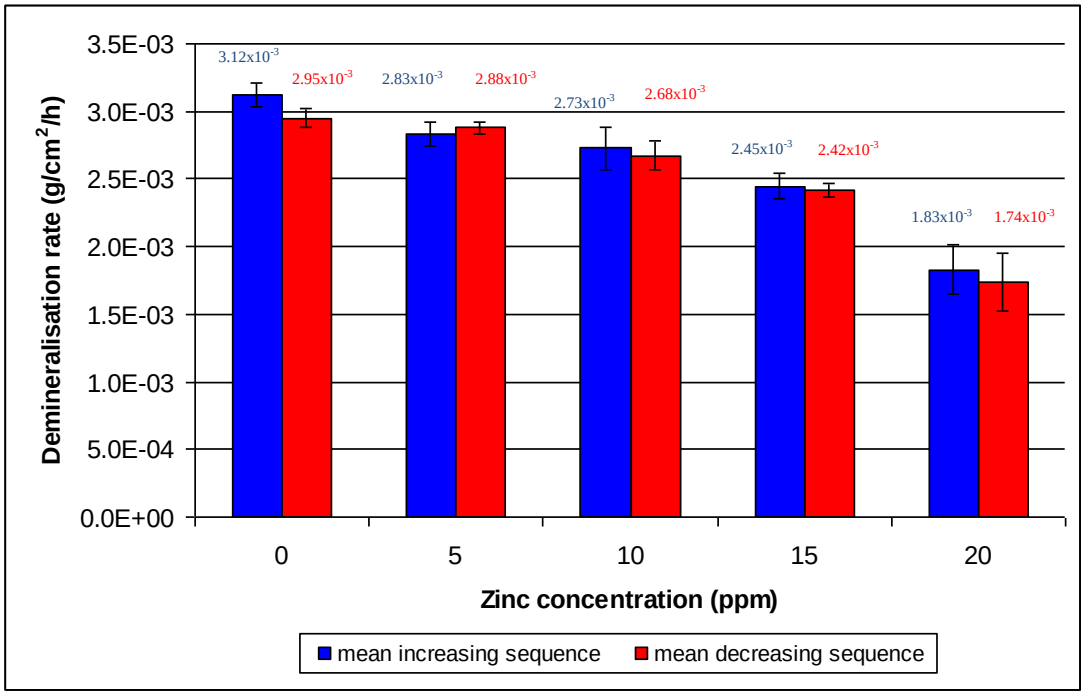

FIGURE 16.11 The effect of 0.3% citric acid pH 2.8 with different Zn^{2+} concentration (ppm) on RD_{HAp} ($g/cm^2/h$) at both increasing and decreasing concentrations sequences

Figure 16.11 shows the relation between Zn^{2+} concentration and RD_{HAp} is the same for both increasing and decreasing concentration sequences. An important outcome of this study is that it demonstrated that the sequence of Zn^{2+} concentration in a series of experiments has no effect on its ability in reducing RD_{HAp}, *i.e.* Zn^{2+} were completely washed away when the HAp disc was rinsed by de-ionised water between the different concentrations. This supports the hypothesis that Zn^{2+} does not incorporate into the HAp structure; instead it adheres to the surface blocking some dissolution nuclei and slowing the demineralisation rate.

An overall comparison between the results of the effect of Zn^{2+} on RD_{HAp} in caries and erosion-like conditions clearly indicates that both showed a decrease in RD_{HAp} with increasing Zn^{2+} concentrations. All solutions with a range of Zn^{2+} concentrations (5, 10, 15 and 20 ppm) showed a significant decrease ($p \leq 0.05$) in RD_{HAp} compared to the control solution (0 ppm Zn^{2+}). This suggests that Zn^{2+} is in a

"loose equilibrium" with the HAp surface mineral, and therefore while there is Zn^{2+} in the surrounding fluid some will be adsorbed onto the surface in a dynamic equilibrium. This finding is in agreement with Tan-Walker and Gilbert (1989), who showed that Zn^{2+} reduced demineralisation significantly at physiologically relevant zinc concentrations added to a gel acid demineralisation system.

16.6 Conclusions

The results of this study demonstrated the inhibitory effect of Zn^{2+} as a divalent metal cation on RD_{HAp} under strictly controlled thermodynamic conditions relevant to dental caries and erosion. The results also support the hypothesis that Zn^{2+} (under the experimental conditions) inhibits HAp dissolution by adsorbing to the surface of the HAp disc rather than having a substitution effect.

CHAPTER 17

Effect of Strontium Ions (Sr^{2+}) at a Range of Concentrations (0-30 ppm) on Hydroxyapatite Dissolution Kinetics Studied Using Scanning Microradiography*

17.1 Introduction

Numerous clinical trials have reported the efficacy of a wide range of Sr^{2+} containing compounds in the management of dentine hypersensitivity. The British and American Dental Associations have accredited various formulations for efficacy, including toothpastes incorporating strontium acetate and strontium chloride (Orchardson and Gillam, 2006). On the other hand the role of Sr^{2+} in the prevention of dental caries shows many controversies. Experimental studies show that the replacement of Ca^{2+} by Sr^{2+} alter the HAp crystal lattice, and the formed strontium calcium apatite is more soluble than the HAp. However clinical studies showed that populations who lived in areas with high Sr^{2+} water concentration level had higher Sr^{2+} concentration in their enamel and experienced less dental caries than those from areas with lower Sr^{2+} water concentration level (Curzon and Crocker, 1978, Curzon *et al.*, 1978, Athanassouli *et al.*, 1983, Curzon, 1985).

* The work described in this chapter was presented at the International Association of Paediatric Dentistry Conference, Athens, Greece, (June, 2011) and at the British Society of Oral and Dental Research, Sheffield, UK (September 2011).

17.2 Aims and objectives

The aim of this study was to investigate the effect of Sr^{2+} at concentrations of 0, 5, 10, 20 and 30 ppm on the dissolution kinetics of permeable HAp disc.

The objectives were to measure the rate of HAp dissolution of a permeable HAp disc using the SMR technique under strictly controlled thermodynamic conditions and Sr^{2+} range of concentrations relevant to concentrations found in drinking water supplies.

17.3 Materials and methods

The protocol of this experiment is illustrated in Figure 17.1.

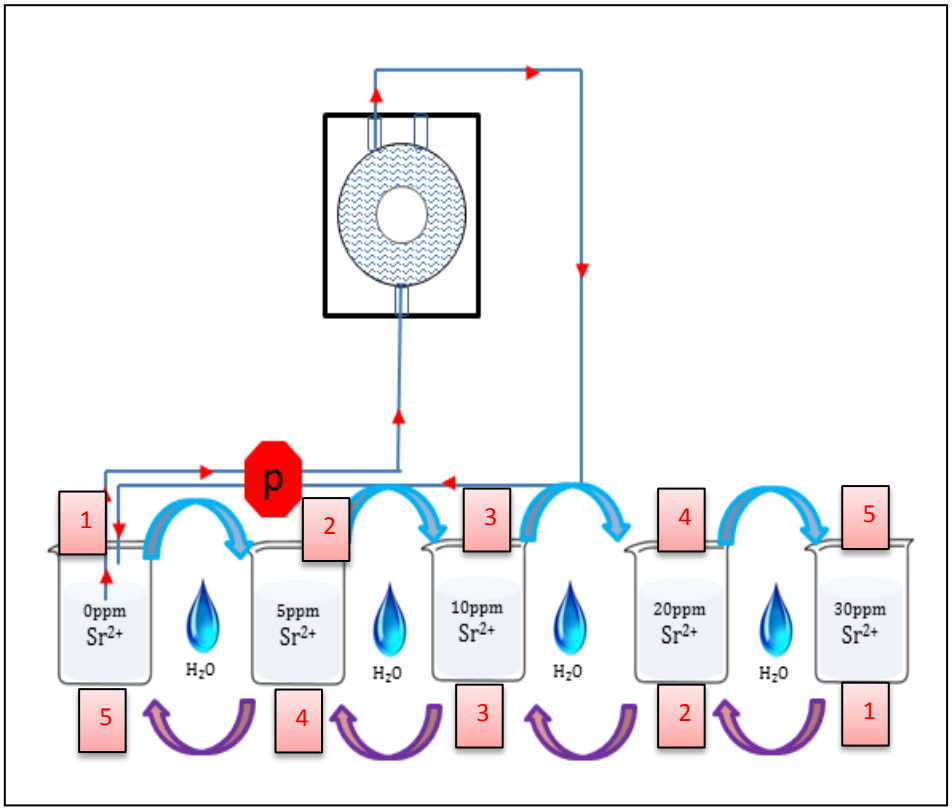

FIGURE 17.1 schematic diagram of an SMR cell with HAp disc in place, connected to the peristaltic pump (p) for circulating the demineralisation solution over a period of 20 h followed by 30 minutes of de-ionised water at both increasing , and decreasing Sr^{2+} concentration sequences

17.3.1 HAp discs

Eight HAp discs were used in this study. The details of the HAp disc preparation were described in Section 10.6.2.

17.3.2 Demineralising solutions

For cariogenic conditions, a 5 litre batch solution of 0.1% acetic acid pH 4.0 was divided into five 1 litre bottles. Into each one, strontium acetate (SIGMA-ALDRICH, Co., St. Louis, USA, product # 388548-500G and batch # 01715JJ *SIGMA-ALDRICH*™) was added, so that the final Sr^{2+} concentration was 0, 5, 10, 20 and 30 ppm Sr^{2+}.

For erosive conditions, a 5 litre batch solution of 0.3% citric acid pH 2.8 was divided into five 1 litre bottles. Into each one, strontium acetate was added, so that the final Sr^{2+} concentration was 0, 5, 10, 20 and 30 ppm Sr^{2+}.

After the addition of strontium acetate, the pH of each demineralising solution was adjusted by using 1 Molar HCl or KOH solutions as necessary (Section 10.7).

17.3.3 SMR

HAp discs were located centrally in the SMR cells and demineralising solutions were circulated at 0.80 ml/min (Chapter 14). The rate of HAp demineralisation was measured at a centrally located point in each disc for a ≈20 h at 22 ± 1°C. Each experiment was repeated twice in both increasing (0 - 30 ppm) and decreasing (30 - 0 ppm) Sr^{2+} concentrations sequence.

For the increasing Sr^{2+}concentration experiments; the HAp disc was exposed for ≈20 h to the demineralising solution with no Sr^{2+} added; followed by 30 min of washing by de-ionised water, followed by ≈20 h of exposure to demineralising solution with 5 ppm Sr^{2+}, followed by 30 min of washing by de-ionised water and so

on through the increasing Sr^{2+} concentrations. All exposures were performed using the same HAp disc. In reverse, for the decreasing sequence Sr^{2+} concentration experiments, the same HAp disc was further exposed for ≈ 20 h to each demineralising solution with 30 min of washing by de-ionised water. The SMR cells were mounted on the SMR stage and scanned at the same time. Each experiment was duplicated.

17.4 Results

17.4.1 0.1% acetic acid pH 4.0

For each experiment of the 20 demineralisation experiments using 0.1% acetic acid pH 4.0 with various Sr^{2+} concentrations, the mineral mass loss of each HAp disc was continuously measured throughout the entire experimental duration. Figure 17.2 and Figure 17.3 are typical examples of the real-time change in the projected HAp mineral mass content in response to the exposure to 0.1% acetic acid pH 4.0 solution with 20 ppm Sr^{2+}concentration in both increasing and decreasing Sr^{2+}concentration sequences respectively.

For Figure 17.2 the HAp projected mineral mass content decreased from 0.776 g/cm^2 to 0.772g/cm^2 in 20 h. This reduction in projected mineral mass content represents only a 0.5% loss of projected HAp mineral content over 20 h. While for Figure 17.3 the HAp projected mineral mass content decreased from 0.677 g/cm^2 to 0.675 g/cm^2 in ≈20 h which represents 0.3% loss of projected mineral content over ≈20 h at a rate of 1.05×10^{-4} g/cm^2/h.

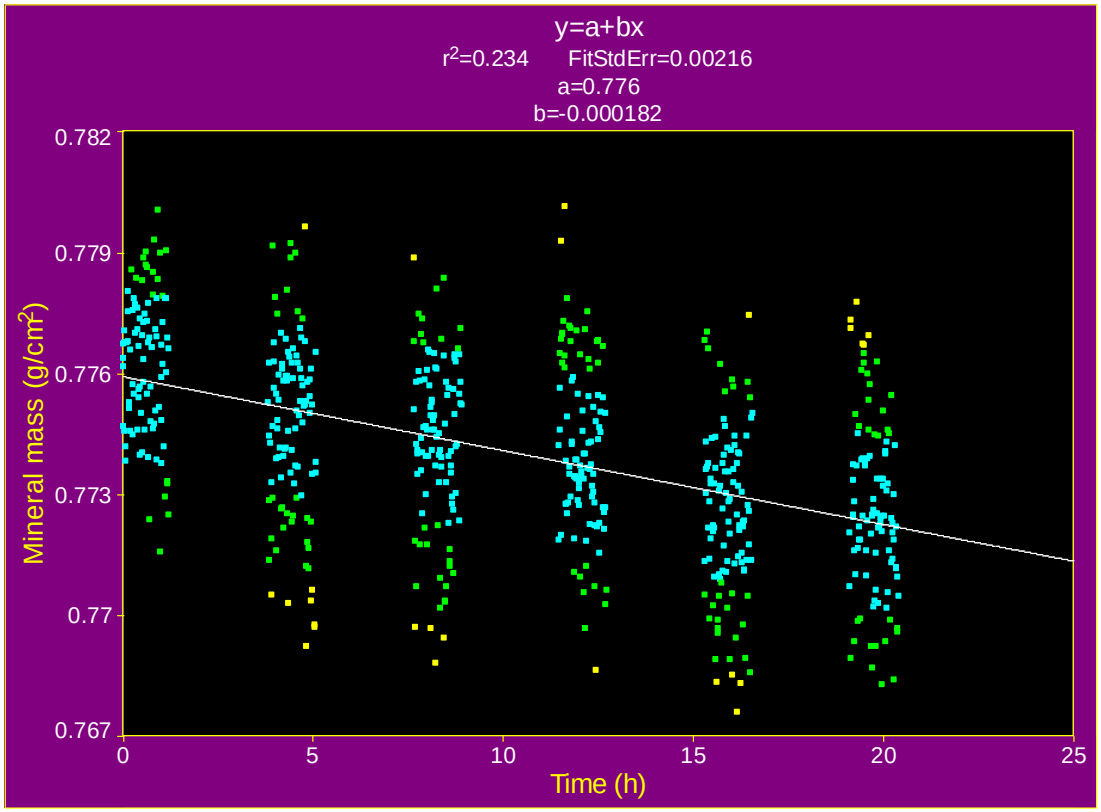

FIGURE 17.2 Typical example of the change in projected HAp mineral mass content over a period of ≈ 20 h in response to 0.1% acetic acid pH 4.0 with 20 ppm Sr^{2+} demineralisation solution at increasing Sr^{2+} concentration sequence.

(Within 1 SD, 1 SD< < 2 SD, 2 SD< < 3 SD, 3 SD< < 4 SD)

TABLE 17.1 Statistical analysis, for the data in Figure 17.2, using TableCurve 2D®

	Value	SE	t-value	95% Confidence Limits	
a (g/cm^2)	0.776	1.651e-04	4697.25	0.7756	0.7762
b (g/cm^2/h)	-1.82e-4	1.35e-05	-13.55	-2.09-4	- 1.57e-4

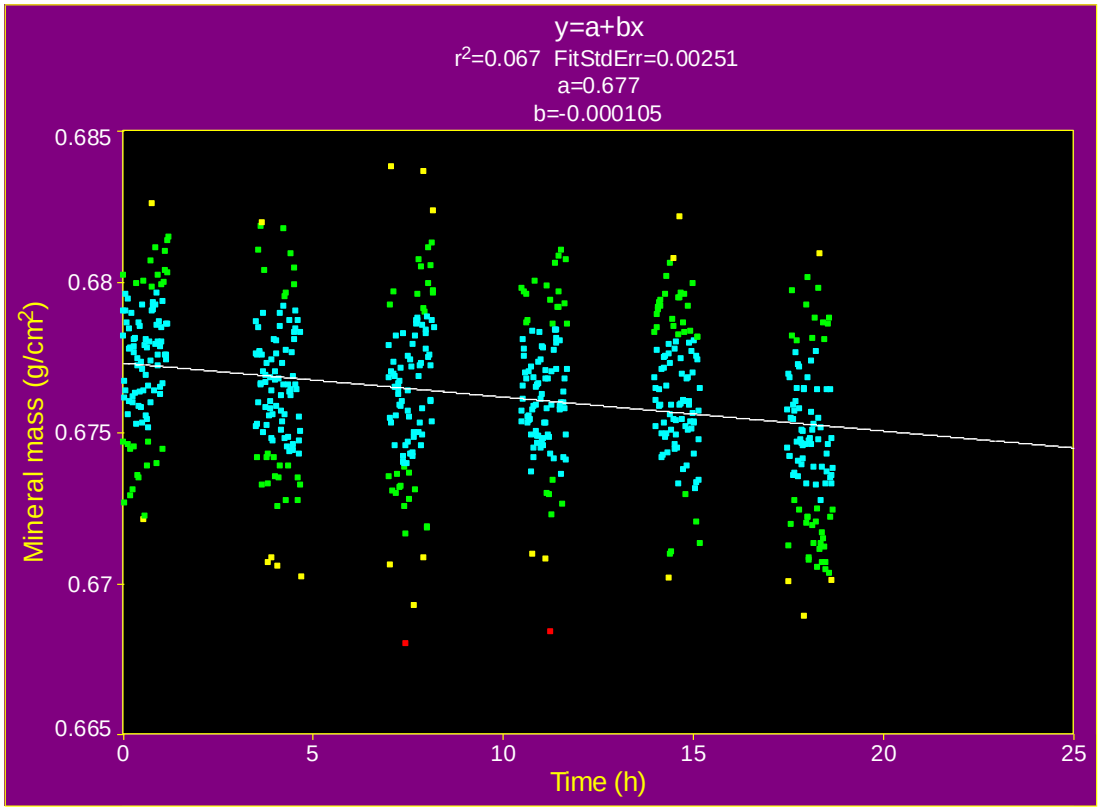

FIGURE 17.3 Typical example of the change in projected HAp mineral mass content over a period of 20 h in response to 0.1% acetic acid pH 4.0 with 20 ppm Sr^{2+} demineralisation solution at decreasing Sr^{2+} concentration sequence

(■ Within 1 SD, 1 SD< ■ < 2 SD, 2 SD< ■ < 3 SD, 3 SD< ■ < 4 SD)

TABLE 17.2 Statistical analysis, for the data in Figure 17.3, using TableCurve 2D®

	Value	SE	t-value	95% Confidence Limits	
a (g/cm^2)	0.677	1.747e-04	3878.92	0.6773	0.6780
b ($g/cm^2/h$)	-1.05e-4	1.331e-05	-7.924	-1.312e-4	- 7.935e-4

The RD_{HAp} and the SE for each of the 20 experiments, using 0.1% acetic acid pH 4.0, was calculated and the results associated errors were summarized in Table 17.3

TABLE 17.3 RD_{HAp} and SE for each demineralisation solution at different Sr^{2+} concentrations at both increasing and decreasing concentration sequences

0.1% acetic acid pH 4.0									
		RD_{HAp} ($g/cm^2/h$) increasing Sr^{2+} concentration sequence				RD_{HAp} ($g/cm^2/h$) decreasing Sr^{2+} concentration sequence			
Sr^{2+} concentration (ppm)		**HAp disc1**	**SE**	**HAp disc2**	**SE**	**HAp disc1**	**SE**	**HAp disc2**	**SE**
	30	1.30×10^{-4}	1.28×10^{-5}	1.00×10^{-4}	1.18×10^{-5}	1.76×10^{-4}	1.31×10^{-5}	1.18×10^{-4}	1.28×10^{-5}
	20	1.82×10^{-4}	1.51×10^{-5}	1.05×10^{-4}	1.43×10^{-5}	1.42×10^{-4}	1.69×10^{-5}	1.06×10^{-4}	1.43×10^{-5}
	10	2.05×10^{-4}	1.23×10^{-5}	1.71×10^{-4}	1.57×10^{-5}	1.18×10^{-4}	1.65×10^{-5}	9.03×10^{-5}	1.30×10^{-5}
	5	2.80×10^{-4}	9.61×10^{-5}	2.66×10^{-4}	1.25×10^{-5}	9.00×10^{-5}	1.28×10^{-5}	3.19×10^{-5}	1.75×10^{-5}
	0	3.20×10^{-4}	1.25×10^{-5}	3.60×10^{-4}	1.38×10^{-5}	2.14×10^{-4}	1.09×10^{-5}	2.63×10^{-4}	1.35×10^{-5}

17.4.2 0.3% citric acid pH 2.8

Figure 17.4 and Figure 17.5 are typical examples of the real-time change in the HAp projected mineral mass content in response to the exposure to 0.3% citric acid pH 2.8 solution with 20 ppm Sr^{2+}concentrations in both increasing and decreasing Sr^{2+}concentrations respectively.

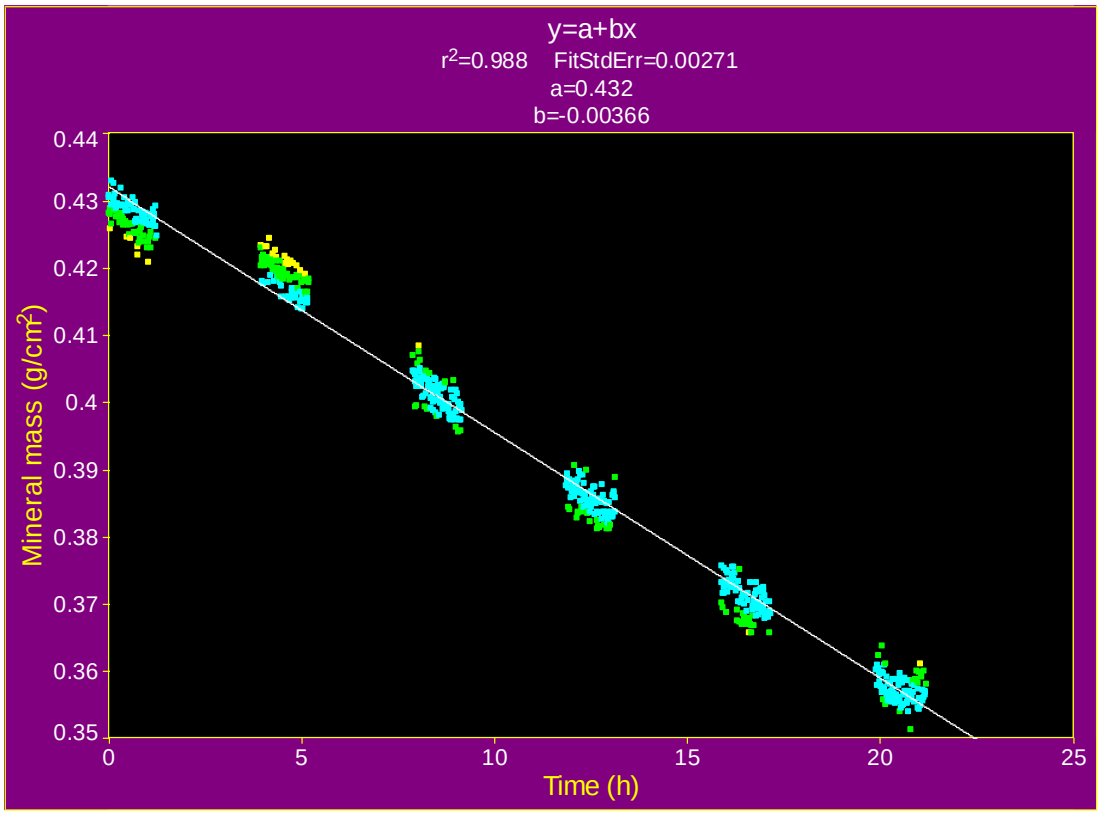

FIGURE 17.4 Typical example of the change in projected HAp mineral mass content over a period of 20 h in response to 0.3% citric acid pH 2.8 with 20 ppm Sr^{2+} demineralisation solution at increasing Sr^{2+} concentration sequence

(■ Within 1 SD, 1 SD< ■ < 2 SD, 2 SD< ■ < 3 SD, 3 SD< ■ < 4 SD)

TABLE 17.4 Statistical analysis, for the data in Figure 17.4, using TableCurve 2D®

	Value	SE	t-value	95% Confidence Limits	
a (g/cm^2)	0.432	2.026e-04	2132.276	0.4317	0.4325
b ($g/cm^2/h$)	-3.66e-3	1.613e-05	-226.720	-3.689e-3	- 3.626e-3

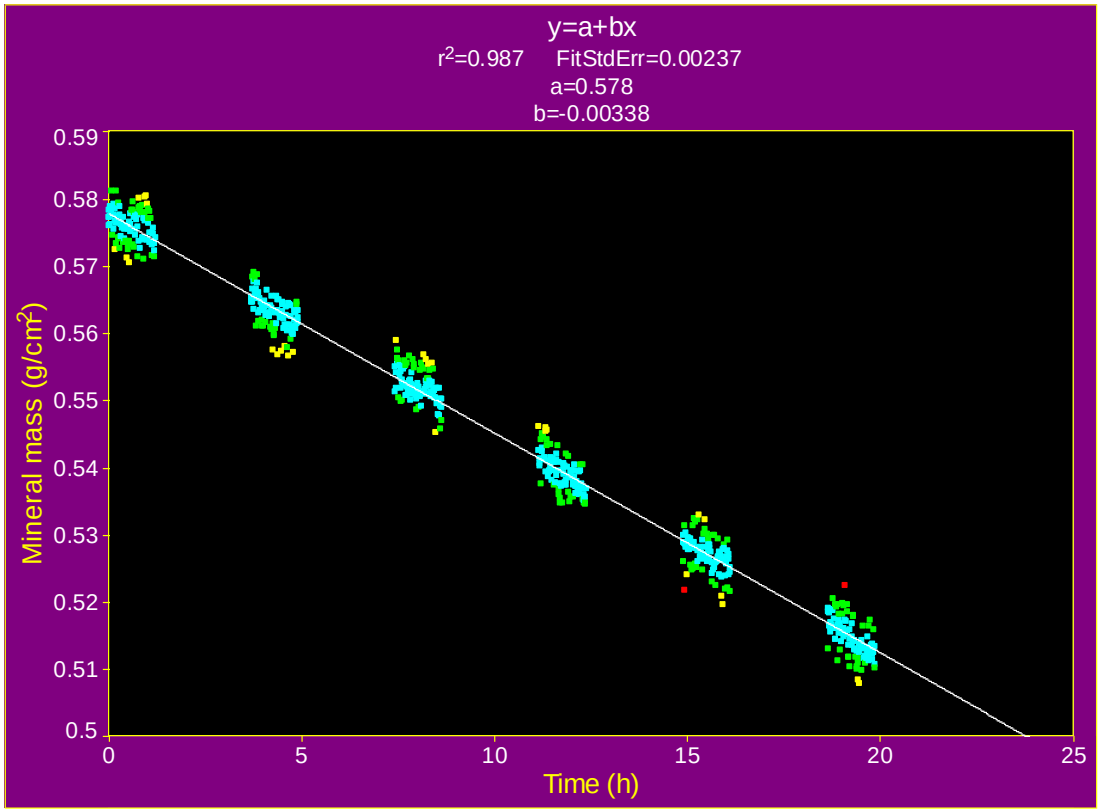

FIGURE 17.5 Typical example of the change in projected HAp mineral mass content over a period of 20 h in response to 0.3% citric acid pH 2.8 with 20 ppm Sr^{2+} demineralisation solution at decreasing Sr^{2+} concentration sequence

(■ Within 1 SD, 1 SD< ■ < 2 SD, 2 SD< ■ < 3 SD, 3 SD< ■ < 4 SD)

TABLE 17.5 Statistical analysis, for the data in Figure 17.5, using TableCurve 2D®

	Value	SE	t-value	95% Confidence Limits	
a (g/cm^2)	0.578	1.779e-04	3248.48	0.5774	0.5781
b ($g/cm^2/h$)	-3.38e-3	1.508e-05	-216.711	-3.298e-3	- 3.239e-3

For each of the 20 demineralisation experiments using 0.3% citric acid pH 2.8 with various Sr^{2+} concentrations, the projected mineral mass loss of each HAp disc was continuously measured throughout the entire experiment duration. The RD_{HAp} and the SE were calculated and the results obtained are summarized in Table 17.6

TABLE 17.6 The RD_{HAp} and SE for each demineralisation solution at different Sr^{2+} concentrations in both increasing and decreasing concentration sequences

0.3% citric acid pH 2.8									
		RD_{HAp} ($g/cm^2/h$) increasing Sr^{2+} concentration sequence				RD_{HAp} ($g/cm^2/h$) decreasing Sr^{2+} concentration sequence			
Sr^{2+} concentration (ppm)		**HAp disc1**	**SE**	**HAp disc2**	**SE**	**HAp disc1**	**SE**	**HAp disc2**	**SE**
	30	3.37×10^{-3}	1.43×10^{-5}	2.87×10^{-3}	1.38×10^{-5}	3.57×10^{-3}	1.41×10^{-5}	4.30×10^{-3}	1.56×10^{-5}
	20	3.66×10^{-3}	1.61×10^{-5}	3.24×10^{-3}	1.46×10^{-5}	3.38×10^{-3}	1.51×10^{-5}	3.72×10^{-4}	1.23×10^{-5}
	10	3.75×10^{-3}	1.95×10^{-5}	3.41×10^{-3}	1.27×10^{-5}	3.21×10^{-3}	1.65×10^{-5}	3.17×10^{-3}	1.34×10^{-5}
	5	4.08×10^{-3}	1.36×10^{-5}	3.95×10^{-3}	1.55×10^{-5}	2.60×10^{-3}	1.19×10^{-5}	2.56×10^{-3}	1.65×10^{-5}
	0	4.31×10^{-3}	1.46×10^{-5}	4.12×10^{-3}	1.22×10^{-5}	5.42×10^{-3}	1.32×10^{-5}	5.88×10^{-3}	1.65×10^{-5}

17.5 Discussion

In this study, Sr^{2+} at drinking water supply concentration levels was investigated at a range between 5 ppm and 30 ppm, based on the literature, particularly the work done by Little and Barrett (1976), Curzon *et al.* (1978), Athanassouli *et al*. (1983), Featherstone *et al*. (1983a), Curzon (1985) and Thuy *et al*. (2008).

The results of strontium 0 ppm solution were used as a control for comparison of the effect of different Sr^{2+}concentrations. Following the same experiment protocol used in the Zn^{2+} experiments, a series of demineralisation solutions was used, that differed only in the Sr^{2+} concentration, in either an increasing or a decreasing concentration sequence on the same permeable HAp disc. Running the experiments in a series of five experiments (≈20 h each), separated by 30 min of washing by stirred de-ionised water removed any loosely adsorbed material from the surface to evaluate the persistence effect of Sr^{2+}.

Figure 17.2 and Figure 17.3 represents typical examples of the change in projected HAp mineral mass content, over a period of ≈20 h when exposed to 0.1% acetic acid pH 4.0 for caries-like conditions with 20 ppm Sr^{2+} demineralisation solution in increasing and decreasing concentration sequences respectively. The data showed a linear regression trend for the projected HAp mineral mass content over time. The systematic gaps in the recording of data over the experimental duration are because more than one SMR cell was scanned simultaneously over the experimental duration. As discussed in Chapter 10, the SMR technique utilizes a large number of data points to obtain good statistical accuracy. Scanning more than one SMR cell requires considerable move time, so bunches of data points were collected for each cell, but this does not affect the calculated RD_{HAp} (Chapter 10).

In Figure 17.2, 606 data counts were measured at a centrally located point on the permeable HAp disc over ≈20 h, of which only 28 data counts were outside 2 SD (4.6%).

Figure 17.3 shows demineralisation in caries-like conditions similar to those in Figure 17.2 but with the sequence of the Sr^{2+} concentration experiments reversed. It shows a similar linear regression trend for the projected HAp mineral mass content over the experimental duration. Six hundred and six data counts were collected at a centrally located point on the permeable HAp disc over ≈20 h out of which 24 data counts were outside 2 SD (3.9%).

Table 17.3 shows the calculated demineralisation rate and the SE for each of the 20 experiments with various Sr^{2+} concentrations.

The effect of Sr^{2+} on RD_{HAp} at increasing concentrations of Sr^{2+} sequence showed that as Sr^{2+} concentration increased in the range from 0-30 ppm, RD_{HAp} decreased (Figure 17.6). The reduction in RD_{HAp} was statistically significant ($P \leq 0.05$) for all Sr^{2+} concentrations investigated when compared to the control group (0 ppm). While the effect of Sr^{2+} on RD_{HAp} at decreasing concentrations of Sr^{2+} sequence showed that as Sr^{2+} concentration decreased in the range from 30 - 0 ppm, the RD_{HAp} continued to decrease significantly, except for 0 ppm where the mean RD_{HAp} increased (Figure 17.7).

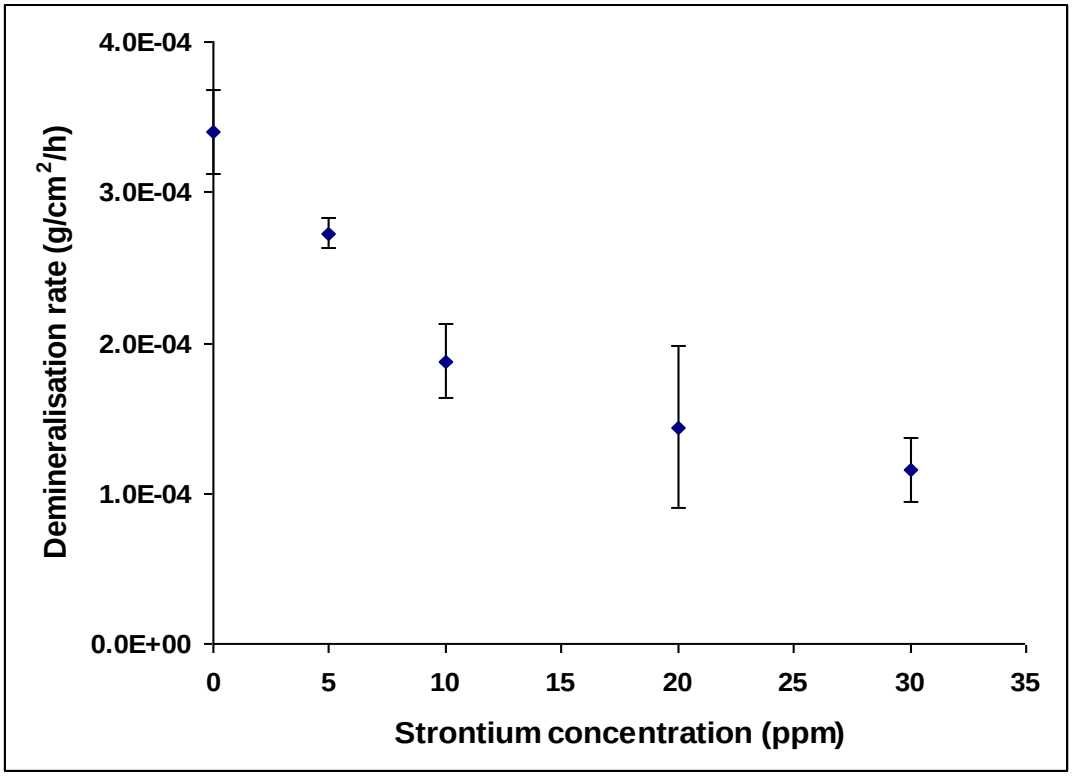

FIGURE 17.6 The effect of Sr^{2+} at a range of 0 -30 ppm on mean RD_{HAp} at increasing Sr^{2+} concentration sequence under caries-like conditions

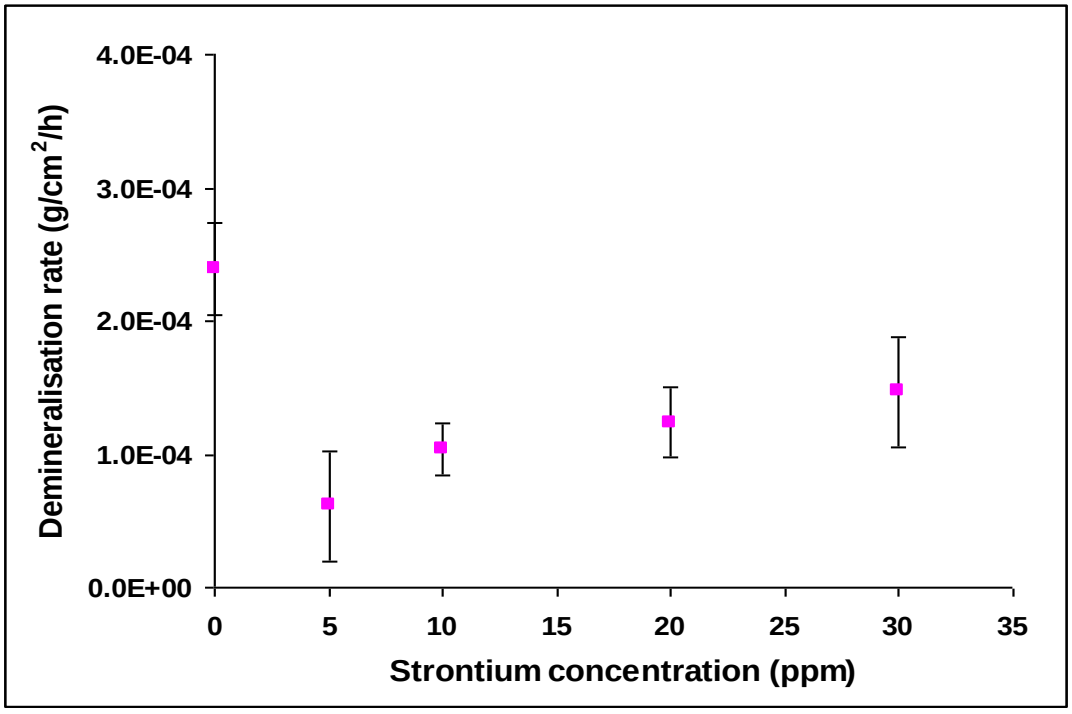

FIGURE 17.7 The effect of Sr^{2+} at a range of 30 - 0 ppm on mean RD_{HAp} at decreasing Sr^{2+} concentration sequence under caries-like conditions

The average of each duplicate experiment, at each Sr^{2+} concentration at increasing and decreasing Sr^{2} concentration sequence was calculated and shown in Figure 17.8.

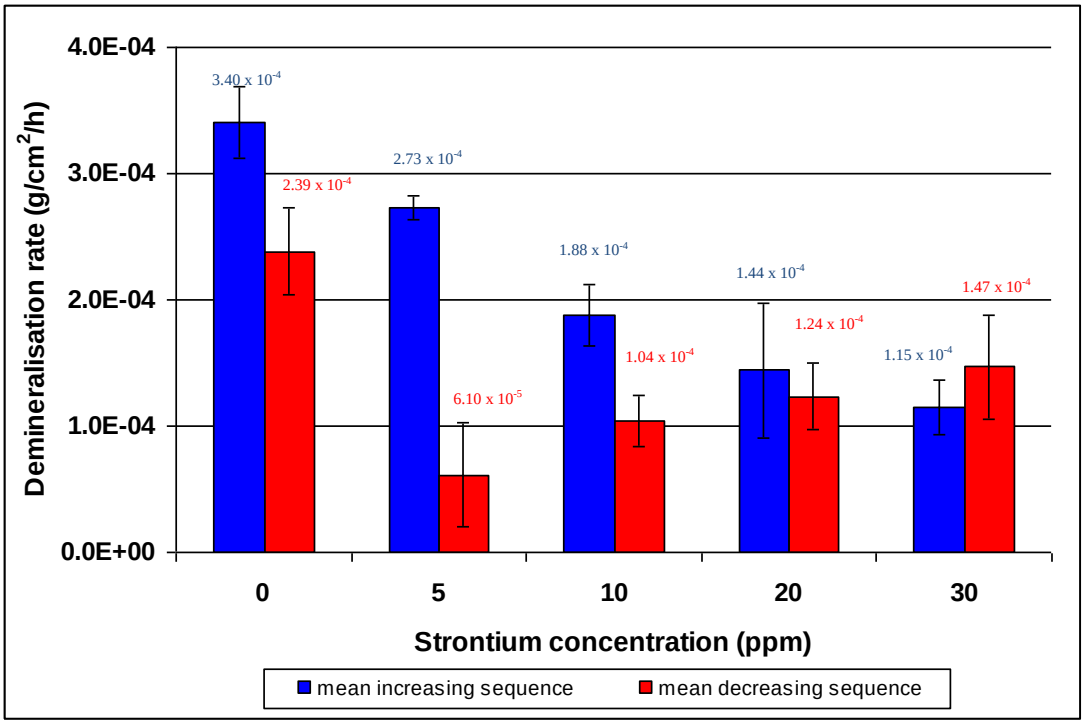

FIGURE 17.8 The effect of 0.1% acetic acid pH 4.0 with different Sr^{2+} concentrations (ppm) on RD_{HAp} (g/cm^2/h) at both increasing and decreasing concentrations sequences

Figure 17.8 shows that Sr^{2+} had an inhibitory effect on the $RD_{HAp.}$ The reduction in RD_{HAp} was statistically significant with $P \leq 0.05$ for all Sr^{2+} concentrations when compared to the control group (0 ppm Sr^{2+} concentration). It also shows that the reduction in RD_{HAp} was affected by the sequence of Sr^{2+} concentration. When the permeable HAp disc was exposed to caries simulating conditions containing 10 ppm Sr^{2+} at increasing Sr^{2+} concentration sequence the mean RD_{HAp} was 1.88×10^{-4} g/cm^2/h. However when the same experiment was repeated in a decreasing concentration sequence, the mean RD_{HAp} was 1.04×10^{-4} g/cm^2/h. A similar observation was seen for all investigated Sr^{2+} concentrations. It was observed that among the investigated Sr^{2+} concentrations, the maximum

reduction in RD_{HAp} in increasing Sr^{2+} concentrations sequence experiments was achieved using 30 ppm Sr^{2+} while for the decreasing Sr^{2+} concentration sequence experiments the maximum reduction in RD_{HAp} was achieved using 5 ppm Sr^{2+}. This supports the idea that Sr^{2+} replaces Ca^{2+} in the HAp crystal lattice and forming a different crystal phase (strontium-calcium-phosphate) which has a more permanent effect.

For erosion-like conditions Figure 17.4 and Figure 17.5 represents typical examples of the change in projected HAp mineral mass content over a period of ≈20 h when exposed to 0.3% citric acid pH 2.8 demineralisation solution containing 20 ppm Sr^{2+} at increasing and decreasing concentration sequence respectively. The data showed a linear regression trend for the projected HAp mineral mass content over time. The systematic periodic interruption in recording the data over the experimental duration is because of more than one SMR cell been scanned simultaneously over the experimental duration. Figure 17.4 shows that 606 data counts were counted at a centrally located point on the permeable HAp disc over ≈20 h out of which only 25 data counts were outside 2 SD (4.1%). The HAp projected mineral mass content decreased at approximately 10 times faster rate than in caries-like conditions. It decreased from 0.432 g/cm^2 to 0.355 g/cm^2 in ≈20 h. This reduction in projected HAp mineral mass content represent a 17.8% loss in projected HAp mineral content over ≈20 h. This further supports that caries is a slowly progressing disease while erosion involves a rapid loss of dental enamel.

Figure 17.5 represents the demineralisation in erosion-like conditions similar to those in Figure 17.4 but with the Sr^{2+} concentration sequence reversed. It shows a similar linear regression trend in projected HAp mineral mass content over the experimental duration. Six hundred and six data counts were counted at a centrally

located point on the permeable HAp disc over ≈20 h out of which only 30 data counts were outside 2 SD (4.9%). The HAp projected mineral mass content decreased from 0.578 g/cm^2 to 0.513g/cm^2 in ≈20 h which represents 11.4% loss of projected mineral content over ≈20 h.

Table 17.4 shows the calculated demineralisation rate and the SE for each of the 20 experiments with various Sr^{2+} concentrations under erosion-like conditions.

The mean effect of Sr^{2+} on RD_{HAp} at increasing concentration sequence showed that as Sr^{2+} concentration increased in the range from 0-30 ppm, the RD_{HAp} decreased (Figure 17.9). The reduction in RD_{HAp} was statistically significant $P \leq 0.05$ for all Sr^{2+} concentrations investigated when compared to the control group (0 ppm). While the mean effect of Sr^{2+} on RD_{HAp} at a decreasing concentration sequence showed that as Sr^{2+} concentration decreased in the range from 30 - 5 ppm, the RD_{HAp} continued to decrease significantly except for 0 ppm where the mean RD_{HAp} increased (Figure 17.10).

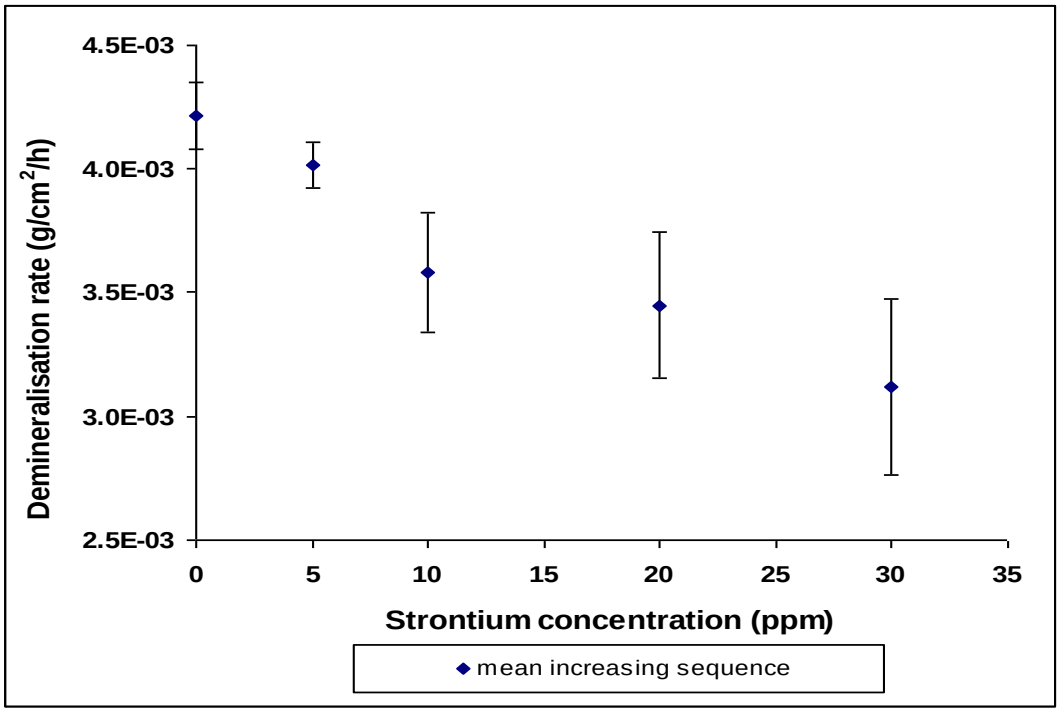

FIGURE 17.9 The effect of Sr^{2+} at a range of 0 - 30 ppm on mean RD_{HAp} at increasing Sr^{2+} concentration sequence under erosion-like conditions

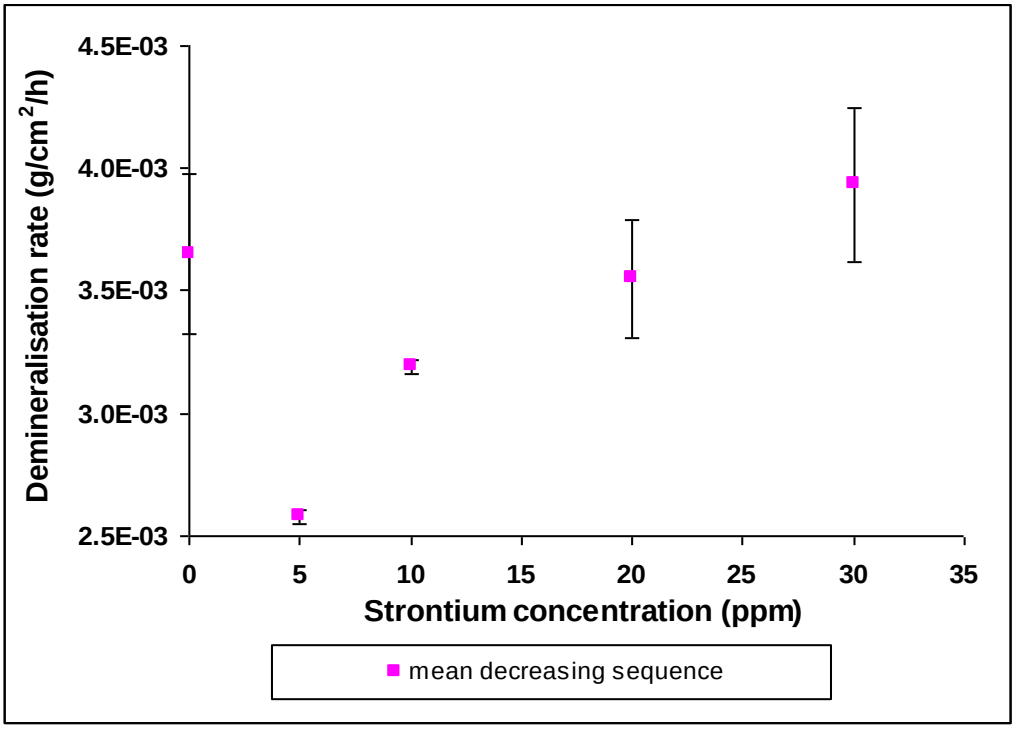

FIGURE 17.10 The effect of Sr^{2+} at a range of 30 - 0 ppm on mean RD_{HAp} at decreasing Sr^{2+} concentration sequence under erosion-like conditions

The average of each duplicate experiments, at each Sr^{2+} concentration, at both increasing and decreasing Sr^{2+} concentration sequence was calculated and shown in Figure 17.11.

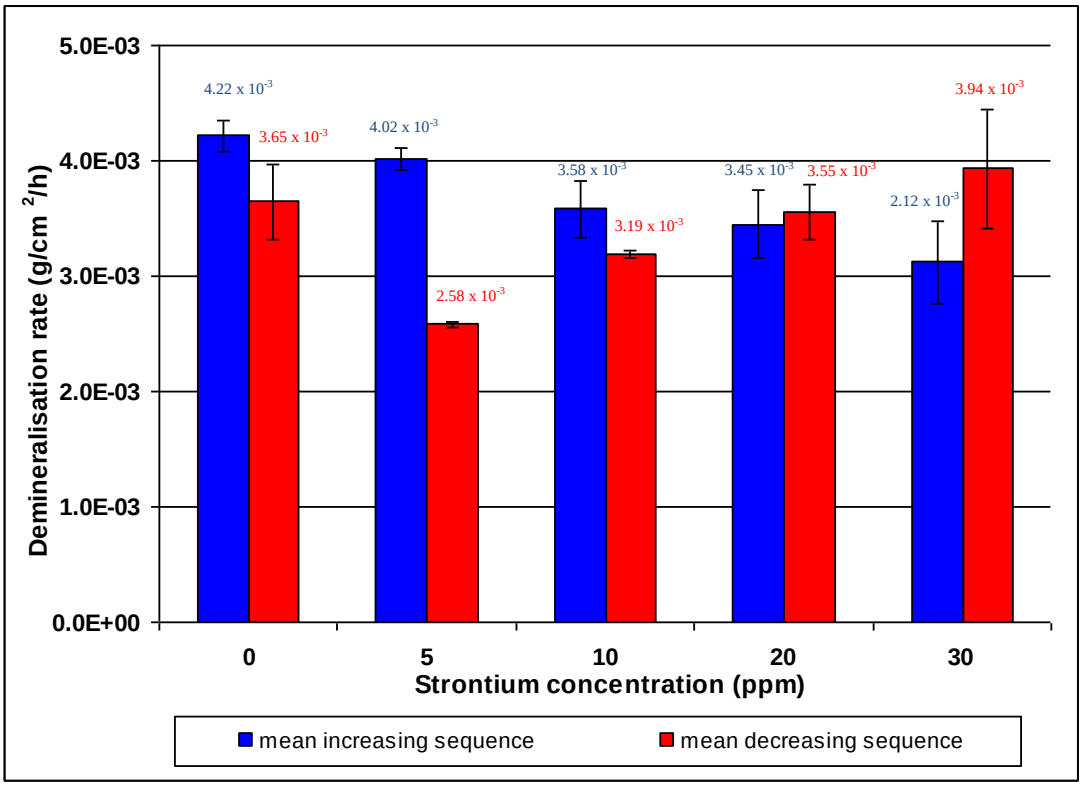

Figure 17.11 The effect of 0.3% citric acid pH 2.8 with different Sr^{2+} concentrations (ppm) on RD_{HAp} ($g/cm^2/h$) at both increasing and decreasing concentrations sequences

Similar to caries-like conditions, Figure 17.11 shows that Sr^{2+} had an inhibitory effect on the $RD_{HAp.}$ The reduction in RD_{HAp} was statistically significant with ($P \leq 0.05$) for all Sr^{2+} concentrations when compared to the control group (0 ppm Sr^{2+} concentration) and the reduction in RD_{HAp} was affected by the sequence of Sr^{2+} concentration in the experimental series. It was observed that among the investigated Sr^{2+} concentrations, the maximum reduction in RD_{HAp} in increasing Sr^{2+} concentrations sequence experiments was achieved using 30 ppm Sr^{2+} while for the decreasing Sr^{2+} concentration sequence experiments the maximum reduction in

RD_{HAp} was achieved using 5 ppm Sr^{2+}, in support of the hypothesis that Sr^{2+} replaces Ca^{2+} in the HAp crystal lattice forming different crystal phase with longer lasting effect on the apatite dissolution. This can be clinically interpreted as better to give a larger dose of a Sr^{2+} containing therapeutic agent (30 ppm of Sr^{2+}) initially, and then provide lower maintenance doses of 5 ppm.

Comparison of the results of the effect of Sr^{2+} on RD_{HAp} under caries and erosion-like conditions shows that they both shared similar regression trend in RD_{HAp} in response to an increase in Sr^{2+} concentrations. The results of this study also confirm that dental caries involves slowly progressive loss of mineral content while erosion involves a faster loss of mineral content (≈10 times faster), which can be explained by the nature of the effect of the two different acids as well as the difference in pH.

17.6 Conclusions

In conclusion, the addition of Sr^{2+} decreased RD_{HAp} under strictly controlled thermodynamic conditions relevant to both dental caries and erosion. However, this decrease was not reversed when the Sr^{2+} concentration was subsequently decreased. This pattern of influence of Sr^{2+} suggests a partial inclusion of Sr^{2+} into the HAp lattice.

CHAPTER 18

Effect of Copper Ions (Cu^{2+}) on Hydroxyapatite Dissolution Kinetics Studied Using Scanning Microradiography

18.1 Introduction

Copper is an essential element required for many normal body functions such as red blood cell synthesis, collagen cross linking as well as metabolism and production of energy.

Copper has been reported to be associated with low caries prevalence in animals such as rats, as well as in human beings. Its caries inhibitory property has been attributed mainly to its antimicrobial effect against oral bacteria associated with dental caries (Section 7.2).

The direct effect of copper ions on hydroxyapatite dissolution has not been studied as extensively as its antimicrobial effect (Section 7.4). There is still much uncertainty about the exact mechanism through which copper increases dental enamel resistance against acid attacks. For further details about copper please refer to Chapter 7.

18.2 Aims and objectives

The aim of this study was to investigate the effect of Cu^{2+} at a range of concentrations of 0 to 180 ppm on the dissolution kinetics of permeable HAp disc.

The objective was to measure the rate of HAp dissolution of a permeable HAp disc using the SMR under strictly controlled thermodynamic conditions relevant to dental caries and erosion at a range of Cu^{2+} concentrations relevant to those used in other studies.

18.3 Materials and methods

The protocol of this experiment is illustrated in Figure 18.1.

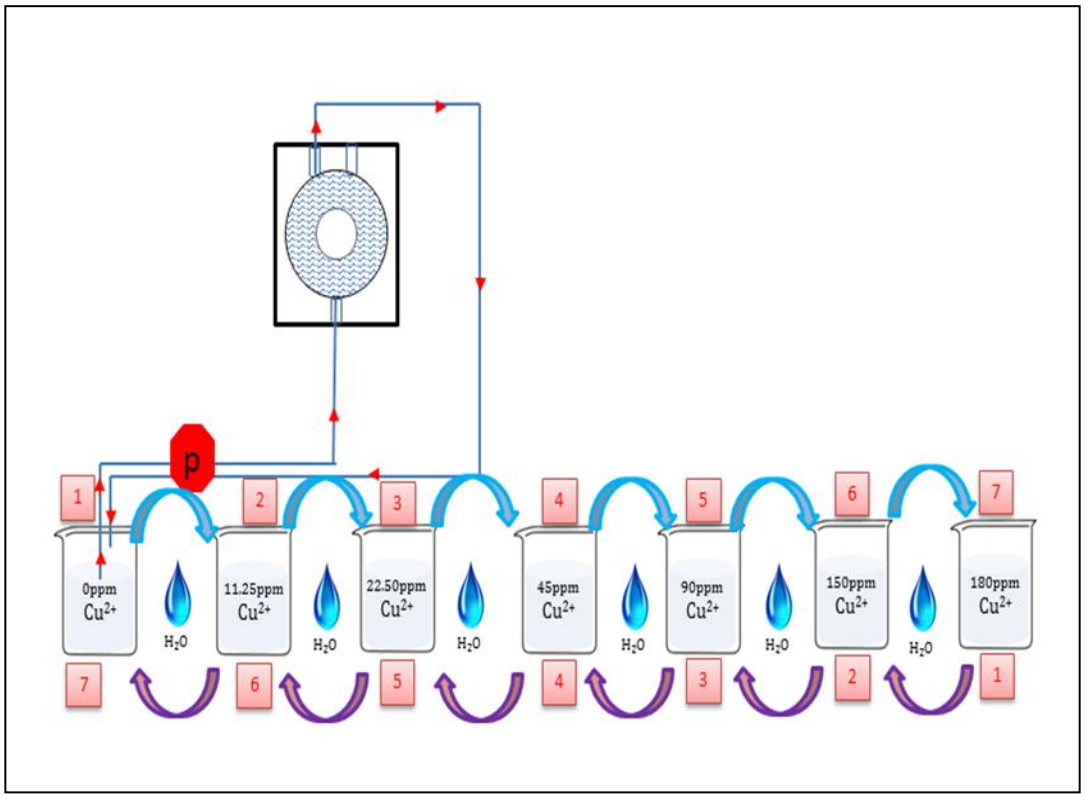

FIGURE 18.1 schematic diagram of an SMR cell with HAp disc in place, connected to the peristaltic pump (p) for circulating the demineralisation solution over a period of 20 h followed by 30 minutes of de-ionised water at both increasing , and decreasing Cu^{2+} concentration sequences

18.3.1 HAp discs

Eight HAp discs were used in this study. The details of the HAp discs preparation were described in Section 10.6.2.

18.3.2 Demineralising solutions

For cariogenic conditions, a 7 litre batch solution of 0.1% acetic acid pH 4.0 was divided into seven 1 liter bottles. Into each one, copper sulphate (*SIGMA-ALDRICH*™, Product code # 1000950043 and batch # 070M0268V) was added, so that the final Cu^{2+} concentrations were 0, 11.25, 22.50, 45, 90, 150, and 180 ppm.

For erosive conditions, a 7 litre batch solution of 0.3% citric acid pH 2.8 was divided into seven 1 liter bottles. Into each one, copper sulphate was added, so that the final Cu^{2+} concentration were of 0, 11.25, 22.50, 45, 90, 150, and 180 ppm.

After the addition of copper sulphate, the pH of each solution was adjusted by using 1 Molar HCl or KOH solutions as necessary (Section 10.6).

18.3.3 SMR

HAp discs were located centrally in the SMR cells and demineralising solutions were circulated at 0.80 ml/min. The rate of HAp demineralisation was measured at a centrally located point in each disc for ≈20 h at 22 ± 1°C. Each experiment was repeated for both increasing (0-180 ppm) and decreasing (180-0 ppm) Cu^{2+} concentration sequences.

For the increasing Cu^{2+} concentration experiments, the HAp disc was exposed for ≈20 h to demineralising solution with no Cu^{2+} added, followed by 30 min of washing by de-ionised water, followed by ≈20 h of exposure to demineralising solution with 11.25 ppm Cu^{2+}, followed by 30 min of washing by de-ionised water and so on through the increasing Cu^{2+} concentrations. All exposures were performed using the same HAp disc (Figure 18.1). In reverse, for the decreasing Cu^{2+}

concentration experiments HAp disc was exposed for ≈20 h to each demineralising solution with 30 min of washing by de-ionised water. The SMR cells were mounted on the SMR stage and scanned simultaneously. Each experiment was duplicated.

18.4 Results

18.4.1 0.1% acetic acid pH 4.0

For each experiment of the 28 demineralisation experiments using 0.1% acetic acid pH 4.0 with various Cu^{2+} concentrations, the mineral mass loss of each HAp disc was continuously measured throughout the entire experimental duration. Figure 18.2 and Figure 18.3 are typical examples of the real-time change in projected HAp mineral mass content in response to exposure to 0.1% acetic acid pH 4.0 solution with 22.5 ppm Cu^{2+} concentration in both increasing and decreasing Cu^{2+} concentration respectively.

Figure 18.2 shows that the projected HAp mineral mass content decreased from 0.671 g/cm^2 to 0.667 g/cm^2 in 20 h. This reduction represents only a 0.5% loss in the projected HAp mineral mass over 20 h at a rate of 1.41×10^{-4} g/cm^2/h. Such subtle changes are difficult to detect and measure without a powerful technique of high precision such as the SMR technique. While for Figure 18.3 the HAp projected mineral mass content decreased from 0.642 g/cm^2 to 0.639 g/cm^2 in ≈20 h which represents a 0.5 % loss in the projected mineral mass over ≈20 h at a rate of 2.1×10^{-4} g/cm^2/h.

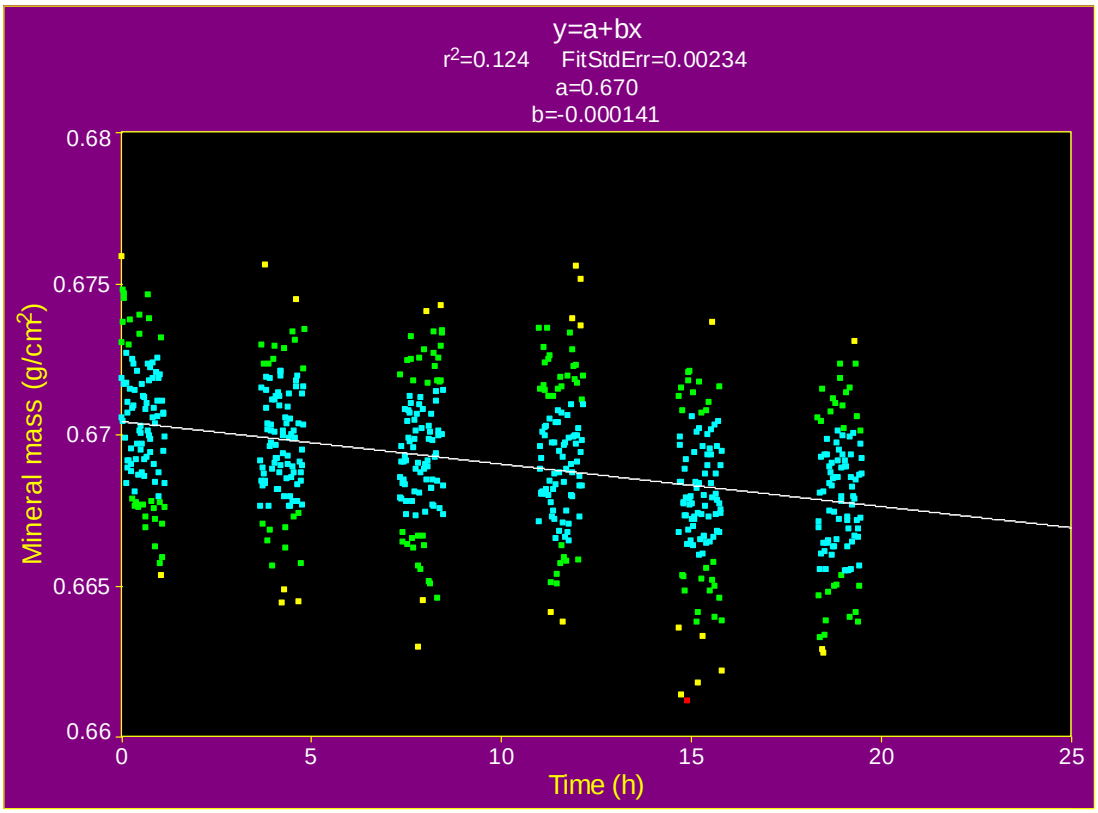

FIGURE 18.2 Typical example of the change in projected HAp mineral mass content over a period of ≈20 h in response to 0.1% acetic acid pH 4.0 with 22.5 ppm Cu^{2+} demineralisation solution at increasing Cu^{2+} concentration sequence

(Within 1 SD, 1 SD< < 2 SD, 2 SD< < 3 SD, 3 SD< < 4 SD)

TABLE 18.1 Statistical analysis, for the data in Figure 18.2, using TableCurve 2D®

	Value	SE	t-value	95% Confidence Limits	
a (g/cm^2)	0.670	1.760e-04	3809.40	0.6701	0.6708
b ($g/cm^2/h$)	-1.41e-4	1.52e-05	-9.26	-1.70-4	- 1.11e-4

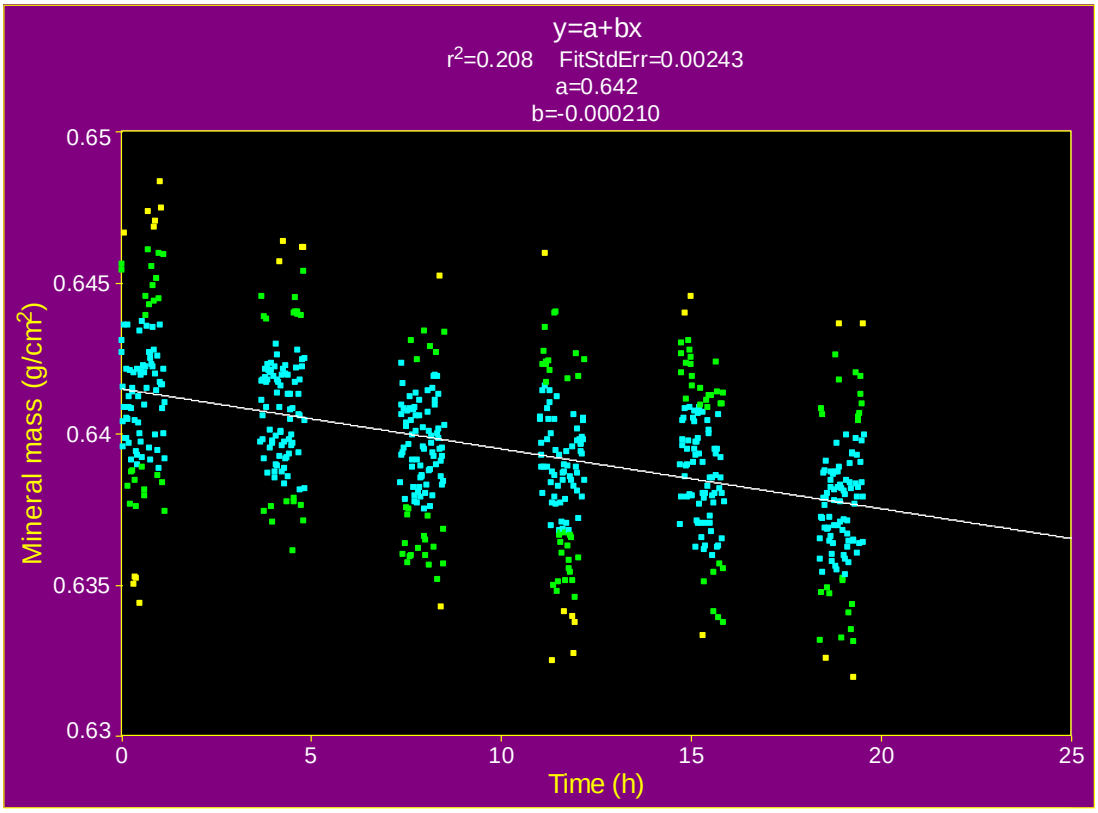

FIGURE 18.3 Typical example of the change in projected HAp mineral mass content over a period of ≈20 h in response to 0.1% acetic acid pH 4.0 with 22.5 ppm Cu^{2+} demineralisation solution at decreasing Cu^{2+} concentration sequence

(■ Within 1 SD, 1 SD< ■ < 2 SD, 2 SD< ■ < 3 SD, 3 SD< ■ < 4 SD)

TABLE 18.2 Statistical analysis, for the data in Figure 18.2, using TableCurve 2D®

	Value	SE	t-value	95% Confidence Limits	
a (g/cm^2)	0.642	1.830e-04	3509.40	0.6111	0.6418
b ($g/cm^2/h$)	-2.10e-4	1.57e-05	-12.59	-2.42-4	- 1.89e-4

The RD_{HAp} and the SE for each of the 28 experiments, using to 0.1% acetic acid pH 4.0 were calculated and the results obtained were summarized in Table 18.3.

TABLE 18.3 RD_{HAp} and SE for each demineralisation solution at different Cu^{2+} concentrations at both increasing and decreasing concentration sequences

0.1% acetic acid pH 4.0									
		RD_{HAp} ($g/cm^2/h$) increasing Cu^{2+} concentration sequence				RD_{HAp} ($g/cm^2/h$) decreasing Cu^{2+} concentration sequence			
Cu^{2+} concentration (ppm)		**HAp disc1**	**SE**	**HAp disc2**	**SE**	**HAp disc1**	**SE**	**HAp disc2**	**SE**
	180	9.40×10^{-5}	2.88×10^{-5}	7.45×10^{-5}	1.57×10^{-5}	8.55×10^{-5}	2.23×10^{-5}	8.01×10^{-5}	2.53×10^{-5}
	150	9.50×10^{-5}	1.30×10^{-5}	1.10×10^{-4}	1.10×10^{-5}	1.56×10^{-4}	1.19×10^{-5}	1.31×10^{-4}	1.13×10^{-5}
	90	1.14×10^{-4}	1.68×10^{-5}	1.23×10^{-4}	1.23×10^{-5}	1.73×10^{-4}	1.43×10^{-5}	1.51×10^{-4}	1.53×10^{-5}
	45	1.26×10^{-4}	1.48×10^{-5}	1.40×10^{-4}	1.40×10^{-5}	1.93×10^{-4}	2.15×10^{-5}	1.74×10^{-4}	1.88×10^{-5}
	22.5	1.41×10^{-4}	1.52×10^{-5}	1.88×10^{-4}	1.88×10^{-5}	2.98×10^{-4}	1.85×10^{-5}	2.10×10^{-4}	1.57×10^{-5}
	11.25	2.30×10^{-4}	1.55×10^{-5}	2.61×10^{-4}	2.61×10^{-5}	2.33×10^{-4}	1.26×10^{-5}	2.61×10^{-4}	1.30×10^{-5}
	0	3.68×10^{-4}	1.49×10^{-5}	3.36×10^{-4}	3.36×10^{-5}	3.20×10^{-4}	1.65×10^{-5}	3.01×10^{-4}	1.45×10^{-5}

18.4.2 0.3% citric acid pH 2.8

Figure 18.4 and Figure 18.5 are typical examples of the real-time change in projected HAp mineral mass content in response to exposure to 0.3% citric acid pH 2.8 solution with 22.5 ppm Cu^{2+} concentration in both increasing and decreasing Cu^{2+} concentration sequences respectively.

Figure 18.4 shows that the HAp projected mineral mass content decreased from 0.640 g/cm^2 to 0.625 g/cm^2 in 20 h. This reduction represents only a 2.3% loss in the projected HAp mineral mass over 20 h. While for Figure 18.5 the HAp projected mineral mass content decreased from 0.600 g/cm^2 to 0.580g/cm^2 in ≈20 h which represents a 3.3% loss in the projected mineral content over ≈20 h.

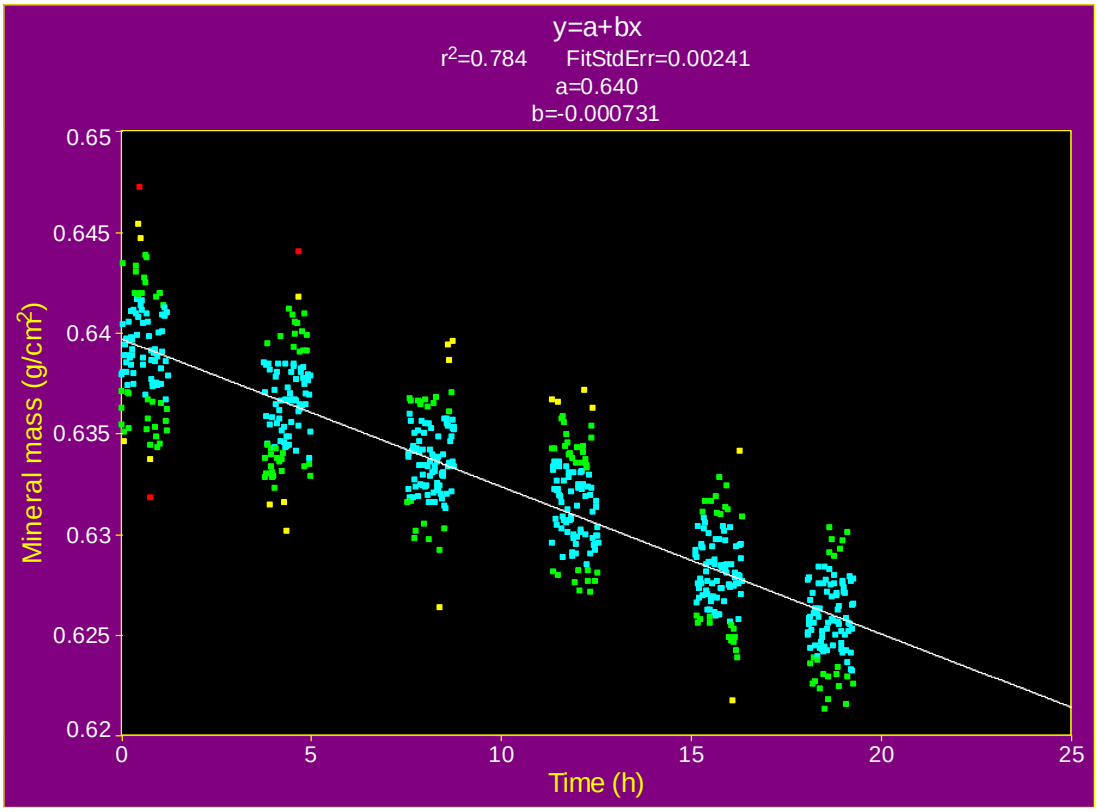

FIGURE 18.4 Typical example of the change in projected HAp mineral mass content over a period of ≈20 h in response to 0.3% citric acid pH 2.8 with 22.5 ppm Cu^{2+} demineralisation solution at increasing Cu^{2+} concentration sequence

(Within 1 SD, 1 SD< < 2 SD, 2 SD< < 3 SD, 3 SD< < 4 SD)

TABLE 18.4 Statistical analysis, for the data in Figure 18.4, using TableCurve 2D®

	Value	SE	t-value	95% Confidence Limits	
a (g/cm^2)	0.640	1.841e-04	3486.08	0.6394	0.6401
b ($g/cm^2/h$)	-7.31e-4	1.56e-05	-46.77	-7.62-4	- 7.00e-4

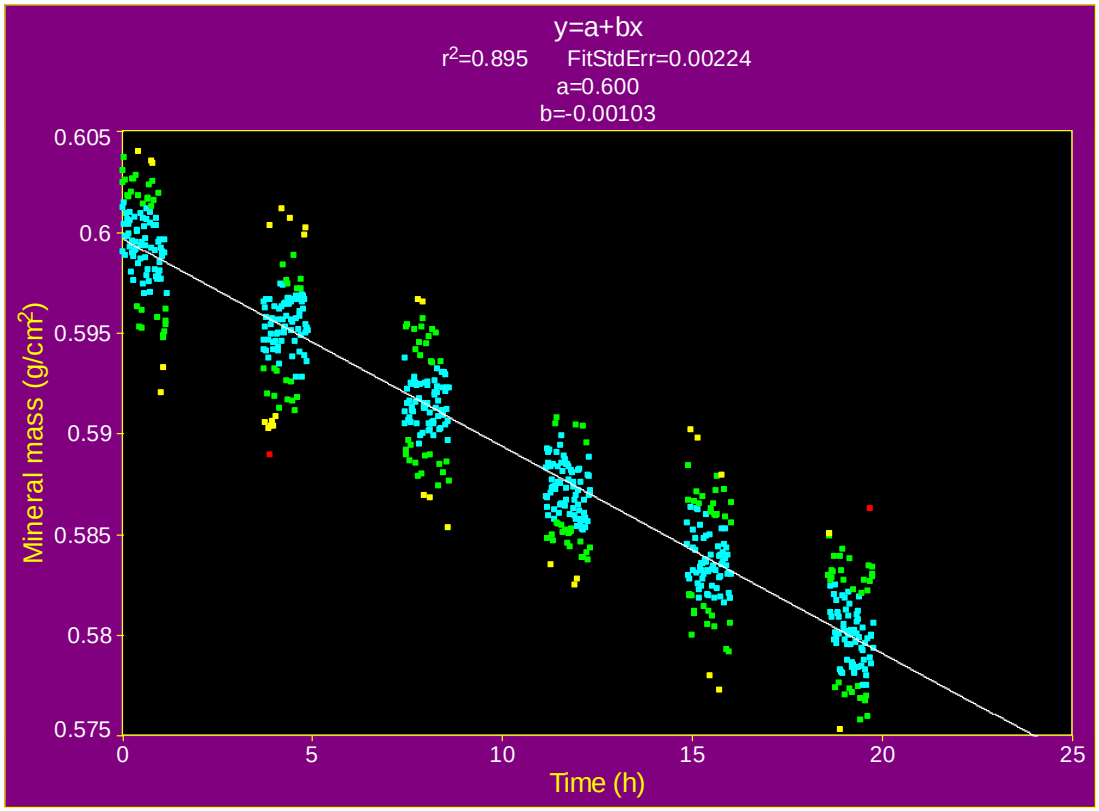

FIGURE 18.5 Typical example of the change in projected HAp mineral mass content over a period of ≈20 h in response to 0.3% citric acid pH 2.8 with 22.5 ppm Cu^{2+} demineralisation solution at decreasing Cu^{2+} concentration sequence

(Within 1 SD, 1 SD< < 2 SD, 2 SD< < 3 SD, 3 SD< < 4 SD)

TABLE 18.5 Statistical analysis, for the data in Figure 18.4, using TableCurve 2D®

	Value	SE	t-value	95% Confidence Limits	
a (g/cm^{2})	0.600	1.681e-04	3565.91	0.5993	0.6000
b ($g/cm^2/h$)	-1.03e-3	1.43e-05	-71.85	-1.06-3	- 9.99e-4

For each of the 28 demineralisation experiments using 0.3% acetic acid pH 2.8 with various Cu^{2+} concentrations, the projected mineral mass loss of each HAp disc was continuously measured throughout the entire experimental duration. The RD_{HAp} and the SE were calculated and the results obtained are summarized in Table 18.6

TABLE 18.6 The RD_{HAp} and SE for each demineralisation solution at different Cu^{2+} concentrations at both increasing and decreasing concentration sequences.

0.3% citric acid pH 2.8									
		RD_{HAp} ($g/cm^2/h$) increasing Cu^{2+} concentration sequence				RD_{HAp} ($g/cm^2/h$) decreasing Cu^{2+} concentration sequence			
Cu^{2+} concentration (ppm)		**HAp disc1**	**SE**	**HAp disc2**	**SE**	**HAp disc1**	**SE**	**HAp disc2**	**SE**
	180	5.95×10^{-4}	2.01×10^{-5}	4.92×10^{-4}	1.43×10^{-5}	6.31×10^{-4}	1.78×10^{-5}	6.33×10^{-4}	1.67×10^{-5}
	150	6.42×10^{-4}	1.75×10^{-5}	5.91×10^{-4}	1.57×10^{-5}	6.36×10^{-4}	2.32×10^{-5}	6.95×10^{-4}	3.21×10^{-5}
	90	6.65×10^{-4}	1.43×10^{-5}	6.12×10^{-4}	1.82×10^{-5}	8.53×10^{-4}	2.13×10^{-5}	7.97×10^{-4}	1.42×10^{-5}
	45	7.06×10^{-4}	1.65×10^{-5}	6.31×10^{-4}	1.18×10^{-5}	9.42×10^{-4}	1.78×10^{-5}	9.42×10^{-4}	1.30×10^{-5}
	22.5	7.07×10^{-4}	1.42×10^{-5}	7.31×10^{-4}	1.56×10^{-5}	1.03×10^{-3}	1.43×10^{-5}	1.07×10^{-3}	2.13×10^{-5}
	11.25	8.78×10^{-4}	1.30×10^{-5}	8.14×10^{-4}	2.70×10^{-5}	1.16×10^{-3}	1.85×10^{-5}	1.14×10^{-3}	1.47×10^{-5}
	0	9.35×10^{-4}	1.56×10^{-5}	8.22×10^{-4}	2.73×10^{-5}	1.21×10^{-3}	1.45×10^{-5}	1.20×10^{-3}	2.41×10^{-5}

18.5 Discussion

The results from this study highlighted the importance of the direct and sole effect of Cu^{2+} as divalent metal cation on the kinetics of HAp dissolution, in isolation from its antibacterial effect. The experiment investigated Cu^{2+} at a range of concentrations from 0-180 ppm. Similar Cu^{2+} concentrations were used in other previous studies (Afseth *et al.*, 1984a, Brookes *et al.*, 2003, Abdullah *et al.*, 2006).

For caries-like conditions; Figure 18.2 and Figure 18.3 represent typical examples of the change in projected HAp mineral mass content, over a period of ≈20 h when exposed to 0.1% acetic acid pH 4.0 with 22.5 ppm Cu^{2+} demineralisation solution in increasing and decreasing concentration sequences respectively. In Figure 18.2 the change in mineral mass content (g/cm^2) was plotted as a function of time (h). The data showed a linear regression trend between the projected HAp mineral mass content over time. The systematic gaps in the recording the data over the experimental duration are because of more than one SMR cell been scanned simultaneously over the experimental duration. In Figure 18.2, 606 data counts were counted at a centrally located point on the permeable HAp disc over ≈20 h out of which 27 data counts were outside 2 SD (4.5%).

Figure 18.3 represents the demineralisation in caries-like conditions similar to those in Figure 18.2 but with the sequence of Cu^{2+} concentrations reversed. It shows a similar linear regression trend in projected HAp mineral mass content over the experimental duration. Six hundred and six data counts were collected at a centrally located point on the permeable HAp disc over ≈20 h out of which 29 data counts were outside 2 SD (4.7%).

Table 18.3 shows the calculated demineralisation rate and the SE for each of the 28 experiments with various Cu^{2+} concentrations.

The mean effect of Cu^{2+} on RD_{HAp} at increasing concentration sequence showed that as Cu^{2+} concentration increased over the range from 0-180 ppm, RD_{HAp} decreased (Figure 18.6). The reduction in RD_{HAp} was statistically significant ($P \leq 0.05$) for all Cu^{2+} concentrations investigated when compared to the control group (0 ppm). These results are in accordance with the observations of Hein *et al.* who reported caries reduction in hamsters with 50 ppm Cu^{2+} as copper sulphate in drinking solutions (Hein, 1953). It also goes in accordance with the results obtained by Afseth *et al.* who reported a significant reduction in caries in rats at 65 ppm Cu^{2+} applied as topical application (Afseth *et al.*, 1984a). When the sequence of Cu^{2+} concentrations was reversed, as Cu^{2+} concentration decreased at a range of 180-0 ppm, RD_{HAp} increased (Figure 18.7).

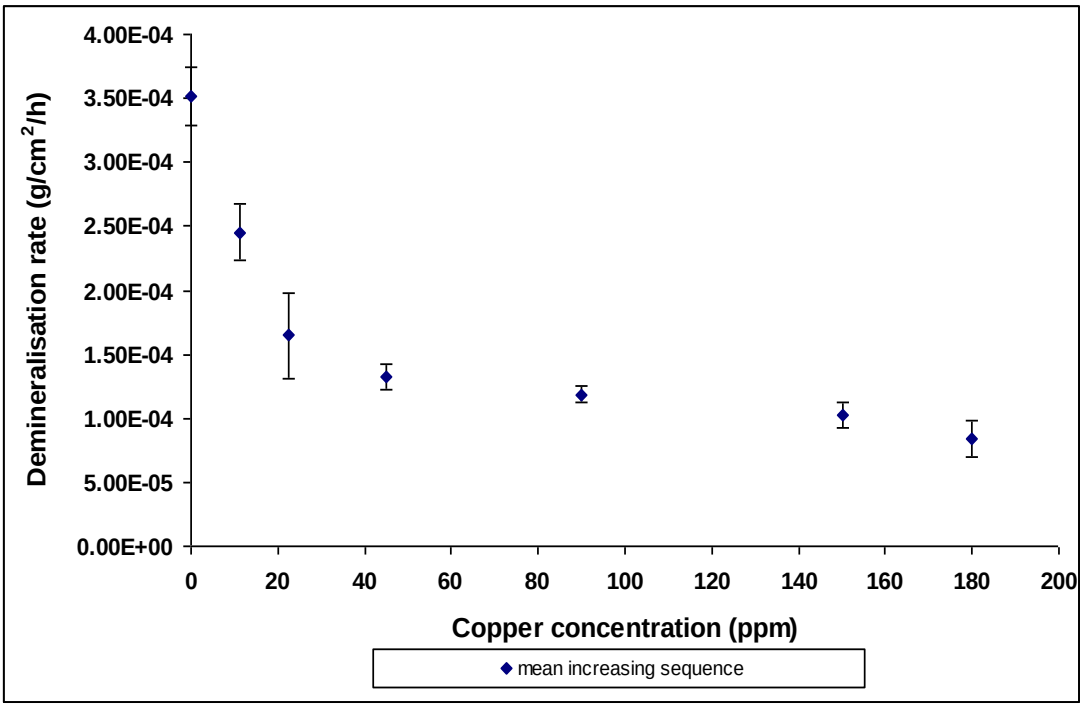

FIGURE 18.6 The effect of Cu^{2+} at a range of 0 - 180 ppm on mean RD_{HAp} at increasing Cu^{2+} concentration sequence under caries-like conditions

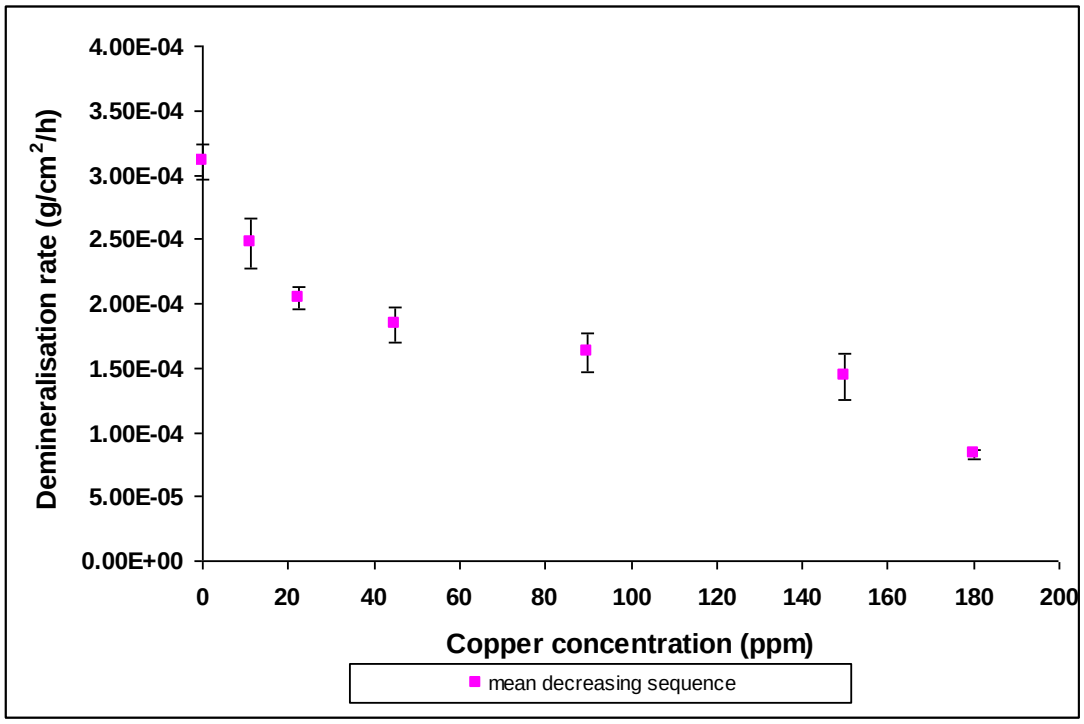

FIGURE 18.7 The effect of Cu^{2+} at a range of 180 - 0 ppm on mean RD_{HAp} at decreasing Cu^{2+} concentration sequence under caries-like conditions

The results of this study also show that the differences in reduction of RD_{HAp} obtained with 150 and 180 ppm Cu^{2+} concentration were not statistically significant when compared to the reduction observed with 90 ppm Cu^{2+}. These results are in agreement with those published by Brookes *et al.*(2003); as illustrated in Figure 18.8.

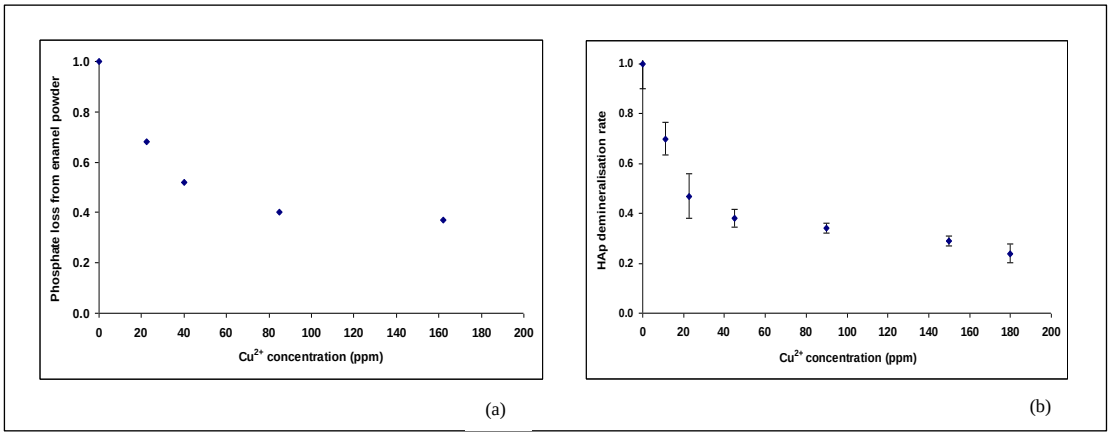

Figure 18.8 (a) The effect of Cu^{2+} concentration on phosphate released from powdered enamel published by Brookes *et al.*(2003) after the conversion of mmol/L to ppm; (b) Example of the effect of Cu^{2+} at a range of 0-180 ppm on mean RD_{HAp} as observed in this study

The average of each duplicate experiment, at each Cu^{2+} concentration, for increasing and decreasing concentration sequence was calculated and presented in Figure 18.9.

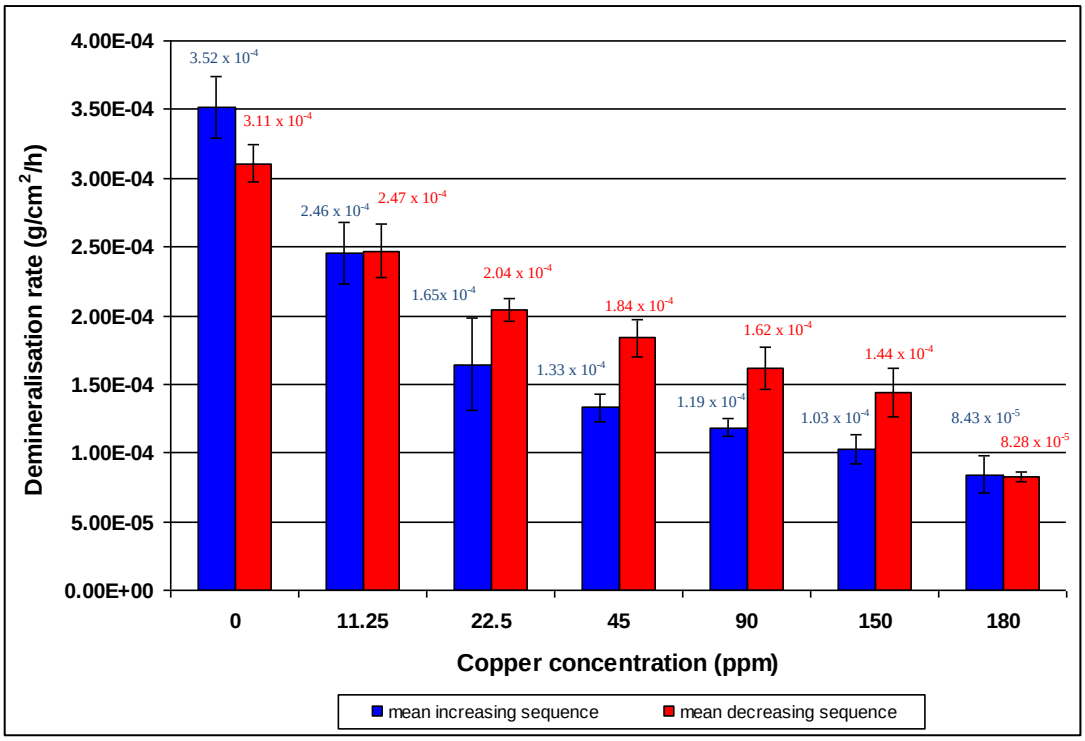

FIGURE 18.9 The effect of 0.1% acetic acid pH 4.0 with different Cu^{2+} concentrations (ppm) on RD_{HAp} ($g/cm^2/h$) at both increasing and decreasing concentrations sequences

Figure 18.9 shows that Cu^{2+} had an inhibitory effect on the RD_{HAp}. The percentage reduction in RD_{HAp} detected in this experiment was around 75% reduction in caries-like conditions at Cu^{2+} concentration of 180 ppm. This percentage is less than the percentage reduction in caries detection reported by Rosalen *et al.* (1996a) who reported 82% reduction at 150 ppm Cu^{2+} concentration. The difference in reduction rate detected can be attributed to the principle difference between the two studies. The Rosalen *et al.* (1996a) study was an *in vivo* study, while this study is *in vitro*. In addition, the effect of Cu^{2+} concentration in this study is determined from its direct effect on HAp reflected as a change in RD_{HAp} whereas in other studies the effect of Cu^{2+} is measured indirectly by its effect on caries score.

For erosion-like conditions Figure 18.4 and Figure 18.5 are typical examples of the change in projected HAp mineral mass content, over a period of ≈20 h when exposed to 0.3% citric acid pH 2.8 demineralisation solution containing 22.5 ppm Cu^{2+} at increasing and decreasing concentration sequences respectively. The change in mineral mass content (g/cm^2) was plotted as a function of time (h). The data showed a linear regression trend between the projected HAp mineral mass content over time. The systematic gaps in recording the data over the experimental duration were because of more than one SMR cell been scanned simultaneously over the experimental duration. In Figure 18.4, 606 data counts were counted at a centrally located point on the permeable HAp disc over ≈20 h out of which 31 data counts were outside 2 SD (5.1%).

Figure 18.5 represents the demineralisation in erosion-like conditions similar to those in Figure 18.4 but with the sequence reversed. It shows a similar linear regression trend in projected HAp mineral mass content over the experimental duration. Six hundred and six data counts were collected at a centrally located point on the permeable HAp disc over ≈20 h out of which 30 data counts were outside 2 SD (4.9%).

Table 18.6 shows the calculated demineralisation rate and the SE for each of the 28 experiments with various Cu^{2+} concentrations.

The mean effect of Cu^{2+} on RD_{HAp} at increasing concentration sequences showed that as Cu^{2+} concentration increased at a range of 0 - 180 ppm, the RD_{HAp} decreased (Figure 18.10). The reduction in RD_{HAp} was statistically significant ($P \leq 0.05$) for all Cu^{2+} concentrations investigated when compared to the control group (0 ppm). However, when the sequence of Cu^{2+} concentrations was reversed, as Cu^{2+}

concentration decreased at a range of 180-0 ppm, the RD_{HAp} increased (Figure 18.11).

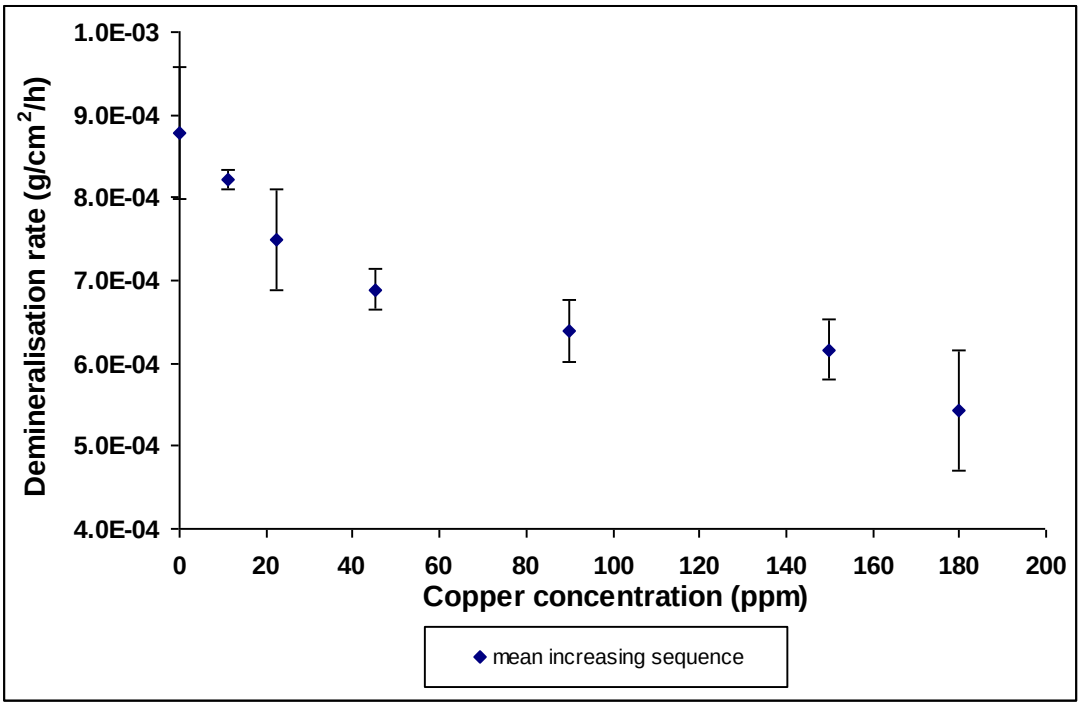

FIGURE 18.10 The effect of Cu^{2+} at a range of 0 - 180 ppm on mean RD_{HAp} at increasing Cu^{2+} concentration sequence under erosion-like conditions

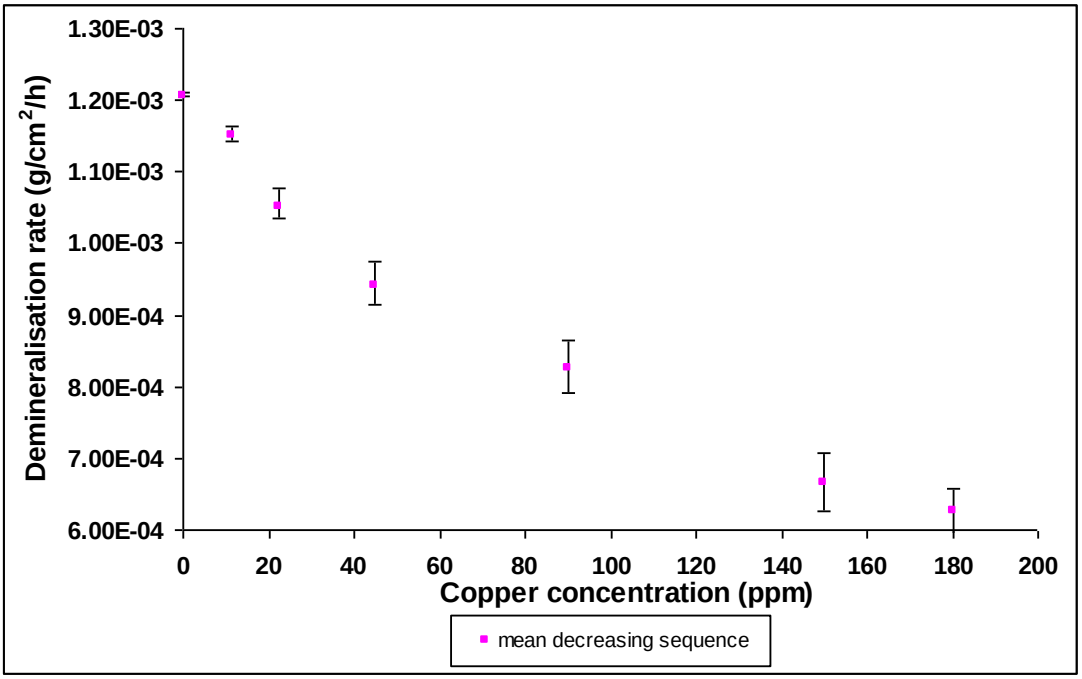

FIGURE 18.11 The effect of Cu^{2+} at a range of 180 - 0 ppm on mean RD_{HAp} at decreasing Cu^{2+} concentration sequence under erosion-like conditions

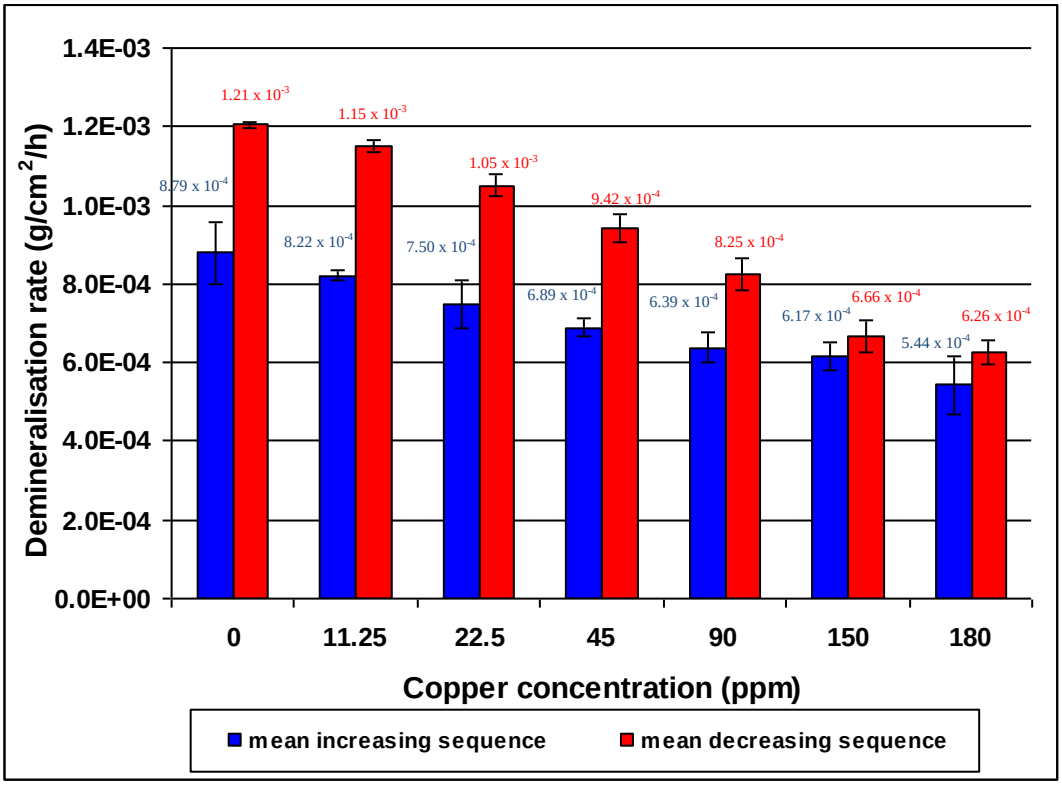

FIGURE 18.12 The effect of 0.3% citric acid pH 2.8 with different Cu^{2+} concentrations (ppm) on RD_{HAp} ($g/cm^2/h$) at both increasing and decreasing concentrations sequences

The average of each duplicate experiment, at each Cu^{2+} concentration, at both increasing and decreasing Cu^{2+} concentration sequences were calculated and shown in Figure 18.12. The dose response data obtained from this study demonstrated a significant and direct effect of Cu^{2+} on RD_{HAp} from the minimal investigated concentration of 11.25 ppm. However, Cu^{2+} concentrations of 150 ppm and 180 ppm did not show a statistically significant reduction in RD_{HAp}. These results are similar to the results obtained from Brookes *et al.* (2003) (Figure 7.1).

Figure 18.12 shows that the mean RD_{HAp} for Cu^{2+} decreasing sequence experiments is higher than the RD_{HAp} for Cu^{2+} increasing sequence experiments. The justification remains unclear and requires further investigations.

All the series of 7 different Cu^{2+} concentrations, whether at increasing or decreasing concentration sequence under conditions resembling artificial caries or erosion, showed the same trend in RD_{HAp} reduction/increase. The reversibility in

RD_{HAp} through the increased or decreased Cu^{2+} concentration sequence supports the hypothesis that Cu^{2+} under the experimental conditions does not permanently change the HAp solid phase. Instead it affected the calcium-rich layer (stern layer) or adhered to the HAp surface blocking the dissolution pit (Wang *et al.*, 2005).

18.6 Conclusions

In conclusion, the results of this study showed the direct inhibitory effect of Cu^{2+} as the divalent metal cation on HAp dissolution kinetics from the minimal investigated concentration as 11.25 ppm. The reversibility of the effect suggests a surface controlled action rather than change in the bulk composition. It demonstrates the potential usefulness of Cu^{2+} as a preventive agent against caries and erosion.

PART V: GENERAL DISCUSSION, CONCLUSIONS, CLINICAL IMPLICATIONS AND RECOMMENDED FUTURE WORKS

CHAPTER 19

General Discussion, Conclusions, Clinical Implications and Future Works

19.1 General discussion

In order to develop an effective preventive strategy for mineral loss in dental caries and erosion, it is essential to fully understand the physico-chemical processes involved in these two conditions and the factors affecting them. Unfortunately many aspects of the dental enamel demineralisation processes are still poorly understood. For example, the direct effects of various divalent cations-enamel interactions, relevant to demineralisation need further investigations and deeper understanding. Therefore, the main aim of this thesis was to investigate the effect of Zn^{2+}, Sr^{2+} and Cu^{2+}, as divalent metal cations, on HAp dissolution kinetics relevant to dental caries and erosion-like conditions.

Ideally dental enamel should have been used. However, it was decided to use permeable compressed sintered HAp discs instead of dental enamel due to the uniformity and homogeneity of its structure compared to enamel. HAp has been extensively used in research as a model system for dental enamel (Margolis and Moreno, 1985, Anderson, 1993, Elliott *et al.*, 2005).

Most previous studies on Zn^{2+} and Cu^{2+} were aiming at investigating their antimicrobial effect. However the scope of interest of this thesis was to investigate the direct and sole effect of divalent cations on the kinetics of HAp dissolution.

As part of this study, new methodologies have been devised. This included modification and optimisation of the SMR technique to obtain sufficient and statistically reliable data over short period of 24 h or less (Chapter 10). Further the developments of the research protocol which involved multiple experiments to investigate the effect of changing various experimental parameters on HAp dissolution kinetics. These studies included the characterization of the different types of HAp discs using XRD, XMT and SMR, the effect of various demineralisation solutions with range of pH on the RD_{HAp}, the effect of demineralisation solution circulation speed on RD_{HAp} and the effect of high Sr^{2+} concentrations on HAp dissolution kinetics. These studies are described in Chapters 11-15.

Studying the effect of divalent cations on the HAp dissolution kinetics via exposing a single HAp disc to a series of demineralisation solutions containing certain cations concentrations in both increasing and decreasing concentration sequence for 20 h at each concentration separated by 30 min of washing by de-ionised water, has proved to be a successful approach in evaluating the persistence/lack of persistence of the effect of the divalent cation under investigation. This experimental approach provided an insight to the different mechanisms through which the various divalent cations under investigation affected the HAp dissolution kinetics.

The results obtained from the effect of Sr^{2+} on RD_{HAp} (Chapter 17) showed that as Sr^{2+} concentrations were increased the RD_{HAp} decreased, and when the Sr^{2+}

concentrations were subsequently decreased, the RD_{HAp} continued to decrease. This "persistence" of Sr^{2+} effect on HAp dissolution was demonstrated in its ability to decrease RD_{HAp} whether it was investigated at an increasing or decreasing concentration sequence. These results support the hypothesis that Sr^{2+} substitutes some Ca^{2+} in the HAp forming Sr-Ca-phosphates phase. The results of this substitution should lead to the formation of a less stable phase (Sr-Ca-phosphates) (LeGeros, 1991, Grynpas, 1993, Kikuchi *et al.*, 1994) due to the difference in size between Sr^{2+} and Ca^{2+} ions (Section6.4). However the explanation for the reduction in RD_{HAp} that was observed from the results of this study, can be justified by the critically low Sr^{2+} concentrations investigated (0–30 ppm) which lead to less than 10% strontium substituted apatites. This comes in agreement with the results reported by (Li *et al.*, 2007) and (Verbeeck *et al.*, 1981).

The results shown in Chapter 16 on the effect of using a range of Zn^{2+} concentrations (0-20 ppm) on RD_{HAp} demonstrated that Zn^{2+} incorporated into caries and erosion-like demineralisation conditions, provided an inhibitory effect. As Zn^{2+} concentrations were increased the RD_{HAp} decreased, but when the Zn^{2+} concentrations were subsequently decreased, the RD_{HAp} increased again. This lack of "persistence" of Zn^{2+} effect on HAp disc dissolution suggests that Zn^{2+} exerts its effect through an adsorption mechanism (Stötzel *et al.*, 2009), rather than incorporation into the crystal lattice mechanism as suggested in earlier studies (Mayer *et al.*, 1994, Li *et al.*, 2008, Ren *et al.*, 2009).

Cu^{2+} showed a similar effect as Zn^{2+}, suggesting similarly a surface controlled effect rather than long term effect in reducing RD_{HAp} under dental caries and erosion-like conditions. However, the metallic taste and ability to cause teeth

discolorations of Cu^{2+} will be limitations of its incorporation into therapeutic agents aiming at the prevention of dental caries and erosion.

Comparison between the results of the effects of the three divalent metal cations at 20 ppm concentration shows that Sr^{2+} provides the best protection against HAp dissolution under both caries and erosion like conditions (58% and 50% respectively). Copper demonstrates a slightly lower inhibitory effect (53% and 15% reduction in RD_{HAp} under caries and erosion like conditions respectively). Zinc demonstrated the lowest efficacy with 38% reduction in RD_{HAp} under caries like conditions and 41% reduction in RD_{HAp} under erosion like conditions. However, although as discussed in sections 16.6, 17.6 and 18.6, the mechanisms are different for the different ions, the dissolution inhibitions are similar.

Strontium and copper showed more protection for HAp against dissolution when exposed to acetic acid pH 4.0, while zinc was more protective under the erosive like conditions of citric acid pH 2.8. The exact reason behind this finding is not known and more research is needed in this area. However it is an interesting finding to be taken in consideration while selecting a suitable divalent cation when designing a therapeutic regimen, or to be incorporated as a food and drink modifier to protect against dental caries or erosion.

19.2 Conclusions

In this thesis, the effect of three divalent cations; Zn^{2+}, Sr^{2+} and Cu^{2+}, on the physical-chemistry influencing HAp dissolution kinetics, under simulated cariogenic and erosive conditions relevant to the oral environment was studied using an SMR technique.

The following conclusions were drawn:

1. SMR has been shown to be a highly suitable technique for investigating the effect of cations on the kinetics of HAp dissolution. Among its advantages are its accuracy in obtaining real-time quantitative measurements, the way it allows alteration of the experimental conditions if required, to simulate the more dynamic environment mimicking the oral cavity, without interrupting the experiment.
2. SMR has previously been successfully used in experiments investigating de/remineralisation over long period of time extending up to several weeks; however the results in this thesis demonstrated that the SMR technique is also capable of obtaining quantitatively reliable data with high accuracy and precision over short time of 24 h or less.
3. The use of Zn^{2+}, Sr^{2+} and Cu^{2+} as therapeutic agents should not be simply confined to their role as antiplaque and calculus agents, or for the treatment and prevention of tooth hypersensitivity. Instead the ions' use should be expanded to include prevention of dental caries and erosion by directly inhibiting dental tissue dissolution.
4. It was observed that Zn^{2+} and Cu^{2+} decreased RD_{HAp} through a surface controlled mechanism whereas Sr^{2+} decreased RD_{HAp} through a solid phase change. This information will be useful as part of the development of therapeutic products which include these ions for the prevention of dental caries and erosion.

19.3 Clinical implications

Dental caries and erosion are worldwide problems, affecting populations in both industrial and developing countries. According to WHO 2003 (Petersen, 2003) dental caries alone affected approximately five billion people worldwide, and prevalence of dental erosion has increased in recent years. The recent increase in dental erosion might be due to a real increase in the disease due to faulty oral hygiene habits and/or diet with high erosive potential, or due to the increased awareness of the disease by both dentists and patients. Dental caries and erosion form a real problem and their control is a challenge.

In the past it was thought that dental caries and erosion are irreversible progressive dental tissue diseases. Nowadays with more research in the field, it has been realized that enamel and dentine constantly undergo through alternating demineralisation and remineralisation according to the surrounding oral environment. It is also known that demineralisation can be stopped at early stages of its development and remineralisation of very early lesions is possible. This depends on the early detection and proper management of the condition via therapeutic agents capable of controlling demineralisation and facilitating remineralisation of the affected enamel.

Nowadays the concept of minimally invasive dentistry is more appreciated by both dentists as well as by patients (Wilson, 2007). It is based on three basic principles; prevention, less intrusive treatment, and conservation of healthy tissues. The research interest in discovering and developing therapeutic agents that inhibit demineralisation and ideally facilitate remineralisation of dental enamel has increased recently. Historically, the ion of most interest in prevention of enamel demineralisation was fluoride. The discovery of fluoride caries-reducing effect was a

landmark in the history of dentistry. Until now almost all successful preventive treatments contain fluoride. Fluoride cariostatic effectiveness does not only lay in its effect on the apatite crystal lattice but also in its inhibition of mineral dissolution, inhibition of acid formation by dental plaque bacteria and promotion of remineralisation. Another element of interest to recent research is silver in its divalent and trivalent cation forms. Silver as a trivalent metal cation has demonstrated its ability in preventing against dental caries through its bacteriostatic effect. Most recent researches on salivary proteins have demonstrated that statherin and a subunit of protein STN21 have considerable effect in preventing HAp demineralisation, and these peptides can be used as therapeutic agents for the prevention or treatment of erosive and carious demineralisation.

In this thesis the three divalent cations of interest (Zn^{2+}, Sr^{2+} and Cu^{2+}) showed positive results in their anti-carious and anti-erosive effect with promising clinical implications.

19.3.1 Zinc

Zn^{2+} has been incorporated in oral hygiene products. It has been used in toothpastes and mouthwashes for its antiplaque effect and for its capability to reduce oral malodor. This is accomplished through its ability to alter bacterial metabolic activity leading to reduction in bacterial growth and capability to adhere to tooth surfaces. However, the results of this study have demonstrated that Zn^{2+} has a direct effect on HAp dissolution kinetics under caries and erosion-like conditions. This effect is significant even at low concentrations such as 5 ppm Zn^{2+}. This expands the potential usefulness of Zn^{2+} in playing a role as a therapeutic agent added to toothpastes and mouthwashes aiming at caries and erosion prevention. However, the results of this thesis have demonstrated that the surface effect of Zn^{2+} in inhibiting

HAp dissolution should be taken into account in the design of the new Zn^{2+} containing therapeutic agents, for example allowing long term release of Zn^{2+} or more frequent applications this can be achieved through the incorporation of Zn^{2+} into chewing gum or mouthwashes. Zn^{2+} toxicity should not be of concern (Section 5.1) as it does not have to be added in high concentrations to provide the preventive effect.

19.3.2 Strontium

The second divalent metal cation studied in this thesis was Sr^{2+}. One of the main clinical uses of Sr^{2+} is for the management of osteoporosis. Sr^{2+} stimulates osteoblast cell activities and inhibits osteoclast cell differentiation, reducing in bone resorption. This characteristic of Sr^{2+} has also led to its being favoured in dental implants, by introducing Sr^{2+} as component in some bioactive glass materials to facilitate the integration between the dental implant and bone.

Sr^{2+} has been also used for the prevention and management of tooth hypersensitivity. Strontium chloride has been introduced commercially as the first tubular occluding agent in Sensodyne™ Original toothpaste (Dowell and Addy, 1983). Sensodyne™ Rapid Relief is one of the latest products on the market to manage tooth hypersensitivity with strontium acetate as a key ingredient. In order for the Sr^{2+} to effectively block the dentinal tubules and reduce tooth sensitivity it has to be incorporated at high concentration (80,000 ppm of strontium acetate) (Layer and Hughes, 2010).

The results presented in this thesis have demonstrated a direct anti-carious and anti-erosive effect of Sr^{2+} through its incorporation into the apatite lattice forming strontium calcium phosphate which lowers the HAp dissolution rate when applied in low concentration (0-30 ppm). A potential clinical implication arising

from this study is the manufacture of toothpastes or mouthwashes with these low Sr^{2+} concentrations for caries and erosion prevention.

Another clinical implication is the use of Sr^{2+} in dental cements and glass ionomer cements. It will not only have the advantage of being more radiopaque which allow better follow up for caries progression, but the Sr^{2+} containing glass ionomer cement will also have the advantage of providing a local anti-carious and anti-erosive effect.

19.3.3 Copper

While Cu^{2+} has been used for its antimicrobial effect against dental plaque bacteria causing caries and periodontal diseases, not much attention has been given to the direct effect of Cu^{2+} in reducing the RD_{HAp}. Cu^{2+} and Zn^{2+} both share the same mechanism of affecting the kinetics of HAp dissolution. However the salty metallic taste of Cu^{2+} and tooth discolouration might be a major drawback to its use in therapeutic agents for the prevention of dental caries and erosion.

19.4 Recommended future works

1) Studies of dental enamel: In this thesis, the SMR technique was successfully used to demonstrate the inhibitory effect of the three investigated divalent cations (Zn^{2+}, Sr^{2+} and Cu^{2+}) on RD_{HAp}. However, knowing that dental enamel consists mainly of impure form of HAp, which contains multiple impurities, it would be beneficial for the results of this study to be used as a base for a future work that involves applying the same experiments using dental enamel.

2) Lower concentrations of investigated cations: The results of this thesis have shown that Zn^{2+}, Sr^{2+} and Cu^{2+}, significantly reduced RD_{HAp} even at the minimal

investigated concentrations. However no concentrations less than 5 ppm were investigated. It would be of interest in future works to investigate the same cations at lower concentrations in an attempt to determine the lowest significantly effective dose for each of the three cations.

3) The use of other techniques: As scanning microradiography is a powerful technique concerned with quantifying changes in projected mineral mass content over a period of time it would be interesting in a future study to combine the SMR technique with another technique such as scanning electron microscopy (SEM) or atomic force microscopy (AFM). The scanning electron microscope can be used to reveal information about the sample including external morphology (texture), chemical composition, and crystalline structure and orientation of materials making up the sample. Using the energy dispersive X-ray spectroscopy (EDS) mode, SEM will be useful in qualitatively or semi-quantitatively determining the chemical compositions at selected point locations on the sample. Therefore, SMR and SEM could complement each other in a future work to obtain more detailed information about the mechanisms through which the investigated cations affect $RD_{Hap.}$ Through applying both techniques we might be able to get a better understanding of whether the divalent cations inhibit the RD_{HAp} through adhering to the surface blocking dissolution nuclei or through replacing calcium ions within the apatite lattice altering the physico-chemical properties of the apatite.

4) Testing of therapeutic agents: Dental caries and erosion are still considered a significant problem affecting societies in both industrial as well as developing countries. Every effort should be made to control these diseases, whether by prevention or treatment. The world of dentistry is moving more towards non-invasive dentistry and the industrial companies are more along the lines of producing

preventive agents such as toothpastes, mouthwashes, gel *etc*. Therefore, considerably more work can be done applying the SMR technology on studying different therapeutic agents when their efficacy and effect on demineralisation/ remineralisation need to be tested. The SMR technique benefits from accuracy and high precision in real-time detection of minute changes in mineral mass content, as well as allowing for the possibility of altering experimental conditions without interrupting the experiment. Taking these advantages into consideration, the SMR technique has superiority over other available techniques of mineral quantification.

REFERENCES

ABDULLAH, A., STRAFFORD, S., BROOKES, S. & DUGGAL, M. (2006) The effect of copper on demineralization of dental enamel. *Journal of Dental Research,* 85**,** 1011.

ADDY, M., RICHARDS, J. & WILLIAMS, G. (1980) Effects of a zinc citrate mouthwash on dental plaque and salivary bacteria. *Journal of Clinical Periodontology,* 7**,** 309-315.

ADDY, M., SLAYNE, M. & WADE, W. (1992) The formation and control of dental plaque—an overview. *Journal of Applied Microbiology,* 73**,** 269-278.

AFSETH, J. (1983) Some aspects of the dynamics of Cu and Zn retained in plaque as related to their effect on plaque pH. *European Journal of Oral Sciences,* 91**,** 169-174.

AFSETH, J., AMSBAUGH, S., MONELL-TORRENS, E., BOWEN, W., RØLLA, G., BRUNELLE, J. & DAHL, E. (1984a) Effect of copper applied topically or in drinking water on experimental caries in rats. *Caries Research,* 18**,** 434-439.

AFSETH, J., AMSBAUGH, S., MONELL-TORRENS, E., BOWEN, W., RÖLLA, G., BRUNELLE, J., LI, S. & DAHL, E. (1984b) Effect of topical application of copper in combination with fluoride in drinking water on experimental caries in rats. *Caries Research,* 18**,** 134-140.

AFSETH, J., HELELAND, K. & BONESVOLL, P. (1983a) Retention of Cu and Zn in the oral cavity following rinsing with aqueous solutions of copper and zinc salts. *European Journal of Oral Sciences,* 91**,** 42-45.

AFSETH, J., OPPERMANN, R. & RØLLA, G. (1983c) Accumulation of Cu and Zn in human dental plaque in vivo. *Caries Research,* 17**,** 310-314.

AFSETH, J., OPPERMANN, R. V. & ROLLA, G. (1980) The in vivo effect of glucose solutions containing Cu^{++} and Zn^{++} on the acidogenicity of dental plaque. *Acta Odontologica,* 38**,** 229-233.

AGUS, H. M., UN, P. S. H., COOPER, M. & SCHAMSCHULA, R. (1980) Ionized and bound fluoride in resting and fermenting dental plaque and individual human caries experience. *Archives of Oral Biology,* 25**,** 517-522.

AICHINHER, H., DIERKER, J., JOINT-BARFUSS, S. & SABEL, M. (2004) *Radiation Exposure and Image Quality in X-Ray Diagnistic Radiology,* Berlin, Springer-Verlag.

AINE, L., BAER, M. & MÄKI, M. (1993) Dental erosions caused by gastroesophageal reflux disease in children. *Journal of Dentistry for Children,* 60**,** 210-214.

AL-DLAIGAN, Y. H., SHAW, L. & SMITH, A. (2001) Tooth surface loss: Dental erosion in a group of British 14-year-old, school children. Part I: Prevalence and influence of differing socioeconomic backgrounds. *British Dental Journal,* 190**,** 145-149.

ALAMOUDI, N., SALAKO, N. & MASSOUD, I. (1996) Caries experience of children aged 6–9 years in Jeddah, Saudi Arabia. *International Journal of Paediatric Dentistry,* 6**,** 101-105.

ALDOSARI, A., WYNE, A., AKPATA, E. & KHAN, N. (2004) Caries prevalence and its relation to water fluoride levels among schoolchildren in Central Province of Saudi Arabia. *International Dental Journal,* 54**,** 424-428.

AMAECHI, B. & HIGHAM, S. (2005) Dental erosion: possible approaches to prevention and control. *Journal of Dentistry,* 33**,** 243-252.

ANDERSON, P. 1988. *Real time X-ray absorption studies and their interpretation via numerical solution of diffusion and reaction equations of model systems for dental caries.* PhD Thesis, Queen Mary, University of London.

ANDERSON, P., BOLLET-QUIVOGNE, F., DOWKER, S. & ELLIOTT, J.C. (2004) Demineralization in enamel and hydroxyapatite aggregates at increasing ionic strengths. *Archives of Oral Biology,* 49**,** 199-207.

ANDERSON, P. & ELLIOTT, J. C. (1985) Scanning X-ray microradiographic study of the formation of caries-like lesions in synthetic apatite aggregates. *Caries Research,* 19**,** 403-406.

ANDERSON, P., ELLIOTT, J.C. (1993) scanning microradiography. *Microbeam Analysis Journal,* March**,** 30-31.

ANDERSON, P., LEVINKIND, M. & ELLIOTT, J.C. (1998) Scanning microradiographic studies of rates of in vitro demineralization in human and bovine dental enamel. *Archives of Oral Biology,* 43**,** 649-656.

ANDRES, C. J., SHAEFFER, J. C. & WINDELER, A. S. (1974) Comparison of antibacterial properties of stannous fluoride and sodium fluoride mouthwashes. *Journal of Dental Research,* 53**,** 457-460.

ANGINO, E. E., BILLINGS, G. K. & ANDERSEN, N. (1966) Observed variations in the strontium concentration of sea water. *Chemical Geology,* 1**,** 145-153.

AOBA, T. (1997) The effect of fluoride on apatite structure and growth. *Critical Reviews in Oral Biology & Medicine,* 8**,** 136-153.

AOBA, T. (2004) Solubility properties of human tooth mineral and pathogenesis of dental caries. *Oral Diseases,* 10**,** 249-257.

ASHER, C. & READ, M. (1987) Early enamel erosion in children associated with the excessive consumption of citric acid. *British Dental Journal,* 162**,** 384.

ASHRAFI, M., SPECTOR, P. & CURZON, M. (1980) Pre-and posteruptive effects of low doses of strontium on dental caries in the rat. *Caries Research,* 14**,** 341-346.

ASSMUS, A. (1995). Early History of X Rays. Beamline, 11-24

ATHANASSOULI, T., PAPASTATHOPOULOS, D. & APOSTOLOPOULOS, A. (1983) Dental caries and strontium concentration in drinking water and surface enamel. *Journal of Dental Research,* 62**,** 989.

BAGRAMIAN, R., GARCIA-GODOY, F. & VOLPE, A. (2009) The global increase in dental caries. A pending public health crisis. *American Journal of Dentistry,* 22**,** 3–8.

BALES, C., FREELAND-GRAVES, J., ASKEY, S., BEHMARDI, F., POBOCIK, R., FICKEL, J. & GREENLEE, P. (1990) Zinc, magnesium, copper, and protein concentrations in human saliva: age-and sex-related differences. *The American Journal of Clinical Nutrition,* 51**,** 462.

BARBOUR, M. E. 2002. *Human tooth enamel dissolution in citric acid as a function of degree of saturation and pH.* PhD Thesis, University of Bristol.

BARMES, D. (1969) Caries etiology in Sepik villages–trace element, micronutrient and macronutrient content of soil and food. *Caries Research,* 3**,** 44-59.

BARON, R. & TSOUDEROS, Y. (2002) In vitro effects of S12911-2 on osteoclast function and bone marrow macrophage differentiation. *European Journal of Pharmacology,* 450**,** 11-17.

BARTLETT, D. & COWARD, P. (2001) Comparison of the erosive potential of gastric juice and a carbonated drink in vitro. *Journal of Oral Rehabilitation,* 28**,** 1045-1047.

BIGI, A., BOANINI, E., CAPUCCINI, C. & GAZZANO, M. (2007) Strontium-substituted hydroxyapatite nanocrystals. *Inorganica Chimica Acta,* 360**,** 1009-1016.

BOLLET-QUIVOGNE, F., ANDERSON, P., DOWKER, S. & ELLIOTT, D. J. C. (2007) Demineralisation of permeable hydroxyapatite with alternating water and acidic buffer: scanning microradiographic study of effect of switching period. *Caries Research,* 41**,** 152-160.

BOLLET-QUIVOGNE, F. R. G., ANDERSON, P., DOWKER, S. E. P. & ELLIOTT, J. C. (2005) Scanning microradiographic study on the influence of diffusion in the external liquid on the rate of demineralization in hydroxyapatite aggregates. *European Journal of Oral Sciences,* 113**,** 53-59.

BONESVOLL, P. & GJERMO, P. (1978) A comparison between chlorhexidine and some quaternary ammonium compounds with regard to retention, salivary concentration and plaque-inhibiting effect in the human mouth after mouth rinses. *Archives of Oral Biology,* 23**,** 289-294.

BONNELYE, E., CHABADEL, A., SALTEL, F. & JURDIC, P. (2008) Dual effect of strontium ranelate: stimulation of osteoblast differentiation and inhibition of osteoclast formation and resorption in vitro. *Bone,* 42**,** 129-138.

BOYDE, A. Year. Microstructure of enamel. *In:* Wiley Ciba foundation symposium 205, 1997. 18-31.

BOYDE, A., FORTELIUS, M., LESTER, K. & MARTIN, L. (1988) Basis of the structure and development of mammalian enamel as seen by scanning electron microscopy. *Scanning Microscopy,* 2**,** 1479.

BOYDE, A. & OKSCHE, A. (eds.) 1989. *Handbook of Microscopic Anatomy,* Berlin: Springer-Verlag.

BRADSHAW, D., MARSH, P., WATSON, G. & CUMMINS, D. (1993) The effects of triclosan and zinc citrate, alone and in combination, on a community of oral bacteria grown in vitro. *Journal of Dental Research,* 72**,** 25.

BRAND, H., GAMBON, D., PAAP, A., BULTHUIS, M., VEERMAN, E. & AMERONGEN, A. (2009) The erosive potential of lollipops. *International Dental Journal,* 59**,** 358-362.

BROOKES, S., SHORE, R., ROBINSON, C., WOOD, S. & KIRKHAM, J. (2003) Copper ions inhibit the demineralisation of human enamel. *Archives of Oral Biology,* 48**,** 25-30.

BROOKS, W. A., SANTOSHAM, M., NAHEED, A., GOSWAMI, D., WAHED, M. A., DIENER-WEST, M., FARUQUE, A. S. G. & BLACK, R. E. (2005) Effect of weekly zinc supplements on incidence of pneumonia and diarrhoea in children younger than 2 years in an urban, low-income population in Bangladesh: randomised controlled trial. *The Lancet,* 366**,** 999-1004.

BRUDEVOLD, F., REDA, A., AASENDEN, R. & BAKHOS, Y. (1975) Determination of trace elements in surface enamel of human teeth by a new biopsy procedure. *Archives of Oral Biology,* 20**,** 667-673.

BRUDEVOLD, F., STEADMAN, L., SPINELLI, M., AMDUR, B. & GRØN, P. (1963) A study of zinc in human teeth. *Archives of Oral Biology,* 8**,** 135-144.

BRUDEVOLD, F., STEADMAN, L. T. & SMITH, F. A. (1960) Inorganic and organic components of tooth structure. *Annals of the New York Academy of Sciences,* 85**,** 110-132.

BUDZ, J. A. & NANCOLLAS, G. H. (1988) The mechanism of dissolution of hydroxyapatite and carbonated apatite in acidic solutions. *Journal of Crystal Growth,* 91**,** 490-496.

BURGUERA-PASCU, M., RODRÍGUEZ-ARCHILLA, A., BURGUERA, J. L., BURGUERA, M., RONDÓN, C. & CARRERO, P. (2007) Flow injection on-line dilution for zinc determination in human saliva with electrothermal atomic absorption spectrometry detection. *Analytica Chimica Acta,* 600**,** 214-220.

CANALIS, E., HOTT, M., DELOFFRE, P., TSOUDEROS, Y. & MARIE, P. (1996) The divalent strontium salt S12911 enhances bone cell replication and bone formation in vitro. *Bone,* 18**,** 517-523.

CARINO, K. M. G., SHINADA, K. & KAWAGUCHI, Y. (2003) Early childhood caries in northern Philippines. *Community Dentistry and Oral Epidemiology,* 31**,** 81-89.

CHADWICK, R. (2008) Summary of: Sour sweets: a new type of erosive challenge? *British Dental Journal,* 204**,** 84-85.

CHAUDHRY, S., HARRIS, J. & CHALLACOMBE, S. (1997) Dental erosion in a wine merchant: an occupational hazard? *British Dental Journal,* 182**,** 226-228.

CHRISTENSEN, L. B., TWETMAN, S. & SUNDBY, A. (2010) Oral health in children and adolescents with different socio-cultural and socio-economic backgrounds. *Acta Odontologica Scandinavica,* 68**,** 34-42.

CHRISTIANSON, D. W. (1991) Structural biology of zinc. *Advances in Protein Chemistry,* 42**,** 281-355.

CHRISTOFFERSEN, J., CHRISTOFFERSEN, M. R., KOLTHOFF, N. & BÃRENHOLDT, O. (1997) Effects of strontium ions on growth and dissolution of hydroxyapatite and on bone mineral detection. *Bone,* 20**,** 47-54.

CHU, C., PANG, K. & LO, E. (2010) Dietary behavior and knowledge of dental erosion among Chinese adults. *BMC Oral Health,* 10**,** 13.

CHURCHLEY, D., NEWBY, C. S., WILLSON, R., HAIDER, A., SCHEMEHORN, B. & LYNCH, R. J. M. (2011) Protection against enamel demineralisation using toothpastes containing o cymen 5 ol, zinc chloride and sodium fluoride. *International Dental Journal,* 61**,** 55-59.

CIANCIO, S. (1992) Agents for the management of plaque and gingivitis. *Journal of Dental Research,* 71**,** 1450-1454.

CLARKSON, B., WEFEL, J. & MILLER, I. (1984) A model for producing caries-like lesions in enamel and dentin using oral bacteria in vitro. *Journal of Dental Research,* 63**,** 1186-1189.

COMPTON, F. H. & BEAGRIE, G. S. (1975) Inhibitory effect of benzethonium and zinc chloride mouthrinses on human dental plaque and gingivitis. *Journal of Clinical Periodontology,* 2**,** 33-43.

CRABB, H. (1966a) 'Arrested caries'. *British Dental Journal,* 121**,** 167.

CRABB, H. (1966b) Enamel caries. Observations on the histology and pattern of progress of the approximal lesion. *British Dental Journal,* 121**,** 115.

CUMMINS, D. (1991) Zinc citrate/Triclosan: a new anti plaque system for the control of plaque and the prevention of gingivitis: short term clinical and mode of action studies. *Journal of Clinical Periodontology,* 18**,** 455-461.

CUMMINS, D. (2010) Recent advances in dentin hypersensitivity: clinically proven treatments for instant and lasting sensitivity relief. *American Journal of Dentistry,* 23**,** 3A.

CURZON, M. (1984) Strontium concentrations in whole human saliva. *Archives of Oral Biology,* 29**,** 211-214.

CURZON, M. (1985) The relation between caries prevalence and strontium concentrations in drinking water, plaque, and surface enamel. *Journal of Dental Research,* 64**,** 1386.

CURZON, M. (1988) Effects of a combination of strontium and fluoride on dental caries in the rat. *Nutrition Research,* 8**,** 321-326.

CURZON, M., ASHRAFI, M. & SPECTOR, P. (1982) Effects of strontium administration on rat molar morphology. *Archives of Oral Biology,* 27**,** 667-671.

CURZON, M. & CROCKER, D. (1978) Relationships of trace elements in human tooth enamel to dental caries. *Archives of Oral Biology,* 23**,** 647-653.

CURZON, M., SPECTOR, P. & IKER, H. (1978) An association between strontium in drinking water supplies and low caries prevalence in man. *Archives of Oral Biology,* 23**,** 317-321.

CURZON, M. E. J. & CUTRESS, T. (1983) *Trace elements and dental disease,* J. Wright/Psg Inc.

DANKS, D. (1988) Copper deficiency in humans. *Annual Review of Nutrition,* 8**,** 235-257.

DAVEY, H. & EMBERY, G. (1992) Metal ions in oral hygiene products. *Clinical and Biological Aspects of Dentifrices. pp165-172. New York: Oxford Medical Publications*.

DAVIS, G. & ELLIOTT, J. (1997) X-ray microtomography scanner using time-delay integration for elimination of ring artefacts in the reconstructed image. *Nuclear Instruments and Methods in Physics Research Section A: Accelerators, Spectrometers, Detectors and Associated Equipment,* 394**,** 157-162.

DEDHIYA, M., YOUNG, F. & HIGUCHI, W. (1973) Mechanism for the retardation of the acid dissolution rate of hydroxyapatite by strontium. *Journal of Dental Research,* 52**,** 1097.

DHAVALIKAR, M. (1997) Meluhha—The Land of Copper. *South Asian Studies,* 13**,** 275-279.

DONAHUE, G. J., WADDELL, N., PLOUGH, A. L., DEL AGUILA, M. A. & GARLAND, T. E. (2005) The ABCDs of treating the most prevalent childhood disease. *American Journal of Public Health,* 95**,** 1322.

DORNER, K., DZIADZKA, S., HOHN, A., SIEVERS, E., OLDIGS, H. D., SCHULZ-LELL, G. & SCHAUB, J. (1989) Longitudinal manganese and copper balances in young infants and preterm infants fed on breast-milk and adapted cow's milk formulas. *British Journal of Nutrition,* 61**,** 559-572.

DOROZHKIN, S. V. (1997a) Acidic dissolution mechanism of natural fluorapatite. II. Nanolevel of investigations. *Journal of Crystal Growth,* 182**,** 133-140.

DOROZHKIN, S. V. (1997b) Surface reactions of apatite dissolution. *Journal of Colloid and Interface Science,* 191**,** 489-497.

DOROZHKIN, S. V. (2002) A review on the dissolution models of calcium apatites. *Progress in Crystal Growth and Characterization of Materials,* 44**,** 45-61.

DOWELL, P. & ADDY, M. (1983) Dentine hypersensitivity-A review. *Journal of Clinical Periodontology,* 10**,** 341-350.

DOWNER, M. (1993) Changing trends in dental caries experience in Great Britain. *Advances in Dental Research,* 7**,** 19-24.

DOWNER, M., NORDLING, H., BLINKHORN, A. & KOISTINEN, A. (1985) The Edinburgh-Helsinki study: a comparison of dental care for children. *International Dental Journal,* 35**,** 226.

DUCKWORTH, R., MORGAN, S. & MURRAY, A. (1987) Fluoride in saliva and plaque following use of fluoride-containing mouthwashes. *Journal of Dental Research,* 66**,** 1730.

ELLIOTT, J. C. (1994) *Structure and chemistry of the apatites and other calcium orthophosphates,* Amsterdam, Elsevier Science B.V.

ELLIOTT, J. C. Year. Structure, crystal chemistry and density of enamel apatites. *In*, 1997. Wiley Online Library, 54-72.

ELLIOTT, J. C., BOLLET-QUIVOGNE, F., ANDERSON, P., DOWKER, S., WILSON, R. & DAVIS, G. (2005) Acidic demineralization of apatites studied by scanning X-ray microradiography and microtomography. *Mineralogical Magazine,* 69**,** 643.

ELLIOTT, J. C., DOWKER, S. & KNIGHT, R. (1981) Scanning X-ray microradiography of a section of a carious lesion in dental enamel. *Journal of Microscopy,* 123**,** 89-92.

ELLIOTT, J. C., HOLCOMB, D. & YOUNG, R. (1985) Infrared determination of the degree of substitution of hydroxyl by carbonate ions in human dental enamel. *Calcified Tissue International,* 37**,** 372-375.

FEATHERSTONE, J., SHIELDS, C., KHADEMAZAD, B. & OLDERSHAW, M. (1983a) Acid reactivity of carbonated apatites with strontium and fluoride substitutions. *Journal of Dental Research,* 62**,** 1049.

FEATHERSTONE, J. D. B., MAYER, I., DRIESSENS, F. C. M., VERBEECK, R. M. H. & HEIJLIGERS, H. J. M. (1983b) Synthetic apatites containing Na, Mg, and CO 3 and their comparison with tooth enamel mineral. *Calcified Tissue International,* 35**,** 169-171.

FEJERSKOV, O., KIDD, E. & KIDD, E. A. M. (2008) *Dental caries: the disease and its clinical management,* Singapore, Wiley-Blackwell.

FILSTRUP, S. L., BRISKIE, D., DA FONSECA, M., LAWRENCE, L., WANDERA, A. & INGLEHART, M. (2003) Early childhood caries and quality of life: child and parent perspectives. *Pediatric Dentistry,* 25**,** 431-440.

FISCHMAN, S., PICOZZI, A., CANCRO, L. & PADER, M. (1973) The inhibition of plaque in humans by two experimental oral rinses. *Journal of Periodontology,* 44**,** 100.

FOSMIRE, G. J. (1990) Zinc toxicity. *The American Journal of Clinical Nutrition,* 51**,** 225.

FRANK, R., SARGENTINI-MAIER, M., TURLOT, J. & LEROY, M. (1989) Zinc and strontium analyses by energy dispersive X-ray fluorescence in human permanent teeth. *Archives of Oral Biology,* 34**,** 593-597.

FROSTELL, G., LARSSON, S., LODDING, A., ODELIUS, H. & PETERSSON, L. (1977) SIMS study of element concentration profiles in enamel and dentin. *European Journal of Oral Sciences,* 85**,** 18-21.

GANDARA, B. K. & TRUELOVE, E. L. (1999) Diagnosis and management of dental erosion. *The Journal of Contemporary Dental Practice,* 1**,** 16.

GAO, X., ELLIOTT, J. & ANDERSON, P. (1993) Scanning Microradlographic Study of the Kinetics of Subsurface Demineralization In Tooth Sections under Constant-composition and Small Constant-volume Conditions. *Journal of Dental Research,* 72**,** 923-930.

GEDALIA, I., ANAISE, J. & LAUFER, E. (1975) Effect of prenatal, preeruptive, and posteruptive strontium administration on dental caries in hamster molars. *Journal of Dental Research,* 54**,** 1240.

GLAS, J. & LAGERGREN, C. (1961) Strontium fixation in the mineral phase of bone. *International Journal of Biochemistry and cell Biology,* 1**,** 25-28.

GOLDEN, M. (1989) The diagnosis of zinc deficiency. *Zinc in human biology,* 323.

GOMES, P. R., COSTA, S. C., CYPRIANO, S. & SOUSA, M. L. R. (2004) Dental caries in Paulinia, Sao Paulo State, Brazil, and WHO goals for 2000 and 2010. *Cadernos de Saúde Pública,* 20**,** 866-870.

GRENBY, T. H. (1996) Lessening dental erosive potential by product modification. *European Journal of Oral Sciences,* 104**,** 221-228.

GRYNPAS, M. (1993) Age and disease-related changes in the mineral of bone. *Calcified Tissue International,* 53**,** 57-64.

HALL, P., GREEN, A., HORAY, C., DE BRABANDER, S., BEASLEY, T., CROMWELL, V., HOLT, J. & SAVAGE, D. (2003) Plaque antibacterial levels following controlled food intake and use of a toothpaste containing 2% zinc citrate and 0.3% Triclosan. *International Dental Journal,* 53**,** 379-384.

HAMBIDGE, M. (2000) Human zinc deficiency. *The Journal of nutrition,* 130**,** 1344S.

HANKE, M. T. (1940) Studies on the local factors in dental Caries 1. Destruction of plaques and retardation of bacterial growth in the oral cavity. *Journal of the American Dental Association,* 27**,** 1379-1393.

HARKER, R. & MORRIS, J. (2005) Children's dental health in the United Kingdom 2003. *London, Office for National Statistics*.

HARLESS, R. I. M. M. H. J. D. & WEFEL, J. (2003) Effect of fluoridated milk on progression of root surface lesions in vitro under pH cycling conditions. *Caries Research,* 37**,** 166-171.

HARRAP, G., BEST, J. & SAXTON, C. (1984) Human oral retention of zinc from mouthwashes containing zinc salts and its relevance to dental plaque control. *Archives of Oral Biology,* 29**,** 87-91.

HARRAP, G., SAXTON, C. & BEST, J. (1983) Inhibition of plaque growth by zinc salts. *Journal of Periodontal Research,* 18**,** 634-642.

HARRIS, R., NICOLL, A. D., ADAIR, P. M. & PINE, C. M. (2004) Risk factors for dental caries in young children: a systematic review of the literature. *Community Dental Health,* 21**,** 71-85.

HEIN, J. (1953) Effect of copper sulfate on initiation and progression of dental caries in the Syrian hamster. *Journal of dental Research,* 32**,** 654.

HENKIN, R., MUELLER, C. & WOLF, R. (1975) Estimation of zinc concentration of parotid saliva by flameless atomic absorption spectrophotometry in normal subjects and in patients with idiopathic hypogeusia. *The Journal of Laboratory and Clinical Medicine,* 86**,** 175.

HESLOP, D., BI, Y., BAIG, A. & HIGUCHI, W. (2003) Metastable equilibrium solubility behavior of carbonated apatite in the presence of solution strontium. *Calcified Tissue International,* 74**,** 72-85.

HIGUCHI, W. I., GRAY, J. A., HEFFERREN, J. J. & PATEL, P. R. (1965) Mechanisms of Enamel Dissolution in Acid Buffers. *Journal of Dental Research,* 44**,** 330.

HUGHES, N., MASON, S., JEFFERY, P., WELTON, H., TOBIN, M., O'SHEA, C. & BROWNE, M. (2010) A comparative clinical study investigating the efficacy of a test dentifrice containing 8% strontium acetate and 1040 ppm sodium fluoride versus a marketed control dentifrice containing 8% arginine, calcium carbonate, and 1450 ppm sodium monofluorophosphate in reducing dentinal hypersensitivity. *The Journal of Clinical Dentistry,* 21**,** 49.

ISAAC, S., BRUDEVOLD, F., SMITH, F. A. & GARDNER, D. E. (1958) Solubility rate and natural fluoride content of surface and subsurface enamel. *Journal of Dental Research,* 37**,** 254.

ISMAIL, A., SOHN, W., TELLEZ, M., AMAYA, A., SEN, A., HASSON, H. & PITTS, N. (2007) The International Caries Detection and Assessment System (ICDAS): an integrated system for measuring dental caries. *Community Dentistry and Oral Epidemiology,* 35**,** 170-178.

ISMAIL, A. I., SOHN, W., TELLEZ, M., WILLEM, J. M., BETZ, J. & LEPKOWSKI, J. (2008) Risk indicators for dental caries using the International Caries Detection and Assessment System (ICDAS). *Community Dentistry and Oral Epidemiology,* 36**,** 55-68.

JOHANSSON, A. K., LINGSTRÖM, P., IMFELD, T. & BIRKHED, D. (2004) Influence of drinking method on tooth‐surface pH in relation to dental erosion. *European Journal of Oral Sciences,* 112**,** 484-489.

JOHNSSON, M. S. A. & NANCOLLAS, G. H. (1992) The role of brushite and octacalcium phosphate in apatite formation. *Critical Reviews in Oral Biology & Medicine,* 3**,** 61-82.

JOSEPH, M., GEDALIA, I. & FUKS, A. (1977) Effect of Strontium and Fluoride Administration on Caries Resistance of Hamster Molars. *Journal of Dental Research,* 56**,** 924.

KIDD, E. & FEJERSKOV, O. (2004) What constitutes dental caries? Histopathology of carious enamel and dentin related to the action of cariogenic biofilms. *Journal of Dental Research,* 83**,** C35-C38.

KIDD, E. A. M. (2005) *Essentials of dental caries: The disease and its management,* Oxford University Press, USA.

KIKUCHI, M., YAMAZAKI, A., OTSUKA, R., AKAO, M. & AOKI, H. (1994) Crystal structure of Sr-substituted hydroxyapatite synthesized by hydrothermal method. *Journal of Solid State Chemistry,* 113**,** 373-378.

KISHI, S. & YAMAGUCHI, M. (1994) Inhibitory effect of zinc compounds on osteoclast-like cell formation in mouse marrow cultures. *Biochemical pharmacology,* 48**,** 1225-1230.

KLEVAY, L. M. (1998) Lack of a recommended dietary allowance for copper may be hazardous to your health. *Journal of the American College of Nutrition,* 17**,** 322-326.

KNOTT, L. & BAILEY, A. (1998) Collagen cross-links in mineralizing tissues: a review of their chemistry, function, and clinical relevance. *Bone,* 22**,** 181-187.

KODAKA, T., KUROIWA, M. & HIGASHI, S. (1991) Structural and distribution patterns of surface 'prismless' enamel in human permanent teeth. *Caries Research,* 25**,** 7-20.

KODAKA, T., NAKAJIMA, F. & HIGASHI, S. (1989) Structure of the so-called 'prismless' enamel in human deciduous teeth. *Caries Research,* 23**,** 290-296.

KOSORIC, J. 2006. *Influence of salivary proteins on biomineralisation of hydroxyapatite and enamel using scanning microradiography: the effect of the N-terminus of statherin on demineralisation of hydroxyapatite.* PhD Thesis, Queen Mary, university of Lonodn.

KOULOURIDES, T., FEAGIN, F. & PIGMAN, W. (1968) Effect of pH, ionic strength, and cupric ions on the rehardening rate of buffersoftened human enamel. *Archives of Oral Biology,* 13**,** 335-341.

LARSON, R. H. & AMSBAUGH, S. M. (1975) Protection against rat caries by fluoride in water vs.diet. *Journal of Dental Research,* 54**,** 118.

LAWLER, M. R. & KLEVAY, L. M. (1984) Copper and zinc in selected foods. *Journal of the American Dietetic Association,* 84**,** 1028.

LAYER, T. & HUGHES, N. (2010) Evidence for the efficacy of an 8% strontium acetate dentifrice for instant and lasting relief of dentin hypersensitivity. *The Journal of Clinical Dentistry,* 21**,** 56.

LAZARCHIK, D. A. & FILLER, S. J. (1997) Effects of gastroesophageal reflux on the oral cavity. *The American Journal of Medicine,* 103**,** 107S-113S.

LEGEROS, R. & TUNG, M. (1983) Chemical stability of carbonate-and fluoride-containing apatites. *Caries Research,* 17**,** 419-429.

LEGEROS, R. Z. (1991) *Calcium phosphates in oral biology and medicine,* Basel, Karger.

LI, Z., LAM, W., YANG, C., XU, B., NI, G., ABBAH, S., CHEUNG, K., LUK, K. & LU, W. (2007) Chemical composition, crystal size and lattice structural changes after incorporation of strontium into biomimetic apatite. *Biomaterials,* 28**,** 1452-1460.

LIKINS, R., POSNER, A., PARETZKIN, B. & FROST, A. Effect of Crystal Growth on the Comparative Fixation of Srsg and Ca45 by Calcified Tissues. *The Journal of Biological Chemistry,* 236,10,2804-2806.

LINNETT, V. & SEOW, W. (2001) Dental erosion in children: a literature review. *Pediatric Dentistry,* 23**,** 37-43.

LITTLE, M. & BARRETT, K. (1976) Trace element content of surface and subsurface enamel relative to caries prevalence on the west coast of the United States of America. *Archives of Oral Biology,* 21**,** 651-657.

LOSEE, F. & ADKINS, B. (1969) A study of the mineral environment of caries-resistant Navy recruits. *Caries Research,* 3**,** 23-31.

LUSSI, A. (2006) *Dental erosion: from diagnosis to therapy,* Basel, Karger.

LYNCH, R. J. M. (2011) Zinc in the mouth, its interactions with dental enamel and possible effects on caries; a review of the literature. *International Dental Journal,* 61**,** 46-54.

MACDONALD, N. S., NUSBAUM, R. E., STEARNS, R., EZMIRLIAN, F., MCARTHUR, C. & SPAIN, P. (1951) The skeletal deposition of non-radioactive strontium. *Journal of Biological Chemistry,* 188**,** 137.

MAFE, S., MANZANARES, J., REISS, H., THOMANN, J. & GRAMAIN, P. (1992) Model for the dissolution of calcium hydroxyapatite powder. *The Journal of Physical Chemistry,* 96**,** 861-866.

MALTZ, M. & EMILSON, C. (1982) Susceptibility of oral bacteria to various fluoride salts. *Journal of Dental Research,* 61**,** 786-790.

MANDEL, I. D. (1988) Chemotherapeutic agents for controlling plaque and gingivitis. *Journal of Clinical Periodontology,* 15**,** 488-498.

MARET, W. & SANDSTEAD, H. H. (2006) Zinc requirements and the risks and benefits of zinc supplementation. *Journal of Trace Elements in Medicine and Biology,* 20**,** 3-18.

MARGOLIS, H. C. & MORENO, E. C. (1985) Kinetics and Thermodynamics of enamel demineralisation. *Caries Research,* 19**,** 22-35.

MARGOLIS, H. C., MORENO, E.C. (1992) Kinetics of hydroxyapatite dissolution in acetic, lactic, and phosphoric acid solutions. *Calcified Tissue International,* 50**,** 137-143.

MARGOLIS, H. C., MORENO, E.C. (1994) Composition and cariogenic potential of dental plaque fluid. *Critical Reviews in Oral Biology & Medicine,* 5**,** 1.

MARIE, P., AMMANN, P., BOIVIN, G. & REY, C. (2001) Mechanisms of action and therapeutic potential of strontium in bone. *Calcified Tissue International,* 69**,** 121-129.

MARSHALL, A. & LAWLESS, K. (1981) TEM study of the central dark line in enamel crystallites. *Journal of Dental Research,* 60**,** 1773-1782.

MARTHALER, T. (2004) Changes in dental caries 1953-2003. *Caries Research,* 38**,** 173-181.

MASON, S., HUGHES, N., SUFI, F., BANNON, L., MAGGIO, B., NORTH, M. & HOLT, J. (2010) A comparative clinical study investigating the efficacy of a dentifrice containing 8% strontium acetate and 1040 ppm fluoride in a silica base and a control dentifrice containing 1450 ppm fluoride in a silica base to provide immediate relief of dentin hypersensitivity. *The Journal of Clinical Dentistry,* 21**,** 42.

MATSUNAGA, K. (2008) First-principles study of substitutional magnesium and zinc in hydroxyapatite and octacalcium phosphate. *The Journal of Chemical Physics,* 128**,** 245101.

MATSUNAGA, K., MURATA, H., MIZOGUCHI, T. & NAKAHIRA, A. (2010) Mechanism of incorporation of zinc into hydroxyapatite. *Acta Biomaterialia,* 6**,** 2289-2293.

MAYER, I., APFELBAUM, F. & FEATHERSTONE, J. (1994) Zinc ions in synthetic carbonated hydroxyapatites. *Archives of Oral Biology,* 39**,** 87-90.

MAYHEW, R. & BROWN, L. (1981) Comparative effect of SnF2, NaF, and SnCl2 on the growth of Streptococcus mutans. *Journal of Dental Research,* 60**,** 1809-1814.

MCELROY, B. H. & MILLER, S. P. (2002) Effectiveness of zinc gluconate glycine lozenges (Cold-Eeze) against the common cold in school-aged subjects: a retrospective chart review. *American Journal of Therapeutics,* 9**,** 472.

MEJÀRE, I. & MJÖNES, S. (1989) Dental caries in Turkish immigrant primary schoolchildren. *Acta Paediatrica,* 78**,** 110-114.

MELLBERG, J. & CHOMICKI, W. (1983) Effect of zinc citrate on fluoride uptake by artificial caries lesions. *Journal of Dental Research,* 62**,** 145.

MEUNIER, P. J., ROUX, C., SEEMAN, E., ORTOLANI, S., BADURSKI, J. E., SPECTOR, T. D., CANNATA, J., BALOGH, A., LEMMEL, E. M. & PORS-NIELSEN, S. (2004) The effects of strontium ranelate on the risk of vertebral fracture in women with postmenopausal osteoporosis. *New England Journal of Medicine,* 350**,** 459-468.

MEURMAN, J. & GATE, J. (1996) Pathogenesis and modifying factors of dental erosion. *European Journal of Oral Sciences,* 104**,** 199-206.

MEURMAN, J. H., TOSKALA, J., NUUTINEN, P. & KLEMETTI, E. (1994) Oral and dental manifestations in gastroesophageal reflux disease. *Oral Surgery, Oral Medicine, Oral Pathology,* 78**,** 583-589.

MILLWARD, A., SHAW, L. & SMITH, A. (1994) Dental erosion in four-year-old children from differing socioeconomic backgrounds. *ASDC Journal of Dentistry for Children,* 61**,** 263.

MILNE, D., CANFIELD, W., MAHALKO, J. & SANDSTEAD, H. (1984) Effect of oral folic acid supplements on zinc, copper, and iron absorption and excretion. *The American Journal of Clinical Nutrition,* 39**,** 535.

MOAZZEZ, R., SMITH, B. & BARTLETT, D. (2000) Oral pH and drinking habit during ingestion of a carbonated drink in a group of adolescents with dental erosion. *Journal of Dentistry,* 28**,** 395-397.

MORTIMER, K. & TRANTER, T. (1971) A scanning electron microscope study of carious enamel. *Caries Research,* 5**,** 240-263.

MURRAY, T. (1993) Elementary Scots. The discovery of Strontium. *Scottish Medical Journal,* 38**,** 188.

NUNN, J., GORDON, P., MORRIS, A. & WALKER, A. (2003) Dental erosion–changing prevalence? A review of British National childrens' surveys. *International Journal of Paediatric Dentistry,* 13**,** 98-105.

NYVAD, M. (1999) Enamel erosion by some soft drinks and orange juices relative to their pH, buffering effect and contents of calcium phosphate. *Caries Research,* 33**,** 81-87.

O'SULLIVAN, E., CURZON, M., ROBERTS, G., MILLA, P. & STRINGER, M. (1998) Gastroesophageal reflux in children and its relationship to erosion of primary and permanent teeth. *European Journal of Oral Sciences,* 106**,** 765-769.

OEZDEMIR, A., SAYAL, A., AKCA, E. & AYDIN, A. (1998) The Determination of Salivary Zinc Level Following Delivery from Zinc Containing Toothpaste. *Turkish Journal of Medical Sciences,* 28**,** 281-284.

OPPERMANN, R. & RÖLLA, G. (1980) Effect of Some Polyvalent Cations on the Acidogenicity of Dental Plaque *in vivo*. *Caries Research,* 14**,** 422-427.

OPPERMANN, R. U. I. V. & JOHANSEN, J. A. N. R. (1980) Effect of fluoride and non‐fluoride salts of copper, silver and tin on the acidogenicity of dental plaque in vivo. *European Journal of Oral Sciences,* 88**,** 476-480.

OPPERMANN, R. U. I. V., ROLLA, G., JOHANSEN, J. A. N. R. & ASSEV, S. (1980) Thiol groups and reduced acidogenicity of dental plaque in the presence of metal ions *in vivo*. *European Journal of Oral Sciences,* 88**,** 389-396.

ORCHARDSON, R. & GILLAM, D. G. (2006) Managing dentin hypersensitivity. *The Journal of the American Dental Association,* 137**,** 990.

PEARCE, E., GUHA-CHOWDHURY, N., IWAMI, Y. & CUTRESS, T. (1995) Stoichiometry of fluoride release from fluorhydroxyapatite during acid dissolution. *Caries Research,* 29**,** 130-136.

PETERSEN, P. (2003) The World Oral Health Report 2003: continuous improvement of oral health in the 21st century–the approach of the WHO Global Oral Health Programme. *Community Dentistry and Oral Epidemiology,* 31**,** 3-24.

PETERSEN, P. E. (2005) Sociobehavioural risk factors in dental caries–international perspectives. *Community Dentistry and Oral Epidemiology,* 33**,** 274-279.

PETERSEN, P. E. & GORMSEN, C. (1991) Oral conditions among German battery factory workers. *Community Dentistry and Oral Epidemiology,* 19**,** 104-106.

PETERSEN, P. E. & YAMAMOTO, T. (2005) Improving the oral health of older people: the approach of the WHO Global Oral Health Programme. *Community Dentistry and Oral Epidemiology,* 33**,** 81-92.

PICOZZI, A., FISCHMAN, S., PADER, M. & CANCRO, L. (1972) Calculus inhibition in humans. *Journal of Periodontology,* 43**,** 692.

PIEKARZ, C., RANJITKAR, S., HUNT, D. & MCINTYRE, J. (2008) An in vitro assessment of the role of Tooth Mousse in preventing wine erosion. *Australian Dental Journal,* 53**,** 22-25.

PITTS, N. (2004) " ICDAS"--an international system for caries detection and assessment being developed to facilitate caries epidemiology, research and appropriate clinical management. *Community Dental Health,* 21**,** 193.

PITTS, N., BOYLES, J., NUGENT, Z., THOMAS, N. & PINE, C. (2007) The dental caries experience of 5-year-old children in Great Britain (2005/6). Surveys co-ordinated by the British Association for the study of community dentistry. *Community Dental Health,* 24**,** 59.

POBE, J. (1998) *Diagnostic X-rays. In: Medical Physics*.

PREVÉY, P. S. (2000) X-ray diffraction characterization of crystallinity and phase composition in plasma-sprayed hydroxyapatite coatings. *Journal of Thermal Spray Technology,* 9**,** 369-376.

REITZNEROVÁ, E., AMARASIRIWARDENA, D., KOP ÁKOVÁ, M. & BARNES, R. M. (2000) Determination of some trace elements in human tooth enamel. *Fresenius' Journal of Analytical Chemistry,* 367**,** 748-754.

REMUN, B., KOSTER, P., HOUTHUU, D., BOLEIJ, J., WILLEMS, H., BRUNEKREEF, B., BIERSTEKER, K. & VAN LOVEREN, C. (1982) Zinc chloride, zinc oxide, hydrochloric acid exposure and dental erosion in a zinc galvanizing plant in the Netherlands. *The Annals of Occupational Hygiene,* 25**,** 299.

RIPA, L., GWINNETT, A. & BUONOCORE, M. (1966) The" prismless" outer layer of deciduous and permanent enamel. *Archives of Oral Biology,* 11**,** 41.

ROBINSON, C., HALLSWORTH, A., SHORE, R. & KIRKHAM, J. (1990) Effect of surface zone deproteinisation on the access of mineral ions into subsurface carious lesions of human enamel. *Caries Research,* 24**,** 226-230.

ROBINSON, C., KIRKHAM, J. & SHORE, R. (1995a) *Dental enamel: formation to destruction,* London, CRC Press.

ROBINSON, C., SHORE, R.C., BROOKES, S.J., STRAFFORD, S., WOOD, S.T., AND KIRKHAM, J., (2000) The chemistry of enamel caries. *Critical Reviews in Oral Biology and Medicine,* 11**,** 481-95.

ROBINSON, C., WEATHERELL, J. & HALLSWORTH, A. (1983). Alterations in the composition of permanent human enamel during carious attack. IRL Press, Oxford.

ROSALEN, P., BOWEN, W. & PEARSON, S. (1996a) Effect of copper co-crystallized with sugar on caries development in desalivated rats. *Caries Research,* 30**,** 367-372.

ROSALEN, P., PEARSON, S. & BOWEN, W. (1996b) Effects of copper, iron and fluoride co-crystallized with sugar on caries development and acid formation in desalivated rats. *Archives of Oral Biology,* 41**,** 1003-1010.

SAXTON, C., HARRAP, G. & LLOYD, A. (1986) The effect of dentifrices containing zinc citrate on plaque growth and oral zinc levels. *Journal of Clinical Periodontology,* 13**,** 301-306.

SCHMID, M., SCHAIT, A. & MUHLEMANN, H. (1974) Effect of a zinc chloride mouthrinse on calculus deposits formed on foils. *Helvetica Odontolgia Acta,* 18**,** 22.

SCHROEDER, P. L., FILLER, S. J., RAMIREZ, B., LAZARCHIK, D. A., VAEZI, M. F. & RICHTER, J. E. (1995) Dental erosion and acid reflux disease. *Annals of Internal Medicine,* 122**,** 809-815.

SCHWEISSING, M. M. & GRUPE, G. (2003) Stable strontium isotopes in human teeth and bone: a key to migration events of the late Roman period in Bavaria. *Journal of Archaeological Science,* 30**,** 1373-1383.

SEIBERT, J. A. (2004) X-ray imaging physics for nuclear medicine technologists. Part 1: Basic principles of X-ray production. *Journal of Nuclear Medicine Technology,* 32**,** 139.

SEIBERT, J. A. & BOONE, J. M. (2005) X-ray imaging physics for nuclear medicine technologists. Part 2: X-ray interactions and image formation. *Journal of Nuclear Medicine Technology,* 33**,** 3.

SGAN-COHEN, H. D. & MANN, J. (2007) Health, oral health and poverty. *The Journal of the American Dental Association,* 138**,** 1437.

SHELLIS, R. (1984) Relationship between human enamel structure and the formation of caries-like lesions in vitro. *Archives of Oral Biology,* 29**,** 975-981.

SHELLIS, R., BARBOUR, M., JONES, S. & ADDY, M. (2010) Effects of pH and acid concentration on erosive dissolution of enamel, dentine, and compressed hydroxyapatite. *European Journal of Oral Sciences,* 118**,** 475-482.

SHELLIS, R. & DIBDIN, G. (2000) Enamel microporosity and its functional implications. *Development, Function and Evolution of Teeth***,** 242-251.

SHELLIS, R. & DUCKWORTH, R. (1994) Studies on the cariostatic mechanisms of fluoride. *International Dental Journal,* 44**,** 263.

SHELLIS, R., WAHAB, F. & HEYWOOD, B. (1993) The hydroxyapatite ion activity product in acid solutions equilibrated with human enamel at 37 C. *Caries Research,* 27**,** 365-372.

SILVERSTONE, L. (1981) *Dental caries: aetiology, pathology and prevention*, Macmillan.

SILVERSTONE, L. M. (1966) The primary translucent zone of enamel caries and of artificial caries-like lesions. *British Dental Journal,* 120**,** 461.

SINGH, J. (2000) *Semiconductor devices : basic principles,* New York, Wiley.

SISCOGLOU, A. (2008). *Determination of diffusion coeffecients in enamel and other permeable solids using X-ray absorption measurements in enamel and other permeable solids using X-ray absorption measurements.* PhD, Queen Mary, University of London.

SKJÖRLAND, K., GJERMO, P. & RÖLLA, G. (1978) Effect of some polyvalent cations on plaque formation in vivo. *European Journal of Oral Sciences,* 86**,** 103-107.

SMITH, B. & KNIGHT, J. (1984) An index for measuring the wear of teeth. *British Dental Journal,* 156**,** 435.

STEADMAN, L., BRUDEVOLD, F. & SMITH, F. (1958) Distribution of strontium in teeth from different geographic areas. *Journal of the American Dental Association (1939),* 57**,** 340.

STÖTZEL, C., MÜLLER, F., REINERT, F., NIEDERDRAENK, F., BARRALET, J. & GBURECK, U. (2009) Ion adsorption behaviour of hydroxyapatite with different crystallinities. *Colloids and Surfaces B: Biointerfaces,* 74**,** 91-95.

TAMM, T. & PELD, M. (2006) Computational study of cation substitutions in apatites. *Journal of Solid State Chemistry,* 179**,** 1581-1587.

TAN-WALKER, R. & GILBERT, R. (1989) Oral delivery of zinc from slurries and separated supernatant fractions of dentifrices. *Journal of Dental Research,* 68**,** 1708-1709.

TANG, R., HENNEMAN, Z. J. & NANCOLLAS, G. H. (2003) Constant composition kinetics study of carbonated apatite dissolution. *Journal of Crystal Growth,* 249**,** 614-624.

TANG, Y., CHAPPELL, H., DOVE, M., REEDER, R. & LEE, Y. (2009) Zinc incorporation into hydroxylapatite. *Biomaterials,* 30**,** 2864-2872.

TATEVOSSIAN, A. (1978) Distribution and kinetics of fluoride ions in the free aqueous and residual phases of human dental plaque. *Archives of Oral Biology,* 23**,** 893-898.

TEN CATE, A. (1998). Oral histology: Development, structure, and function, St. Louis, MO: Mosby-Year Book. Inc.

TEN CATE, J. (1993) The caries preventive effect of a fluoride dentifrice containing Triclosan and zinc citrate, a compilation of in vitro and in situ studies. *International Dental Journal,* 43**,** 407.

TEN CATE, J. & FEATHERSTONE, J. (1991) Mechanistic aspects of the interactions between fluoride and dental enamel. *Critical Reviews in Oral Biology & Medicine,* 2**,** 283-296.

TERRA, J., JIANG, M. & ELLIS, D. (2002) Characterization of electronic structure and bonding in hydroxyapatite: Zn substitution for Ca. *Philosophical Magazine A,* 82**,** 2357-2377.

THAVEESANGPANICH, P., ITTHAGARUN, A., KING, N. & WEFEL, J. (2005) The effects of child formula toothpastes on enamel caries using two in vitro pH cycling models. *International Dental Journal,* 55**,** 217-223.

THOMANN, J., VOEGEL, J. & GRAMAIN, P. (1990) Kinetics of dissolution of calcium hydroxyapatite powder. III: pH and sample conditioning effects. *Calcified Tissue International,* 46**,** 121-129.

THOMAS, B. & BISHOP, J. (2007) *Manual of dietetic practice,* Wiley-Blackwell.

THUY, T. T., NAKAGAKI, H., KATO, K., HUNG, P. A., INUKAI, J., TSUBOI, S., HIROSE, M. N., IGARASHI, S. & ROBINSON, C. (2008) Effect of strontium in combination with fluoride on enamel remineralisation in vitro. *Archives of Oral Biology,* 53**,** 1017-1022.

TURNLUND, J. R., KEEN, C. L. & SMITH, R. G. (1990) Copper status and urinary and salivary copper in young men at three levels of dietary copper. *The American Journal of Clinical Nutrition,* 51**,** 658-664.

TURNLUND, J. R., KEYES, W. R., PEIFFER, G. L. & SCOTT, K. C. (1998) Copper absorption, excretion, and retention by young men consuming low dietary copper determined by using the stable isotope 65Cu. *The American Journal of Clinical Nutrition,* 67**,** 1219-1225.

VERBEECK, R., DRIESSENS, F., THUN, H. & VERBEEK, F. (1981) Stability of Calcium-Strontium Hydroxyapatite Solid Solutions in Aqueous Solutions at 25°. *Bulletin des Societes Chimiques Belges,* 90**,** 409-417.

VERBEECK, R. M. H. (1986) *Minerals in human enamel and dentin. In:Tooth development and caries. Drissene F.C.M. Woltgens J.M.H.,* CRC Press.

WAERHAUG, M., GJERMO, P. & JOHANSEN, J. R. (1984) Comparison of the effect of chlorhexidine and CuSO4 on plaque formation and development of gingivitis. *Journal of Clinical Periodontology,* 11**,** 176-180.

WAGONER, S. N., MARSHALL, T. A., QIAN, F. & WEFEL, J. S. (2009) In vitro enamel erosion associated with commercially available original-flavor and sour versions of candies. *The Journal of the American Dental Association,* 140**,** 906-913.

WALER, S. M. & ROLLA, G. (1982) Comparison between plaque inhibiting effect of chlorhexidine and aqueous solutions of copper ‐ and silver ions. *European Journal of Oral Sciences,* 90**,** 131-133.

WANG, L., NANCOLLAS, G. H., HENNEMAN, Z. J., KLEIN, E. & WEINER, S. (2006) Nanosized particles in bone and dissolution insensitivity of bone mineral. *Biointerphases,* 1**,** 106.

WANG, L., TANG, R., BONSTEIN, T., ORME, C., BUSH, P. & NANCOLLAS, G. (2005) A new model for nanoscale enamel dissolution. *The Journal of Physical Chemistry B,* 109**,** 999-1005.

WAPNIR, R. A. (2000) Zinc deficiency, malnutrition and the gastrointestinal tract. *The Journal of nutrition,* 130**,** 1388S.

WATANABE, M., ASATSUMA, M., IKUI, A., IKEDA, M., YAMADA, Y., NOMURA, S. & IGARASHI, A. (2005) Measurements of several metallic elements and matrix metalloproteinases (MMPs) in saliva from patients with taste disorder. *Chemical Senses,* 30**,** 121.

WEATHERELL, J., HALLSWORTH, A. & ROBINSON, C. (1973) The effect of tooth wear on the distribution of fluoride in the enamel surface of human teeth. *Archives of Oral Biology,* 18**,** 1175-1189, IN5.

WEATHERELL, J., ROBINSON, C. & HALLSWORTH, A. (1972) Changes in the fluoride concentration of the labial enamel surface with age. *Caries Research,* 6**,** 312-324.

WEISMANN, K., JAKOBSEN, J. P., WEISMANN, J. E., HAMMER, U. M., NYHOLM, S. M., HANSEN, B., LOMHOLT, K. & SCHMIDT, K. (1990) Zinc gluconate lozenges for common cold. *Danish Medical Bulletin,* 37**,** 279-281.

WELBURY, R., DUGGAL, M. S. & HOSEY, M. T. (2005) *Paediatric Dentistry,* Oxford, Oxford university press.

WHITE, D. (1995) The application of in vitro models to research on demineralization and remineralization of the teeth. *Advances in Dental Research,* 9**,** 175-193.

WHITE, S. & PHAROAH, M. (2004) Intraoral radiography. *Oral radiology: principles and interpretation. 5th ed. St. Louis: Mosby***,** 77-90.

WHITE, S. C. & PHAROAH, M. J. (2008) The evolution and application of dental maxillofacial imaging modalities. *Dental Clinics of North America,* 52**,** 689-705.

WHITE, W. & NANCOLLAS, G. H. (1977) Quantitative study of enamel dissolution under conditions of controlled hydrodynamics. *Journal of Dental Research,* 56**,** 524-530.

WHITTAKER, D. (1982) Structural variations in the surface zone of human tooth enamel observed by scanning electron microscopy. *Archives of Oral Biology,* 27**,** 383-392.

WHO (2004) Copper in drinking-water. *Background document for development of WHO Guidelines for Drinking water Quality*.

WILSON, R., ELLIOTT, J. & DOWKER, S. (1999) Rietveld refinement of the crystallographic structure of human dental enamel apatites. *American Mineralogist,* 84**,** 1406.

XU, Y., SCHWARTZ, F. W. & TRAINA, S. J. (1994) Sorption of Zn^{2+} and Cd^{2+} on hydroxyapatite surfaces. *Environmental Science & Technology,* 28**,** 1472-1480.

YAMAGUCHI, M. (1998) Role of zinc in bone formation and bone resorption. *The Journal of Trace Elements in Experimental Medicine,* 11**,** 119-135.

YAMAGUCHI, M., OISHI, H. & SUKETA, Y. (1987) Stimulatory effect of zinc on bone formation in tissue culture. *Biochemical Pharmacology,* 36**,** 4007-4012.

YOON, N. A. & BERRY, C. W. (1979) The antimicrobial effect of fluorides (acidulated phosphate, sodium and stannous) on Actinomyces viscosus. *Journal of Dental Research,* 58**,** 1824-1829.

YOUNG, A., JONSKI, G. & ROLLA, G. (2003) Inhibition of orally produced volatile sulfur compounds by zinc, chlorhexidine or cetylpyridinium chloride-effect of concentration. *European Journal of Oral Sciences,* 111**,** 400-404.

YOUNG, A., JONSKI, G., RÖLLA, G. & WÅLER, S. (2001) Effects of metal salts on the oral production of volatile sulfur containing compounds (VSC). *Journal of Clinical Periodontology,* 28**,** 776-781.

ZAHRADNIK, R. & MORENO, E. (1977) Progressive stages of subsurface demineralization of human tooth enamel. *Archives of Oral Biology,* 22**,** 585-591.

ZAHRADNIK, R., MORENO, E. & BURKE, E. (1976) Effect of salivary pellicle on enamel subsurface demineralization in vitro. *Journal of Dental Research,* 55**,** 664-670.

ZEROB, A. L. T. J. D. (2004) The role of diet in the aetiology of dental erosion. *Caries Research,* 38**,** 34-44.

APPENDIX I

ABSTRACTS FOR CONFERENCE PRESENTATIONS AND PAPERS IN PREPARATION

List of conferences presentations that have arisen from the work presented in this thesis

1. H. Lingawi, M.E. Barbour, P. Anderson

Effect of Replenishment Rate of Demineralisation Solutions on Hydroxyapatite Dissolution Kinetics Studied Using Scanning Microradiography, International Caries Research Conference, Montpellier, France (July, 2010)

ORAL PRESENTATION

2. H. Lingawi, M.E. Barbour, R.J.M. Lynch, P. Anderson

Effect of Zinc ions (Zn^{2+}) on Hydroxyapatite Dissolution Kinetics Studied Using Scanning Microradiography, 2nd UK Zinc meeting, London, UK, (October, 2010)

ORAL PRESENTATION

3. H. Lingawi, M.E. Barbour, P. Anderson

Effect of Demineralisation Solutions Circulation Rates on Hydroxyapatite Dissolution Kinetics Studied Using Scanning Microradiography, William Harvey Day, QMUL, (October, 2010)

POSTER PRESENTATION

4. H. Lingawi, M.E. Barbour, R.J.M. Lynch, P. Anderson

Effect of Zinc (Zn^{2+}) and Strontium (Sr^{2+}) Ions on Hydroxyapatite Thermodynamic Dissolution Kinetics, Weybridge Scientific Conference, Surry, UK, (April 2011)

ORAL PRESENTATION

5. H. Lingawi, M.E. Barbour, R.J.M. Lynch, P. Anderson

Effect of Zinc (Zn^{2+}) and Strontium (Sr^{2+}) Ions on Hydroxyapatite Dissolution Relevant to Dental Caries and Erosion, International Association of Paediatric Dentistry, Athens, Greece, (June 2011)

POSTER PRESENTATION

6. H. Lingawi, M.E. Barbour, R.J.M. Lynch, P. Anderson

Effect of Zinc as Divalent Metal Cation on Hydroxyapatite Dissolution Kinetics Studied Using Scanning Microradiography, International Caries Research Conference, Kaunas, Lithuania (July, 2011)

ORAL PRESENTATION

7. H. Lingawi, M.E. Barbour, P. Anderson

Cariostatic Influence of Sr^{2+} on Hydroxyapatite-disc Tooth Analogue Demineralisation, The British Society of Oral and Dental Research, Sheffield, UK (September 2011)

ORAL PRESENTATION

8. H. Lingawi, M.E. Barbour, P. Anderson

Effect of Sr^{2+} on Hydroxyapatite Dissolution Kinetics Studied Using Scanning Microradiography, William Harvey Day, QMUL, (October, 2011)

POSTER PRESENTATION

9. H. Lingawi, M.E. Barbour, P. Anderson

Effect of Divalent Metal Cations on Hydroxyapatite Dissolution Relevant to Dental Caries and Erosion, London Oral Biology Club, QMUL, London (November, 2011)

ORAL PRESENTATION

List of papers in preparation that have arisen from the work presented in this thesis

1. H. Lingawi, P. Anderson

Real-time Scanning Microradiography for the Quantitative Measurements of Dissolution Kinetics of Compressed Hydroxyapatite Pellets

Scanning

2. H. Lingawi, M.E. Barbour, R.J.M. Lynch, P. Anderson

Effect of Zinc (Zn^{2+}) and Strontium (Sr^{2+}) Ions on Hydroxyapatite Dissolution Relevant to Dental Caries and Erosion

Caries Research

Published abstracts for oral presentations

1. H. Lingawi, M.E. Barbour, P. Anderson. Effect of Replenishment Rate of Demineralisation Solutions on Hydroxyapatite Dissolution Kinetics Studied Using Scanning Microradiography. The European Organization for Caries Research Conference, France, (July, 2010)

Abstract

The replenishment of demineralising solution adjacent to a dissolving surface has considerable influence on the rate of dissolution of solids. This is particularly pertinent to dissolution studies of enamel, and similar studies of model systems for dental caries using compressed powders of hydroxyapatite as the substrate. As part of an overall investigation of the fundamental mechanisms influencing kinetics of enamel and hydroxyapatite dissolution, the aim was to compare the dissolution rates of compressed hydroxyapatite (HAP) powder discs as a function of replenishment rate of demineralising solution, using scanning microradiography (SMR).
Compressed HAP powder discs product of Plasma –Biotal with 20 wt% nominal porosity were sterilised, coated with acid-resistant varnish on all surfaces except one, preconditioned, and located in an SMR cell volume 1.96 cm^3. Demineralising solution (0.1% acetic acid buffered with 1M KOH, pH 4.0) was pumped at various replenishments rates using a variable speed circulating pump. The rate of HAP dissolution (RDHAP) was measured using SMR at a single centrally located point on each disc for periods of 24 h at 22°C. Each measurement was repeated in triplicate.
The mean RDHAP was; $6.58x10^{-6}$, $1.18\ x10^{-4}$, $1.70\ x10^{-4}$, $2.40\ x10^{-4}$, $2.72\ x10^{-4}$, $3.13\ x10^{-4}$, $3.16\ x10^{-4}$g.cm-2.h-1 at circulation speeds of 0, 0.19, 0.39, 0.58, 0.80, 0.97 and 1.17cm3.min-1 respectively.
The RDHAP statistically significantly increased for circulation speeds up to 0.78 cm3.min-1, but did not change significantly at higher speeds.
This study demonstrates that the solution composition in contact with a demineralising HAP surface achieved by sufficient replenishment rate, or stirring, is an important parameter in HAP dissolution studies. Diffusive transport of dissolved substrate away from the dissolving HAP surface will influence the kinetics of the process.

2. H. Lingawi, M.E. Barbour, R.J.M. Lynch, P. Anderson. Effect of Zinc Ions (Zn^{2+}) on Hydroxyapatite Dissolution Kinetics Studied Using Scanning Microradiography. The European Organization for Caries Research Conference, Lithuania, (July, 2011)

Abstract

Zinc (Zn^{2+}) is a dietary essential trace element necessary for various body functions. It is used in toothpaste for its anti-calculus properties and reducing oral malodour, but it may also have a role in inhibiting dissolution kinetics of enamel's principal inorganic component; hydroxyapatite (HAp).

The aim of this study was to investigate the effect of Zn^{2+} on surface physical chemistry influencing HAp dissolution by measuring the rate of HAp dissolution (RD_{HAp}) under strictly controlled thermodynamic conditions relevant to caries and erosion using scanning microradiography (SMR) at a range of Zn^{2+}concentrations.

Compressed sintered HAp discs (*Plasma-Biotal, UK*) were coated with acid-resistant varnish on all surfaces except one, and located in an SMR cell. A bulk solution of 0.1% acetic acid pH4, divided into five (1 litre bottle) with the addition of 0, 5, 10, 15, 20 ppm Zn^{2+} respectively was prepared. 0.3% citric acid pH2.8 solutions were similarly prepared.

The demineralising solution was circulated at 0.80cm^3/min, and the RD_{HAp} was measured using SMR at a single centrally located point on each disc for 24h at 22°C. Each experiment was repeated in duplicate for both increasing, and decreasing, Zn^{2+} concentrations.

For acetic acid, the mean RD_{HAp} decreased significantly ($p< 0.05$) from 4.38 $x10^{-4}$ (with no Zn^{2+} added) to 3.81$x10^{-4}$, 3.19$x10^{-4}$, 3.02$x10^{-4}$, and 2.71$x10^{-4}$g/cm^2/h at Zn^{2+} concentrations of 5, 10, 15 and 20 ppm respectively.

For citric acid, the mean RD_{HAp} decreased significantly ($p<0.05$) from 3.12 $x10^{-3}$ (with no Zn^{2+} added) to 2.83$x10^{-3}$, 2.73$x10^{-3}$, 2.45$x10^{-3}$ and 1.83$x10^{-3}$g/cm^2/h at Zn^{2+} concentrations of 5, 10, 15 and 20 ppm respectively.

This study demonstrates that Zn^{2+} decreased RD_{HAp} under strictly controlled thermodynamic conditions relevant to caries and erosion, possibly due to inhibition of dissolution nuclei on the HAp surfaces.

3. H. Lingawi, M.E. Barbour, P. Anderson. Cariostatic Influence of Sr^{2+} on Hydroxyapatite-Disc Tooth Analogue Demineralisation. The British Society of Oral and Dental Research, Sheffield, UK (September 2011).

Abstract

Objectives: Strontium (Sr^{2+}) has been demonstrated to be cariostatic. The evidence is controversial and the exact mechanism by which strontium decreases dental caries is unclear. Our aim is to study the effect of the divalent metal cation Sr^{2+} on the kinetics of porous hydroxyapatite (HAp) disc dissolution using scanning microradiography (SMR) under artificial caries and erosion conditions.
Methods: Compressed 1mm thick sintered HAp discs (Plasma-Biotal, UK. 20wt% nominal porosity) used as tooth analogues, were preconditioned, coated with acid-resistant varnish on all surfaces leaving one surface exposed, and located centrally in SMR cell. 1L 0.1% acetic acid pH 4.0 (caries conditions) and 0.3% citric acid pH 2.8 (erosion conditions) demineralising solutions were prepared with each of 0, 5, 10, 20 and 30 ppm Sr^{2+} respectively. Demineralising solution was circulated at 0.80 cm^3/min, and the HAp demineralisation rate (RDHAp) was measured at a single centrally located point on each disc for 24 h at 22±1°C using SMR. Each experiment was repeated twice for both increasing, and decreasing sequences of Sr^{2+} concentrations.
Results: Caries conditions: mean RD_{HAp} decreased significantly from $3.40x10^{-4}$ (0 ppm Sr^{2+}) to $2.73x10^{-4}$ (5 ppm), $1.88x10^{-4}$ (10 ppm), $1.44x10^{-4}$ (20 ppm), and $1.15x10^{-4}$ (30 ppm) g/cm^2/h for increasing concentration sequence, and from 1.47 $x10^{-4}$ (30ppm Sr^{2+}) to $1.24x10^{-4}$ (20 ppm), $1.04x10^{-4}$ (10 ppm), $6.10x10^{-5}$ (5 ppm) and $2.39x10^{-4}$ (0 ppm) g/cm^2/h for decreasing concentration sequence.
Erosion conditions: mean RD_{HAp} decreased significantly from 4.22 $x10^{-3}$ (0 ppm Sr^{2+}) to $4.02x10^{-3}$ (5 ppm), $3.58x10^{-3}$ (10 ppm), $3.45x10^{-3}$ (20 ppm) and $2.83x10^{-3}$ (30 ppm) g/cm^2/h for increasing concentration sequence, and from $3.94x10^{-3}$ (30 ppm Sr^{2+}) to $3.55x10^{-3}$ (20 ppm), $3.19x10^{-3}$ (10 ppm) , $2.58x10^{-3}$ (5 ppm) , and $3.65x10^{-3}$ (0 ppm) g/cm^2/h for decreasing concentration sequence.
Conclusion: Sr^{2+}decreased RD_{HAp} under strictly controlled thermodynamic conditions relevant to dental caries and erosion. The non-reversibility in RD_{HAp} throughout the increasing and decreasing Sr^{2+} sequences may be due to lasting effects of phase changes in HAp. This study demonstrates the potential usefulness of Sr^{2+} in caries prevention.

4. H. Lingawi, M.E. Barbour, P. Anderson. Effect of Sr^{2+} on Hydroxyapatite Demineralisation Using Scanning Microradiography. The European Organization for Caries Research Conference, Brazil, (June, 2012)

Abstract

The literature on the cariostatic effects of strontium (Sr^{2+}) remains controversial and the mechanism is obscure. The aim was to study the effect of $Sr2^{+}$ in the demineralising solution on the kinetics of hydroxyapatite (HAp) dissolution using scanning microradiography (SMR) under artificial caries and erosion conditions.
Hydroxyapatite discs (Plasma-Biotal, UK. 20wt% porosity) 1mm thick sintered, were used as enamel analogues, coated with acid-resistant varnish leaving one surface exposed, and located in an SMR cell. Demineralising solutions of 0.1% acetic acid pH4 simulating caries conditions, and 0.3% citric acid pH2.8, simulating erosive conditions were circulated through the SMR cells. The rate of demineralisation of the HAp discs (RD_{HAp}) was measured using SMR. Further SMR measurements were carried out using identical demineralising conditions, but with increasing Sr^{2+} concentrations of 5, 10, 20 and 30 ppm, and SMR measurements were continued for each case. The SMR measurements were then repeated at decreasing Sr^{2+} concentrations (30, 20, 10, 5 and 0 ppm).
Results for Caries-like conditions showed RD_{HAp} decreased ($3.40x10^{-4}$, $2.73x10^{-4}$, $1.88x10^{-4}$ $1.44x10^{-4}$, $1.15x10^{-4}$ $g.cm^{-2}.h^{-1}$) at increasing Sr^{2+} concentrations. RD_{HAp} also decreased ($1.47x10^{-4}$, $1.24x10^{-4}$, $1.04x10^{-4}$, $6.10x10^{-5}$ $g.cm^{-2}.h^{-1}$) at decreasing Sr^{2+} concentrations, except for $2.39x10^{-4}$ $g.cm^{-2}.h^{-1}$ at 0 ppm.
Erosive-like conditions RD_{HAp} decreased ($4.22x10^{-3}$, $4.02x10^{-3}$, $3.58x10^{-3}$, $3.45x10^{-3}$, $3.12x10^{-3}$ $g.cm^{-2}.h^{-1}$) at increasing Sr^{2+} concentrations. RD_{HAp} also decreased ($3.94x10^{-3}$, $3.55x10^{-3}$, $3.19x10^{-3}$, $2.58x10^{-3}$ $g.cm^{-2}.h^{-1}$) at decreasing Sr^{2+} concentrations except for $3.65x10^{-3}$ $g.cm^{-2}.h^{-1}$ at 0 ppm.
In conclusion, Sr^{2+}decreased RD_{HAp} under strictly controlled thermodynamic conditions relevant to caries and erosion. However, this decrease was not reversed when the Sr^{2+} concentration was subsequently decreased. This pattern of the influence of Sr^{2+} may result from the partial inclusion of Sr^{2+} into the HAp lattice.

Samples of poster presentations

1. H. Lingawi, M.E. Barbour, P. Anderson. Effect of Demineralisation Solutions Circulation Rate on Hydroxyapatite Dissolution Kinetics Studied Using Scanning Microradiography. William Harvey Day, QMUL (October, 2010)

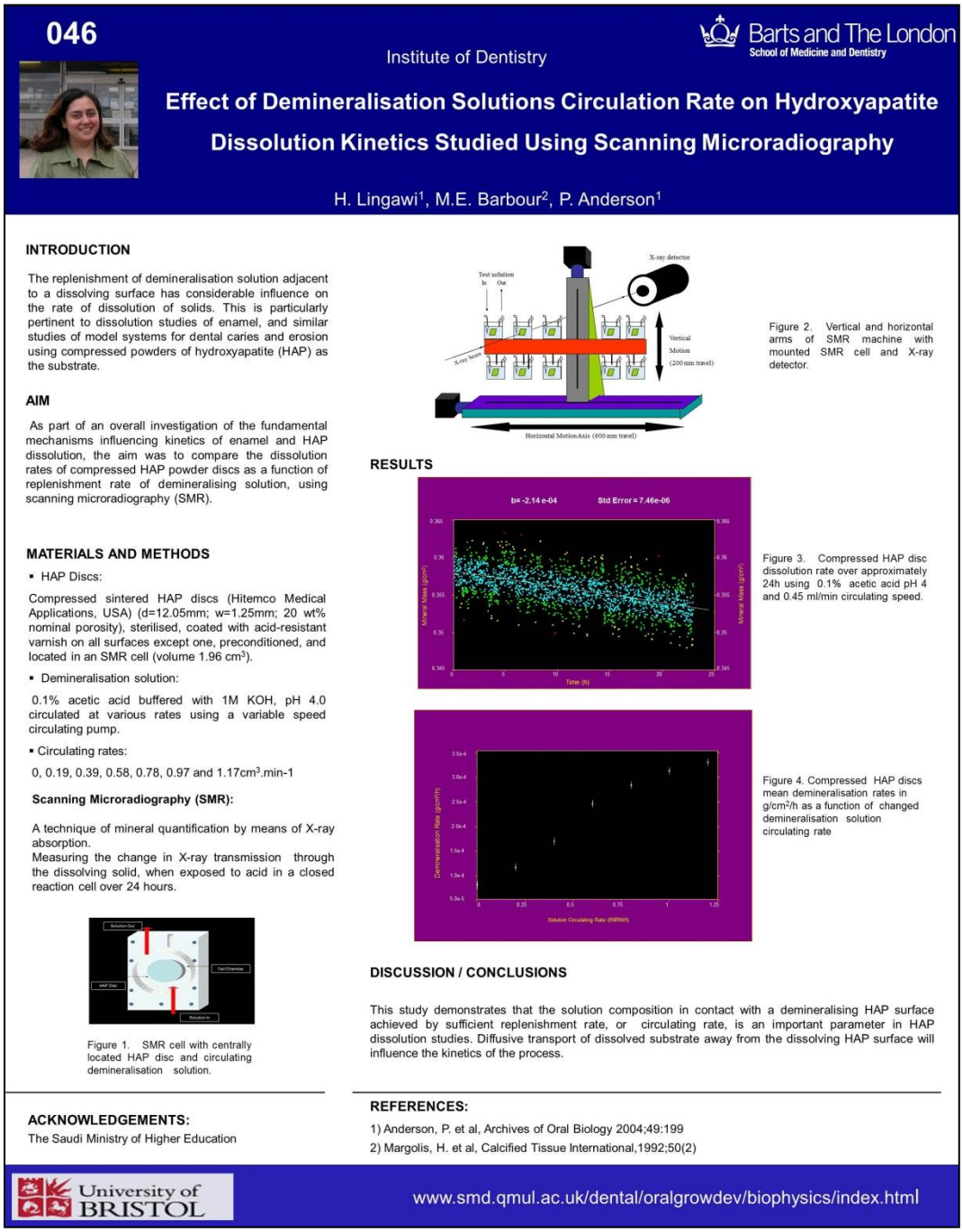

046

Institute of Dentistry

Barts and The London School of Medicine and Dentistry

Effect of Demineralisation Solutions Circulation Rate on Hydroxyapatite Dissolution Kinetics Studied Using Scanning Microradiography

H. Lingawi[1], M.E. Barbour[2], P. Anderson[1]

INTRODUCTION

The replenishment of demineralisation solution adjacent to a dissolving surface has considerable influence on the rate of dissolution of solids. This is particularly pertinent to dissolution studies of enamel, and similar studies of model systems for dental caries and erosion using compressed powders of hydroxyapatite (HAP) as the substrate.

AIM

As part of an overall investigation of the fundamental mechanisms influencing kinetics of enamel and HAP dissolution, the aim was to compare the dissolution rates of compressed HAP powder discs as a function of replenishment rate of demineralising solution, using scanning microradiography (SMR).

MATERIALS AND METHODS

- HAP Discs:

Compressed sintered HAP discs (Hitemco Medical Applications, USA) (d=12.05mm; w=1.25mm; 20 wt% nominal porosity), sterilised, coated with acid-resistant varnish on all surfaces except one, preconditioned, and located in an SMR cell (volume 1.96 cm^3).

- Demineralisation solution:

0.1% acetic acid buffered with 1M KOH, pH 4.0 circulated at various rates using a variable speed circulating pump.

- Circulating rates:

0, 0.19, 0.39, 0.58, 0.78, 0.97 and 1.17cm^3.min-1

Scanning Microradiography (SMR):

A technique of mineral quantification by means of X-ray absorption.
Measuring the change in X-ray transmission through the dissolving solid, when exposed to acid in a closed reaction cell over 24 hours.

Figure 1. SMR cell with centrally located HAP disc and circulating demineralisation solution.

Figure 2. Vertical and horizontal arms of SMR machine with mounted SMR cell and X-ray detector.

RESULTS

Figure 3. Compressed HAP disc dissolution rate over approximately 24h using 0.1% acetic acid pH 4 and 0.45 ml/min circulating speed.

Figure 4. Compressed HAP discs mean demineralisation rates in $g/cm^2/h$ as a function of changed demineralisation solution circulating rate

DISCUSSION / CONCLUSIONS

This study demonstrates that the solution composition in contact with a demineralising HAP surface achieved by sufficient replenishment rate, or circulating rate, is an important parameter in HAP dissolution studies. Diffusive transport of dissolved substrate away from the dissolving HAP surface will influence the kinetics of the process.

ACKNOWLEDGEMENTS:
The Saudi Ministry of Higher Education

REFERENCES:

1) Anderson, P. et al, Archives of Oral Biology 2004;49:199
2) Margolis, H. et al, Calcified Tissue International,1992;50(2)

University of BRISTOL

www.smd.qmul.ac.uk/dental/oralgrowdev/biophysics/index.html

2. H. Lingawi, M.E. Barbour, P. Anderson. Effect of Strontium Ions on Hydroxyapatite Dissolution Kinetics Studied Using Scanning Microradiography. William Harvey Day, QMUL, (October, 2011).

27

Effect of Strontium Ions on Hydroxyapatite Dissolution Kinetics Studied Using Scanning Microradiography

H. Lingawi[1], M.E. Barbour[2], P. Anderson[1]

INTRODUCTION

Strontium (Sr^{2+}) is a dietary essential trace element essential for many body functions such as collagen synthesis, mineralisation of bone and immune system function. It is used in toothpastes and mouthwashes to reduce oral malodour as well as its anti calculus properties, but may also have a role in inhibiting the dissolution kinetics of hydroxyapatite (HAP).

AIM

To investigate the effect of Sr^{2+} as a divalent metal cation on the surface physical chemistry influencing HAP dissolution kinetics by measuring the rate of HAP dissolution (RD_{HAP}) under strictly controlled thermodynamic conditions relevant to dental caries and erosion using scanning microradiography technique (SMR) at a range of Sr^{2+} concentrations.

MATERIALS AND METHODS

- **HAP Discs:**

Compressed sintered HAP discs (Plasma Biotal, UK.) (d=13mm; w=2mm; 20 wt% nominal porosity), coated with acid-resistant varnish on all surfaces leaving one surface exposed to the demineralising solution, preconditioned, sterilised, and located centrally in an SMR cell (volume 1.96 cm^2).

- **Demineralisation solution:**

Bulk solution of 0.1% acetic acid pH 4.0 buffered with 1M KOH, divided into five (1liter bottle) with the addition of 0, 5, 10, 20 and 30ppm Sr^{2+} respectively was prepared. demineralising solution was circulated at 0.80$cm^3.min^{-1}$.

- **Scanning Microradiography (SMR):**

Technique of mineral quantification by means of X-ray absorption.
Measuring the change in X-ray transmission through the dissolving solid, when exposed to acid in a closed reaction cell over 24 hours

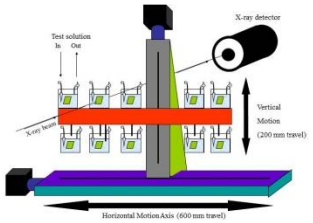

Figure 1. Vertical and horizontal arms of SMR machine with mounted SMR cells and X-ray detector.

RESULTS

For citric acid pH 2.8; the RD_{HAP} decreased significantly ($p<0.05$) from 4.22 $x10^{-3}$(with 0 Sr^{2+} added) to 4.02$x10^{-3}$, 3.58$x10^{-3}$, 3.45$x10^{-3}$and 2.12$x10^{-3}$g.cm^{-2}.h^{-1} at Zn^{2+} concentrations of 5, 10, 15 and 20ppm respectively and from 3.94$x10^{-3}$ to 3.55$x10^{-3}$, 3.19$x10^{-3}$, 2.58$x10^{-3}$ and 3.65$x10^{-3}$ g.cm^{-2}.h^{-1} at Sr^{2+} concentration of 30, 20, 10, 5and 0ppm respectively .

For acetic acid pH4; the RD_{HAP} decreased significantly ($p<0.05$) from 3.40$x10^{-4}$ (with 0 Sr^{2+} added) to 2.73$x10^{-4}$, 1.88$x10^{-4}$, 1.44$x10^{-4}$, and 1.15$x10^{-4}$ g.cm^{-2}.h^{-1} at Sr^{2+} concentration of 5, 10, 20and 30ppm respectively in increasing Sr^{2+} concentration sequences, and from 1.47$x10^{-4}$ to 1.24 $x10^{-4}$, 1.04 $x10^{-4}$, 6.10$x10^{-5}$ and 2.39$x10^{-4}$ g.cm^{-2}.h^{-1} at Sr^{2+} concentration of 30, 20, 10, 5and 0ppm respectively .

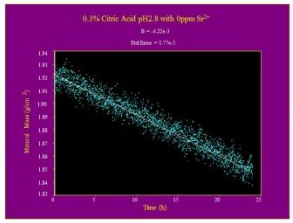

Figure 2. RD_{HAP} over approximately 24h using 0.3% citric acid pH 2.8 with 0ppm Sr^{2+}.

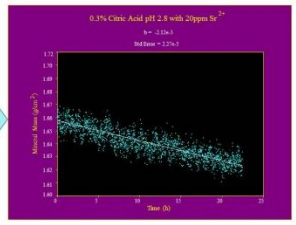

Figure 3. RD_{HAP} over approximately 24h using 0.3% citric acid pH 2.8 with 20ppm Sr^{2+}.

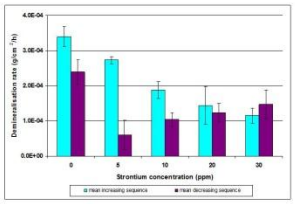

Figure 4. Mean RD_{HAP} using 0.1% acetic acid pH 2.8. with various Sr^{2+} concentrations in both increasing and decreasing orders.

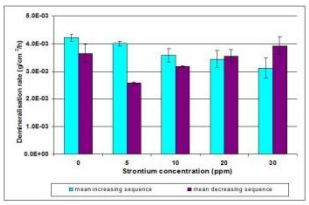

Figure 5. Mean RD_{HAP} using 0.3% citric acid pH 2.8. with various Sr^{2+} concentrations in both increasing and decreasing orders.

CONCLUSIONS

This study demonstrates that Sr^{2+}as divalent metal cation decreases RD_{HAP} under strictly controlled thermodynamic conditions relevant to dental caries and erosion, possibly due to lasting effect of phase changes in HAP.

REFERENCES:

ANDERSON, P. & ELLIOTT, J. (1992) Subsurface demineralization in dental enamel and other permeable solids during acid dissolution. *Journal of Dental Research,* 71, 1473.

INGRAM, G., HORAY, C. & STEAD, W. (1992) Interaction of zinc with dental mineral. *Caries research,* 26, 248-253.

MATSUNAGA, K., MURATA, H., MIZOGUCHI, T. & NAKAHIRA, A. (2010) Mechanism of incorporation of zinc into hydroxyapatite. *Acta biomaterialia,* 6, 2289-2293.

University of BRISTOL

Acknowledgements to The Saudi Ministry of Higher Education

www.smd.qmul.ac.uk/dental/oralgrowdev/biophysics/index.htm

Barts and The London School of Medicine and Dentistry